Design, Synthesis and Evaluation of Somatostatin Analogs for Improved Imaging and Radionuclide Therapy

Inauguraldissertation

zur

Erlangung der Würde eines Doktors der Philosophie

vorgelegt der

Philosophisch-Naturwissenschaftichen Fakultät

der Universität Basel

von

Mihaela Ginj

aus Iasi, Rumänien

Basel, 2005

Genehmigt von der Philosophisch-Naturwissenschaftichen Fakultät auf Antrag von

Prof. Dr. Helmut R. Mäcke

Prof. Dr. Helma Wennemers

Prof. Dr. Urs Sequin

Basel, den 11 Mai 2005

Prof. Dr. Hans-Jacob Wirz (Dekan)

Acknowledgements

The work presented in this dissertation was carried out at the Division of Radiological Chemistry, Department of Radiology, University Hospital Basel with financial support from the Swiss National Science Foundation and COST B12 action. Many people contributed to the completeness of this thesis and I would like to acknowledge them.

The first person to whom I would like to express my gratitude is ***Prof. Manfred Mutter*** *who made this thesis possible by forwarding my PhD application to Prof. Maecke.*

I am deeply indebted to my ''Doktorvater'' ***Prof. Helmut R. Maecke*** *first of all for accepting me in his group, and thus rescuing me from ''computer modeling poisoning''. And then for his encouraging guidance and generous support over the course of my thesis. The granted freedom for the design and execution of the projects, his confidence, as well as his constant interest in the progress of my work have made the past years a great experience.*

I am grateful to ***Prof. Helma Wennemers*** *for accepting the co-examination of my thesis and for being a constant model of scientific enthusiasm.*

Many thanks also to ***Prof. Jean-Claude Reubi*** *and his research group for the precious help with binding affinity measurements for so many compounds.*

I have been fortunate to have had ***Jörg Schmitt*** *as mentor in my early days in Basel, a competent and patient teacher. His help and guidance were crucial for a good start.*

I would like to express my gratitude also to ***Dr. Stefan Schulz*** *and his group in Magdeburg for the generous help provided in the last year.*

I would like to acknowledge the help all along these years provided by Novartis Pharma and particularly by ***Dieter Staab*** *and* ***Kayhan Akyel*** *in terms of analytics. And I am also grateful to* ***Dr. Peter Burkhard*** *for his assistance in molecular modeling and peptide crystallization (still waiting for the magic pearls…).*

And what would have been my days (and nights) in the lab without the continuous support of ***''the weasels''****… So many neurons saved from apoptosis only by talking, singing, laughing and racing chairs together! So little people and so many lessons to learn from! I'll always envy Hanwen's serenity (the mamahuhu state) and Patricia's swimming technique! Obrigado para tudo!*

My first years of thesis wouldn't have been so smooth and cheerful without the French touch. Merci **Val** *pour me faire découvrir la vraie culture française (l'humour disjoncté), pour avoir été la meilleure co-locataire qu'on peut désirer et pour toujours me soutenir, même de loin. Merci aussi* **Sandrine** *pour ton équilibre dans toutes les circonstances.*

I will always be indebted to **Karin** *not only for the subtle insights into the Swiss German dialect, but also for the precious help with the biological in vitro studies. Many, many thanks to* **Sibylle** *(alias Bill) as well for backing me up with the hundreds of experiments planned every time at the last minute.*

I am also grateful to all the **routine personnel** *for always keeping the things going, to* **Claudine** *for dealing with my sometimes peculiar administrative problems and to* **Joos Dürr** *for his remarkable skills in repairing everything at any time. I would like also to acknowledge the help with the animal experiments from the part of* **Christian**, **Damian, Jianhua** *and* **Martin**.

I cannot forget my other present and past labmates, each one bringing his/her personal contribution to the good lab atmosphere: **Simona**, **Klaus**, **Stephan**, **Daniel** *and* **Michi**.

Many thanks to all the members of the Institute of Nuclear Medicine and to **Prof. Jan Müller** *for accepting our (I and some weasels) sometimes noisy presence.*

Special thanks go to my family in Romania and to my husband, friend and cook, **Cristian**:

Va multumesc, mama si tata, pentru sprijinul vostru continuu si increderea (uneori exagerata!) pe care ati avut-o si o aveti in mine! Cine stie unde ma va purta inca destinul, sper doar sa ma pot revansa pentru tot ceea ce ati facut si faceti pentru mine.

Dragul meu Cristi, cine stie ce-ar fi ajuns teza asta fara cantitatile enorme de strudele, clatite, sarmale si alte bunatati facute de miinile tale cu atita dragoste! Te iubesc, iti multumesc si sper sa mai avem destul timp impreuna sa recuperam toate zilele si noptile pierdute de dragul stiintei.

This thesis is based on the following papers, which will be referred to in the text by their roman numerals **I-VI**:

I **Ginj M** and Maecke HR. in *Radiometallo-Labeled Peptides in Tumor Diagnosis and Therapy*; Sigel, A., Sigel, H., Eds.; **Metal ions in biological systems**; Marcel Dekker, New York, **2004**; Vol. 42, p. 109-142.

II **Ginj M**, Schmitt JS, Chen J, Waser B, Reubi JC, de Jong M, Schulz S, Maecke HR. Design, synthesis and biological evaluation of new somatostatin based radiopeptides, Manuscript in preparation.

III Wild D, Schmitt JS, **Ginj M**, Macke HR, Bernard BF, Krenning E, de Jong M, Wenger S, Reubi JC. DOTA-NOC, a high affinity ligand of somatostatin receptor subtypes 2, 3 and 5 for labeling with various radiometals, *Eur J Nucl Med Mol Imaging*, **2003**, 30: 1338-1347.

IIIa Wild D, Maecke HR, Waser B, Reubi JC, **Ginj M**, Rasch H, Muller-Brand J, Hofmann M. (68)Ga-DOTANOC: a first compound for PET imaging with high affinity for somatostatin receptor subtypes 2 and 5, *Eur J Nucl Med Mol Imaging*, **2005**, 32: 724.

IV **Ginj M**, Chen J, Walter MA, Eltschinger V, Reubi JC, Maecke HR. Preclinical evaluation of new and highly potent analogues of octreotide for predictive imaging and targeted radiotherapy, *Clin Cancer Res*, **2005**;11(3):1136-45.

V **Ginj M**., Maecke HR. Synthesis of trifunctional somatostatin based derivatives for improved cellular and subcellular uptake, *Tetrahedron Lett*, **2005,** 46 (16): 2821-2824.

VI **Ginj M**, Hinni K, Tschumi S, Schulz S, Maecke HR. Trifunctional somatostatin based derivatives designed for targeted radiotherapy using Auger electron emitters, *J Nucl Med,* **2005**, 46:2097-2103.

Contents

Abbreviations

^{18}FDG	2-deoxy-2-[^{18}F]fluoro-D-glucose
DCM	Dichloromethane
DIC	*N,N'*-Diisopropylcarbodiimide
DIPEA	Diisopropylethylamine
DMF	Dimethylformamide
DOTA	1,4,7,10-tetraazacyclododecane-1,4,7,10-tetraacetic acid
DTPA	Diethylentriaminepentaacetic acid
ESI-MS	Electron spray ionization-mass spectroscopy
GH	Growth hormone
GPCR	G-protein coupled receptor
HATU	2-(1H-9-Azabenzotriazole-1-yl)-1,1,3,3-tetramethyluronium hexafluorophosphate
HEK	Human embryonic kidney (cells)
HOBt	*N*-Hydroxybenzotriazole
hsstr	Human somatostatin receptor
HYNIC	2-hydrazinonicotinic acid
MALDI-MS	Matrix assisted laser desorbtion/ionization-mass spectroscopy
mRNA	Messenger ribonucleic acid
p.i.	Post injection
PAH	Para-aminohippurate
PCR	Polymerase chain reaction
PET	Positron emission tomography
PRRT	Peptide receptor radionuclide therapy
RP-HPLC	Reverse phase-high performance liquid cromatography
RT-PCR	Reverse phase-polymerase chain reaction
SAR	Structure-activity relationship
SPECT	Single photon emission computer tomography
SPPS	Solid phase peptide synthesis
SRIF	Somatotropin release inhibiting factor
SS	Somatostatin
sstr	Somatostatin receptor
TIS	Triisopropylsilane
TNBS	2,4,6-Trinitrobenzene sulfonic acid

‘’My idea is that chemistry is the central science.
Everything that goes on in biology or medicine
has a chemical basis.”
R. Lerner, *Chem. Eng. News* 1996, *74(20)*, 39.

Foreword

The term **target** *carries several connotations in the overall context of drug discovery. Remarkable progress in molecular biology has led to the identification of numerous proteins with key roles in the function of both normal and abnormal cells, which has allowed the formation of specific hypotheses about how modulating the function of defined proteins that are linked to disease could be a route to new drugs.*

Although there are many exciting new targets for treating and/or preventing cancer, classical chemotherapy and radiotherapy approaches remain the mainstay of cancer treatment for tumors that cannot be cured solely by surgical excision. The preparation of new radiopharmaceuticals for diagnosis or targeted therapy will evolve only if close interactions between biologists, chemists, and physicians continue. As new biological targets are identified, the synthetic challenges presented to the radiopharmaceutical chemists will be faced and hopefully mastered.

Regardless of the beauty of the science involved in the development of the radiotracer, the ultimate goal in nuclear medicine is not the science, but the ability to improve the quality of life. Therefore, the current challenge in this field is to achieve a balance between the specificity of a radiotracer, the required validation of the radiotracer, and the number of patients the radiotracer can help.

1. INTRODUCTION

The major advantage of nuclear medicine methods is that only picomolar concentrations of radiotracers are required to provide a measurable signal without interfering with the process under investigation. It is often true that biochemical or metabolic changes can therefore be identified before a significant change in structure or anatomy can be determined. In oncology this has the potential advantage of not only being able to detect abnormal function related to malignant tissue at diagnosis but also to identify changes as a result of therapy earlier than is possible with anatomical techniques alone. The discovery that many tumor types overexpress receptors for peptide hormones dates back to the mid-1980s. Since then there has been an exponential growth in the development of radiolabeled peptides for diagnostic and therapeutic applications in oncology. Much can be said on the advantages of peptides as targeting agents over proteins, e.g. antibodies, and on the potential targets of metallo-peptides in diagnosis and therapy. For a more comprehensive reading on this matter please see **paper I**.

The first diagnostically studied and also radiotherapeutically employed regulatory peptides were analogs of somatostatin. The high level of expression of somatostatin receptors on various tumor cells has provided the molecular basis for successful use of radiolabeled somatostatin analogs as tumor tracers in nuclear medicine. [1-3]

Throughout this thesis the discussion will be focused on the somatostatin derivatives and their use in peptide receptor mediated radionuclide targeted therapy (PRRT) and diagnostic, with emphasis on the design of new derivatives with improved pharmacological profiles and on strategies to increase their retention time and cytotoxicity in the tumor cells.

1.1. Somatostatin

Somatostatin (somatotropin release-inhibiting factor, SRIF or SS) was originally discovered as a hypothalamic neurohormone that inhibits growth hormone (GH) secretion [4]. Subsequently, SRIF was detected both in the central and peripheral nervous systems and in peripheral tissues where it plays many different roles. In the periphery, the endocrine pancreas and the gut are the main sources of SS, but SRIF-producing cells are also present in the thyroid, adrenals, submandibular glands, kidneys, prostate, and placenta [5, 6, 7]. Its functions include inhibition of endocrine and exocrine secretions, modulation of neurotransmission, motor and cognitive functions, inhibition of intestinal motility, absorption of nutrients and

ions, vascular contractility, and cell proliferation (for a review, see Ref. [8]). Another action of SS is the inhibition of proliferation of various normal and tumor cells [9]. Somatostatin occurs naturally in two molecular forms: a tetradecapeptide (SS-14) and a 28-amino acid peptide (SS-28) containing the amino acid sequence of SS-14, N-terminally extended by 14 amino acid residues (Figure 1) [7, 10]. The SS peptides are synthesized as part of a large precursor molecule that undergoes tissue-specific enzymatic cleavage to yield either SS-14 or SS-28 [10]. Although the biological significance of the two forms of peptide is not yet completely understood, SS-14 is thought to function predominantly as a neuropeptide whereas SS-28 mostly acts as a circulating hormone [11], [12]. The diverse actions of SS peptides are mediated through interaction with a family of five specific SS receptors (sstr) expressed by a variety of normal and malignant tissues [8]. Because of its dual role in inhibiting hormone release and cell growth, it was a logical step to evaluate SS as an anticancer drug for the treatment of neuroendocrine tumors. Various studies demonstrated inhibitory effects of SS in patients with acromegaly, endocrine pancreatic tumors such as insulinomas and glucagonomas, ectopic tumors like gastrinomas, and VIP-(vasoactive intestinal peptide)-producing tumors [7]. However, the short half-life of SS in vivo (about 2–3 min) prevented its application in the clinic.

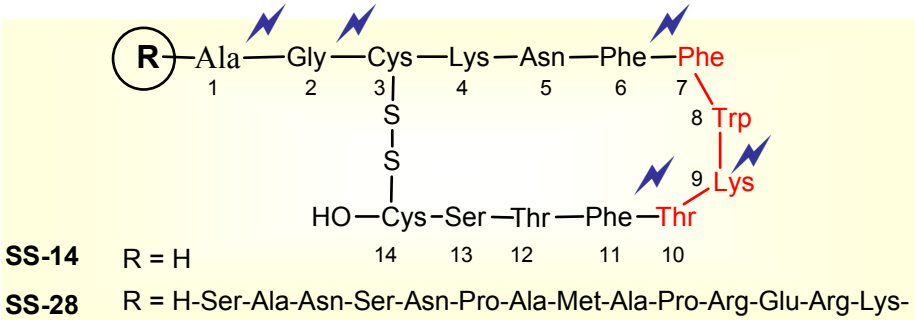

Figure 1. *Structures of the natural somatostatin peptide agonists SS-14 and SS-28. The pharmacophore is highlighted in red. The sites of enzymatic degradation are indicated in blue [13].*

1.2. Somatostatin receptors

Since the original demonstration that the physiological actions of SRIF are mediated by high-affinity plasma membrane receptors, five SS receptors have been cloned and termed sstr1 through sstr5. They belong to the superfamily of G-protein coupled receptors (GPCRs) and the genes encoding the five sstr subtypes are localized on different chromosomes [14]. Via alternative splicing, two forms of sstr2 can be generated, *i.e.*, sstr2A and sstr2B [15, 16], the only difference between them being the length of their cytoplasmatic tail. All the five

receptor subtypes share a coupling to the second messenger systems known to be activated upon SS binding to its receptor. These systems include inhibition of adenylyl cyclase activity and activity of calcium channels, as well as stimulation of phosphotyrosine phosphatase or MAPK activity. These features have been extensively reviewed, [8, 14, 17]. Particular interest has been devoted to the inhibitory action of SS through MAPK pathways [18], this being likely to contribute to the antiproliferative effect of somatostatin. The role of SS in stimulating apoptotic mechanisms in sstr2- or sstr3-expressing cells [19, 20] is another notable antiproliferative mechanism. Recent data reveal that sstr form homo- and heterodimers and also that they physically interact with a class of proteins displaying anchoring and scaffolding functions [21, 22, 23].

Pharmacological studies reveal that all five human subtypes bind SS-14 and SS-28 with high affinity; only SS-28 displays a 10-fold higher affinity for sstr5 than SS-14. Nevertheless, there are differences in the binding affinities of structural analogs of somatostatin and this topic will be discussed later in this study.

1.2.1. Agonist-induced internalization of sstr subtypes

The ability of sstr subtypes to undergo agonist-induced internalization is an important characteristic of these receptors for transporting radiolabeled SS-analogs into the cell, thereby making sstr-targeted radiotherapy a feasible approach. Generally, the mechanism and route of internalization of sstr-agonist complexes follow those described for many other GPCRs and involve aggregation of the hormone receptor complex in specialized areas of the membrane, followed by internalization of the hormone-receptor complex via clathrin-coated, as well as uncoated, pits. After internalization and pit formation, fusion of these vesicles with lysosomes occurs, resulting in hormone degradation or receptor recycling to the cell surface (Figure 2) [24, 25].

There are though differences in the cell trafficking and internalization capabilities of the different receptor subtypes [8, 26, 27, 28]. Thus, using CHO-K1 cells stably expressing one of the hsstr1-5, Hukovic et al. [27] found that [^{125}I]LTT-SS-28 was internalized in the order: hsstr3>hsstr5>hsstr4 >hsstr2 >>hsstr1. On the other hand, by confocal microscopy with fluorescent SS derivatives, Beaudet et al. [29] obtained another classification: hsstr2>hsstr5 >>hsstr1, the only accordance being the very weak internalization of sstr1.

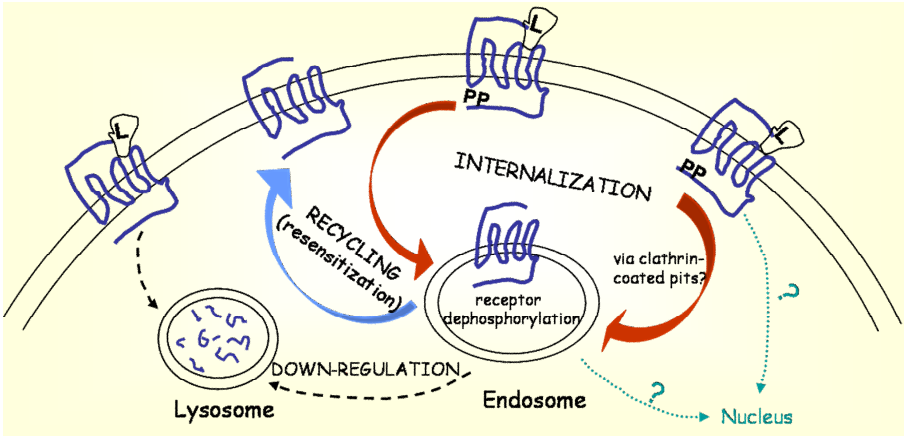

Figure 2. *Schematic representation of intracellular routing of GPCRs after agonist activation (L = ligand, PP = phosphate group). [adapted from ref. [30]]*

The recent observations on homo- and heterodimerization of human sstr [21, 23] showed the influence of co-expression of several sstr subtypes on the cell on the functionality of individual sstr types. Moreover, sstr may also form heterodimers with other GPCRs, e.g., dopamine and opioid receptors, these constructs having different properties from the individual receptors [22].

There are still questions to be answered on the topics of sstr agonist-induced internalization and cell trafficking; apparently, there are several factors influencing the outcome of such studies:

- the technique of investigation employed;
- the nature of the ligand used;
- the cell type utilized for transfection of sstr DNA;
- the species of sstr analyzed;
- the presence of different sstr subtypes or of other GPCRs on the same cell.

In addition, it is worth mentioning that another open question is: are the receptor trafficking mechanisms the same in tumors and in normal tissues?

1.2.2. Somatostatin receptor subtype expression in normal tissues

Receptor binding studies, mRNA determination, and/or receptor immunohistochemistry have been used to identify somatostatin receptors in human brain [31], as well as in numerous peripheral tissues, including pituitary, pancreas, gut, thyroid,

adrenal, kidney and the immune system; a complex pattern of somatostatin receptor subtype expression has been observed, including co-expression of multiple subtypes in a tissue-specific pattern [32, 33, 34]. The most frequently expressed subtype is sst2A in pancreatic islets, in specific regions of the brain and in the peripheral nervous system, but also in the immune system, adrenals and kidneys. The precise localization of the other sstrs in human tissues is not yet fully established. Sstr3 and sstr5 have been identified in T lymphocytes. The human placenta as well as the fetal and adult lung display predominantly sstr4.

1.2.3. Somatostatin receptor subtype expression in human tumors

A very high incidence and often a high density of sstrs have been found in neuroendocrine tumors, in particular in pituitary adenomas, islet cell tumors, carcinoids, paragangliomas, pheochromocytomas, small cell lung cancers and medullary thyroid carcinomas (MTCs). Non-neuroendocrine tumors such as breast carcinomas, lymphomas, renal cell cancers, brain tumors, prostatic, ovarian, gastric, hepatocellular and nasopharyngeal carcinomas were also shown to express sstrs (for a review see [38]). The majority of human sstr-positive tumors express simultaneously multiple sstr subtypes, although there is a considerable variation in sstr subtype expression between the different tumor types and among tumors of the same type. Parts of these differences are also due to the method used to investigate the somatostatin receptor subtype occurrence.

There are several methods for the *in vitro* evaluation of peptide receptor expression, the techniques employed being dependent on what it is analyzed: either the receptor protein or the receptor mRNA expression. Because it is the receptor protein that is ultimately targeted *in vivo*, it should also be the protein that is investigated *in vitro*, rather than the receptor mRNA. In addition, there is variation in the methods used to identify the mRNA (in situ hybridization, Northern blots, RNase protection assays, RT-PCR and real-time PCR) or the protein expression (receptor autoradiography, *in vitro* binding assays, immunohistochemistry). Each method has its own advantages and drawbacks, e.*g*. the techniques used for mRNA detection are highly sensitive, but potentially without morphological correlates; while the receptor autoradiography localizes, identifies the receptor protein through its binding site and quantifies the receptor, but it has limited cellular resolution and not always specific receptor antibodies are available for each of the peptide receptor subtypes under investigation. Combination of these methods could give more reliable results, than the use of one technique alone.

Most of the data available up to now on sstrs expression in human tumors originates from mRNA detection, but more recently several groups provided information on sstr subtype protein expression [35, 36, 37]. Frequently, there are disagreements between the outcomes from different authors, depending on the method of analysis employed. Nevertheless, there are some distinct conclusions:

- all the studies conclude that sstr2 is the most frequently expressed in a majority of cancers;
- there is a considerable heterogeneity in the expression of individual sstr within and between different tumors;
- sstr1, 2, 3 and 5 are often found in GEP tumors [38], MTCs [39] and in epithelial ovarian cancers [40];
- sstr3 is predominantly expressed in inactive pituitary adenomas and in thymomas [35, 41, 42];
- high incidence of sstr1, 2 and 3 has been revealed in human cervical and endometrial cancers [43];
- GH-secreting pituitary adenomas express sstr2 and 5 [35, 44];
- sstr2, 3 and 5 were detected in human lung tumors [45].

The predominant expression of sstr2 in human tumorous tissues forms the basis for the successful clinical application of radiolabeled octapeptide SS-analogs in imaging of sstr-positive tumors (see section 1.6.). It is important to mention also that in a significant number of tumors sstr2 is absent or expressed in low density, therefore, knowledge of the sstr subtype expression patterns in human tumors it is very important for the development of the concept of sstr-targeted radiotherapy (or chemotherapy).

1.3. Somatostatin analogs

As specified in section 1.1., SRIF has a short half-life *in vivo*, hence preventing its application in the clinic. As a consequence, it has been a long-standing objective of pharmacological studies to develop synthetic analogs selective for all sstr or for subsets of them.

1.3.1. Strategies for targeting GPCRs

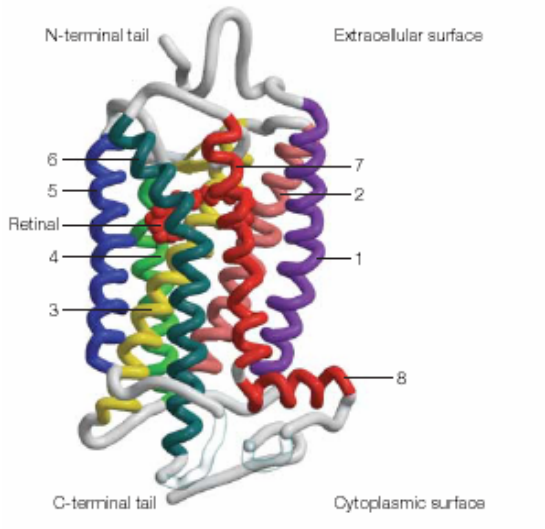

Figure 3. *The crystal structure of rhodopsin. The protein folds into seven transmembrane helices (labeled 1 through 7) and a short helix (8) that runs across the cytoplasmatic surface of the membrane. The crystal structure was obtained in the presence of the retinal chromophore (the red spheres). [46]*

GPCRs represent by far the largest class of targets for modern drugs. The natural ligands of this superfamily of seven transmembrane receptors (7TM) are extremely diverse, comprising peptide and protein hormones, biogenic amines, nucleosides and nucleotides, lipids and eicosanoids and others (such as glutamate, Ca^{2+} ions, etc). Despite this ''popularity'', there is still limited structural data available on GPCRs. The only resolved crystal structure of a heptahelical receptor up to date is the one of bovine rhodopsin [46] (Fig.3).

Incontestably, this crystal structure provides significant insights concerning structure/activity relationships in visual pigments and related GPCRs. Nevertheless, the rhodopsin structure represents the inactive state of the receptor. Moreover, although GPCRs share a common membrane topology, they are remarkably diverse in sequence and vary especially in size of the extracellular amino-terminal tails, cytoplasmatic loops and carboxy-terminal tails. These structural differences are the basis of their classification into three major families: A (rhodopsin-like), B (glucagon-receptor-like) and C (GABA-receptor-like). Therefore, it is unlikely that existing GPCR models, either based on rhodopsin or designed *ab initio*, will be sufficient to be used for *in silico* screening of compound libraries.

Consequently, the design of ligands for this receptor family still heavily relies on **ligand-based drug design** techniques. For many GPCRs the natural ligand can provide a good starting point in the lead finding process. Structure-activity relationships (SAR) can be directly derived from the natural ligand and its analogs. The resulting pharmacophore models can then be employed for virtual screening to identify lead structures with novel scaffolds.

This is the case also for the somatostatin receptor subtypes, as part of the GPCR superfamily. All the analogs synthesized world-wide over the years, either via the ''classical'' approach (progressive shortening of the peptide from N- and C-terminus; Ala-scans; D-amino

acid scans; cyclization, etc.) or using the ‘’modern’’ combinatorial chemistry and molecular modeling, were based on SS-14. As there is a vast number of SRIF analogs and this dissertation does not claim to be an exhaustive study on this matter, I will point out only the ‘’milestones’’ in the development of SS-derivatives, emphasizing on the analogs relevant for nuclear medicine. For simplification I will classify these compounds as shown in scheme 1.

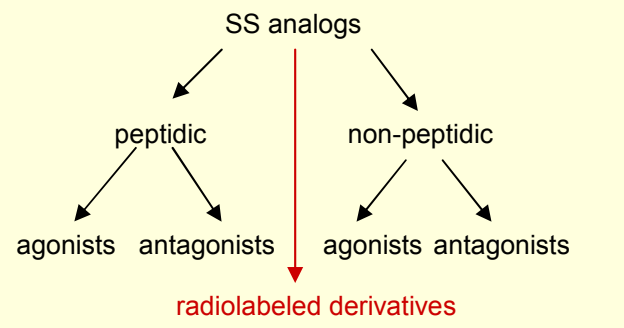

Scheme 1. *Informal classification of SRIF-analogs.*

1.3.2. Peptide analogs of somatostatin

A) AGONISTS

Initial work in the development of somatostatin analogs was carried out by the Salk group [47]. They synthesized several series of somatostatin-related peptides, employing different approaches like:

- systematic deletion of single residues;
- Ala-scans;
- D-amino acid scans;
- deletion and/or modification of multiple residues.

In these series, [D-Trp^{8}]SRIF was the first analog reported to have significantly higher potency than somatostatin (on the inhibition of GH *in vitro* and glucagon and insulin *in vivo*). The Ala-scans revealed that the fragment to be the essential pharmacophore of SS is Phe^{7}-D-Trp^{8}-Lys^{9}-Thr^{10} [47]. Based on these results, Veber *et al*. [48] synthesized a series of reduced-size somatostatin analogs, the most interesting being L-363,301 (structure **1** in Figure 4). This molecule showed higher biological activity than the native SRIF in inhibiting the release of GH, insulin and glucagon. From NMR studies Freidinger *et al*. [49] proposed a type II’ β-turn about the tetrapeptide sequence Phe^{7}-D-Trp^{8}-Lys^{9}-Thr^{10} (the numbering in the sequence refers to the position of the residue in SS-14), which they considered to be the biologically active portion interacting with the receptor.

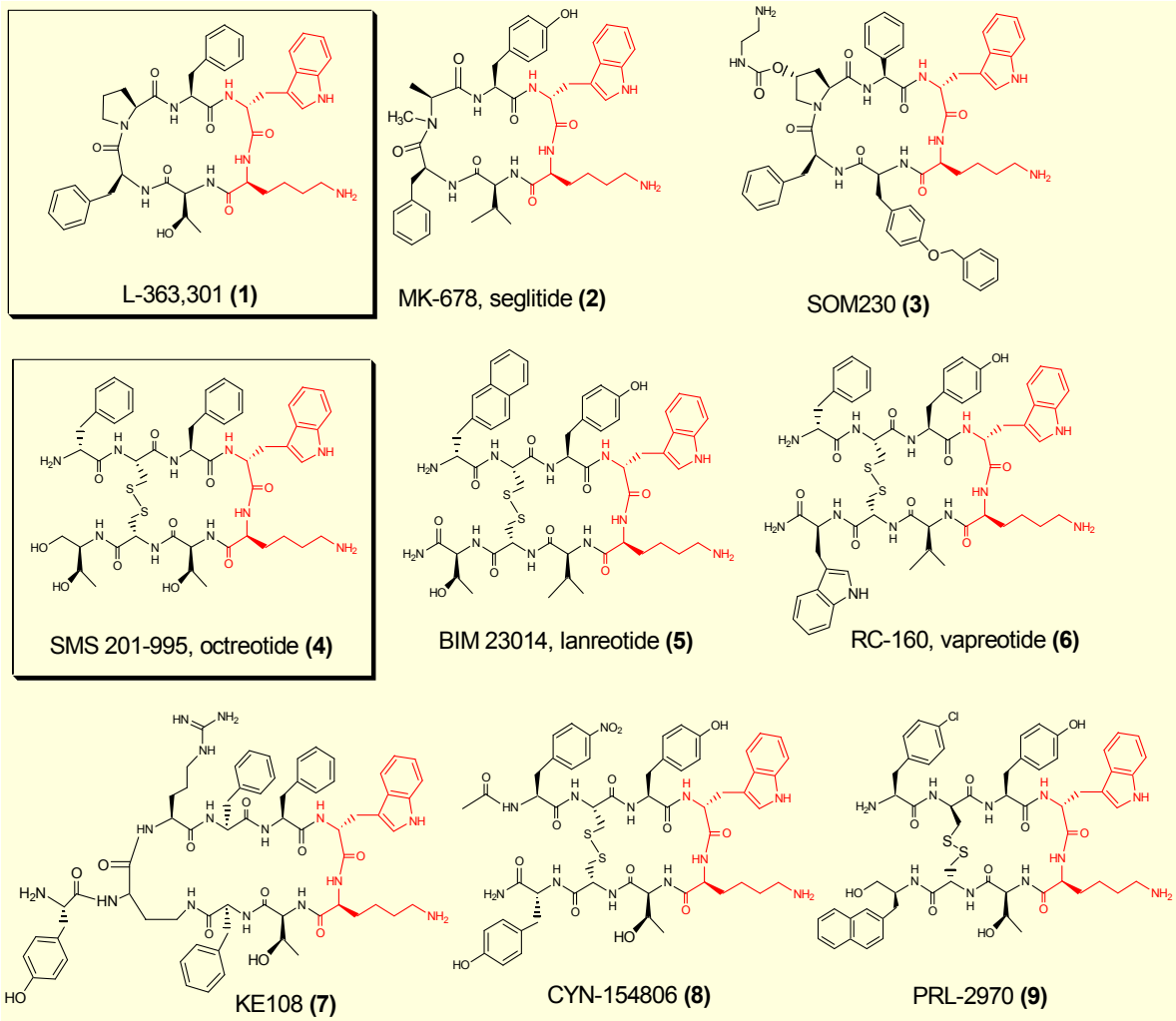

Figure 4. *Structures of selected peptidic somatostatin analogs.*

Further modifications of (**1**) resulted in the synthesis of MK-678 (structure **2**, Fig. 4), which showed at least 10-fold greater potency than the parent compound in all biological tests [50].

Starting from Vale's research on truncated somatostatin analogs [47], Bauer *et al.* [51] synthesized octreotide (SMS 201-995, Sandostatine®) (structure **4**, Fig. 4), a cyclooctapeptide derivative of SRIF. This analog is protected against enzymatic degradation by the presence of D-Phe residue at the N-terminus and by the amino alcohol Thr-ol at the C-terminus. The bridging unit Cys^2-Cys^7 provides as well enhanced metabolic stability. Octreotide was characterized by greater potency than the native SS-14, longer duration of action (half-life ≈ 117 min) and higher selectivity in GH inhibition compared with insulin and glucagon [52].

Incontestably, it can be stated that the hexapeptide L-363,301 and the octapeptide octreotide represent the ''milestones'' in the development of clinically useful SRIF-

derivatives. These analogs were, and still are, subjected to numerous modifications in the search for even more potent agonists. Thus, in the octapeptide series, lanreotide (**5**) [53] and vapreotide (**6**) [54] were developed (Fig. 4). To further investigate the structural role played by the Pro^{1}-Phe^{6} sequence in the hexapeptide L-363,301 (**1**) several conformational studies have been made by Goodman and coworkers [55, 56, 57]. It turned out that this sequence is needed to maintain the proper orientation of the biologically important side-chains, stabilizing the β II' turn.

Following the cloning of SS receptor subtypes in the early 90s [58], the quest for new SRIF analogs reached a new dimension - the receptor subtype affinity profile. Investigations of the binding affinities for the five sstr subtypes revealed that (**1**), (**2**), (**4**), (**5**) and (**6**) are very potent on sstr2, moderate on sstr3 and 5 and have no affinities for sstr1 and 4 [59, 60]. However, the situation has recently changed with the discovery of the new cyclohexapeptide SOM230 (**3**) (Fig. 4) [61] which has affinity for sstr1, 2, 3 and 5. In a novel approach for generating a universal analog, in our group a nonapeptide scaffold was used as the basis for the agonist KE108 (**7**) (Figure 4), which binds with nanomolar affinity to all sstr1-5 [62].

Although most likely of moderate clinical relevance, but very important for the study of somatostatin receptor subtypes is the research on subtype selective SS-analogs [63, 64, 65].

B) ANTAGONISTS

For elucidating the many physiological functions of SRIF, but also for the possible clinical interest (*e.g.*, the stimulation of GH levels in elderly patients), the research of somatostatin receptor antagonists continues to be noteworthy. The first reported competitive peptide antagonist of SRIF was CYN-154806 (**8**) (Fig. 4) [66]. From a weak octapeptide agonist with sstr2 affinity, the authors described the conversion to an antagonist by the inversion of chirality at positions 5 and 6. Coy and co-workers further explored the effect of this putative L^{5}, D^{6} motif on various series of SRIF antagonists. The most potent antagonist found to date is PRL-2970 (**9**) (Fig. 4), binding to sstr2 [67].

1.3.3. Non-peptidic analogs of somatostatin

Selective non-peptide SS agonists and antagonists can provide complementary information on the role of each receptor subtype. Moreover, they can improve the poor oral bioavailability of peptide analogs. Mix-and-split combinatorial library synthesis followed by iterative deconvolution enabled the identification of a complete set of non-peptide agonists

with pronounced selectivity and affinity for each sstr subtype [68]. Pioneering work on monosaccharides as scaffolds led to SRIF mimics with a new non-peptide backbone [69].

*

* *

From all the mentioned analogs of somatostatin, only three of them are approved for clinical use: octreotide (**4**), lanreotide (**5**) and vapreotide (**6**). Giving the broad antisecretory action of the natural SRIF, the therapeutical potential of SS-analogs is very large: neuroendocrine tumors of the gastrointestinal tract, pituitary tumors, prevention and treatment of pancreatic surgery complications, malignant bowel obstruction, acromegaly [70, 71, 72]. The main limitation of the therapeutic effectiveness of the above-mentioned SS-analogs is their selectivity for particular sstr subtypes (see Table 1). That is why the new universal binders like KE108 or the multi-sstr binder SOM230 are very promising drugs. The latter is already in early clinical trials. Nevertheless, giving the recent findings on sstr homo- and heterodimerization (pointing to the possibility that SS can trigger signalling events normally controlled by other receptor systems and vice versa), at present it is still difficult to predict which properties will be most relevant for the therapeutic potential of new SRIF analogs.

Table 1. *Binding affinities (K_i, nM) to hsstr of clinically used SS-analogs [73].*

Compound	*hsstr1*	*hsstr2*	*hsstr3*	*hsstr4*	*hsstr5*
SS-14	1.1	1.3	1.6	0.53	0.9
SS-28	2.2	4.1	6.1	1.1	0.07
Octreotide	> 1000	2.1	4.4	> 1000	5.6
Lanreotide	> 1000	1.8	43	66	0.62
Vapreotide	> 1000	5.4	31	45	0.7

1.3.4. Radiolabeled SRIF analogs

The clinical implications based on the presence of somatostatin receptors in human tumors involve not only long-term therapy with non-cytotoxic SS-analogs as presented above, but also tumor diagnosis and therapy with radioactive analogs.

There are two techniques for diagnosis using radionuclides in nuclear medicine: γ-scintigraphy and positron emission tomography (PET). The first method requires a radiopharmaceutical containing a radionuclide that emits γ radiation with energy between 100-250 keV and a γ camera or a SPECT camera. PET necessitates a radiopharmaceutical

labeled with a positron (β^+) emitting radionuclide and a PET camera. For more details on this type of radionuclides please see **paper I**.

The first ever used radiolabeled peptide for γ-scintigraphy was [^{123}I-Tyr^3]-octreotide (Figure 1c [paper I]) [74]. Being too lipophilic, hence having increased hepatobiliary excretion, this radiopharmaceutical did not prove to be the best diagnostic tool, especially for the abdominal area. Linking the chelator DTPA to octreotide and thus allowing complexation with ^{111}In, improved the biodistribution profile very much, with a shift from a gastrointestinal excretion pathway to a predominant renal excretion. This conjugate ^{111}In-DTPA-octreotide (Figure 1d [paper I]) became the first commercialized imaging vector based on a radiopeptide (Octreoscan®, ^{111}In-pentetreotide, Mallinckrodt Med., St. Louis, MO, USA).

Because of the very favorable properties of ^{99m}Tc including low-cost production, on-demand availability, short half-life (6h) (see **paper I** for further reading), various attempts to develop efficacious ^{99m}Tc-labeled somatostatin analogs have been published. Two successful conjugates are ^{99m}Tc-HYNIC-[Tyr^3]-octreotide (HYNIC-TOC) [75] and ^{99m}Tc-N_4-[Tyr^3]-octreotide [76] (Figure 6 [paper I]). In the clinic these derivatives showed good results when compared with Octreoscan [77].

Several strategies have been studied to develop SS analogs-based tracers for PET. Wester *et al* successfully labeled octreotide with ^{18}F [78], but despite specific accumulation in the tumor, this radioligand was of limited clinical application, because of the fast tumor washout, high liver uptake and hence insufficient visualization of abdominal tumors. Very recently the same group reported the preclinical data on a pharmacokinetically improved ^{18}F-octreotide derivative [79]. Also various ^{64}Cu-labeled SS-analogs were synthesized, showing favorable biodistribution in animal models [80] and good performance for PET imaging in patients [81]; however, the use of ^{64}Cu relies on the availability of a cyclotron.

A major advance was however the introduction of the macrocyclic chelator DOTA (1,4,7,10-tetraazacyclododecane-1,4,7,10-tetraacetic acid) (Figure 2 [paper I]). It forms kinetically and thermodynamically stable metal complexes even if one carboxymethyl group is used for coupling. The radiometal is encapsulated and 'embedded' inside the macrocyclic cage [82] which protects it from the attack of competing ligands present in human tissue and body fluids. It is the chelator of choice for the stable complexation of lanthanides or lanthanide-like radionuclides like $^{90/86}$Y, ^{177}Lu, ^{111}In and of $^{66/67/68}$Ga. The use of ^{68}Ga-DOTA conjugated to the somatostatin analog [Tyr^3]-octreotide (^{68}Ga-DOTATOC) in PET is a success story, offering excellent imaging properties and a very high tumor-to-background ratio [83]. This was previously shown in preclinical studies [84]. A logical consequence of

peptide receptor mediated scintigraphy was peptide receptor mediated radionuclide therapy (PRRT). Still, there are certain prerequisites for an efficient PRRT: the number of receptors in the treated tumors needs to be high, the radiopeptide should internalize in the targeted tissue, the employed radionuclides should emit radiations that have a high linear energy transfer (LET) in order to destroy the tumor tissue and the whole metal-chelator-peptide complex should have suitable pharmacokinetics. There are three main categories of therapeutic radionuclides: β-emitters, α-emitters and Auger-electron emitters, each type of these particles having different range of energy deposition and LET properties (see **paper I**).

The most frequently used analog for radiotherapy is ^{90}Y-DOTA-[Tyr^3]-octreotide (^{90}Y-DOTATOC) [85, 86]. Main indications are metastatic neuroendocrine tumors, in particular endocrine pancreatic tumors and carcinoids, but it proved its efficacy also in other malignancies [87]. An overview of patient studies imaged and/or treated with DOTATOC labeled with various radionuclides in our clinic is given in **paper I**.

Recently, the Thr^8-version of DOTATOC was introduced in imaging and therapy – DOTA-TATE [88]. The 7-fold higher binding affinity of Y^{III}-DOTA-TATE on hsst2 compared with Y^{III}-DOTATOC (Table 2, [89]) and the very promising preclinical data of ^{177}Lu-DOTA-TATE [90] were not confirmed by Forrer *et al*. [91] in imaging and dosimetric comparison studies between ^{111}In-DOTATOC and ^{111}In-DOTA-TATE. Their analysis showed no significant difference between the two radiopeptides. Nevertheless, therapeutic studies on mice bearing sstr-positive tumors showed the efficacy of ^{177}Lu over ^{90}Y in small to medium tumors [90]. The reason is the difference in the β-energy emission: ^{90}Y is a pure high energy β-emitter with a maximum range in tissue of up to 12 mm, being more suitable for large tumors, while ^{177}Lu is a low energy β-emitter, more appropriate for medium to small neoplasia. Moreover, ^{177}Lu emits also γ radiation with energy suitable for scintigraphy and dosimetry. That is why recently more and more ^{90}Y is replaced by ^{177}Lu in therapy studies.

Chelator-derivatives of lanreotide and vapreotide have been developed as well. Y- and In- labeled DOTA-lanreotide (Mauritius, Figure 2c [paper I]) have been claimed to be universal binders to somatostatin receptors [92]. As seen in Table 2, Reubi *et al*. [89] could not confirm this assertion. The reported improvement of *in vivo* visualization using ^{111}In-DOTA-lanreotide as compared with Octreoscan in some cases [93] may be primarily due to the higher affinity of this compound for sstr5. ^{111}In- [94] and ^{188}Re-labeled [95] versions of vapreotide have been also reported, as alternative tracers.

Table 2. *Affinity profiles for human sstr1-5 of a series of somatostatin analogs (values are expressed as $IC_{50} \pm SEM$, in nM) [89].*

Compound	hsst 1	hsst 2	hsst 3	hsst 4	hsst 5
SS-28	5.2±0.3	2.7±0.3	7.7±0.9	5.6±0.4	4.0±0.3
In^{III}-DTPA-octreotide	> 10,000	22±3.6	182±13	> 1,000	237±52
Y^{III}-DOTA-OC	>10,000	20±2	27±8	>10,000	57±22
Y^{III}-DOTA-TOC	>10,000	11±1.7	389±135	>10,000	114±29
Y^{III}-DOTA-TATE	>10,000	1.6±0.4	>1,000	523±239	187±50
Y^{III}-DOTA-Lanreotide	>10,000	23±5	290±105	>10,000	16±3.4
Y^{III}-DOTA-Vapreotide	>10,000	12±2	102±25	778±225	20±2.3

Summarizing, the radioactive somatostatin analogs used for the *in vivo* visualization and treatment of human tumors are derivatives of octreotide, lanreotide and vapreotide, the three octapeptides already used in the clinic, described in the previous section. Comparing the data from the Tables 1 and 2, the influence of the additional chelate on the pharmacological profile of the peptides can be seen, with significant loss in binding affinity especially for sstr5, but also sstr3 and sstr2. Although the *in vivo* metabolism, excretion pathway and retention times of a molecule are important parameters for its evaluation as a new tracer for diagnosis or therapy, there is no doubt that the *in vitro* characterization of the receptor binding affinity of such a molecule is crucial information, particularly nowadays when several studies on the receptor expression pattern on tumors are available. Therefore, the conclusion from the information presented here is that the efficacy of the currently used radiolabeled somatostatin analogs derives mainly from their moderate to high affinity for sstr2, the receptor with the widest distribution among the sstr family. The improved sstr5-profile of metal-complexed-DOTA-lanreotide and –vapreotide is an advantage for visualization of tumors such as pituitary adenomas [41] and colorectal cancers [96] known to express sstr5. Nevertheless, they are still far from being optimal candidates.

Having complex structures, in which every component influences the biological efficacy *in vivo* (see also **paper I**), it is still a challenge to find the best **metal-chelator-SS analog** structure with not only suitable pharmacological properties, but also with optimal pharmacokinetics and pharmacodynamics.

The only real valuable thing is intuition.
Albert Einstein

2. HYPOTHESES - AIMS – RATIONALE

2.1. Improved pharmacological profile for radiolabeled somatostatin-based derivatives

The unique pharmacological effects of SRIF-14 derive probably from its universal high-affinity binding to all somatostatin receptor subtypes [8]. As shown in section *1.3.4*., the somatostatin derivatives used currently for the visualization and targeted radiotherapy of cancers have high affinity only for sstr2 and some moderate affinity for sstr3 and sstr5 (Table 2, section *1.3.4*.). Although sstr2 is overexpressed in a majority of neuroendocrine tumors, there are still a significant number of malignancies where this subtype is absent or expressed in low density; moreover, in most of the sstr-positive cancers the somatostatin receptor subtypes are co-expressed (see paragraph *1.2.3.*).

Therefore, targeting with high affinity subsets or all sstr subtypes simultaneously, would imply not only aiming to identify and treat a wider range of tumors, but also increase the amount of radioactivity brought to the malignant cells.

In paragraph *1.3.1*. I pointed out the obstacles in designing effective somatostatin analogs based on the receptor structure. The ligand based design is the only applicable approach and SS-14 served as model for all the analogs synthesized over the years. Two lead compounds emerged from this research, the hexapeptide L-363,301 and the octapeptide octreotide (Sandostatin®, SMS 201-995) (Figure 4, section *1.3.2.*). While no successful radiopharmaceuticals were developed based on Veber's hexapeptide (except for P829 [154], a peptide conjugate designed for ^{99m}Tc labeling and having moderate success in clinic), all the radiolabeled somatostatin based compounds used in clinical applications are derivates of octreotide (see paragraph *1.3.4.*).

This is one of the reasons for the extensive structural studies including NMR [97, 98], CD [99] and X-ray analysis [100] performed on this octapeptide. These studies showed SMS 201-995 to adopt, like the endogenous peptide, a type II or type II' β-turn conformation around Phe^3-D-Trp^4-Lys^5-Thr^6. Constituting the pharmacophoric unit, modifications on this

sequence can have profound consequences on the biological properties. That is why all the peptide analogs of SRIF conserved the center of this β-turn, D-Trp^4-Lys^5, in their structures (see Figure 4, section *1.3.2.*). Nevertheless, referring to the four major radiolabeled SS-analogs used in clinic, two main modifications have been done for the two side amino acids of this β-turn. Thus, Phe^3 has been replaced with Tyr (in lanreotide, vapreotide and [Tyr^3]-octreotide) and Thr^6 was substituted with Val (in lanreotide and vapreotide). Because lanreotide and vapreotide have modifications also at the N- and, respectively, at the C-terminus compared with octreotide, the alterations in the binding affinity profiles (Table 2, paragraph *1.3.4.*) can not be exclusively attributed to the two amino acids in the 3rd and 6th positions, respectively.

However, it has to be said that, in general, cyclic octapeptides in the octreotide series have high affinity to sstr2 and no affinity for sstr1 and sstr4. Modifications to these analogs can have tremendous effects on their residual affinity for sstr3 and sstr5.

Thus, taking a closer look to the binding profile of Y^{III}-DOTA-OC and Y^{III}-DOTA-TOC in Table 2, one can see the consequences of substituting Phe^3 for Tyr^3: a gain in affinity to sstr2, but a significant loss to sstr3 and sstr5.

Compiling the involvement of the 3rd position amino acid of octreotide in the β-turn (Figure 5) with the observations on the affinities to somatostatin receptors of Y^{III}-DOTA-OC and Y^{III}-DOTA-TOC, two conjugates differing only in the 3rd peptidic amino acid, one can readily see a new strategy for lead optimization. Exchanging the aminoacid in the 3rd position of octreotide with different other aromatic and bulky side-chain residues, modulation of the pharmacological properties of octreotide-type derivatives could be acquired.

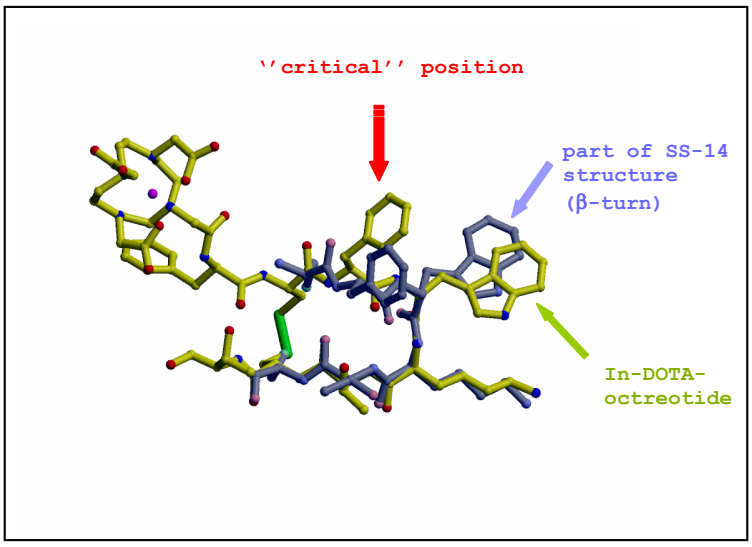

Figure 5. *Scheme illustrating the importance of the 3rd aa position in octreotide due to its involvement in the β-turn essential for pharmacological activity.*

2.2. Modification of pharmacokinetics/pharmacodynamics of radiolabeled somatostatin-based analogs

Despite good pharmacological profiles many drugs fail the clinical trials because of inadequate pharmacokinetics and pharmacodynamics. Pharmacokinetics (PK) is the study of the time course of a drug within the body and incorporates the processes of absorption, distribution, metabolism and excretion (ADME). Pharmacodynamics (PD) can be defined as the study of the mechanisms of drug action, including the relationship between drug concentration at the site of action and the drug effect. In simple terms, pharmacokinetics is the study of what the body does to a drug and pharmacodynamics is the study of what a drug does to the body. Therefore, the effectiveness of a drug is a very complex notion, involving several *in vitro* and *in vivo* parameters and the best estimation should be a measure of the ultimate goal: the benefit to the patient. Although this is conceptually sound and logical, in practice the leap between the experimental development of a drug and the ultimate benefit to the patient can be extremely large.

These rules apply to the radiopharmaceuticals as well. A perfect example is the first radiopeptide used for *in vivo* localization of tumors: ^{123}I-[3-iodo-Tyr^3]-octreotide. Despite some spectacular early imaging results [101] and an almost optimal pharmacologic profile showing high sstr2 affinity (IC_{50} = 2.0 ± 0.7 nM) and a high rate of internalization in tumor cells, this radioligand finally turned out not to be useful as a diagnostic tool. The reasons are its lipophilicity causing hepatobiliary excretion and therefore a very low diagnostic sensitivity in the abdomen. Contrary, the chelator-modified molecule, DTPA-octreotide, designed to be complexed with $^{111}In^{3+}$, shows a rather low *in vitro* pharmacologic profile (low binding affinity, IC_{50} = 22 ± 3.6 nM, and slow internalization rate), but the hydrophilic metal complex conveys high hydrophilicity to the targeting molecule and changes its pharmacokinetics, including predominant kidney excretion. Consequently, it became the first imaging vector based on a radiopeptide (Octreoscan®), registered worldwide.

2.2.1. Modulation of hydrophilicity/ lipophilicity

Clearance of a drug normally occurs through the liver and kidneys and it is an important assumption that only free (*i. e*. not protein bound) drug is available for clearance. One of the decisive parameters is lipophilicity. This is the key physicochemical factor linking membrane permeability – and hence drug absorption and distribution - with the route of clearance (metabolic or renal). For radiopharmaceuticals the excretion pathways are of crucial

importance for early and high tumor/background ratios and thus signal intensity in diagnostic by SPECT or PET and low toxicity for therapy. As pointed out above, the *in vitro* or the *in vivo* studies in animals can not always predict the drug ''performance'' in humans.

In addition to the above presented approach, also other strategies have been employed in order to reduce the metabolic clearance of radioiodinated somatostatin analogs. Thus, Schottelius *et al*. [102] reported improved pharmacokinetics, translated by reduced hepatic uptake and biliary excretion, clearance through the kidney and increased tumor-to-nontumor ratios, for carbohydrated derivatives of ^{125}I-[Tyr^3]-octreotide. Wester *et al.* [103] applied the same method of carbohydration for ^{125}I-[Tyr^3, Thr^8]-octreotide], obtaining also improved biokinetics. Lin *et al.* [104] synthesized very recently a ^{99m}Tc-bombesin analog derivative with low abdominal accumulation due to the introduction of DTPA at the N-terminus of the peptide.

DOTA-somatostatin based radiopharmaceuticals are generally hydrophilic compounds (log P < 0) with a predominant renal clearance. Nevertheless, log P calculation can only be a first estimate of the lipophilicity of a compound in a biological environment. Small differences in the partition coefficient values could be translated into considerable biodistribution modifications in humans, particularly in the case of radiopharmaceuticals, due the sensitivity of the technique.

Some of the modifications we performed on the octreotide sequence (paragraph *2.1*.) introduced increased lipophilicity to the whole metal-DOTA-peptide conjugate. Although preclinical *in vivo* biodistribution studies in rats showed very positive and promising results, with predominant kidney clearance, very low liver uptake and high tumor/background ratios, in patients the pharmacokinetics are different. Despite the improved diagnostic potential, due to the superior pharmacological profile, the ^{111}In- or ^{90}Y-labeled DOTA-octreotide derivatives in question exhibit increased metabolic clearance, with gall bladder accumulation. The same conjugates labeled with ^{68}Ga do not show the high abdominal uptake anymore. Assuming that this outcome correlates with the coordination chemistry difference between Ga^{3+} and In^{3+} or Y^{3+} [82], the hexacoordination of the Ga^{III}-complex versus the octacoordinate complexes of In^{III} and Y^{III} implying the presence versus the absence of a free carboxymethyl arm bound to the peptide, new strategies to decrease the lipophilicity of such conjugates can be designed.

These results prompted us to test the influence of different hydrophilic spacers between the chelator DOTA and the peptide, hoping in improved pharmacokinetics without loss of pharmacological performance.

2.2.2. Lowering the kidney radioactivity levels

The kidney is the dose-limiting organ in peptide receptor mediated radionuclide therapy. While favoring the renal clearance route, nephrotoxicity can be one of the consequences, particularly in the case of radiotherapy with strong β-emitters like ^{90}Y [105]. Boerman *et al*. plastically compared the dilemmatic situation of hitting the tumor while saving the kidney with ‘’sailing between Scylla and Charybdis’’, the two ancient sea monsters [106].

Although the mechanistic details involved in the renal radiobiological response remain unclear, it is established that during the excretion process these radioligands are filtered through the glomerular barrier and to a small part reabsorbed at the proximal tubular cells (PTC) [105]. Very recently, Barone *et al.* proved that two endocytotic pathways are contributing to the reabsorption of radiolabeled somatostatin analogs by PTC: receptor-mediated endocytosis via megalin/cubilin interaction and fluid-phase endocytosis [107]. The same group [108] underlined in another study the necessity of obtaining individual dosimetry measurement, because other factors like preexisting hypertension, diabetes or previous chemotherapy, may accelerate renal function loss induced by radiation.

Nevertheless, several strategies to reduce the renal-absorbed dose have been developed over the years. Among them, the coinfusion of basic amino acids [109] is a methodology followed frequently in PRRT protocols. However, the complete reduction of the kidney uptake is not attained using this method and several more or less severe side-effects are associated with this treatment [110]. Other strategies concern structural modifications of the radiolabeled compounds. Thus, the approaches for radiolabeled peptide conjugates involve mainly the lipophilicity alteration, as reviewed in the precedent section. Therefore, also our and others [111] hypothesis of addition of a cleavable linker possessing good plasma stability could accelerate the generation of radiometabolites and their renal elimination rate, without impairing the tumor uptake is to be considered.

Another hypothesis of ours is based on previous work reported by Arano *et al.* [112, 113]. They showed that the radiochemical design of radiolabeled antibody fragments that liberate radiometabolites of urinary excretion from antibody fragments by the action of brush border enzymes may constitute a new strategy for reducing the renal radioactivity levels. They used a hippuric acid radiolabeled derivative conjugated to the antibody, since para-amino-hippuric acid (PAH) is recognized by the organic anion transporter (OAT) system of the kidneys. That is why we assumed that the introduction of a PAH moiety in different

positions in the radiometal-DOTA-peptide conjugates derivatives of somatostatin could have the same effect on the renal uptake.

2.2.3. Targeting the cell nucleus

In paragraph *1.2.1.* I resumed the complexity of sstr cell trafficking after agonist activation. Like for all the other GPCRs still much research is needed to completely clarify the route followed by both receptor and ligand, once inside the cell. What makes PRRT a feasible approach is the ability of sstr to undergo agonist-induced internalization, allowing radioactivity accumulation in the tumor cells. This accumulation depends on several factors like: sstr subtype, agonist pharmacological profile, agonist exposure time, agonist concentration etc., but also sstr-expressing cell type and cell-specific regulatory functions. No irrefutable evidence has been brought up to now, proving a privileged route of the ligand toward nucleus after internalization.

What would be the advantages of nuclear localization of a radiolabeled ligand? First, it would mean longer retention time and secondly, higher accumulation in the cell. Clinically, these effects could signify lower radioactivity dose administered to the patient and a real possibility of using Auger-electron* emitters as therapeutic radionuclides. Most of the therapeutic radionuclides used at present are β-emitters, like ^{90}Y or ^{177}Lu, having high or intermediate energy, therefore being suitable for large or medium tumors, their cytotoxic effectiveness being due to the cross-fire effect (see **paper I** for details on β-emitter radionuclides). This is clinically significant, because it means that metastatic small cell clusters cannot be efficiently killed using β-emitters. In very small lesions PRRT with Auger-electron emitting radiopharmaceuticals may be the best choice. This type of radionuclides offer the advantages of a *short effect range* (several nanometers) and *high toxicity*, thus fulfilling two major requirements for the idealized targeted therapy (the other two being *specificity* and *universality*, in agreement with Ehrlich's theory of ''magic bullet''). Approximately half of the known radionuclides emit Auger electrons. This means that, in principle, there is a choice of which radionuclide to use in a particular therapeutic context. Table 3 lists some of the Auger-emitting radionuclides together with their half-lives and

* Inner shell electron vacancies are created when radionuclides decay by electron capture (EC) and/or internal conversion (IC) processes; these are subsequently filled by electronic transitions from shells of higher energy. The differences in electron energy may be emitted as photons, but can also be transferred to other orbital electrons which are consequently released from the atom. Non-radiative transitions are classified into Auger, Coster-Kronig and super-Coster-Kronig processes, depending on the relationship between the electron shells involved. Generally, the electrons emitted as a consequence of these processes are referred to as **Auger electrons**. Auger electron energies can be between tens of KeV and several eV 114. O'Donoghue, J.A., and T. E. Wheldon, *Targeted radiotherapy using Auger electron emitters.* Phys. Med. Biol., **1996** *41*: 1973-1992..

Auger energy. Beside the Auger energy, the half-life of the radionuclide is extremely important, a too long or a too short one being unsuitable for targeted therapy.

The biological effects of Auger emitters are critically dependent on their subcellular localization [114]. Auger electron emitters decaying in the neighborhood of the DNA produce similar amounts of reactive chemical radical species as do α-emitters, which are regarded as the classical form of high linear energy transfer (LET) radiation [115]. Recently, the hypothesis that the radiotoxicity of Auger electrons is caused only by direct ionization of the DNA has been proved inaccurate. Apparently 90 % of Auger electrons toxicity is due mainly to indirect mechanisms [116, 117]. Nevertheless, a long enough time of retention in the targeted cells and intranuclear or in nucleus proximity location of the radioligand would ensure the success of this type of therapy [118]. This conclusion is confirmed by several therapeutic studies using internalizing antibodies labeled with Auger-electron emitting radionuclides [119], but also by preclinical and clinical studies with ^{111}In-DTPA-octreotide [120, 121].

***Table 3**. Characteristics of some Auger-emitting radionuclides [114]. The Auger yield is the mean number of Auger and Coster-Kronig electrons emitted per decay. The Auger energy is the average total kinetic energy of Auger and Coster-Kronig electrons emitted per decay.*

Radionuclide	Half-life	Auger yield	Auger energy (keV)
^{51}Cr	27.7 d	5.4	3.65
^{55}Fe	2.73 d	5.1	4.17
^{67}Ga	3.26 d	4.7	6.26
^{75}Se	120 d	7.4	5.74
^{99m}Tc	6.01 h	4.0	0.89
^{111}In	2.8 d	14.7	6.75
^{113m}In	1.66 h	4.3	2.04
^{115m}In	4.5 d	6.1	2.84
^{123}I	13.2 h	14.9	7.42
^{125}I	60.1 d	24.9	12.24
^{193m}Pt	4.33 d	26.4	10.35
^{195m}Pt	4.02 d	32.8	22.52
^{203}Pb	2.16 d	23.3	11.63

Therefore derivatives with a longer retention time in the cell and aiming at the nucleus would increase the potential of Auger-electron emitters in radiotherapy, but also improve other targeted therapy strategies. We assumed that a new functional unit for nucleus targeting and prolonged cell retention could be added to the DOTA-TOC conjugate - a standard in PRRT with radiolabeled somatostatin analogs [85]. For this we have chosen the ‘’classical’’ nuclear targeting signal (NLS) of the SV40 large T antigen, the heptapeptide PKKKRKV [122]. This sequence serves as a tag to proteins, indicating their destination to the cell nucleus and assisting in the transport through the nuclear membrane. To function properly, the NLS conjugates must be located in the cytoplasm, but they are not readily incorporated into cells [123]. Consequently, [Tyr^3]-octreotide should serve as a function of targeting the cell and internalization, the NLS sequence is supposed then to ‘’find its way’’ through cytoplasm to the nucleus and the ^{111}In- or ^{67}Ga-DOTA moiety ought to manifest afterward its cytotoxic effect. The success of such a ‘’trifunctional’’ derivative (Figure 7) would probably depend on its architecture, on the lack of hindrance between the three constitutive elements.

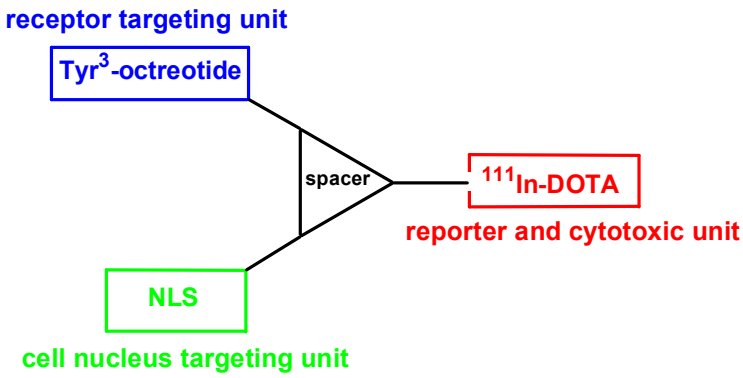

***Figure 7**. The principle of a double targeting with a trifunctional construct*

2.3. Understanding the post-endocytic pathway of somatostatin receptors

As underlined in paragraph *1.2.*, somatostatin receptors, as all the members of the GPCR superfamily, transduce the information provided upon agonist binding into intracellular second messengers that are interpreted as meaningful signals by the cell. GPCR activity represents a coordinated balance between molecular mechanisms governing receptor signaling, internalization, desensitization and resensitization [25, 124]. The processes of internalization and desensitization are adaptive mechanisms that prevent persistent receptor

stimulation from producing detrimental cellular effects. Internalization may also play a role in receptor resensitization. A critical first step in both GPCR internalization and desensitization is believed to be receptor phosphorylation by G-protein kinases and second messenger-activated kinases. Phosphorylated receptors then bind regulatory proteins called arrestins, which inhibit further signaling by blocking receptor- G protein interaction [124, 125].

Several studies have proved the phosphorylation of different sstr subtypes upon agonist activation [126, 127, 128]. Special attention has been given to sstr2 subtype [129, 130], because – due to its presence in a wide range of tumors- modulation of sstr2 receptor function is likely to have important therapeutic consequences and possibly may be exploited to improve sstr2 receptor-mediated radioligand internalization. Therefore, elucidation of early events, which occur after exposure to agonist as well as heterologous hormones, may provide new strategies to enhance the clinical utility of sstr2 receptor-targeted drugs.

Willing to contribute to this endeavor, we collaborated with the group of Dr. S. Schulz from the Department of Pharmacology and Toxicology at Otto-von-Guericke University in Magdeburg, Germany. Having a rich experience in the study of somatostatin receptors signaling and trafficking [131, 132], they intended to demonstrate that a certain amino acid sequence from the C-terminus of sstr2 is phosphorylated. For that they needed to develop an antibody against the specific amino acid phosphorylated sequence in the sstr2 carboxyl-terminus. Therefore, we planned to synthesize that 15 amino acid sequence having four phosphorylated threonine residues corresponding to the carboxylic terminus of sstr2A receptor, which could subsequently be used for antibody production.

If we knew what it was we were doing,
it would not be called research, would it?
Albert Einstein

3. SUMMARY OF RESULTS AND DISCUSSION

3.1. Synthesis and biological evaluation of new radiolabeled somatostatin analogs (papers II, III, IIIa, IV)

The heterogeneous expression of somatostatin receptor subtypes within and between different tumors (section *1.2.3.*) and the predominant sstr2 affinity of the somatostatin-based radioligands used in the clinic (section *1.3.4.*) prompted us to start a programme to design and synthesize radiopeptides with affinity to all sstr subtypes. The strategy in our laboratory was based on two methods:

a) progressive extension of the peptide cycle from octreotide to SS-14 [62];

b) modification of octreotide.

This second approach is discussed in the above mentioned papers attached to this thesis. Our premise, as described in paragraph *2.1.*, was that replacement of Phe^3 in octreotide with different aromatic side-chain amino acids may modulate the binding affinity to sstr3 and sstr5. As part of the β-turn, critical for preserving the binding to somatostatin receptors, subtle changes at this position may have profound effects on the pharmacological profile.

Thus, we synthesized a small library of DOTA-octreotide derivatives, substituting Phe^3 with a variety of aromatic residues, but also with some aliphatic amino acids for structure-activity relationship investigation reasons. In a second step we modified also the 8^{th} residue (from Thr-*ol* to Thr) for the two best compounds emerged from this library, DOTA-[1-Nal^3]-octreotide (DOTA-NOC) and DOTA-[$BzThi^3$]-octreotide (DOTA-BOC).

3.1.1. Preclinical data

A) Synthesis (papers II and IV)

The 24 derivatives (**1**-**24**, paper II) were synthesized by parallel solid phase synthesis using Fmoc/*t*Bu strategy on 2-chlorotritylchloride resin preloaded with Fmoc-Thr(*t*Bu)*ol*. The average yields after purification were 25-30 % based on the first Fmoc cleavage. The

structures of the synthesized conjugates are shown in Figure 1[paper II]. All the compounds were characterized by ESI-MS and RP-HPLC.

The two additionally Thr^{8}-modified derivatives (compounds **1** and **2**, paper IV) were synthesized on tritylchloride resin. Their structural formulae are displayed in Figure 1 [paper IV].

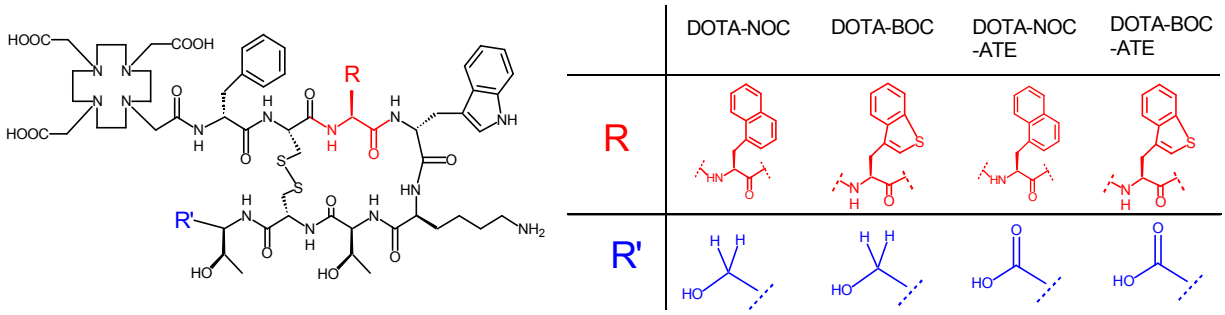

***Figure 8**. Structural formulae of the four best ligands in this series.*

B) Partition coefficient determination (paper II)

The log P values for all the ^{111}In/In^{III}-labeled conjugates **1-24** (Figure 2 [paper II]) were determined using the shake flask method. Giving the structural variety of the residues employed in the 3rd position we considered necessary to evaluate the influence of lipophilicity on the pharmacological profile.

C) Binding affinity profiles (papers II, III and IV)

Table 1 [paper IV], table 2 [paper III] and table 2 [paper IV] show the IC_{50} values of the metal-complexed versions of all synthesized derivatives in comparison with SS-28. The values were obtained by performing complete displacement experiments with the universal somatostatin radioligand [^{125}I][Leu^{8}, D-Trp^{22}, Tyr^{25}]-SS-28 on membranes from cells expressing the receptor subtypes. The broadest affinity spectra correspond to M^{III}-DOTA-NOC (compound **3** [paper II]), M^{III}-DOTA-BOC (compound **5** [paper II]), In^{III}-DOTA-NOC-ATE (compound **1** [paper IV]) and In^{III}-DOTA-BOC-ATE (compound **2** [paper IV]). These compounds confirmed our starting hypothesis: not only have they enhanced binding affinity to sstr3 and sstr5, but also superior sstr2 affinity in comparison to the starting conjugate M^{III}-DOTA-octreotide. The structural formulae of these four best conjugates are shown in Figure 8. The affinities to all sstr subtypes obtained for the other compounds of this series provide a useful structure-activity relationship tool, as discussed in paper II.

D) Internalization and externalization in vitro studies (papers II, III, IV)

In a first step we evaluated the internalization capacity for all the ^{111}In-labeled conjugates **1-24** after 4 h incubation at 37 ^{0}C in sstr2- (AR42J) and in sstr3-expressing cells (HEK-sstr3), respectively (Table 2 [paper II]). The ability to induce receptor internalization is important for the success of sstr-mediated targeted radiotherapy, therefore this first estimation was necessary to further select the best conjugates. Complete kinetics of the uptake in these cell-lines for ^{111}In-DOTA-NOC, -DOTA-NOC-ATE and –DOTA-BOC-ATE are shown in Figure 3 [paper III], Figure 2 [paper IV]. In all these internalization experiments the uptake is expressed as percentage of specifically internalized compound from the total amount of added radiopeptide.

Externalization studies were done in order to evaluate the retention of the radiopeptides in the cell, after internalization. The results are expressed as percentage retained in cell from the total amount internalized (Figure 3 [paper II], Figure 3 [paper IV]) or as percentage externalized from the total amount internalized (Figure 5 [paper III]). We found that the Thr^{8} modified conjugates have a higher externalization rate than the Thr(ol)^{8} derivatives in AR42J cells. Giving the complexity of intracellular trafficking, we do not know if this is due to the relatively higher affinity of these derivatives for sstr2, to the charge difference or to both other reasons. The metabolic stability does not seem to be the issue, since the γ-detector monitored HPLC of the externalized fractions of these radiopeptides shows them intact even after 24 h.

E) In vivo biodistribution studies (papers II, III, IV)

Animal experiments were performed in male Lewis rats bearing CA20948 or AR42J pancreatic tumors. Both types of tumor are sstr-positive, CA20948 tumor expressing several somatostatin receptor subtypes [133] and AR42J tumor functionally expressing only sstr2 [129]. The four best compounds from the *in vitro* studies were tested in biodistribution in animals in comparison with ^{111}In-DOTA-TOC (our internal standard). The results are shown in Figure 5 [paper II], Table 3 [paper III], Table 3 [paper IV] and Figure 4 [paper IV]. The uptake is expressed as percentage of the injected activity per gram tissue. The monitored aspects are not only the accumulation in sstr-positive tissues (including the tumor), but also the excretion pathways (liver and kidneys), the specificity (proved by the blocking studies with excess of non-radioactive peptide, also shown in the rat γ-scintigraphy in Figure 5 [paper IV]) and the tumor:kidney ratios.

COMMENTS

This study revealed four DOTA-peptide conjugates (Figure 8) with improved pharmacological profile if compared with the existent clinically used somatostatin based radiolabeled derivatives. These compounds can be labeled with γ- (^{111}In, ^{67}Ga), β^-- (^{90}Y, ^{177}Lu) or β^+-emitting radionuclides (^{68}Ga) and be used for imaging or therapy of sstr-expressing tumors (see the first preliminary clinical data in the next paragraph). The data of the small library from which these conjugates emerged may further contribute in developing computer programs for the *in silico* prediction of binding affinity for such derivatives. Nevertheless, auxiliary structural studies (CD, NMR, X-ray) are in progress to better understand these data. The broader affinity profile of the new conjugates may permit not only the targeting of a wider range of sstr-positive tumors, but also the increase of radiotoxicity to the malignant tissue, due to the co-expression of several somatostatin receptor subtypes.

3.1.2. Preliminary clinical data

A) DOTA-NOC (in collaboration with Hannover University Medical School and University Hospital Rotterdam)

The first derivative among the four best compounds emerged from this library to enter clinical trials was DOTA-NOC. A comparison between the PET imaging with ^{68}Ga-DOTA-NOC and γ-scintigraphy with ^{111}In-DOTA-TOC of a patient having multiple liver and bone metastases originating from a neuroendocrine tumor is given in **paper IIIa**. The scans not only show the high resolution of the PET technology, but also additional lesions which are visible only with ^{68}Ga-DOTA-NOC.

At the University Hospital Rotterdam DOTA-NOC labelled with different radionuclides was studied in several patients using also ^{111}In-Octreoscan for comparison. A first case is shown in Figure 9. After administration of ^{111}In-DOTA-NOC to a patient having papillary thyroid carcinoma with lung metastases, the scintiscans revealed high background, the tumor/background ratio being the same as with ^{111}In-Octreoscan.

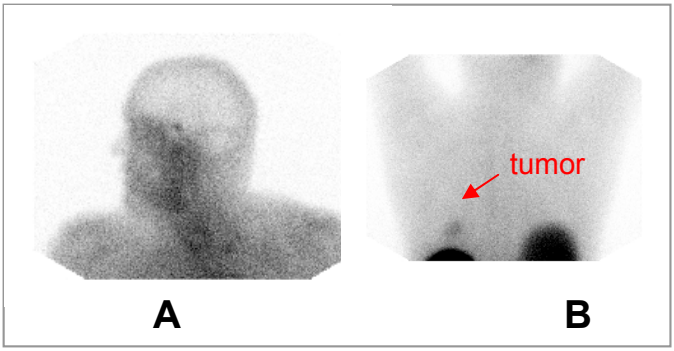

***Figure 9**. Gamma-scintigraphy of a patient with papillary thyroid carcinoma. **A**: high background in the thyroid region; **B**: faint visualization of lung lesions (previously confirmed by computer tomography).*

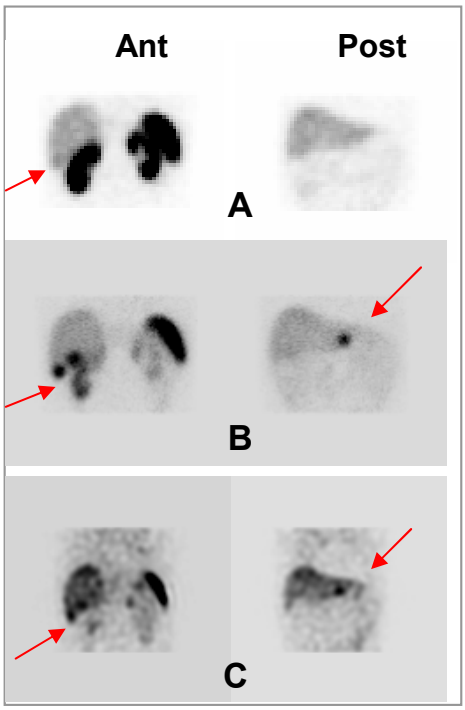

On the contrary, in another patient with follicular thyroid carcinoma both ^{111}In- and ^{68}Ga-labeled DOTA-NOC were superior imaging agents compared to ^{111}In-Octreoscan (Figure 10). The images were done one year after thyroidectomy, the patient having a raising tumor marker (thyroglobulin) and ^{131}I-negative lesions. The liver and lung metastases were confirmed by CT and ^{18}FDG-PET. The ^{111}In-Octreoscan scintigraphies (Fig. 10A) show high renal uptake and faint liver metastasis. The ^{111}In-DOTA-NOC images (Fig. 10B) reveal low kidney uptake and three clear liver metastases. The overall tumor:background ratio is enhanced in this case. The 90 min p.i. PET scans done with ^{68}Ga-DOTA-NOC (Fig. 10C) confirm the three liver lesions and the lower kidney uptake.

***Figure 10**. Imaging comparison between ^{111}In-Octreoscan (**A**), ^{111}In-DOTA-NOC (**B**) and ^{68}Ga-DOTA-NOC (**C**) in a patient with follicular thyroid carcinoma having multiple liver and lung metastases.*

These results prompted the clinicians to start therapy with DOTA-NOC labeled with the medium energy β- and γ-emitter ^{177}Lu for this patient. After three cycles of treatment at every two months interval only 18 % of the initial tumor mass is still visible (Figure 11). Moreover, the tumor marker (thyroglobulin) shows a significant decrease after ^{177}Lu-DOTA-NOC therapy (Figure 12). Although ^{177}Lu-DOTA-NOC had low renal uptake, the treatment has been done with concomitant basic amino acids infusion (Lys/Arg).

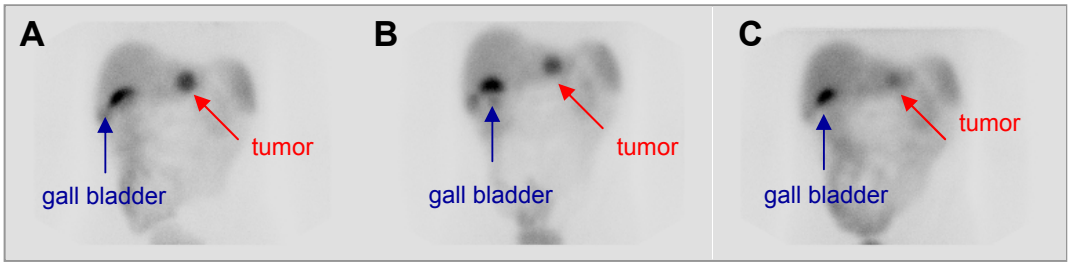

***Figure 11**. Scintigraphy of a patient with follicular thyroid carcinoma during treatment with ^{177}Lu-DOTA-NOC. (**A**): first cycle of therapy with 100 mCi (tumor size considered 100%); (**B**): 2nd cycle of therapy with 200 mCi, partial tumor remission (66% from initial size); (**C**) 3rd cycle of therapy with 200 mCi, enhanced tumor remission (18% of the initial size).*

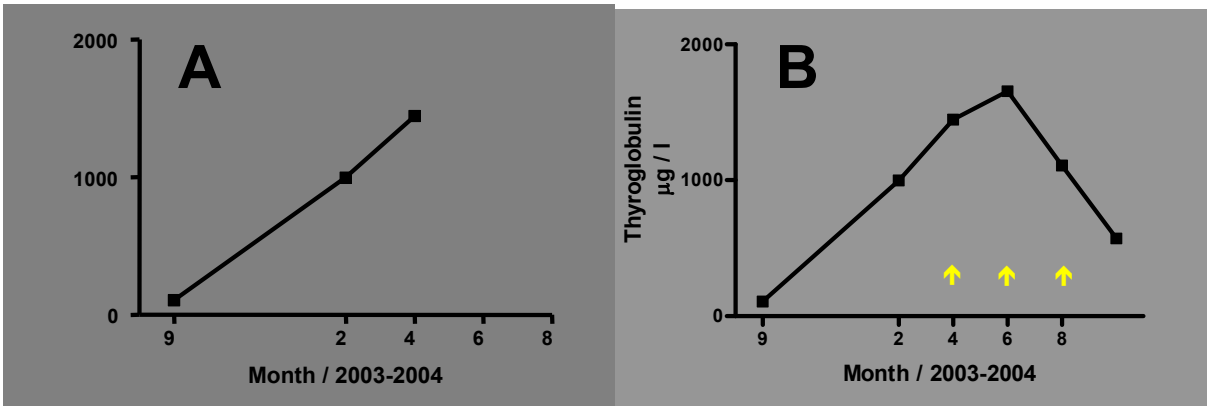

***Figure 12**. Schematic representation of the thyroglobulin marker level before the ^{177}Lu-DOTA-NOC therapy (**A**) and after the treatment (**B**). The yellow arrows indicate the therapy dates.*

These promising results confirmed our preclinical studies and encouraged further clinical trials in patients with neuroendocrine tumors concomitantly expressing several somatostatin receptor subtypes.

B) DOTA-NOC-ATE (IN OUR CLINIC)

At the end of 2004 several clinical trials started in our clinic using ^{177}Lu-DOTA-NOC-ATE as tracer. Up to now only patients with medullary thyroid carcinoma have been studied, a type of tumor known to express also other somatostatin receptor subtypes beside sstr2 [134]. Such a case is shown in Figure 13 of a patient previously negatively-scanned with ^{111}In-Octreoscan. Although the tumor visualization with ^{177}Lu-DOTA-NOC-ATE is faint, it proves that this tracer can be used for the imaging of other sstr subtypes than sstr2.

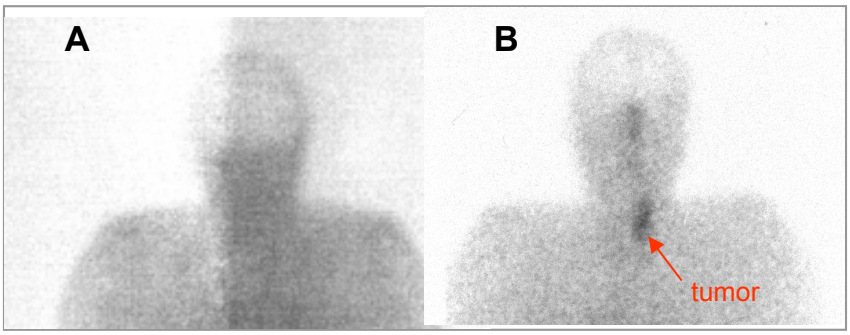

***Figure 13**. Scintiscans of a patient with medullary thyroid carcinoma: (**A**) with ^{111}In-Octreoscan; (**B**) with ^{177}Lu-DOTA-NOC-ATE.*

Further studies are in progress with these derivatives, but also with DOTA-BOC and DOTA-BOC-ATE, respectively.

3.2. PK/PD modified radiolabeled somatostatin analogs

3.2.1. Increasing the hydrophilicity (unpublished results)

As seen in the previous section, the best compounds obtained by modification of the 3rd amino acid in the octreotide sequence are more lipophilic than the parent compound. Although the differences in the log P values are not very significant, the patient images performed with ^{111}In-DOTA-NOC (Fig. 11), albeit giving additional details, show some more gall bladder accumulation (hepatobiliary excretion, sign of increased lipophilicity) in comparison with Octreoscan. We concluded that the introduction of hydrophilic moieties between the chelator and the peptide sequence could improve this issue without impairing the pharmacological profile.

The work presented below is part of a larger project completed on DOTA-NOC, which will be published in the near future.

A) Synthesis

Three DOTA-NOC derivatives have been synthesized using the same methods as in **paper IV**, having a neutral, a cationic and an anionic spacer between DOTA and NOC (Fig. 14A). The same approach has been also used for DOTA-BOC (Fig. 14B).

B) Partition coefficient determination

The log P values for all these compounds complexed with $^{111/115}In^{3+}$ have been established using the shake flask method depicted in **paper IV**. The results are summarized in Table 4. Except for MG32, all the new derivatives are more hydrophilic than the parent compounds with the lowest log P for the Lys-spacer-conjugates.

C) Binding affinity profiles

Using the same competition assay as described in **paper III** or **IV**, the IC_{50} values for all the human sstr subtypes have been determined (Table 5). Both in the DOTA-NOC series as in the DOTA-BOC series, the more hydrophilic derivatives have a drop in their binding affinities to hsstr3. Except for In^{III}-MG78 which shows a 4-fold decrease in the binding affinity to hsstr5, all the derivatives maintain the good binding profile for hsstr2 and 5 as the parent compounds.

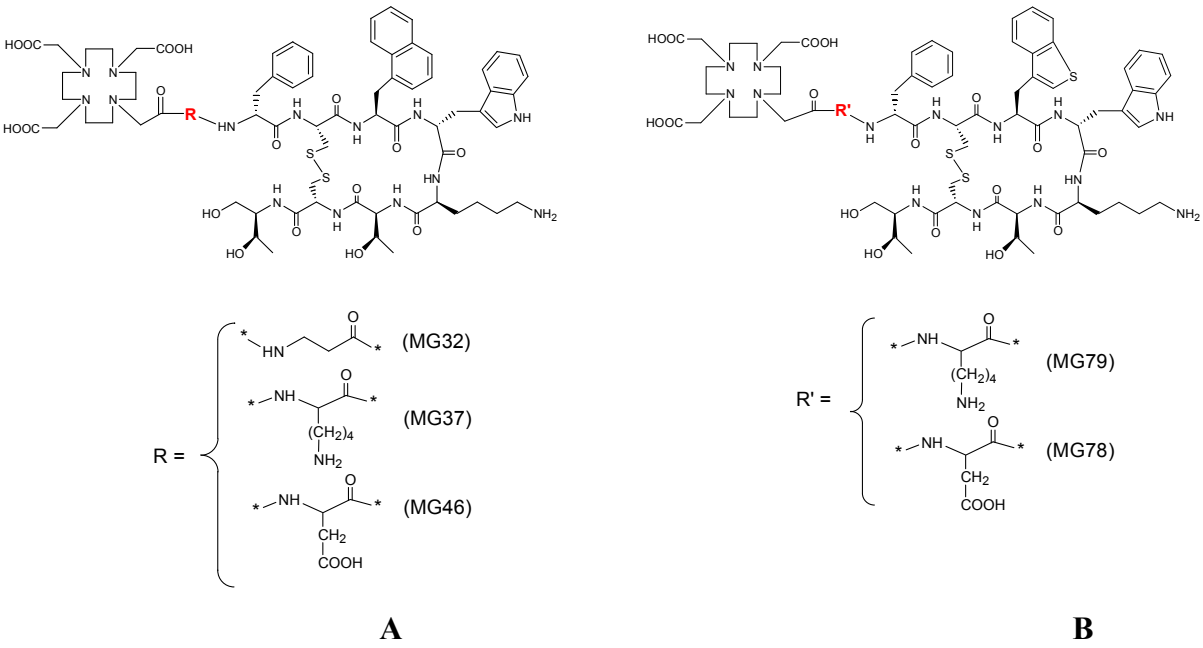

***Figure 14**. The chemical structures of the spacer-modified derivatives of DOTA-NOC (**A**) and DOTA-BOC (**B**).*

***Table 4**. Partition coefficient values (n =6).*

Compound	log P
In^{III}-DOTA-NOC	**- 2.0 ± 0.4**
In^{III}-MG32	-2.13 ± 0.2
In^{III}-MG37	-3.04 ± 0.01*
In^{III}-MG46	-2.71 ± 0.03*
In^{III}-DOTA-BOC	**- 2.1 ± 0.06**
In^{III}-MG78	-2.79 ± 0.04#
In^{III}-MG79	-3.1 ± 0.05#

*P < 0.001 relative to In^{III}-DOTA-NOC
# P < 0.001 relative to In^{III}-DOTA-BOC

***Table 5**. Binding affinities to hsstr subtypes (IC_{50} ± SEM, nM; n ≥ 2).*

Compound	hsstr1	hsstr2	hsstr3	hsstr4	hsstr5
In^{III}-DOTA-NOC	> 10 000	2.9 ± 0.1	8.0 ± 2.0	227 ± 18	11.2 ± 3.5
Y^{III}-MG32	> 1000	4.7 ± 0.4	33.5 ± 3.5	> 1000	8.6 ± 3.4
Y^{III}-MG37	> 1000	4.6 ± 2.0	77 ± 35	243 ± 63	3.8 ± 2.2
In^{III}-MG46	> 1000	1.65 ± 0.5	82.5 ± 27.5	370 ± 170	9.2 ± 4.7
In^{III}-DOTA-BOC	> 1000	4.3 ± 1.3	6.8 ± 0.3	213 ± 83	10 ± 1.0
In^{III}-MG78	> 1000	2.9 ± 0.8	200 ± 72	189 ± 18	47 ± 16
In^{III}-MG79	> 1000	4.6 ± 0.9	113 ± 43	436 ± 122	11 ± 0.5

D) Internalization rates in AR42J and in HEK-sstr3 cell-lines

The apparatus and procedures for the cell internalization experiments are based on previously described methods (**paper III**). The outcome of the internalization experiments in AR42J cells is illustrated in Figure 15. This cell-line has been previously shown to functionally express only sstr2 [129]. In the DOTA-NOC series (Fig. 15A) the highest internalization rate corresponds to the Asp-derivative, correlating with the binding affinity data. While MG32 and MG37 have similar binding affinities to sstr2, they slightly differ in their potency to activate the internalization of this receptor (13.0% versus 17.5%). In the DOTA-BOC series (Fig. 15B) the Asp-derivative is the best internalizer as well, with 44.2 % after 4h.

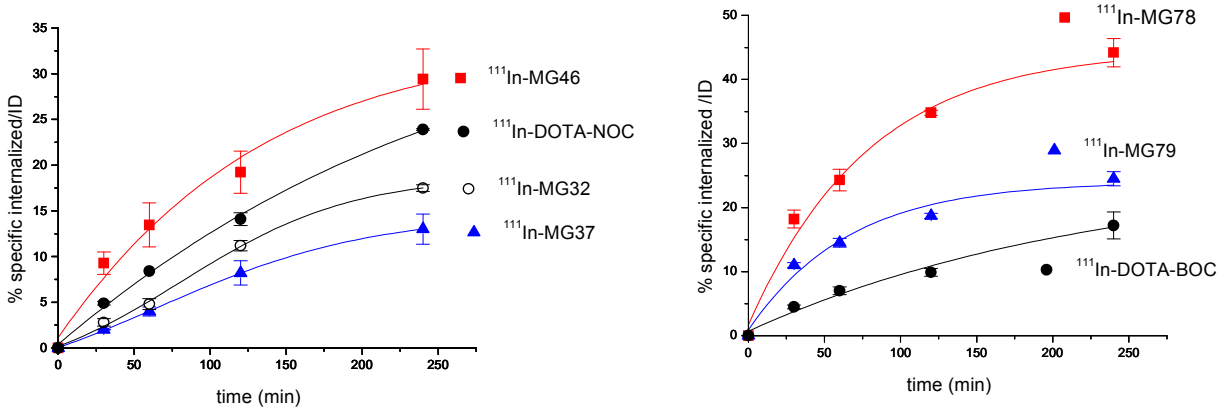

(A) **(B)**

***Figure 15**. Comparison of the internalization rate of ^{111}In-labeled DOTA-NOC (A) and DOTA-BOC derivatives (B) into AR4-2J cells. Values are expressed as specific internalization (percentage of dose added to 1 million cells at 1.67 nM concentration) and are the result of three independent experiments with triplicates in each experiment.*

Despite the drop in the binding affinities to sstr3 of these new derivatives, we were interested to probe the effect on the activation of this receptor by evaluating the 4h internalization rate in HEK cells stably expressing rsstr3. The results are summarized in Table 6. Thus, the hypothesis stated also in **paper IV** that, apparently, more lipophilic derivatives internalize better on somatostatin receptor subtype 3, was confirmed with these studies. All the conjugates with increased hydrophilicity exhibit very little internalization compared with the parent compounds. Further confirmation of this observation comes from the 4h rate of internalization for ^{111}In-MG32, which remains practically unchanged in comparison with ^{111}In-DOTA-NOC.

***Table 6**. Comparison in the 4h internalization rates in HEK cells stably transfected with rsstr3. The values are expressed as in Figure 15.*

Compound	%ID internalized after 4h	Compound	%ID internalized after 4h
^{111}In-DOTA-NOC	13.1 ± 0.3	^{111}In-DOTA-BOC	24.3 ± 0.4
^{111}In-MG32	14.0 ± 1.8	^{111}In-MG78	2.2 ± 0.7
^{111}In-MG37	1.2 ± 0.5	^{111}In-MG79	3.2 ± 0.6
^{111}In-MG46	1.8 ± 0.6		

E) Biodistribution studies in AR42J tumor bearing rats

In order to study the *in vivo* pharmacokinetics of the DOTA-NOC derivatives we analyzed the 4h biodistribution profile of the ^{111}In-labeled newly synthesized compounds in comparison with ^{111}In-DOTA-NOC in Lewis rats bearing subcutaneous AR42J tumors in the left leg. Figure 16 displays the outcome of this assay.

***Figure 16**. Biodistribution comparison in AR42J tumor bearing rats between the ^{111}In-labeled DOTA-NOC derivatives 4h after injection*

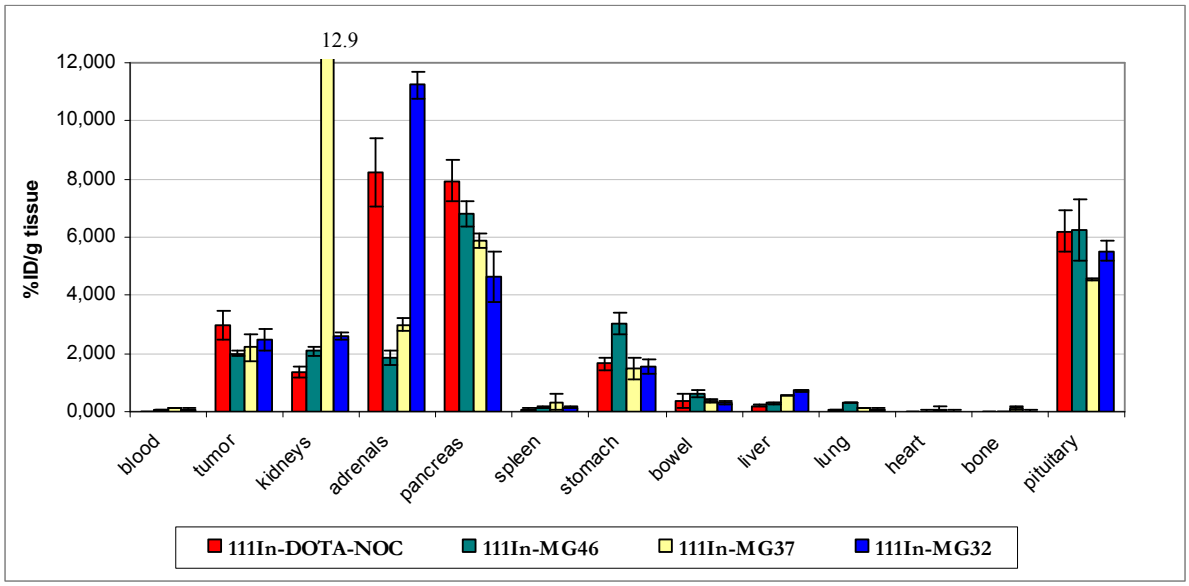

All the derivatives have a specific distribution in the sstr-expressing tissues, except for the kidneys, as proved by the blocking studies (data not shown). The tumor uptakes are similar, but still the highest one corresponds to the parent compound. The insertion of an additional Lys residue to the [1-Nal^3]-octreotide sequence tremendously increases the kidney accumulation (MG37); however, theoretically this uptake can be blocked by coinfusion of basic amino acid (see section *2.2.2.*). It is difficult to explain the decreased pancreas uptake which can be due either to the modified pharmacokinetic profile (more hydrophilic derivatives, less metabolic excretion) or to the change in the pharmacological properties (drop in affinity and internalization to sstr3, and the pancreas expresses sstr 2, 3 and 5).

It has to be said that this animal model may not be the most appropriate for this type of analysis, because ^{111}In-DOTA-NOC does not exhibit enhanced hepatobiliary clearance when compared to ^{111}In-DOTA-TOC in this model (see **paper II**). Therefore we can not rely on these *in vivo* studies to fully predict the PK/PD profile of these spacer-modified compounds.

COMMENTS

As mentioned at the beginning of this paragraph the work presented here represents just a part of a more ample project on spacer-modified analogs of DOTA-NOC. Several other structurally different moieties (polyethylenglycols, sugar-derivatives) have been placed between DOTA and the peptide sequence in the hope of improving the pharmacokinetic profile of this new drug lead. The spacers employed in the above presented work were chosen on the charge criterion: positive-negative-neutral. For comparison reasons I utilized the positive and the negative spacers also for DOTA-BOC, a conjugate similar with DOTA-NOC in all aspects (pharmacological properties, lipophilicity). Previous studies have been shown that the introduction of a negative charge at the N-terminal amino acid of ^{111}In-DTPA-octreotide would not only increase the hydrophilicity, but also would prevent the renal radioaccumulation [135]. We could not confirm these results with our Asp-derivatives. Moreover, our findings validate previous studies done in our laboratory, showing higher kidney uptake for the negatively charged conjugates [84]. Although it is not simple to correlate all the aspects of this type of research, a partial conclusion may be drawn: increasing the hydrophilicity of this kind of compounds (DOTA-NOC, DOTA-BOC) would mean a partial or total loss in affinity and internalization to sstr3, but also an increase in the kidney clearance. The only possible way to genuinely evaluate the impact of these new features on the *in vivo* pharmacokinetics is in the patient studies.

3.2.2. Decreasing the kidney uptake (unpublished results)

Also the work that I will describe below is part of a wider project on the utilization of PAH moiety as a scaffold to modulate the transport through the kidneys.

The transport systems responsible for renal tubular secretion of drugs have been classified as either organic anion (OAT) or cation transport (OCT) systems based on their preferential substrate selectivity. The secretory transport process is performed effectively by two distinct classes of transporters: one localized at the basolateral membranes to mediate cellular uptake of substrates from blood and the other at the brush-border membranes to mediate exit of cellular substrates into the tubular lumen. The reabsorption of the most

peptide-like drugs from the glomerular filtrate is mediated by oligopeptide transporters localized at the brush-border membranes of proximal tubular cells, influencing their pharmacokinetic profiles and therapeutic efficacy. Para-aminohippurate (PAH) is a marker substrate for the renal organic anion transport system.

With the aim of decreasing the renal radioaccumulation during therapy with radiolabeled somatostatin derivatives and based on previous studies of Arano *et al.* [113], we envisaged the use of PAH as a third function in a DOTA-somatostatin analog, assuming its recognition by the OAT system and subsequent stimulation of faster renal excretion. For this we chose the ''gold standard'' of targeted radiotherapy in our clinic, DOTA-TOC, and we placed the PAH unit in different positions relative to the peptide sequence (C-terminus, N-terminus or on the DOTA) in order to evaluate the best design.

Below I will present the results of the C-terminus PAH modified DOTA-TOC derivative.

A) Synthesis

The DOTA-TOC-PAH derivative (MG122, Fig. 17) was synthesized by solid phase peptide synthesis on TCP resin. Coupling of Fmoc-Gly-OH to the solid support was performed in dry DCM in the presence of an excess of DIPEA for 4h. After Fmoc deprotection with 20% piperidine/DMF Fmoc-para-aminobenzoic acid was coupled using HATU as activating agent. In order to prevent a potential steric hindrance 5-aminopentanoic acid (Apt) was used as a spacer between the PAH moiety and the [Tyr^3]-octreotide sequence. Therefore after Fmoc removal from the para-aminobenzoic acid the HATU activated Fmoc-Apt-OH in DIPEA/DMF was coupled for 5 h. Because the TNBS test was still positive after this interval the coupling was repeated for other 4 h. Giving the negative TNBS test, the synthesis was continued in a similar manner as described in **paper IV**. After HPLC purification the final product was obtained in 15 % yield and the correct mass was confirmed by ESI-MS analysis.

B) In vitro and in vivo evaluation

Being placed in close proximity to the pharmacophore the PAH building block might impair the pharmacological properties of DOTA-TOC. This concern was unfortunately confirmed by the *in vitro* internalization studies in AR42J cells (Table 7) and by the *in vivo* biodistribution experiments in Lewis rats bearing AR42J tumors (Figure 18).

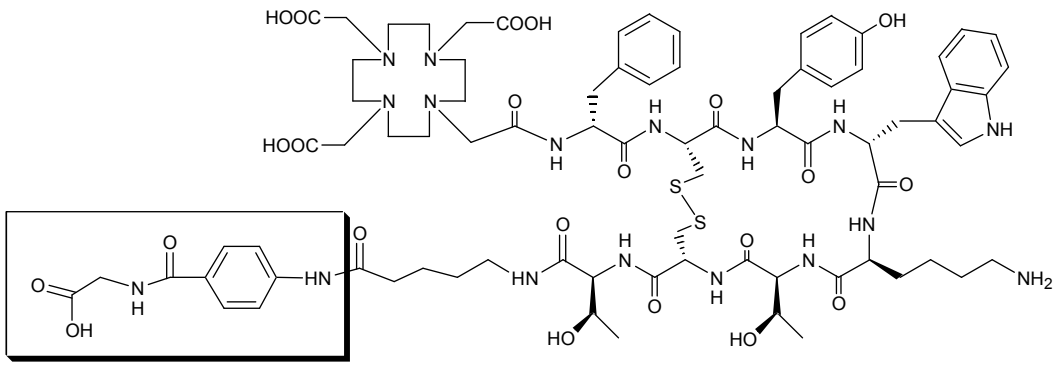

***Figure 17**. Structure of DOTA-TOC-PAH derivative (MG122).*

***Table 7**. Comparison in the 4 h internalization rate in AR42J cells*

Compound	% specific internalized after 4h in AR42J cells
^{111}In-DOTA-TOC	12.5 ± 1.0
^{111}In-MG122	0.82 ± 0.06

***Figure 18**. Comparison in 4 h p.i. biodistribution in AR42J tumor bearing rats.*

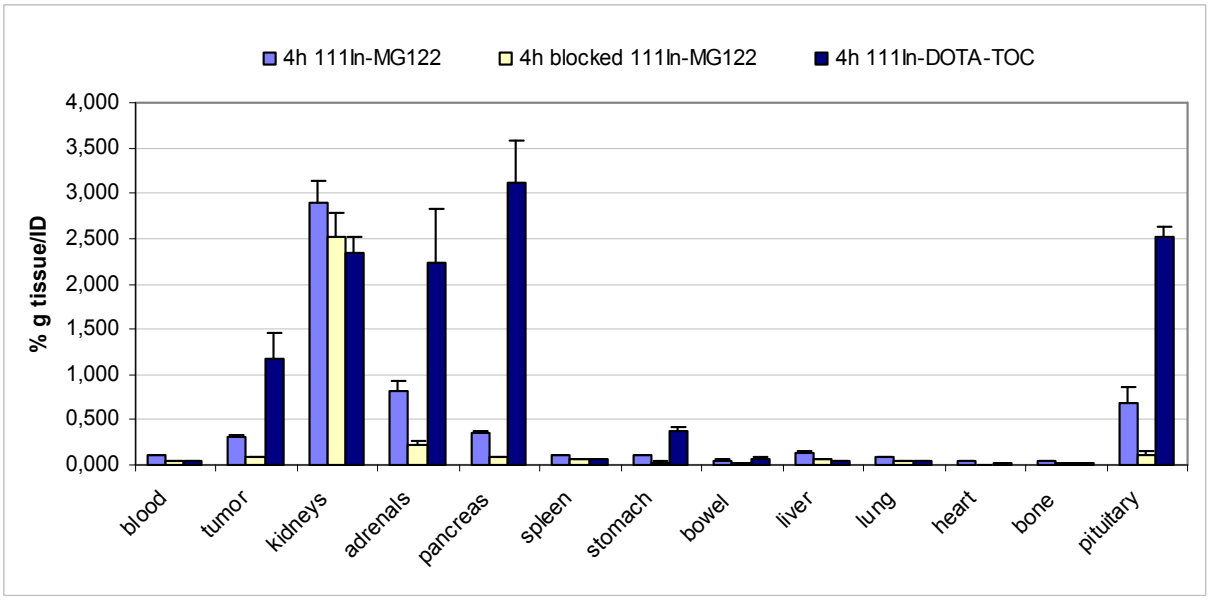

The loss of internalization capability is reflected also in the biodistribution studies. The uptake in sstr-positive tissues is specific, as proved by the blocking experiment (coinjection with excess of cold-labeled compound), but much diminished in comparison with

^{111}In-DOTA-TOC. The only comparable accumulation is in the kidneys, indicating maybe an inappropriate design of this compound.

COMMENTS

This first conjugate of a series of PAH-modified DOTA-TOC derivatives did not confirm our hypothesis regarding a potential decrease in the kidney uptake. This result is mainly due to the unsuitable structure of MG122 with the PAH building block encumbering on the pharmacological properties of DOTA-TOC. An N-terminus modification, remote from the pharmacophore, should not have such a dramatic effect on the biological properties of the parent compound. The synthesis of this type of derivatives is in progress and the final results will be published as soon as possible.

*3.2.3. Nucleus targeting modified radiolabeled somatostatin analogs (papers **V** and **VI**)*

The nucleus is the defining feature of the eukaryotic cell. All known transport between the nucleus and the cytoplasm occurs through the nuclear pore complex (NPC), a large structure spanning the nuclear envelope. Molecules can enter the nucleus either by diffusion or by signal-mediated transport. Although molecules (or cargoes) with masses < 40 kDa should be able to enter the nucleus by passive diffusion [136], many small molecules are imported by a signal-mediated pathway [137]. This route requires energy and a nuclear localization signal (NLS). The mechanism of this transport is not fully understood yet, but it can be described as three steps: a) docking at the NPC; b) translocation; c) nuclear deposition of the cargo [138]. The best characterized import signals are the simian virus 40 (SV40) large T-antigen (also known as the classical NLS) [139], containing a stretch of basic amino acids. A sequence of only seven amino acids rich in basic residues (Lys and Arg) was found to be sufficient for nuclear localization of this antigen. Moreover, it was demonstrated that, when synthetic peptides containing the sequence are conjugated to non-nuclear proteins such as bovine serum albumine (BSA), the conjugates entered the nucleus [140].

We proposed the use of a similar approach for the radiolabeled somatostatin-based derivatives. Thus papers **V** and **VI** describe the design, synthesis and *in vitro* evaluation of NLS-conjugated DOTA-TOC derivatives. The potential impact of such conjugates in nuclear medicine is explained in section *2.2.3.* and in the mentioned papers.

A) Design and Synthesis (PAPER V)

As seen in the previous section, the pharmacological profile of DOTA-TOC-like conjugates is greatly influenced by any structural alterations and care should be taken when designing new modifications. Using combined solid and solution phase peptide synthesis three trifunctional derivatives of DOTA-TOC bearing the NLS sequence PKKKRKV in three different positions relative to the somatostatin analog sequence were synthesized. In order to evaluate the most appropriate design a *C*-terminus modification (compound **1**) and the two *N*-terminus derivatives (compounds **2** and **3**) were generated (Figure 19). Compound **3** has a branched structure in which the NLS sequence is inverted (VKRKKKP). Compound **4** (DOTA-Ahx-PKKKRKV) was synthesized to be used as negative control for the biological studies. All the conjugates were analyzed by MALDI-MS and multiwavelength RP-HPLC and successfully complexed with $^{111/115}$In.

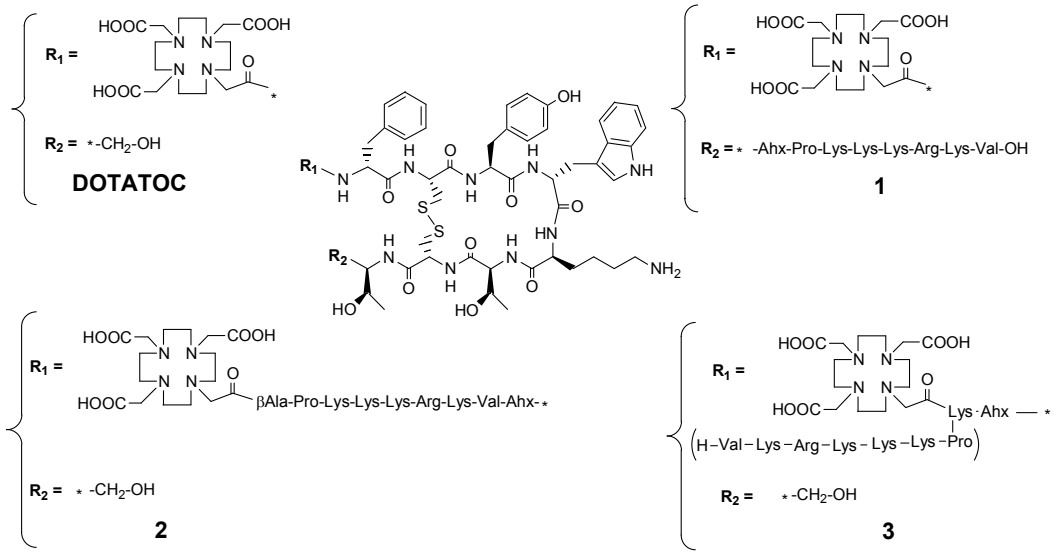

***Figure 19**. Chemical structures of the trifunctional conjugates, DOTA-TOC and DOTA-NLS.*

B) Biological evaluation (PAPER VI)

Paper **VI** summarizes the first series of *in vitro* studies completed with these conjugates: binding affinity determination, internalization in AR42J and HEK-sstr2A cell-lines, cellular and nuclear retention in HEK-sstr2A cells.

Table 1[paper VI] illustrates the preservation of binding affinity to sstr2A for the conjugates **2** and **3**, while the C-terminus derivative **1** shows an accentuated drop in affinity compared with ^{111}In-DOTA-TOC. This result together with the internalization studies presented in **Figure 2**[paperVI] corroborates the findings on MG122 from the previous section of this thesis. That is, modifications at the C-terminus of octreotide-type analogs have dramatic effects on the pharmacological outcome. On the other hand, the N-terminus modified conjugates **2** and **3** revealed increased internalization rates in both studied cell-lines (Fig.2[paperVI]). Another interesting aspect unveiled by these experiments was the high amount of surface-bound radioligand for the NLS-DOTA-TOC conjugates (Fig.3[paperVI]), a potential useful feature for Auger-electron emitter targeting. The control effected with ^{111}In-**(4)** confirmed the premise of Yoneda *et al* [123] that the NLS-cargo has to be located in cytoplasm in order to be directed to the nucleus, because no internalizated or surface-bound radiopeptide **4**, specific or unspecific, has been found (Fig.2 and 3[paperVI]).

Based on these two first assays (binding affinity and internalization investigations) ^{111}In-**(3)** proved to have the best ''architecture'', therefore we used it for further studies in comparison with the parent compound, ^{111}In-DOTA-TOC. The cellular retention assay performed after 2h of allowed internalization at 37^{0}C followed by 4h externalization is illustrated in **Figure 4** [paperVI]. The prolonged cellular retention proposed for such trifunctional derivatives was thus validated, with ^{111}In-**(3)** having only a smooth externalization pattern (70% of the internalized fraction is retained in cell after 4h), while ^{111}In-DOTA-TOC shows a steeper loss of the internalized fraction (about 40% retained in cell).

The nuclear uptake assay performed using a nuclei isolation kit from Sigma-Aldrich further confirmed the initial hypothesis. **Figure 5** [paperVI] and **table 2** [paperVI] summarize the results of this experiment. Already after one hour of incubation at 37^{0}C 11.2% of the internalized ^{111}In-**(3)** is located in the nucleus, whereas only 0.7% of the parent compound reaches the nucleus. Independently of the way of expressing the outcome of this assay, the gap between the two compounds is maintained at all three time points.

COMMENTS

Disseminated cancers have very few therapeutic options with chemotherapy being most frequently used. Because of its very low selectivity systemic cytotoxic chemotherapy is often limited by potential serious side effects. A consequence of these side effects is *e.g.* the application of suboptimal doses which in turn may cause failure of therapeutic success and the development of drug resistance. Encouraging reports on radiotherapy using internalizing

antibodies conjugated to radionuclides emitting low energy electrons have been recently published [119, 141, 142]. They prove the superior targeting efficacy and specificity of Auger-electron emitters in small cancers, due to their high level of cytotoxicity, low energy and short-range biological effectiveness. But they also demonstrate that the success of this therapeutic strategy relies on the concentration of the radioligand within tumor cells and in close nuclear proximity.

Whetstone *et al.* recently reported modified DOTA-[Tyr^3, Thr^8]-octreotide derivatives for longer intracellular residence [143], incorporating cathepsin-B-cleavable linkers between the chelator and the peptide. Their reasoning was that, if somatostatin analogues would escape recycling, they would accumulate in the cell. Although confirming an increased internalization of these derivatives, the subcellular localization of radioactivity was detected only in the lysosomes, unsatisfactory for an efficacious Auger-electron targeting.

Our approach was based on the two step targeting concept: first specific transport through the cellular membrane and then translocation of the cytotoxic moiety to the nucleus. The N-terminus conjugation of a NLS sequence to DOTA-TOC seems to be a good strategy. The first series of *in vitro* studies confirmed the initial hypothesis, although at this stage we cannot fully explain the intracellular mechanism. Nevertheless, further studies have to be completed, to ascertain the viability of this concept, particularly cytotoxicity assays *in vitro* and *in vivo*.

3.3. Synthesis of the phosphorylated sequence corresponding to the sstr2A C-terminus (unpublished results)

Activation of G protein-coupled receptors by their ligands is a process that is still poorly understood. It is generally accepted that phosphorylation of GPCRs is a key step in desensitization, which is essential for the subsequent binding of proteins of the arrestin family, and that is therefore also necessary for endocytosis [25]. However, the mechanism is still not completely clear, but of considerable clinical importance for the somatostatin receptors, because all the therapies with SS analogs (targeted radiotherapy, long term treatment of neuroendocrine tumors with cold SS analogs) presumably rely on the internalization of the ligand by its target cells.

As demonstrated by other studies [144, 145], sequence-specific antiphosphopeptide antibodies are powerful tools to study the phosphorylation events within cells. In

collaboration with Dr. S. Schulz's group (Department of Pharmacology and Toxicology, Otto-von-Guericke University in Magdeburg, DE) we intended the production of an antibody against the estimated phosphorylated fragment from the C-terminus of sstr2A. For this we planned the synthesis of the 15 amino acid sequence corresponding to the carboxylic part of sstr2A, having four (expected) phosphorylated Thr residues. Subsequently this peptide would be used to generate antibodies in a rabbit.

A) Synthesis

Phosphopeptides can be synthesized by either of two general methods: *global phosphorylation* or the *building block approach*. The first method, also known as *postassembly phosphorylation*, involves the synthesis of a peptide in which the residues to be phosphorylated (S, T or Y) are incorporated without side-chain protection; phosphorylation is then accomplished by treating the peptide with a phosphoramidite followed by oxidation. In the *building block approach* the phosphate is integrated into an N^{α} protected amino acid prior to peptide assembly. The phosphoamino acid building block is then incorporated into the growing peptide chain.

We opted for the second method, using protected phosphorylated threonine building blocks. There are two possibilities of protection of a phosphoamino acid: utilization of phosphotriesters (two phosphate protecting groups) (Fig. 20A) or of phosphodiesters (mono-benzyl phosphate protection) (Fig. 20B). A major drawback of serine and threonine phosphotriesters is the piperidine-mediated β-elimination to dehydroalanine or α-amino-butenoate in syntheses employing N^{α}-Fmoc based methods [146]. The mono-benzyl phosphate protection was found to be superior to the dialkyl or dibenzyl phosphate protecting groups and therefore nowadays this type of derivatives become commercially available and is intensively use in Fmoc SPPS approach [147, 148].

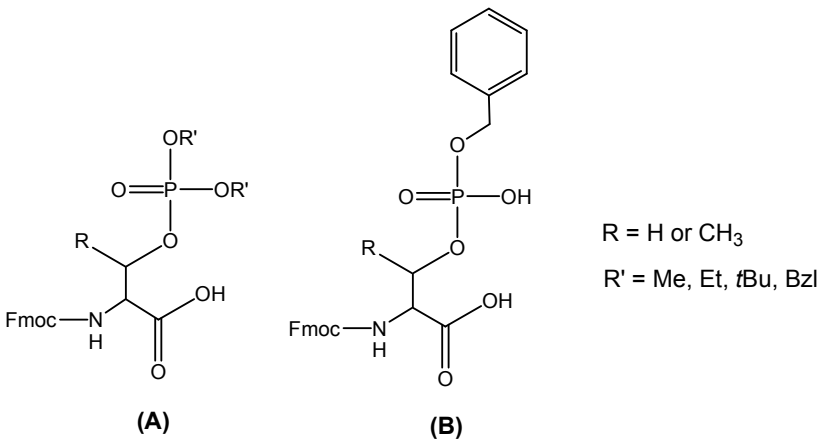

Figure 20. *Structures of protected phosphorylated amino acids used in Fmoc SPPS approach: phosphotriesters (A) and phosphodiesters (B).*

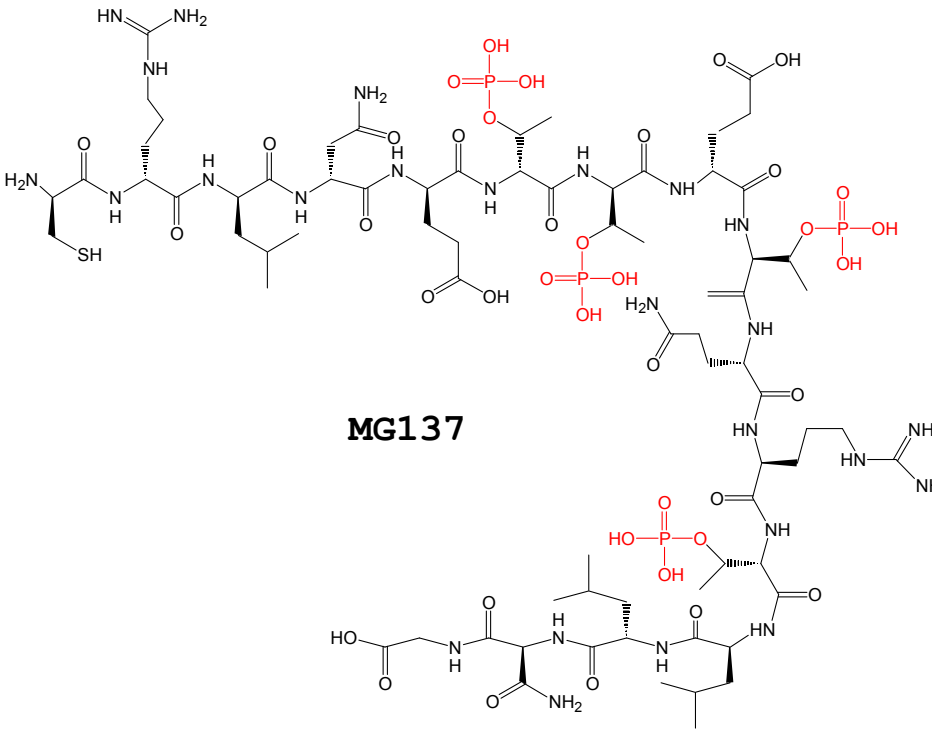

***Figure 21**. Structural formula of the phosphopeptide MG137.*

The 15 amino acid peptide sequence corresponding to the carboxylic intracellular segment of sstr2A is: RLNETTETQRTLLNG. It contains four threonine residues suspected of phosphorylation, therefore for their incorporation we used the Fmoc-Thr(PO(OBzl)OH)-OH building block available from Novabiochem (Merck Biosciences, Switzerland). An N-terminal Cys has been added to the 15 amino acid sequence in order to allow the cross-linking to a suitable carrier protein for antibody production [145] (Figure 21).

This 16 amino acid peptide (named MG137) was assembled on TCP resin. The other amino acids side chains were protected as follows: Asn, trityl (Trt); Arg, 2, 2, 4, 6, 7-pentamethyl-dihydrobenzofurane-5-sulfonyl (Pbf); Gln, trityl; Glu, *tert*-butyl (tBu); Cys, trityl. After Fmoc-Gly-OH loading for 4 h in dry DCM and in the presence of DIPEA, and subsequent Fmoc removal with 20 % piperidine/DMF, the next three protected residues were coupled using DIC, HOBt and DIPEA in DMF. Capping with acetic anhydride and TNBS or Kaiser test were performed after each coupling step. For the incorporation of the mono-benzyl phosphate protected threonine residue we chose HATU/DIPEA, since Perich *et al*. [149] have found that uronium-based coupling agents in conjunction with DIPEA are the most effective coupling agents for these building blocks. The same group observed that a higher that usual excess of DIPEA (3 eq relative to the phosphorylated amino acid) could improve the yield of coupling, because 1 eq of base will be consumed by the acidic partially protected phosphate group. Therefore the coupling was achieved using 5 eq Fmoc-Thr(PO(OBzl)OH)-OH, 5 eq HATU and 15 eq DIPEA in DMF for 20 h. The negative TNBS test confirmed the

completeness of reaction. Still, capping with acetic anhydride was done. After Fmoc removal a washing step with DMF containing DIPEA (20 eq relative to phosphate content of resin) and TFA (1.8 eq relative to phosphate content of resin) was carried out. This step is necessary to exchange the piperidine counterion of the phosphate, which could affect the yield of the next residue coupling [150].

The rest of the peptidic chain was assembled in the same manner: with DIC/HOBt/DIPEA for the coupling of regular Fmoc-residues and with HATU/DIPEA for phosphothreonine incorporation. For the coupling of the 3rd and 4th phosphorylated threonine residues increased excesses of amino acid were used and double couplings. The average yield of phosphorylated-residues couplings was 80 %. After cleavage from the resin with 20% AcOH/DCM, co-evaporation with toluene and *in vacuo* drying, all the protecting groups were removed by 2 h incubation in 95 % TFA solution (2.5 % H_2O, 2.5 % TIS). The crude peptide was obtained in ~ 20 % yield relative to the resin loading and in ~ 70 % purity as assessed by analytical HPLC (Figure 22).

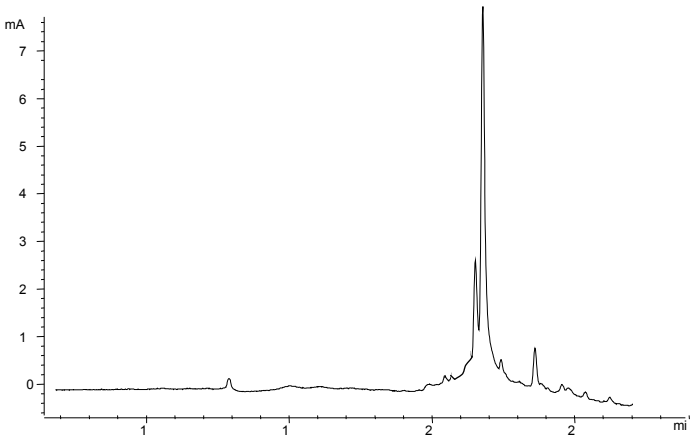

***Figure 22**. HPLC chromatogram of crude MG137; gradient used: 0-10 min: 5 % A, 10-30 min: 5-50 % A; λ = 230 nm (eluents: A = ACN, B = 0.1% TFA/H_2O).*

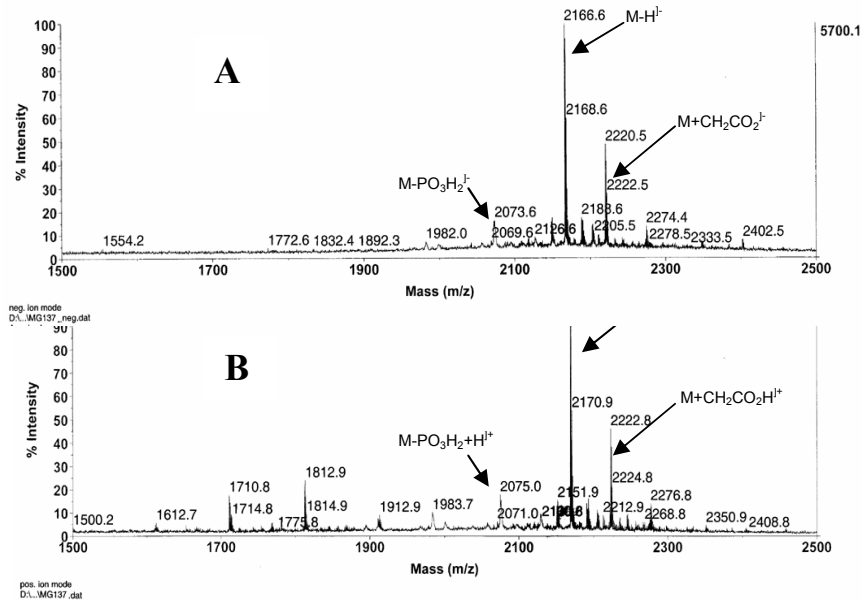

***Figure 23**. MALDI spectra of crude compound MG137 in negative (A) and in positive (B) mode.*

The correct mass was confirmed by MALDI-MS in negative and in positive mode (Figure 23). After purification on RP-HPLC, the final compound was obtained in > 96% purity (Figure 24).

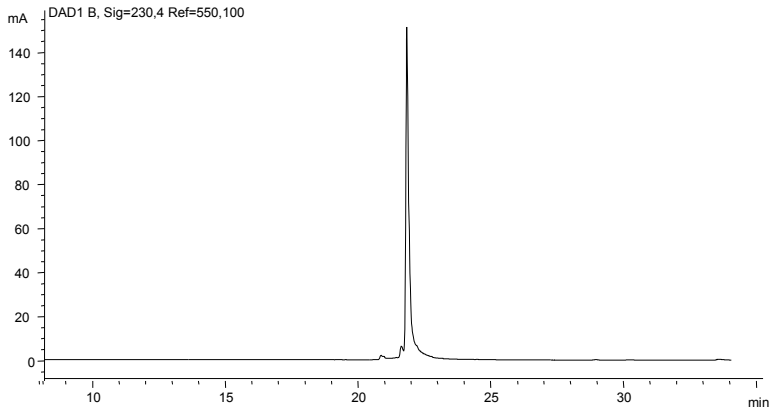

***Figure 24**. Analytical HPLC of purified MG137 (same system as in Figure 22).*

B) QUANTITATION OF PHOSPHORYLATION

Although the mass spectroscopy confirmed the correct molecular weight of this peptide and therefore the presence of four phosphorylated threonine residues, we still carried out an additional experiment in order to certify and quantify the phosphate amount in this molecule. Thus we used the Lanzetta method [151], a colorimetric assay for the determination of nanomole amounts of inorganic phosphate. Briefly, the amount of phosphate released from the organophosphate compound (after digestion with HCl fumans) is measured spectrophotometrically at 660 nm by correlation with a standard inorganic phosphate solution. The dye reagent used was a 3:1 mixture of malachite green hydrochloride (0.045 %) and ammonium molybdate solution (4.2 % in 4 N HCl) and the calibration curve was obtained using as standard a 10 mM solution of $Na_3PO_4.12H_2O$.

This experiment confirmed the presence of 4 moles of phosphate in 1 mole of peptide.

C) FIRST BIOLOGICAL RESULTS (in Dr.Schulz's group, at Magdeburg University)

After cross-linking of MG137 to a protein carrier and immunization of rabbits, the antibody was collected by bleedings started one week after the third injection. After affinity purification, the antibody was tested by Western blotting (Figure 25).

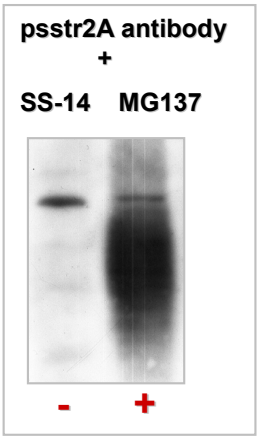

***Figure 25**. Western blotting using the obtained anti-psstr2A antibody preincubated with SS-14 (negative control) and with MG137 (positive control).*

The activity of this antibody was also tested *in vitro* in HEK cells stably expressing sstr2A. The agonist-induced phosphorylation of sstr2A could be proved after 30 min incubation with SS-14 (Figure 26). Further studies are in progress.

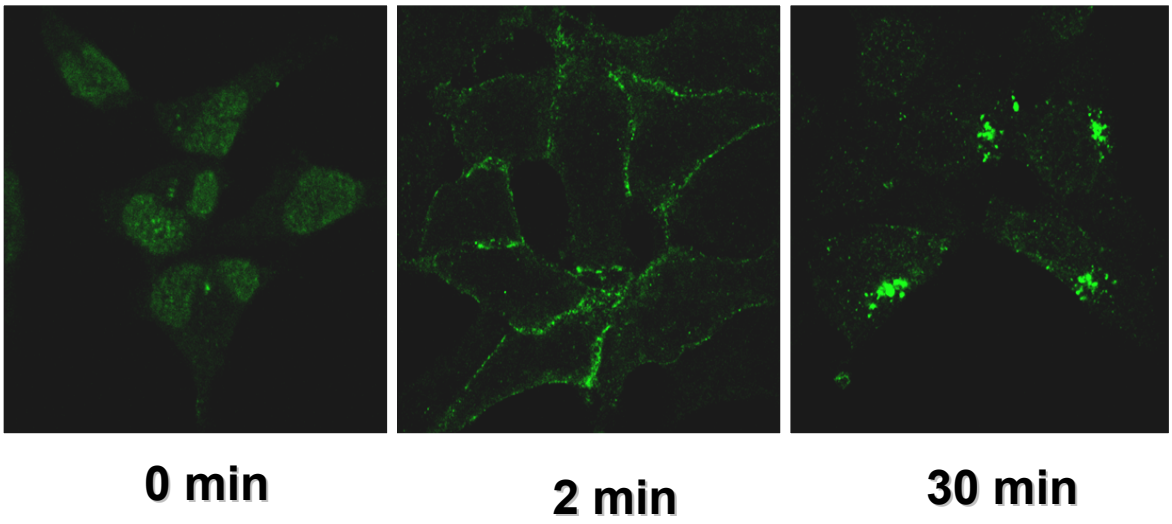

***Figure 26.** Confocal microscopy analysis of agonist-induced phosphorylation of sstr2A using the newly generated anti-**p**sstr2A antibody.*

COMMENTS

Although apparently aside from the topic of my herein described thesis projects, this phosphopeptide (MG137) was a challenge I was willing to take. Not only because of the special features encountered during the solid phase peptide synthesis of this compound, but also due to the analytical aspects comprised and mostly because of the potential utility of such a derivative. There are several techniques to study the phosphorylation of GPCRs: two-dimensional tryptic phosphopeptide mapping, phosphor-amino acid analysis, phosphopeptide sequencing etc. None of these techniques is easy to master and there are technical problems that frequently cannot be solved, *e.g.*, large peptides may be insoluble and thus cannot be separated [145]. The advantage of anti-phosphopeptides antibodies is that they permit rapid analysis of intracellular phosphoproteins without the need to employ complex structural protein analyses (*e.g.*, protease digestion of orthophosphate-labeled proteins) [145].

And once again I would like to underline the importance of the studies that can be completed with such an antibody in the specific case of sstr2A. The overexpression of this receptor in a multitude of tumors, the desensitization and down-regulation of this sstr - potentially responsible for resistance to SS-analog therapy, its newly discovered heterologous regulation [129], are as many clinically relevant reasons to study the post-endocytic pathway of this receptor by these means.

Logic will get you from A to B.
Imagination will take you everywhere.
The important thing is not to stop questioning.
Albert Einstein

4. Conclusions – Outlook

Despite the explosion of knowledge in recent years in the somatostatin field, a great deal remains to be discovered. In particular, developing the potential of somatostatin analogs for cancer treatment will require a more complete understanding of their intracellular actions and interactions. However, there is no doubt that SS-analog radiotherapy has significantly improved the quality of life of many patients and this is very important for a palliative treatment. Limitations to somatostatin-based peptide receptor radiotherapy are principally due to poor tumor penetration of the radioligand and insufficient accumulation within the neoplastic cell. In addition, low or variable expression of somatostatin receptor subtypes may lead to poor tumor localization of radiolabeled somatostatin analogs.

This dissertation presents attempts to overcome these problems associated with targeted therapy and/or imaging with radiolabeled somatostatin analogs. In a first step, we focused on the developing of new radiolabeled somatostatin-based analogs with improved pharmacological profile. Thus, employing parallel solid phase we synthesized a series of analogs of DOTA-octreotide with modifications on the third residue (Phe^3). From the small library synthesized two conjugates showed very promising preclinical properties, DOTA-NOC and DOTA-BOC. Moreover, the Thr^8-modified versions of these two compounds (DOTA-NOC-ATE and DOTA-BOC-ATE) also displayed superior preclinical profiles if compared with somatostatin analogs used in the clinic. Subsequently, these four new derivatives are currently in clinical trials and the first promising results are already described herein. Nevertheless, we planned additional structural studies to better understand the results obtained in this series of compounds.

In a second step we aimed at the improvement of pharmacokinetics for this type of conjugates. The biggest problem associated with this category of drugs is their excretion pathway. A drawback of the derivatives discussed above is their increased lipophilicity. This is translated *in vivo* by increased hepatobilliary excretion, hence impairing on the abdominal imaging. Our strategy was the introduction of hydrophilic spacers between the chelator and the peptide. The derivatives thus obtained partially lose the broad affinity profile of the parent compounds, although the modifications performed are remote from the pharmacophore. Nevertheless, they show increased internalization in sstr2-expressing cells and good

biodistribution profile in rats. However, the animal tumor model used did not permit a genuine evaluation of the hepatobiliary excretion pathway.

While favoring the kidney clearance route, nephrotoxicity can be one of the consequences, particularly in case of targeted radiotherapy. That is why we proposed the addition of a PAH unit (recognized by the OAT system of the kidneys) to the DOTA-somatostatin analogs, expecting a faster excretion, without accumulation in these organs. Nevertheless, this unit should probably be situated on the chelator or at the peptide *N*-terminus, because the conjugate described herein, with PAH at the *C*-terminus of DOTA-[Tyr^3]-octreotide, loses almost completely the pharmacological properties of the parent compound (probably due to the proximity to the pharmacophore sequence).

In a third step we proposed a strategy to modify the pharmacodynamics of DOTA-somatostatin derivatives, by targeting the cell nucleus. Thus, we added an NLS unit to DOTA-[Tyr^3]-octreotide. After testing the best design of such a construct, we selected the best derivative and performed biological trials. Our hypothesis was confirmed in nuclei isolation assays, showing increased cell nuclear uptake for the trifunctional NLS-conjugate in comparison with the parent compound. Moreover, the new molecule has increased uptake and higher retention in tumoral cells *in vitro*. These promising results, if confirmed *in vivo*, could allow the successful use of Auger-electron emitting radionuclides in targeted radiotherapy.

As mentioned at the beginning of this section, understanding the intracellular trafficking of somatostatin receptors is part of the work for developing the potential of somatostatin analogs for therapy. Since phosphorylation is believed to be a critical step in both receptor internalization and desensitization, an antibody directed against the phosphorylated receptor may give useful insights into this process. This is the reason for the phosphorylated peptide synthesis described herein, meant for antibody production. The first biological assays performed with the obtained antibody are encouraging.

***

Although still far from being ‘’magic bullets’’, the radiolabeled somatostatin analogs remain the mainstay of peptide receptor mediated targeted radionuclide imaging and therapy. The recent findings concerning the homo- and hetero-oligomerization of somatostatin receptors and the concomitant expression of several peptide receptors on the same tumor may open new prospects of therapy. Since the receptors combine with each other, why not combining also the peptides directed against them? The use of cocktails of peptide radioligands recognizing their respective receptors may increase the scintigraphic signal of the scanned tumors and may reach superior therapeutic levels. A more chemically interesting

version of this approach would be the synthesis of polyfunctional radioligands. These constructs should incorporate the sequences of several peptides linked by appropriate spacers and including one or more chelators able to complex radiometals.

The same concept of combination therapy or combination targeting may be applied in the field of chemotherapy. Due to the limited efficacy and considerable toxicity of conventional chemotherapy, novel cytotoxic agents are being developed. An example is targeted chemotherapy. By synthesizing conjugates of somatostatin analogs and cytotoxic drugs (doxorubicin, paclitaxel) [152], [153], selective accumulation of cytotoxic radicals in somatostatin receptor-positive tumor cells would be possible. Moreover, adding a radionuclide to this ensemble would increase the potential of therapy.

The targeting combination illustrated also by the cell nucleus targeting through the somatostatin receptors in this thesis may be further applied to achieve more selectivity for cytotoxic drugs.

With the advances in proteomics and genomics more targets are being identified and the opportunities of using combined therapies are increasing. The treatment of any cancer is unlikely to be optimal with a single drug. There are of course major issues to be addressed, including the difficulty of selecting the best combination, uncertain predictability of preclinical models, the design of clinical trials etc. But a major problem remains the complete elucidation of intracellular trafficking of such drugs and their targets, particularly in the field of GPCRs as molecular targets for cancer diagnosis and therapy.

References:

1. Reubi, JC, Laissue, J, Krenning, E, Lamberts, SW. *Somatostatin receptors in human cancer: incidence, characteristics, functional correlates and clinical implications.* J Steroid Biochem Mol Biol, **1992** *43*: 27-35.
2. Reubi, JC, Schaer, JC, Waser, B, Mengod, G. *Expression and localization of somatostatin receptor SSTR1, SSTR2 and SSTR3 mRNAs in primary human tumors using in situ hybridization.* Cancer Res, **1994** *54*: 4355-5459.
3. Reubi, JC, *Neuropeptide receptors in health and disease: the molecular basis for in vivo imaging.* J Nucl Med, **1995** *36*: 1825-1835.
4. Brazeau, P, Vale, W, Burgus, R, et al. *Hypothalamic polypeptide that inhibits the secretion of immunoreactive pituitary growth hormone.* Science, **1973** *179*: 77–79.
5. Alumets, J, Sundler, F, Hakanson, R. *Distribution, ontogeny and ultrastructure of somatostatin immunoreactive cells in the pancreas and gut.* Cell Tissue Res, **1977** *185*: 465–479.
6. Hokfelt, T, Efendic, S, Hellerstrom, C, Johansson, O, Luft, R, Arimura, A. *Cellular localization of somatostatin in endocrine-like cells and neurons of the rat with special references to the A1-cells of the pancreatic islets and to the hypothalamus.* Acta Endocrinol Suppl, **1975** *200*: 5-41.
7. Reichlin, S. *Somatostatin.* N Engl J Med, **1983** *309*: 1495–1501.
8. Patel, YC. *Somatostatin and its receptor family.* Front. Neuroendocrinol, **1999** *20*: 157-198.
9. Bousquet, C, Puente, E, Buscail, L, Vaysse, N, Susini, C. *Antiproliferative effect of somatostatin and analogs.* Chemotherapy, **2001** *47*: 30–39.
10. Gillies, G. *Somatostatin: the neuroendocrine story.* Trends Pharmacol Sci, **1997** *18*(3): 87-95.
11. D'Alessio, D, Sieber, C, Beglinger, C, Ensinck, JW. *A physiologic role for somatostatin 28 as a regulator of insulin secretion.* J Clin Invest, **1989** *84(3)*: 857-862.
12. Reichlin, S. *Secretion of somatostatin and its physiologic function.* J Lab Clin Med, **1987** *109(3)*: 320-326.
13. Marks, N, Stern, F. *Inactivation of somatostatin (GH-RIH) and its analogs by crude and partially purified brain extracts.* FEBS Lett, **1975** *55*: 220-224.
14. Patel, YC. *Molecular pharmacology of somatostatin receptor subtypes.* J Endocrinol. Invest., **1997** *20*: 348-367.
15. Vanetti, M, Kouba, M, Wang, X, Vogt, G, Hollt, V. *Cloning and expression of a novel mouse somatostatin receptor (SSTR2B).* FEBS Lett, **1992** *311*: 290-294.
16. Patel, YC, Greenwood, M, Kent, G, Panetta, R, Srikant, CB. *Multiple gene transcripts of the somatostatin receptor SSTR2: tissue selective distribution and cAMP regulation.* Biochem Biophys Res Commun, **1993** *192*: 288-294.
17. Reisine, T, Bell, GI. *Molecular biology of somatostatin receptors.* Endocr. Rev., **1995** *16*: 427-442.
18. Seger, R, Krebs, EG. *The MAPK signaling cascade.* FASEB J, **1995** *9*: 726-735.
19. Guillermet, J, Saint-Laurent, N, Rochaix, P, et al. *Somatostatin receptor subtype 2 sensitizes human pancreatic cancer cells to death ligand-induced apoptosis.* Proc Natl Acad Sci U S A, **2003** *100(1)*: 155-160.
20. Sharma, K, Srikant CB, *Induction of wild-type p53, Bax, and acidic endonuclease during somatostatin-signaled apoptosis in MCF-7 human breast cancer cells.* Int J Cancer, **1998** *76(2)*: 259-266.
21. Rocheville, M, Lange, DC, Kumar, U, Sasi, R, Patel, RC, Patel, YC. *Subtypes of the somatostatin receptor assemble as functional homo- and heterodimers.* J Biol Chem, **2000** *275(11)*: 7862-7869.
22. Rocheville, M, Lange, DC, Kumar, U, Patel, SC, Patel, RC, Patel, YC. *Receptors for dopamine and somatostatin: formation of hetero-oligomers with enhanced functional activity.* Science, **2000** *288*: 154-157.
23. Pfeiffer, M, Koch, T, Schroder, H, et al. *Homo- and heterodimerization of somatostatin receptor subtypes. Inactivation of sst(3) receptor function by heterodimerization with sst(2A).* J Biol Chem, **2001** *276*(17): 14027-36.
24. Koenig, JA, Edwarson, JM. *Endocytosis and recycling of G-protein coupled receptors.* Trends Pharmacol Sci, **1997** *18*: 276-287.
25. Ferguson, SSG, Barak, LS, Zhang, J, Caron, MG. *G-protein-coupled receptor regulation: role of G-protein-coupled receptor kinases and arrestins.* Can J Physiol Pharmacol, **1996** *74*: 1095-1110.
26. Nouel, D, Gaudriault, G, Houle, M, Reisine, T, Vincent, J, Vicentini, LM. *Differential internalization of somatostatin in COS-7 cells transfected with SST1 and SST2 receptor subtypes: a confocal microscopic study using novel fluorescent somatostatin derivatives.* Endocrinology, **1997** *138*: 296-306.
27. Hukovic, N, Panetta, R, Kumar, U, Patel, YC. *Agonist-dependent regulation of cloned human somatostatin receptor types 1-5 (hSSTR1-5): subtype selective internalization or upregulation.* Endocrinology, **1996** *137*: 4046-4049.

28. Hukovic, N, Rocheville, M, Kumar, U, Sasi, R, Khare, S, Patel, YC. *Agonist-dependent up-regulation of human somatostatin receptor type 1 requires molecular signals in the cytoplasmatic C-tail.* J Biol Chem, **1999** *274*: 24550-24558.
29. Beaudet, A, Nouel, D, Stroh, T, et al. *Fluorescent ligands for studying neuropeptide receptors by confocal microscopy.* Braz J Med Biol Res, **1998** *31*: 1479-1489.
30. Hofland, LJ, Lamberts, WJ. *The pathophysiological consequences of somatostatin receptor internalization and resistance.* Endocr Rev, **2003** *24(1)*: 28-47.
31. Csaba, Z, Dournaud, P. *Cellular biology of somatostatin receptors.* Neuropeptides, **2001** *35(1)*: 1-23.
32. Thoss, VS, Perez, J, Probst, A, Hoyer, D. *Expression of five somatostatin receptor mRNAs in the human brain and pituitary.* Naunyn Schmiedebergs Arch Pharmacol, **1996** *354(4)*: 411-419.
33. Le Romancer, M, Cherifi, Y, Levasseur, S, et al. *Messenger RNA expression of somatostatin receptor subtypes in human and rat gastric mucosae.* Life Sci, **1996** *58(13)*: 1091-1098.
34. Kumar, U, Sasi, R, Suresh, S, et al. *Subtype-selective expression of the five somatostatin receptors (hSSTR1-5) in human pancreatic islet cells: a quantitative double-label immunohistochemical analysis.* Diabetes, **1999** *48(1)*: 77-85.
35. Reubi, JC, Waser, B, Schaer, JC, Laissue, JA. *Somatostatin receptor sst1-sst5 expression in normal and neoplastic human tissues using receptor autoradiography with subtype-selective ligands.* Eur J Nucl Med, **2001** *28*: 836-846.
36. Hofland, LJ, Liu, Q, Van Koetsveld, PM, et al. *Immunohistochemical detection of somatostatin receptor subtypes sst1 and sst2A in human somatostatin receptor positive tumors.* J Clin Endocrinol Metab, **1999** *84(2)*: 775-780.
37. Kulaksiz, H, Eissele, R, Rossler, D, et al. *Identification of somatostatin receptor subtypes 1, 2A, 3, and 5 in neuroendocrine tumours with subtype specific antibodies.* Gut, **2002** *50(1)*: 52-60.
38. Reubi, JC, Waser, B. *Concomitant expression of several peptide receptors in neuroendocrine tumors: molecular basis for in vivo multipreceptor tumor targeting.* Eur J Nucl Med Mol Imaging., **2003** *30*: 781-793.
39. Forssell-Aronsson, E, Nilsson, O, Benjegard, SA, et al. *^{111}In-DTPA-D-Phe^{1}-octreotide binding and somatostatin receptor subtypes in thyroid tumors.* J Nucl Med, **2000** *41*: 636-642.
40. Halmos, G, Sun, B, Schally, AV, Hebert, F, Nagy, A. *Human ovarian cancers express somatostatin receptors.* J Clin Oncol Metab, **2000** *85(10)*: 3509-3512.
41. Greenman, Y, Melmed, S. *Expression of three somatostatin receptor subtypes in pituitary adenomas: evidence for preferential sstr5 expresison in the mammosomatotroph lineage.* J Clin Endocrinol Metab, **1994** *79*: 724-729.
42. Ferone, D, Van Hagen, MP, Kwekkeboom, DJ, et al. *Somatostatin receptor subtypes in human thymoma and inhibition of cell proliferation by octreotide in vitro.* J Clin Endocrinol Metab, **2000** *85*: 1719-1726.
43. Schulz, S, Schmitt, J, Weise W. *Frequent expression of immunoreactive somatostatin receptors in cervical and endometrial cancer.* Gyn Oncol, **2003** *89*: 385-390.
44. Miller, G, Alexander, JM, Bikkal, HA, Katznelson, L, Zervas, NT, Klibanski, A. *Somatostatin receptor subtype gene expression in pituitary adenomas.* J Clin Endocrinol Metab, **1995** *80*: 1386-1392.
45. Papotti, M, Croce, S, Bello, M, et al. *Expresion of somatostatin receptor types 2, 3 and 5 in biopsies and surgical specimens of human lung tumours.* Virchows Arch., **2001** *439*: 787-797.
46. Palczewski, K, Kumasaka, T, Hori, T, et al. *Crystal Structure of Rhodopsin: A G Protein–Coupled Receptor.* Science, **2000** *289*: 739-745.
47. Vale, W, Rivier, C, Rivier, J, Brown, M. *Diverse roles of hypothalamic regulatory peptides.*, in *Medicinal Chemistry*, A.M.J. Gotto, Peck, E.J. Jr, Boyd, A.E., Editor. 1977, Elsevier Scientific: Amsterdam. p. 25-62.
48. Veber, DF, Freidinger, RM, Schwenk-Perlow, D, et al. *A potent cyclic hexapeptide analogue of somatostatin.* Nature, **1981** *292*: 55-58.
49. Freidinger, RM, Schwenk-Perlow, D, Randall, WC, Saperstein, R, Arison, BH, Veber, D.H. *Conformational modifications of cyclic hexapeptide somatostatin analogs.* Int J Peptide Protein Res, **1984** *23*: 142-150.
50. Veber, DF, Saperstein, R, Nutt, RF, et al. *A super active cyclic hexapeptide analog of somatostatin.* Life Sci, **1984** *34*: 1371-1378.
51. Bauer, W, Briner, U, Doepfner, W. et al. *SMS-201-995: a very potent and selective octapeptide analogue of somatostatin with prolonged action.* Life Sci, **1982** *31*: 1133-1140.
52. Marbach, P, Briner, U, Lemaire, M, Schweizer, A, Terasaki, T. *From somatostatin to sandostatin: pharmacodynamics and pharmacokinetics.* Metab Clin Exp, **1992** *41*: 7-10.
53. Murphy, W, Lance, VA, Moreau, S, Moreau, JP, Coy, DH. *Inhibition of rat prostate tumor growth by an octapeptide analog of somatostatin.* Life Sci, **1987** *40(26)*: 2515-2522.
54. Cai, R, Szoke, B, Lu, R, Fu, D, Redding, TW, Schally, AV. *Synthesis and biological activity of highly potent octapeptide analogs of somatostatin.* Proc Natl Acad Sci U S A, **1986** *83(6*): 1896-1900.

55. Pattaroni, C, Lucietto, P, Goodman, M, et al. *Cyclic hexapeptides related to somatostatin. Synthesis and biological testing.* Int J Pept Protein Res, **1990** *36(5*): 401-417.
56. Huang, Z, Probstl, A, Spencer, JR, Yamazaki, T, Goodman, M. *Cyclic hexapeptide analogs of somatostatin containing bridge modifications. Syntheses and conformational analyses.* Int J Pept Protein Res, **1993** *42(4)*: 352-365.
57. Mierke, D, Pattaroni, C, Delaet, N, et al. *Cyclic hexapeptides related to somatostatin. Conformational analysis employing 1H-NMR and molecular dynamics.* Int J Pept Protein Res, **1990** *36(5)*: 418-432.
58. Yamada, Y, Post, SR, Wang, K, Tager, HS, Bell, GI, Seino, S. *Cloning and functional characterization of a family of human and mouse somatostatin receptors expressed in brain, gastrointestinal tract and kidney.* Proc Natl Acad Sci U S A, **1992** *89*: 251-255.
59. Weckbecker, G, Lewis, I, Albert, R, Schmid, HA, Hoyer, D, Bruns, C. *Opportunities in somatostatin research: biological, chemical and therapeutical aspects.* Nature Rev Drug Discovery, **2003** *2*: 999-1017.
60. Janecka, A., Zubrzycka, M, Janecki, T. *Somatostatin analogs.* J Peptide Res, **2001** *58*: 91-107.
61. Lewis, I, Bauer, W, Albert, R, et al. *A novel somatostatin mimic with broad somatotropin release inhibitory factor receptor binding and superior therapeutic potential.* J Med Chem, **2003** *46*: 2334-2344.
62. Reubi, JC, Eisenwiener, KP, Rink, H, Waser, B, and Mäcke, HR. *A new peptidic somatostatin agonist with high affinity to all somatostatin receptors.* Eur J Pharmacol, **2002** *456*: 45-49.
63. Reubi, JC, Schaer, JC, Wenger, S, Hoeger, C, Erchegyi, J, Waser, B, Rivier, J. *SST3-selective potent peptidic somatostatin receptor antagonists.* Proc Natl Acad Sci U S A., **2000** *97(25)*: 13973-13978.
64. Grace, C, Koerber, SC, Erchegyi, J, Reubi, JC, Rivier, J, Riek, R. *Novel sst(4)-selective somatostatin (SRIF) agonists. 4. Three-dimensional consensus structure by NMR.* J Med Chem, **2003** *46(26)*: 5606-5618.
65. Rivier, J, Kirby, DA, Erchegyi, J, et al. *Somatostatin receptor 1 selective analogues: 3. Dicyclic peptides.* J Med Chem, **2005** *48(2)*: 515-522.
66. Bass, RT, Buckwalter BL, Patel, BP, et al. *Identification and characterization of novel somatostatin antagonists.* Mol Pharmacol, **1996** *50*: 709-715.
67. Hocart, SJ, Jain, R, Murphy, WA, Taylor, JE, Coy DH, et al. *Highly potent cyclic disulfide antagonist of somatostatin.* J Med Chem, **1999** *42*: 1863-1871.
68. Rohrer, SP, Birzin, ET, Mosley RT, et al. *Rapid identification of subtype-selective agonists of the somatostatin receptor through combinatorial chemistry.* Science, **1998** *282*: 737-740.
69. Hirschmann, R, Nicolau, KC, Pietranico, S, et al. *Nonpeptidal peptidomimetics with β–D-glucose scaffolding. A partial somatostatin agonist bearing a close structural relationship to a potent, selective substance P antagonist.* J Am Chem Soc, **1992** *114(23):* 9217-9218.
70. De Herder, WW, Lamberts, SWJ. *Somatostatin analog therapy in treatment of gastrointestinal disorders and tumors.* Endocrine, **2003** *20*: 285-290.
71. Colao, A, Filippella, M, Di Somma, C, et al. *Somatostatin analogs in treatment of non-growth hormone-secreting pituitary adenomas.* Endocrine, **2003** *20*: 279-283.
72. Danoff, A, Kleinberg, D. *Somatostatin analogs as primary medical therapy for acromegaly.* Endocrine, **2003** *20*: 291-297.
73. Patel, YC, Srikant, CB. *Subtype selectivity of peptide analogs for all five cloned human somatostatin receptors (hSSTR 1-5).* Endocrinology, **1994** *135*: 2814-2817.
74. Krenning, E, Bakker, WH, Breeman, WA, et al. *Localisation of endocrine-related tumours with radioiodinated analogue of somatostatin.* Lancet, **1989** *1*: 242-244.
75. Behe, M, Maecke HR. *New somatostatin analogues labeled with technetium-99m [abstract]*. Eur J Nucl Med, **1995** *22*: 791.
76. Maina, T, Nock, B, Nikolopoulou, A, et al. *[^{99m}Tc]Demotate, a new ^{99m}Tc-based [Tyr^3]octreotate analogue for the detection of somatostatin receptor-positive tumours: synthesis and preclinical results.* Eur J Nucl Med Mol Imaging, **2002** *29*: 742-753.
77. Bangard, M, Behe, M, Guhlke, S, et al. *Detection of somatostatin receptor-positive tumours using the new ^{99m}Tc-tricine-HYNIC-D-Phe^1-Tyr^3-octreotide: first results in patients and comparison with ^{111}In-DTPA-D-Phe^1-octreotide.* Eur J Nucl Med, **2000** *27*(6): 628-637.
78. Wester, H, Brockmann, J, Rosch, F, et al. *PET-pharmacokinetics of ^{18}F-octreotide: a comparison with ^{67}Ga-DFO- and ^{86}Y-DTPA-octreotide.* Nucl Med Biol, **1997** *24(4)*: 275-286.
79. Schottelius, M, Poethko, T, Herz, M, et al. *First ^{18}F-labeled tracer suitable for routine clinical imaging of sst receptor-expressing tumors using positron emission tomography.* Clin Cancer Res, **2004** *10*: 3593-3606.
80. Anderson, C., Pajeau, TS, Edwards, WB, Sherman, EL, Rogers, BE, Welch, MJ. *In vitro and in vivo evaluation of copper-64-octreotide conjugates.* J Nucl Med, **1995** *36(12)*: 2315-2325.
81. Anderson, C., Dehdashti, F, Cutler, PD, et al. *^{64}Cu-TETA-octreotide as a PET imaging agent for patients with neuroendocrine tumors.* J Nucl Med, **2001** *42(2)*: 213-221.

82. Heppeler, A, Froidevaux, S, Maecke, HR, et al. *Radiometal-labelled macrocyclic chelator-derivatised somatostatin analogue with superb tumour targeting properties and potential for receptor-mediated internal radiotherapy.* Chem Eur J, **1999** *5*: 1974-1981.
83. Henze, M., Schuhmacher, J, Hipp, P, et al. *PET imaging of somatostatin receptors using [^{68}GA]DOTA-D-Phe^{1}-Tyr^{3}-octreotide: first results in patients with meningiomas.* J Nucl Med, **2001** *42(7)*: 1053-1056.
84. Froidevaux, S, Eberle, AN, Christe, M, et al. *Neuroendocrine tumor targeting: study of novel gallium-labeled somatostatin radiopeptides in a rat pancreatic tumor model.* Int J Cancer, **2002** *98(6*): 930-937.
85. Otte, A, Mueller-Brand, J, Dellas, S, Nitzsche, E, Herrmann, R, Maecke, H. *Yttrium-90-labelled somatostatin-analogue for cancer treatment.* Lancet, **1998**: 417-418.
86. Bodei, L., Cremonesi, M, Grana, C, et al. *Receptor radionuclide therapy with ^{90}Y-[DOTA]^{0}-Tyr^{3}-octreotide (^{90}Y-DOTATOC) in neuroendocrine tumours.* Eur J Nucl Med Mol Imaging, **2004** *31(7)*: 038-46.
87. Reubi, JC. *Peptide receptors as molecular targets for cancer diagnosis and therapy.* Endocr Rev, **2003** *24(4)*: 389-427.
88. Kwekkeboom DJ, Bakker, WH, Kooij PP, et al. *[^{177}Lu-DOTA^{0},Tyr^{3}]octreotate: comparison with [^{111}In-DTPA^{0}]octreotide in patients.* Eur. J. Nucl. Med., **2001** *28*: 1319-1325.
89. Reubi, JC, Schaer, JC, Waser, B, et al. *Affinity profiles for human somatostatin receptor sst1-sst5 of somatostatin radiotracers selected for scintigraphic and radiotherapeutic use.* Eur J Nucl Med, **2000** *27*: 273-282.
90. de Jong, M, Breeman, WA, Bernard, BF, et al. *[^{177}Lu-DOTA^{0},Tyr^{3}] octreotate for somatostatin receptor-targeted radionuclide therapy.* Int J Cancer, **2001** *92(5)*: 628-633.
91. Forrer, F, Uusijärvi, H, Waldherr, C, et al. *A comparison of ^{111}In-DOTATOC and ^{111}In-DOTATATE: biodistribution and dosimetry in the same patients with metastatic neuroendocrine tumours.* Eur J Nucl Med Mol Imaging, **2004** *31*: 1257-1262.
92. Smith-Jones, P, Bischof, C, Leimer, D, et al. *"Mauritius", a novel somatostatin analog for tumor diagnosis and therapy.* J Nucl Med, **1998** *39 Suppl*: 223P.
93. Virgolini, I, Szilvasi, I, Kurtaran, A, et al. *Indium-111-DOTA-lanreotide: biodistribution, safety and radiation absorbed dose in tumor patients.* J Nucl Med, **1998** *39*: 1928-1936.
94. Breeman, W, van Hagen, PM, Kwekkeboom, DJ, Visser, TJ, Krenning, EP. *Somatostatin receptor scintigraphy using [^{111}In-DTPA^{0}]RC-160 in humans: a comparison with [^{111}In-DTPA^{0}]octreotide.* Eur J Nucl Med, **1998** *25*: 182-186.
95. Zamora, P, Guhlke, S, Bender, H, et al. *Experimental radiotherapy of receptor-positive human prostate adenocarcinoma with ^{188}Re-RC-160, a directly-radiolabelled somatostatin analogue.* Int J Cancer, **1996** *65*: 214-220.
96. Buscail, L, Saint-Laurent, N, Chastre, E, et al. *Loss of sst2 somatostatin receptor gene expression in human pancreatic and colorectal cancer.* Cancer Res, **1996** *56*: 1823-1827.
97. Melacini, G, Zhu, Q, Goodman, M. *Multiconformational NMR analysis of Sandostatin (octreotide): equilibrium between β-sheet and partially helical structures.* Biochemistry, **1997** *36*: 1233-1241.
98. Wynants, C, Van Binst, G, Loosli, HR. *SMS 201-995, an octapeptide somatostatin analogue. Assignment of the ^{1}H 500 MHZ NMR spectra and conformational analysis of SMS 201-995 in dimethylsufoxide.* Int J Pept Protein Res, **1985** *25(6*): 615-621.
99. Criado, J, Li, H, Jiang, X, et al. *Structural and compositional determinants of cortistatin activity.* J Neurosci Res, **1999** *56(6)*: 611-619.
100. Pohl, E, Heine, A, Sheldrick, GM, et al. *Structure of octreotide, a somatostatin analogue.* Acta Crystallogr D Biol Crystallogr, **1995** *51*: 48-59.
101. Lamberts, S, Bakker, WH, Reubi, JC, Krenning EP. *Somatostatin-receptor imaging in the localization of endocrine tumors.* N Engl J Med, **1990** *323(18)*: 1246-1249.
102. Schottelius, M, Wester, HJ, Reubi, JC, Senekowitsch-Schmidtke, R, Schwaiger, M. *Improvement of pharmacokinetics of radioiodinated Tyr^{3}-octreotide by conjugation with carbohydrates.* Bioconj Chem, **2002** *13*: 1021-1030.
103. Wester, H, Schottelius, M, Scheidhauer, K, Reubi, JC, Wolf I, Schwaiger, M. *Comparison of radioiodinated TOC, TOCA and Mtr-TOCA: the effect of carbohydration on the pharmakinetics.* Eur J Nucl Med Mol Imaging., **2002** *29(1)*: 28-38.
104. Lin, K., Luu, A, Baidoo, KE, et al. *A new high affinity Technetium-99m-bombesin analogue with low abdominal accumulation.* Bioconj Chem, **2005** *16*: 43-50.
105. Cybulla, M, Weiner, SM, Otte, A. *End-stage renal disease after treatment with ^{90}Y-DOTATOC.* Eur J Nucl Med Mol Imaging, **2001** *28*(10): 1552-1554.
106. Boerman, OC, Oyen, WJG, Corstens, FHM. *Between the Scylla and Charybdis of peptide radionuclide therapy: hitting the tumor and saving the kidney.* Eur J Nucl Med Mol Imaging, **2001** *28*(10): 1447-1449.
107. Barone, R, Van der Smissen, P, Devuyst, O, et al. *Endocytosis of the somatostatin analogue, octreotide, by the proximal tubule-derived opossum kidney (OK) cell line.* Kidney Int, **2005** *67*: 969-976.

108. Barone, R, Borson-Chazot, F, Valkema, R, et al. *Patient-specific dosimetry in predicting renal toxicity with ^{90}Y-DOTATOC: relevance of kidney volume and dose rate in finding a dose-effect relationship.* J Nucl Med, **2005** *46*: 99S-106S.
109. Behr, TM, Becker, W, Sharkey, RM, et al. *Reduction of the renal uptake of monoclonal antibody fragments by amino acid infusion.* J Nucl Med, **1996** *37*: 829-833.
110. Barone, R, De Camps, J, Smith, C, et al. *Metabolic effects of amino acids (aa) solutions infused for renal protection.* J Nucl Med, **2000** *41*: 94P.
111. Akizawa, H, Arano, Y, Mifune, M, et al. *Effect of molecular charges on renal uptake of ^{111}In-DTPA-conjugated peptides.* Nucl Med Biol, **2001** *28*: 761-768.
112. Arano, Y, Matsushima, H, Tagawa, M. et al. *A newly designed radioimmunoconjugate releasing a hippurate-like radiometal chelate for enhanced target/non-target radioactivity.* Nucl Med Biol, **1994** *21(1)*: 63-69.
113. Arano, Y., Fujioka, Y., Akizawa, H. et al. *Chemical design of radiolabeled antibody fragments for loe renal radioactivity levels.* Cancer Res., **1999** *59*: 128-134.
114. O'Donoghue, JA, Wheldon, TE, *Targeted radiotherapy using Auger electron emitters.* Phys Med Biol, **1996** *41*: 1973-1992.
115. Behr, T, Behe, M, Lohr, M, et al. *Therapeutic advantages of Auger electron- over beta-emitting radiometals or radioiodine when conjugated to internalizing antibodies.* Eur J Nucl Med, **2000** *27(7)*: 753-765.
116. Walicka, M, Adelstein, SJ, Kassis, AI. *Indirect mechanisms contribute to biological effects produced by decay of DNA-incorporated iodine-125 in mammalian cells in vitro: clonogenic survival.* Radiat Res, **1998** *149(2)*: 142-146.
117. Walicka, M, Ding, Y, Adelstein, SJ, Kassis, AI. *Toxicity of DNA-incorporated iodine-125: quantifying the direct and indirect effects.* Radiat Res, **2000** *154*(3): 326-330.
118. Kassis, AI. *Cancer therapy with Auger Electrons: are we almost there?* J Nucl Med, **2003** *44(9)*: 1479-1481.
119. Behr, T, Sgouros, G, Vougiokas, V, et al. *Therapeutic efficacy and dose-limiting toxicity of Auger-electron vs. beta emitters in radioimmunotherapy with internalizing antibodies: evaluation of ^{125}I- vs. ^{131}I-labeled CO17-1A in a human colorectal cancer model.* Int J Cancer, **1998** *76(5)*: 738-748.
120. De Jong, M, Breeman, WA, Bernard, HF, et al. *Therapy of neuroendocrine tumors with radiolabeled somatostatin-analogues.* Q J Nucl Med, **1999** *43(4)*: 356-366
121. Capello, A, Krenning, EP, Breeman, WAP, Bernard, BF, De Jong, M. *Peptide receptor radionuclide therapy in vitro using [^{111}In-DTPA^{0}]octreotide.* J Nucl Med, **2003** *44(1*): 98-104.
122. Conti, E, Uy, M, Leighton, L, Blobel, G, Kuriyan, J. *Crystallographic analysis of the recognition of a nuclear localization signal by the nuclear import factor karyopherin alpha.* Cell, **1998** *94(2)*: 193-204.
123. Yoneda, Y, Hieda, M, Nagoshi, E, Miyamoto, Y. *Nucleocytoplasmic protein transport and recycling of Ran.* Cell Struct Funct, **1999** *24(6)*: 425-33.
124. Ferguson, SSG. *Evolving concepts in G protein-coupled receptor endocytosis: the role in receptor desensitization and signaling.* Pharmacol Rev, **2001** *53*: 1-24.
125. Prossnitz, ER. *Novel roles for arrestins in the post-endocytic trafficking of G-protein coupled receptors.* Life Sci, **2004** *75*: 893-899.
126. Hipkin, R, Friedman, J, Clark, RB, Eppler, CM, Schonbrunn, A. *Agonist-induced desensitization, internalization and phosphorylation of the sst2A somatostatin receptor.* J Biol Chem, **1997** *272*(21): 13869-13876.
127. Schwartkop, C, Kreienkamp, HJ, Richter, D. *Agonist-independent internalization and activity of a C-terminally truncated somatostatin receptor subtype 2 (Δ349).* J Neurochem, **1999** *72*: 1275-1282.
128. Roth, A, Kreienkamp, HJ, Meyerhof, W, Richter, D. *Phosphorylation of four amino acid residues in the carboxyl terminus of the rat somatostatin receptor subtype 3 is crucial for its desensitization and internalization.* J Biol Chem, **1997** *272*: 23769-23774.
129. Elberg, G, Hipjin, RW, Schonbrunn, A. *Homologous and heterologous regulation of somatostatin receptor 2.* Mol Endocrinol, **2002** *16(11)*: 2502-2514.
130. Liu, Q, Reubi, JC, Wang, Y, Knoll, BJ, Schonbrunn, A. *In vivo phosphorylation of the somatostatin 2A receptor in human tumors.* J Clin Endocrinol Metab, **2003** *88(12*): 6073-6079.
131. Pfeiffer, M, Koch, T, Schroder, H, Laugsch, M, Hollt, V, Schulz, S. *Heterodimerization of somatostatin and opioid receptors cross-modulates phosphorylation, internalization, and desensitization.* J Biol Chem, **2002** *277(22*): 19762-19772.
132. Tulipano, G, Stumm, R, Pfeiffer, M, Kreienkamp, HJ, Hollt, V, Schulz, S. *Differential beta-arrestin trafficking and endosomal sorting of somatostatin receptor subtypes.* J Biol Chem., **2004** *279*: 21374-82.
133. Stolz, B, Weckbecker, G, Smith-Jones, PM, Albert, R, Raulf, F, Bruns, C. *The somatostatin receptor-targeted radiotherapeutic [^{90}Y-DTPA-DPhe^{1},Tyr^{3}]octreotide (^{90}Y-SMT 487) eradicates experimental rat pancreatic CA 20948 tumours.* Eur J Nucl Med, **1998** *25*: 668-674.

134. Kolby L, WB, Ahlman H, Tisell LE, Fjalling M, Forssell-Aronsson E, Nilsson O. *Somatostatin receptor subtypes, octreotide scintigraphy, and clinical response to octreotide treatment in patients with neuroendocrine tumors.* World J Surg, **1998** *22(7)*: 679-683.
135. Akizawa, H, Takimoto, H, Saito, M. et al. *Effect of carboxylation of N-terminal phenylalanine of ^{111}In-DTPA (diethylentriaminepentaacetic acid)-octreotide on accumulation of radioactivity in kidney.* Biol Pharm Bull, **2004** *27(2)*: 271-272.
136. Davis, L. *The nuclear pore complex.* Annu Rev Biochem, **1995** *64*: 865-896.
137. Schwamborn, K., Albig, W, Doenecke, D. *The histone H1(0) contains multiple sequence elements for nuclear targeting.* Exp Cell Res, **1998** *244*: 206-217.
138. Kaffman, A, O'Shea, EK. *Regulation of nuclear localization: a key to a door.* Annu Rev Cell Dev Biol, **1999** *15*: 291-339.
139. Kalderon, D, Roberts, BL, Richardson, WD, Smith, AE. *A short amino acid sequence able to specify nuclear location.* Cell, **1984** *39*: 499-509.
140. Yoneda, Y, Arioka, T, Imamoto-Sonobe, N, Sugawa, H, Shimonishi, Y, Uchida, T. *Synthetic peptides containing a region of SV40 large T antigen involved in nuclear localization direct the transport of proteins into the nucleus.* Exp Cell Res, **1987** *170*: 439-452.
141. Michel, R, Castillo, ME, Andrews, PM, Mattes, MJ. *In vitro toxicity of A-431 carcinoma cells with antibodies to epidermal growth factor receptor and epithelial glycoprotein-1 conjugated to radionuclides emitting low-energy electrons.* Clin Cancer Res, **2004** *10*: 5957-5966.
142. Michel, R, Rosario, AV, Andrews, PM, Goldenberg, DM, Mattes, MJ. *Therapy of small subcutaneous B-lymphoma xenografts with antibodies conjugated to radionuclides emitting low-energy electrons.* Clin Cancer Res, **2005** *11*: 777-786.
143. Whetstone, PA, Akizawa, H, Meares, CF. *Evaluation of cleavable (Tyr^3)-octreotate derivatives for longer intracellular probe residence.* Bioconj Chem, **2004** *15*: 647-657.
144. Canman, C, Lim, DS, Cimprich, KA, et al. *Activation of the ATM kinase by ionizing radiation and phosphorylation of p53.* Science, **1998** *281*: 1677-1679.
145. Sun, T, Campbell, M, Gordon, W, Arlinghaus, RB. *Preparation and application of antibodies to phosphoamino acid sequences.* Biopolymers, **2001** *60*: 61-75.
146. Lacombe, J, Andriamanampisoa, F, Pavia, AA. *Solid-phase synthesis of peptides containing phosphoserine using phosphate tert.-butyl protecting group.* Int J Pept Protein Res, **1990** *36*(3): 275-280.
147. Vorherr, T, Bannwarth, W. *Phospho-serine and phospho-threonine building blocks for the synthesis of phosphorylated peptides by the Fmoc solid phase strategy.* Bioorg Med Chem Let, **1995** *5(22)*: 2661-2664.
148. McMurray, J, Coleman, DR, Wang, W, Campbell, ML. *The synthesis of phosphopeptides.* Biopolymers, **2001** *60*: 3-31.
149. Perich, J, Ede, NJ, Eagle, S, Bray, AM. *Synthesis of phosphopeptides by the Multipinast method: Evaluation of coupling methods for the incorporation of Fmoc- Tyr(PO$_3$Bzl,H)-OH, Fmoc-Ser(PO$_3$Bzl,H)-OH and Fmoc- Thr(PO$_3$Bzl,H)-OH.* Lett Pept Sci, **1999** *6*: 91-97.
150. Pascal, R, Schmit, PO, Mendre, C, Dufour, MN, Guillon, G. *Use of diisopropylcarbodiimide in the solid-phase synthesis of phosphorylated peptides by the preformed phosphoamino acid building block approach*. In *Peptides 2000, Proc. 26th European Peptide Symposium.* **2001**. Paris: Editions EDK.
151. Lanzetta, P, Alvarez, LJ, Reinach, PS, Candia, OA. *An improved assay for nanomole amounts of inorganic phosphate.* Anal Biochem, **1979** *100*: 95-97.
152. Schally, A, Nagy, A. *Chemotherapy targeted to cancers through tumoral hormone receptors.* Trends Endocrinol Metab, **2004** *15(7)*: 300-310.
153. Huang, C, Wu, YT, Chen, ST. *Targeting delivery of paclitaxel into tumor cells via somatostatin receptor endocytosis.* Chem Biol, **2000** *7(7)*: 453-461.
154. Vallabhajosula, S, Moyer, BR, Lister-James, J, et al. *Preclinical evaluation of technetium-99m-labeled somatostatin receptor-binding peptides.*J Nucl Med, **1996** 37(6): 1016-1022.

4

Radiometallo-labeled Peptides in Tumor Diagnosis and Therapy

Mihaela Ginj and Helmut R. Maecke

University Hospital Basel,
Institute of Nuclear Medicine, Radiological Chemistry Unit
CH-4031 Basel, Switzerland

1. INTRODUCTION

1.1. Peptides in Medicine

Peptides are necessary elements in more fundamental biological processes than any other class of molecules. The most ubiquitous mode for controlling and modulating cellular function, intercellular communication, immune response and information-transduction pathways is through peptide-protein non-covalent interactions. For example, peptides function as hormones, neurotransmitters, neuromodulators, growth and growth inhibition factors and cytokines. Although there are numerous exceptions, such as insulin, oxytocin and calcitonin, most peptide-ligands are not used directly as drugs, and often the most useful ligands for therapy would be analogues that act as agonists or antagonists of the native ligands. The development of peptides or peptide-mimetics that can target the receptors modulating the biological activities is a top priority in biology, chemistry and medicine.

Peptides play important roles in growth and other cellular functions not only in normal tissues but also in tumors. Most tumors express receptors for different peptides, frequently in high density, and many of these receptors mediate growth-regulating effects *in vitro*. Certain types of tumors also respond to the growth inhibition or growth promoting signals of peptides *in vivo*, an effect which has become an important clinical approach to treatment of tumors in man. An ubiquitous example is the use of somatostatin analogues whose receptors are overexpressed in many neoplastic tissues. A new development to visualize tumors through peptide receptor targeting began about thirteen years ago when radiolabeled somatostatin analogues were introduced into nuclear medicine for *in vivo* imaging of human tumors

using a γ camera. Nuclear medicine is mainly a diagnostic discipline; its strength has been the ability to provide images of (patho)physiological functions rather than morphological information. The development in this field advances into the direction of *in vivo* tissue characterization through imaging of biochemical markers. The use of radiolabeled analogues of regulatory peptides in nuclear oncology is an important step into this direction. The peptides as targeting agents offer several advantages over proteins as for instance antibodies. Because of their high molecular weight, antibodies have often shown limited binding and uptake at the target site and slow blood clearance, which results in modest target-to-background ratios [1,2]. In contrast, peptides are readily synthesized (solid phase synthesis, parallel and combinatorial approaches, phage-display), cheaper and can withstand harsher conditions for modification and labeling. They are less likely to produce immunogenic response, and blood clearance, tissue penetration and tumor uptake are faster.

However, there are several prerequisites for peptides used as radiopharmaceuticals. Primarily, the corresponding receptors have to be expressed on the target in suitable amounts, overexpression or unique expression being desirable. The peptide ligand should retain the high affinity to the receptor as the natural compound. For therapeutic applications internalization by endocytosis appears to be an absolute precondition, because of higher residence time. Also the preclinical biodistribution studies should provide suitable results. Last, but not least, a main concern of radiolabeled peptides is their metabolic stability, concerning not only the peptide part (i.e., peptide fragmentation by peptidases), but also the stability of the metal-chelator complex. Other aspects have to be considered when developing radiometal conjugated peptides, i.e., a high rate of complexation, the practicability of radiolabeling, the availability of the radionuclide and some other biochemical properties of the metal and metal-chelator complex that will be discussed later in this chapter.

1.2. Potential Targets of Metallo-Peptides in Diagnosis and Therapy

The main challenge in the development of targeting agents is to identify specific, relevant, easily accessible and highly expressed targets. They can be situated inside the cell (DNA, m-RNA, enzymes, proteins), on

the cell membrane (receptors) or in the cell environment (pH, pO_2, neovasculature). Proteins as targets on the plasma membrane will permit an optimal selection of disease markers and more accessible drug targets. An important target family is the one of G-protein coupled receptors which are being internalized upon peptide ligand binding.

The molecular biology studies preceding successful receptor targeting with metallo-peptides include in vitro identification and analysis of receptors with biochemical, biomolecular and immunological techniques [3]. For example, radioligand binding analysis and bioassays with cells or membrane preparations are the means to characterize high affinity binding sites and the pharmacological profile of a given peptide. Anatomical information about the distribution of receptors in tissues is obtained by quantitative receptor autoradiography which measures radioligand binding on tissue sections and thus enables localization of receptors at the microscopic level [4]. Only a minority of the large number of potentially useful regulatory peptides and peptide families has been more or less thoroughly investigated so far and future work will probably reveal a multitude of clinically useful peptide-based radioligands. Table 1 gives an overview of some typical receptors for regulatory peptides, which are (over)expressed on various human cancers and it lists the peptides studied for receptor targeting. Once the structure of the natural peptide ligand has been obtained, there are several other steps to follow until the accomplishment of a new radiopharmaceutical [5].

1.3. Prototypical Peptides for Imaging and Targeted Radiotherapy

The first diagnostically studied and also radiotherapeutically employed regulatory peptides were analogs of somatostatin (SS). Throughout this chapter the discussion will solely be based on radiometal labeled somatostatin analogs. Somatostatin is a peptide hormone with a variety of functions in many tissues throughout the body. It binds with high affinity to somatostatin receptors expressed on target tissues exerting a large number of biological effects. Five such receptor subtypes (hsst1-5) have been cloned in recent years. An important aspect with regard to targeting is the finding that these receptors are overexpressed on a variety of human tumors, mainly of neuroendocrine origin [6]. The most relevant receptor

TABLE 1

Expression of receptors on human tumors

Ligand	Receptors	Tumor type
somatostatin	somatostatin receptor subtypes sst1-5	neuroendocrine tumors, SCLC, MTC, tumors of the nervous system, lymphoma(non-Hodgkin's lymphoma, Hodgkin's disease)
VIP / PACAP	$VPAC_1$, $VPAC_2$, PAC_1 receptors	various adenocarcinomas (stomach, colon, pancreas, lung etc.)
CCK/gastrin	CCK_1, CCK_2 receptors	MTC, SCLC, stromal ovarian cancer, astrocytoma
LHRH	LHRH receptors	breast, prostate cancer
α-MSH	MSH receptors	melanoma
bombesin/GRP	BB_1, BB_2, BB_3 and BB_4 receptors	SCLC, MTC, glioblastoma, colonic cancer, prostate cancer
neurotensin	NTR1, NTR2 and NTR3 receptors	Ewing sarcoma, meningioma, MTC, astrocytoma, SCLC, exocrine pancreatic cancer
opioid	opioid receptors	SCLC, neuroblastoma, breast cancer
substance P	NK1 receptors	glioblastoma, astrocytoma, MTC, breast, peri- and intratumoral blood vessels
GLP-1	GLP-1 receptors	Insulinomas
oxytocin	oxytocin receptors	endometrium, breast cancer
neuropeptide Y	NPY receptors subtypes Y_1-Y_6	breast, brain cancer

subtype is hsst2, but all the other receptor subtypes are to some degree also overexpressed on human tumors. There are two biologically active forms of SS consisting of 14 (SS-14) and 28 (SS-28) amino acids that

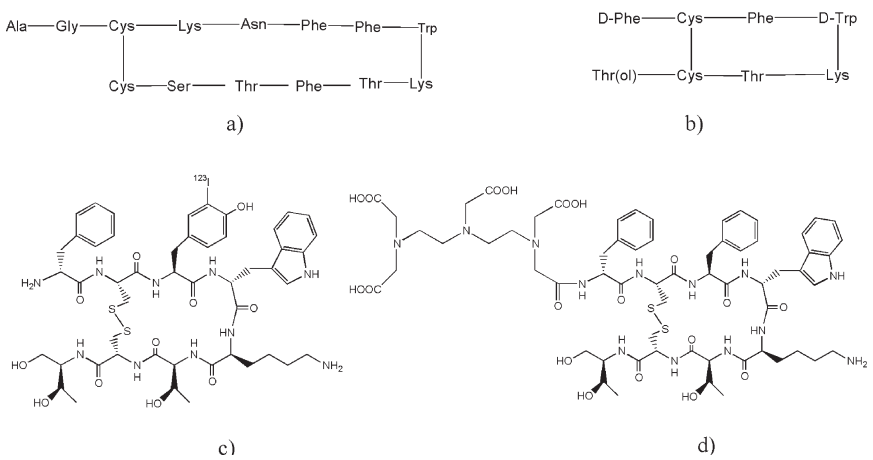

FIG. 1. Structural formula for: (a) SS-14; (b) octreotide; (c) [^{123}I]-[3-iodo-Tyr^3]-octreotide; (d) DTPA-octreotide (Octreoscan®).

show only very low metabolic stability in human blood with half lives of 2-3 min and can therefore not be used clinically. Modifications leading to octapeptides afforded somatostatin receptor binding ligands with much lower proteolytic degradation rate. One of the clinically approved peptides is octreotide, a short analog of somatostatin which retained a high binding affinity to hsst2, reduced affinity to hsst3 and hsst5 and absent affinity to hsst1 and hsst4 (see Table 4 in Section 3.3). The chemical structures of SS-14 and octreotide are shown in Figure 1.

The first radiopeptide used for *in vivo* localization of tumors was [^{123}I]-[3-iodo-Tyr^3]-octreotide (Figure 1c). Despite some spectacular early imaging results [7] and an almost optimal pharmacologic profile showing high somatostatin receptor affinity (IC_{50} = 2.0 ± 0.7 nM) and a high rate of internalization into tumor cells, this radioligand finally turned out not to be useful as a diagnostic tool. The reasons are its lipophilicity causing hepatobilary excretion and therefore a very low diagnostic sensitivity in the abdomen. Contrary, the chelator-modified molecule, DTPA-octreotide (Figure 1d), which was designed to be complexed with the diagnostic radiometal $^{111}In^{3+}$, shows a rather low *in vitro* pharmacologic profile (low

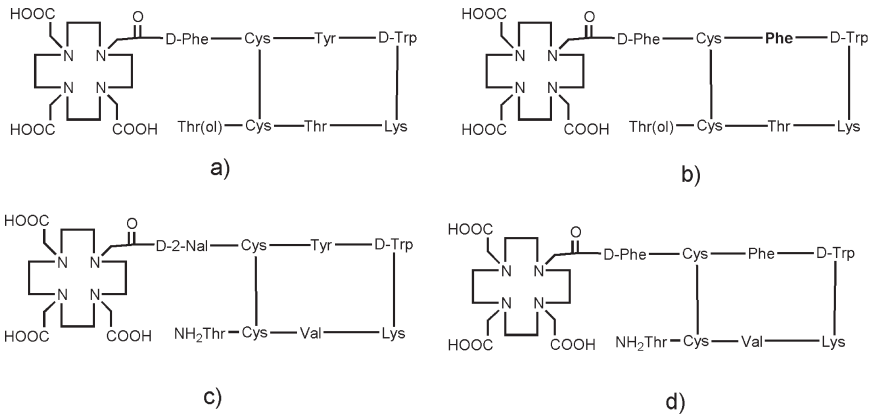

FIG. 2. Prototypical DOTA-peptides used for radiotherapy: (a) DOTA-[Tyr^3]-octreotide (DOTA-TOC); (b) DOTA-octreotide (DOTA-OC); (c) DOTA-lanreotide (DOTA-LAN); (d) DOTA-vapreotide.

binding affinity $IC_{50} = 22 \pm 3.6$ nM and slow internalization rate), but the hydrophilic metal complex conveys high hydrophilicity to the targeting molecule and changes its pharmacokinetics, including predominant kidney excretion. Consequently, it became the first imaging vector based on a radiopeptide (the commercial name is Octreoscan®), registered worldwide. In addition, the advantage of the DTPA-peptide conjugate was the highly practical labeling kinetics which can be performed in any nuclear medicine department or even in a private nuclear medicine practice, whereas the iodination labeling process is tedious, needs well educated and trained personnel and can therefore only be performed in specialized laboratories.

^{111}In is not an useful therapeutic radionuclide (see Section 2.1.), therefore conjugates were designed, synthesized and evaluated preclinically which fulfilled the need for the labeling with the β-emitters, e.g., ^{90}Y and ^{177}Lu. DOTA (1,4,7,10-tetraazacyclododecane-1,4,7,10-tetraacetic acid) was the preferred chelator, forming kinetically and thermodynamically stable metal complexes. The prototypical DOTA-coupled somatostatin based octapeptides used for radiotherapy are shown in Figure 2.

2. RADIOMETALS OF INTEREST FOR PEPTIDE LABELING AND LABELING APPROACHES

2.1. Radiometals for Peptide Labeling

The use of metal complexes as diagnostic and therapeutic agents is a relatively new area of medical research. The introduction of radiometals in nuclear medicine has started in 1959 when the first $^{99}Mo/^{99m}Tc$ generator was developed at Brookhaven National Laboratory. Since then ^{99m}Tc is the most widely used radionuclide for diagnostic imaging. From the perspective of coordination chemistry there are two important features of clinically used ^{99m}Tc: (1) The generator defines the starting material of any ^{99m}Tc radiopharmaceutical preparation to be an aqueous sodium chloride solution of $^{99m}TcO_4^-$ and $^{99}TcO_4^-$. (2) Because of the nature of the generator decay scheme $^{99}Mo \rightarrow {}^{99m}Tc \rightarrow {}^{99}Tc$ the concentration of $^{99m}TcO_4^-$ and $^{99}TcO_4^-$ are variable depending mainly on the time elapsed since the last generator elution. The total concentration of $^{99}TcO_4^- + {}^{99m}TcO_4^-$ in generator eluents is in the range of 10^{-6} - 10^{-8} M. So the synthesis of a ^{99m}Tc radiopharmaceutical must be done at very low concentrations and must start with TcO_4^-. The first step will be a reduction of TcO_4^- to lower oxidation states, most importantly Tc^V and Tc^I.

For therapeutic applications radioisotopes of Re, the group VIIA congener of Tc, became of interest. Two isotopes are of importance for targeted radiotherapy: ^{186}Re and ^{188}Re (see Table 3 below). Both have suitable properties as they do not only emit β but also γ rays allowing to follow the biodistribution. Rhenium-186 is reactor produced and contains carrier ^{185}Re, whereas rhenium-188 is carrier free and is obtained from a $^{188}W/^{188}Re$ generator.

Because of the periodic relationship Tc and Re are called “matched pair”, one used for diagnostic and dosimetric purposes and as model for Re radiopharmaceuticals development and the Re-labeled agent for therapeutic applications. However there are important chemical differences. Despite this, the strategies to label peptides with Tc and Re are until now the same.

Today there is a large variety of radiometals used in γ scintigraphy and positron emission tomography for diagnosis and in targeted radiotherapy.

The γ scintigraphy requires a radiopharmaceutical containing a radionuclide that emits γ radiation with an energy between 100-250 keV and a

γ camera or a SPECT camera. PET requires a radiopharmaceutical labeled with a positron emitting radionuclide (β^+) and a PET camera. A variety of metallic gamma- and positron-emitters have been used for peptide labeling (Table 2) [8]. Besides the energy of emission there are some other factors to consider in designing a radiometal-based radiopharmaceutical, like the physical half-life, the type of decay, cost and availability of the radioisotope.

TABLE 2

Important γ and positron emitting radionuclides for biomolecule labeling

Isotope	Physical Half-life (h)	Decay Mode	E_γ (keV)	$E_{\beta+}$ (keV)
Ga-67	78.26	EC (100%)	91, 93, 185, 296, 388	
Tc-99m	6.0	IT (100%)	141	
In-111	67.9	EC (100%)	245, 172	
Co-55	17.5	β (77%) EC (23%)		1513, 1037
Cu-62	0.16	β (98%) EC (2%)		2910
Cu-64	12.7	β (19%) EC (41%) β^- (40%)		656
Ga-68	1.1	β (90%) EC (10%)		1880, 770
Y-86	14.7	β (33%) EC (66%)		2335, 2019, 1603, 1248, 1043

EC = electron capture, IT = internal transfer

Unlike radionuclides used for diagnostic imaging, therapeutic radionuclides by definition emit radiations that have a high linear energy transfer (LET) in order to destroy tumor tissue. These species with potential for

therapy fall into three main categories: (i) β emitting radionuclides; (ii) α emitting radionuclides; (iii) Auger electron emitting radionuclides. Each type of these particles has different effective range of energy deposition and LET properties.

The physical characteristics and range in tissues of commonly used beta and alpha emitters are summarized in Table 3 [9]. In cases where the γ ray emission is in the diagnostically useful range, the imaging of the tracer biodistribution is also feasible [10]. Radionuclides that decay by β particle emission are used most extensively for therapeutic applications in current clinical practice. A unique advantage of β emitters over other therapeutic modalities is that not every cell needs to be targeted to be killed (crossfire effect, low LET). This result is efficient for lesions larger in diameter than the average path length. Humm [11] has classified β-emitting radionuclides as low-range (mean range < 200 μm, i.e., Lu-177), medium-range (mean range 200 μm to < 1 mm, i.e. Cu-67, Sm-153) and high range (mean range > 1 mm, i.e., Y-90). Radioactive emission of α particles results in high LET over a path length of 3-4 cells diameters. The advantage of this property lies in their capability of producing a high degree of tumoricidal activity while sparing the surrounding normal tissues.

However, the ultimate success of the targeted radiodiagnosis and -therapy depends, of course, on the biological properties (e.g., specificity, affinity, blood and tumor clearance rates, etc.) of the radiopharmaceutical (metal-chelator-peptide conjugate).

2.2. Labeling Approaches

2.2.1. Direct Labeling

Because of the kinetic lability of hard radiometals like Y^{3+}, Lu^{3+}, lanthanides in general, but also Cu^{2+}, Co^{2+}, etc., and the competition in human blood and other body fluids by proteins like transferrin, albumin and anions like PO_4^{3-}, CO_3^{2-}, etc., peptides can not offer any functional groups which provide enough kinetic stability to ensure intact arrival of the radiometal-peptide conjugate at the target. This is different for the pair Tc and Re which form kinetically inert metal complexes in several oxidation states. In addition, both metals show a high degree of thiophilicity

TABLE 3

Nuclear properties of several therapeutic radiometals

Isotope	Physical Half-life	Decay mode		Range	
		max β^- (MeV)	γ (keV)	mean (mm)	Approximate Cell Diameter[a]
Cu-67	2.58 d	0.577 (20%)	91 (7%) 93 (16%) 185 (48%)	0.27	20
Y-90	2.67 d	2.27 (100%)	none	2.8	150
Pm-149	2.21 d	1.07	286 (3%)	0.71	60
Dy-166	3.40 d	0.40	82.5	0.18	15
Lu-177	6.71 d	0.50 (79%)	208 (11%) 113 (6.4 %)	0.24	20
Re-186	90.6 h	1.071	137	0.7	60
Re-188	16.98 h	2.116	155	2.4	130
Bi-212	1 h	1.36 (β, 64%) 6.1 (α, 36%)	727 (7%)	0.09 0.06	2-3 3-4
Bi-213	46 min	5.8 (α, 2.2%) 8.4 (α, 97.8%)	440	0.06 0.08	2-3 3-4
Ac-225	10 d	5.83 (α,100%)	none	0.06	2-3

[a] Refers to the number of cells in length crossed by these radiations.

making sulfur containing peptidic sequences attractive for the binding of these radiometals. Several groups took advantage of this thiophilicity and labeled disulfide-bridged analogs of somatostatin like octreotide, lanreotide and vapreotide directly with ^{99m}Tc and ^{188}Re [12]. Unfortunately,

none of these peptides is very well characterized; in addition, they are too lipophilic, mainly excreted by the hepatobiliary system and never made the step from preclinical studies to the clinic. Still, Re-vapreotide (Figure2d) was synthesized on a macroscopic level and studied using two dimensional ^{1}H-NMR spectroscopy and molecular dynamic simulations [13]. It was found that the metal coordinated peptide maintains the spatial topography and solution conformation as the unmodified peptide consisting of an antiparallel β sheet and type II β turn around D-Trp^{4}-Lys^{5}. The study did not confirm the hypothesis that during synthesis the disulfide bridge is opened creating two thiolate groups for ^{99m}Tc and ^{188}Re coordination and no receptor affinities have been reported for these peptides.

2.2.2. The Bifunctional Chelator Approach

As shown in the previous paragraph in some cases a direct labeling approach can be adopted. However, labeling strategies usually rely on the utilization of a multidentate ligand capable of chelation of the desired radionuclide. For example, all radiometals except ^{67}Cu and ^{55}Co listed in Table 3 are hard acids with 3+ as the major oxidation state in solution. As they are kinetically labile, polydentate chelators need to be utilized for an efficient encapsulation and *in vivo* stabilization.

There are mainly two strategies: the prelabeling and the postlabeling methods. The prelabeling approach involves the formation of the radionuclide-chelator complex prior to conjugation to the peptide. If the radionuclide is introduced into its chelator after the chelator has been attached to the carrier, this is referred to as postlabeling. The decision on which strategy is to be adopted will be influenced by a variety of considerations. For example, when complex formation can only be achieved under non-aqueous or otherwise harsh conditions and the biomolecule is sensitive to these conditions, the prelabeling approach is more indicated. Still, this method is complicated and time-consuming because of multiple steps in preparation and purification and therefore not suitable for routine clinical applications [14]. The postlabeling approach is the most practical method for the development of commercial peptide-based radiopharmaceuticals.

The ideal chelator should satisfy requirements correlating aspects of coordination chemistry with *in vivo* behavior. Factors to be considered

include the redox properties, stability, stereochemistry, charge and lipophilicity of the metal complex [14]. For lanthanides and lanthanide-like radiometals, the bifunctional octadentate chelators satisfy these requirements. Derivatives of diethylentriaminepentaacetic acid (DTPA) are used for the fast incorporation of radiometals; the first clinically approved peptide-based imaging agent has been the DTPA-derivatised somatostatin analogue octreotide labeled with ^{111}In (Figure 1d). The coupling to the peptide is achieved either by using DTPA dianhydride [15] or tri-*t*butyl-DTPA [16] as prochelators (Figure 3). This potential octadenticity of DTPA may convey additional stability to the radiometal complex as $In(DTPA)^{2-}$ was shown to have coordination number 8 in the solid state and in solution [17]. Because of *in vivo* instability, DTPA is not suitable for any other nuclide than ^{111}In. Attempts to use DTPA-peptide conjugates labeled with ^{90}Y for therapy [18] have not been as successful as the use of macrocyclic BFC for labeling of peptides [19].

Radiolabeling with Ga^{III} is of interest because of the access to three radioisopes for imaging (Table 2). Two approaches were used to label somatostatin analogs with radio-gallium. The use of DFO (desferrioxamine B) (Figure 4a) allowed fast complexation, whereas the new chelator NODASA (1,4,7-triazacyclononane-1-succinic acid-4,7-diacetic acid) (Figure 4b) [20] has three 5-membered chelate rings involving carboxylate groups which are thus protected by Ga(III) allowing a free β carboxylate group for coupling to a somatostatin analog. This prelabeling strategy allows the covalent coupling of a well defined radiometal complex of high specific activity to a biomolecule. The same type of chelator has been derivatized in order to make it available also for the postlabeling approach [21].

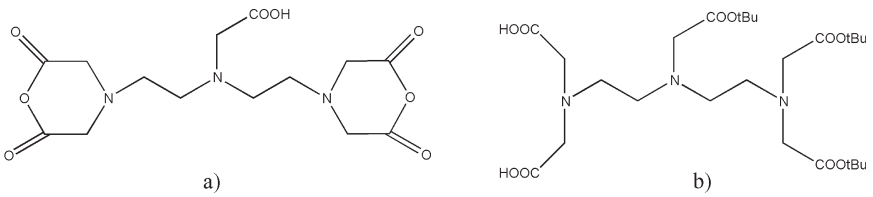

FIG. 3. Precursors of diethylentriaminepentaacetic acid (DTPA) for biomolecule coupling: (a) DTPA dianhydride (cDTPA); (b) tri-t-butyl-DTPA (activated via cyclic anhydride formation).

Unlike the acyclic analogs, the polyazamacrocyclic polycarboxylate ligands provide a higher degree of rigidity to the resulting metal complexes, and therefore improved kinetic inertness *in vivo* [14]. The DOTA-based BFCs (Figure 5 a-c) continue to be the most widely studied ligands for linking trivalent metallic radioisotopes to biomolecules [22-25]. The most common method involves the attachment of the peptide to one of the four acetate groups via a CO-NH bond. This conjugation can be made either via an activated ester of one carboxylate group, like NHS esters (Figure 5a), or using a monoreactive DOTA prochelator like DOTA$(tBu)_3$ (Figure 5b) [26]. The prochelator approach is perfectly compatible with peptide synthesis in solid phase or in solution and DOTA$(tBu)_3$ was coupled to somatostatin analogs with 65 ± 5 % yields after deprotection and purification. DOTA, used unprotected, was also coupled to the same peptide with about 40 % overall yield [26].

A disadvantage of this type of conjugation is the loss of one acetate arm for coordination to the radiometal center. To provide eight donor atoms for coordination, DOTA has been modified at one of the nitrogen atoms (Figure 5c) [27]. After coupling to the biomolecule and deprotection a BFC-peptide conjugate is obtained, available for the labeling with different radiometals (^{111}In, ^{90}Y, ^{177}Lu, and other lanthanides).

The labeling of peptides with radioisopes of Cu(II) is of interest mainly because of its two radionuclides ^{64}Cu and ^{67}Cu. The chemistry of copper

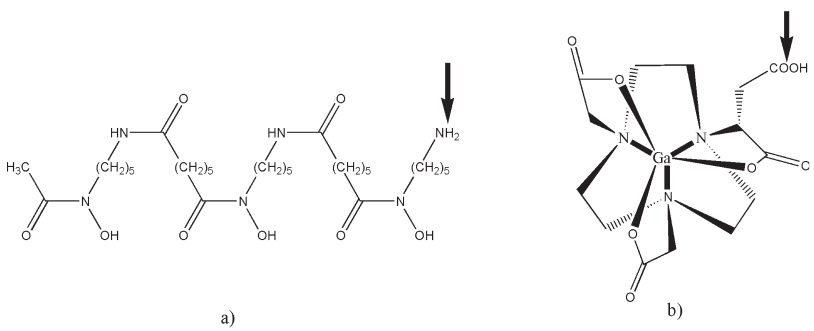

FIG. 4. (a) Desferrioxamine-B (DFO), a bifunctional chelator for labeling with $^{67/68}$Ga; (b) Ga(NODASA), a (radio)metal complex with three metal-protected carboxylate groups and the potential for biomolecule coupling using the prelabeling approach. The coupling site is indicated by the arrow.

radiopharmaceuticals has been reviewed extensively and comprehensively [28]. BFCs for Cu(II) include 4-(1,4,8,11-tetraazacyclotetradec-1-yl)methyl)benzoic acid (CPTA) (Figure 5d), 1,4,8,11-tetra-azacyclotetradecane-1,4,8,11-tetraacetic acid (TETA) (Figure 5e) and DOTA. All three chelators were coupled to the somatostatin analogs through a carboxylate group.

Several approaches to label somatostatin analogs with BFCs for ^{99m}Tc labeling have been published. HYNIC (2-hydrazinonicotinic acid) (Figure 6a) is of interest as a ^{99m}Tc-binding unit because of the potential monodenticity of this ligand which leaves coordination sites on the Tc atom free to be completed by different coligands which may be beneficial for the fine tuning of the biodistribution. HYNIC was described before to label successfully different biomolecules with ^{99m}Tc [29,30]. [^{99m}Tc-N_4-D-Phe^1]-octreotide (FIG. 6b) was shown to bind with high affinity to the SRIF receptor and showed high and specific uptake in a SRIF

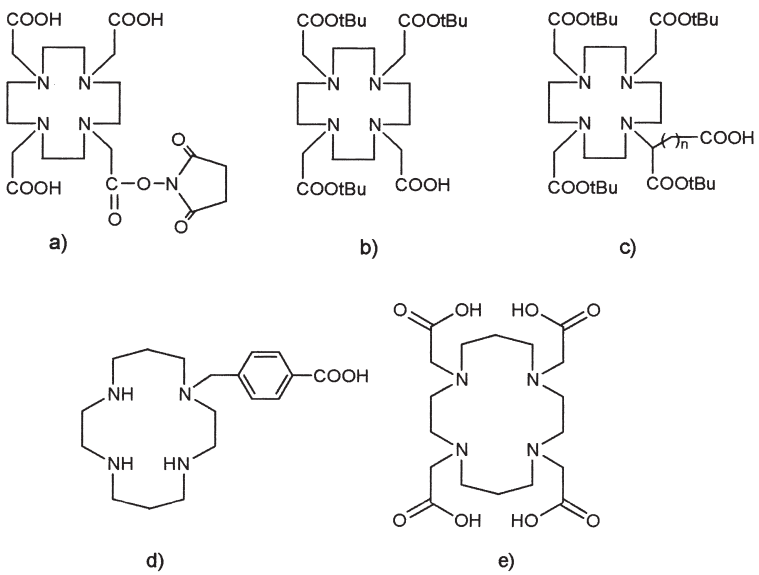

FIG. 5. Structures of DOTA derivatives: (a) *N*-hydroxysuccinimide (NHS) ester of DOTA; (b) tri-*t*-butyl-DOTA; (c) DOTASA(tBu)$_4$, n = 1 and DOTAGA(tBu)$_4$, n = 2; (d) CPTA; (e) TETA.

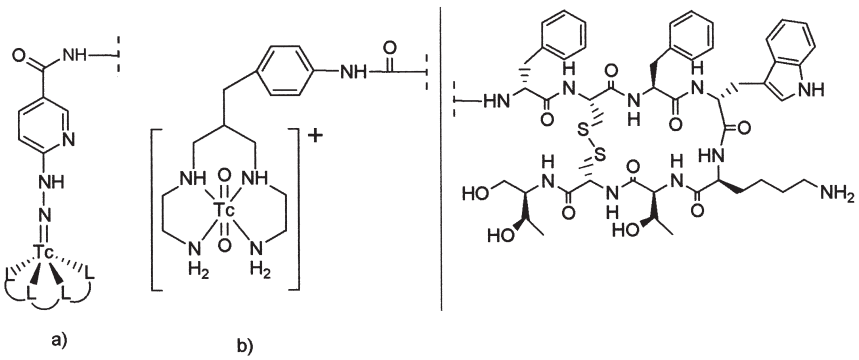

FIG. 6. (a) Structure of Tc-HYNIC-octreotide; (b) ^{99m}Tc-labeling of octreotide, using the N_4-tetraamine chelator.

receptor-positive tumor [31].

3. *IN VITRO* CHARACTERIZATION OF RADIOMETALLO-PEPTIDES

3.1. Labeling Protocols

Because of the low concentrations of radiometal solutions (often lower than 10^{-6} M, showing the need to choose optimal complexation conditions) and the necessity to produce the radiopeptides in high purity in a safe and rapid way, the labeling (complexation) protocols are of major importance. The choice of the radiolabeling approach depends on the type of biomolecules to be labeled and the purpose of the study. As mentioned in Section 2.2.2., there are mainly two labeling strategies: the pre- and the postconjugation labeling.

DTPA-peptide-conjugates can be readily radiolabeled within 10 min at room temperature and pH 5-7, using an acetate or a citrate buffer. The high radiolabeling efficiency can be attributed to the linear chelator backbone of DTPA analogues. However, the kinetic lability of their metal complexes may prove to be problematic when they are used as BFCs for biomolecules having a long blood retention.

The radiolabeling efficiency of a macrocyclic chelator is largely dependent upon radiolabeling conditions: concentration of BFC-conju-

gate, concentration of trace metal contaminants, pH, temperature, reaction time. There are several studies on the influence of all these factors on the radiolabeling efficiency for lanthanides (^{177}Lu) and ^{90}Y, these being the most often used radionuclides in radiotherapy. Summarized e.g., for ^{90}Y, the conclusions are: the radiolabeling efficiency is maximal when the chelator-to-metal ratio is > 3; the presence of increasing amounts of trace metals (Ca^{2+}, Fe^{2+}, Zn^{2+}), commonly found in commercial ^{90}Y preparations, inhibits the labeling in a concentration-dependent manner; higher pH results in faster complexation rate [35], but the potential precipitation of $Y(OH)_3$ has to be taken into consideration, weakly coordinating buffer anions stabilize the radiometals in solution; higher temperature and longer reaction time usually gives better radiolabeling yield provided that the biomolecule is not subjected to thermal decomposition.

3.2. Stability Measurements

The *in vivo* stability of the metal-chelate bond is critical in a metalloradiopharmaceutical. When ^{90}Y or a radiolanthanide is released *in vivo*, it accumulates in bone giving a radiation dose to the radiosensitive bone marrow [32]. There appear to be three major mechanisms that challenge the coordination complex stability: transchelation to metal-seeking serum proteins, competition with anions (see above) and exposure to the acidic environment of the tumor and of the lysosomes as a result of biomolecule catabolism [33, 34] .

High thermodynamic stability is not the sole requirement of a metal chelate complex because it only reflects the direction, not the rate of the reaction. As a matter of fact, the solution stability of a metalloradiopharmaceutical in the blood stream is predominantly determined by the kinetic inertness of the metal chelate. While fast dissociation kinetics are characteristic of metal complexes of acyclic chelators, many references have shown that metal complexes containing macrocyclic chelators are much more kinetically inert [35-37]. This has been clearly demonstrated by the extremely high solution stability of ^{90}Y-labeled macrocycles such as DOTA even though the thermodynamic stability constant of $Y(DOTA)^-$ is comparable to that of $Y(DTPA)^{2-}$.

Human serum stability measurements are accepted methods for the evaluation of radiolabeled ligands, along with pH stability. Neither of these two *in vitro* analyses alone can mimic the challenging environment that a radiolabeled chelator complex encounters *in vivo*. However, both analyses can be useful in determining the optimal chelator for utilization with the metal of choice [21, 38, 39].

Focusing on the peptide part in a peptide-based radiopharmaceutical, it is clear that lipophilicity, peptide size and susceptibility to degradation by peptidases play a vital role [40].

3.3. Determination of the Binding Affinity of Radiometallo-Peptides to Their Targets

After testing the stability of a radiometallo-peptide, the next in vitro assay is the determination of the receptor binding affinity of the radiopharmaceuticals designed for receptor targeting. Introducing a chelator may strongly affect the biological and pharmacological properties of a peptide. This assay can be performed on intact cells or on membrane preparations, either by direct or competitive binding assays, thereby assessing alterations in affinity and specificity of the radiopeptide compared to the natural peptide [41]. As shown in Table 1, there are several receptors (over)expressed on different types of tumors, therefore knowing the affinity pattern for receptor subtypes is very important, since each subtype usually has a different expression profile on different tumor types. This is definitely true especially for somatostatin receptors, sstr1-5 [6]. Table 4 displays the affinity profiles of the somatostatin analogues shown in Figure 2 a-c, along with their Y(III)-chelator-peptide conjugates in comparison with the natural peptide somatostatin-28 (SS-28) and with octreotide. The binding affinities are expressed as IC_{50} values, using ^{125}I-[Leu^{8}, D-Trp^{22}, Tyr^{25}]-somatostatin 28 as radioligand. The assumption made is that non-radioactive metals behave like their radioactive congeners. Although remote to the pharmacophoric site of the peptide, the chelator and the metal exert their influence on the binding affinity profile. Moreover, the same chelator-peptide conjugate complexed with different metals has a different binding affinity for the same receptor subtype (Figure 7). Details on this item are given in Section 5 of this chapter.

TABLE 4

Affinity profiles (IC_{50}) for human sst1-sst5 receptors for a series of somatostatin analogues.

Compound	sst1	sst2	sst3	sst4	sst5
SS-28	5.2±0.3	2.7 ± 0.3	7.7 ± 0.9	5.6 ± 0.4	4.0 ± 0.3
Octreotide	>10000	2.0 ± 0.7	187 ± 0.355	>1000	22 ± 6
DOTA-octreotide	>10000	14 ± 3	27 ± 9	>1000	103 ± 39
Y-DOTA-octreotide	>10000	20 ± 2	27 ± 8	>10000	57 ± 22
[Tyr^3]-octreotide	>1000	2.1±1.0	85 ± 21	350 ± 110	5.0 ± 2.0
DOTA-[Tyr^3] -octreotide	>10000	14 ± 2.6	880 ± 324	>1000	393 ± 84
Y- DOTA-[Tyr^3] -octreotide	>10000	11 ± 1.7	389 ± 135	>1000	114 ± 29
DOTA-lanreotide	>10000	26 ± 3.4	771 ± 229	>1000	73 ± 12
Y-DOTA-lanreotide	>10000	23 ± 5	290 ± 10	>1000	16 ± 3.4

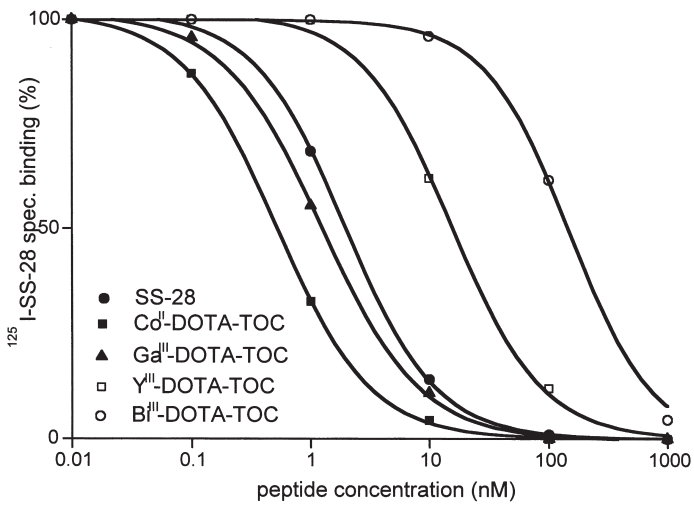

FIG. 7. Influence of (radio)metal on receptor (sst2) binding affinities: competitive binding experiments using ^{125}I-[Leu^8, D-Trp^{22}, Tyr^{25}]-somatostatin-28 as radioligand and various metal-DOTA-TOC complexes as competitors. SS-28 was used as a control peptide.

4. ANIMAL MODELS TO STUDY TARGETING OF TUMORS. BIODISTRIBUTION AND THERAPY STUDIES

The *in vivo* evaluation in animal models of radiometallo-peptides is of major importance, since it is the first "real" indicator of compound pharmacokinetics. As a model, tumor cells for which the peptide is being investigated are transferred from cell culture into nude mice or rats, inducing tumor growth. Upon administration of the labeled peptide in these experimentally grown tumors, the potential of tumor targeting can be evaluated. An important aspect of this is the proof of specificity of tumor targeting due to the possibility to block the receptors with excess cold (non-radioactive signal producing) peptide. Such an example is shown in Figure 8 with two rats bearing subcutaneous tumors in the left hind leg. One animal was only injected with ^{111}In-DOTA-TOC (Figure 8b) and the tumor is nicely shown as well as the receptor positive pancreas. In the second rat (Figure

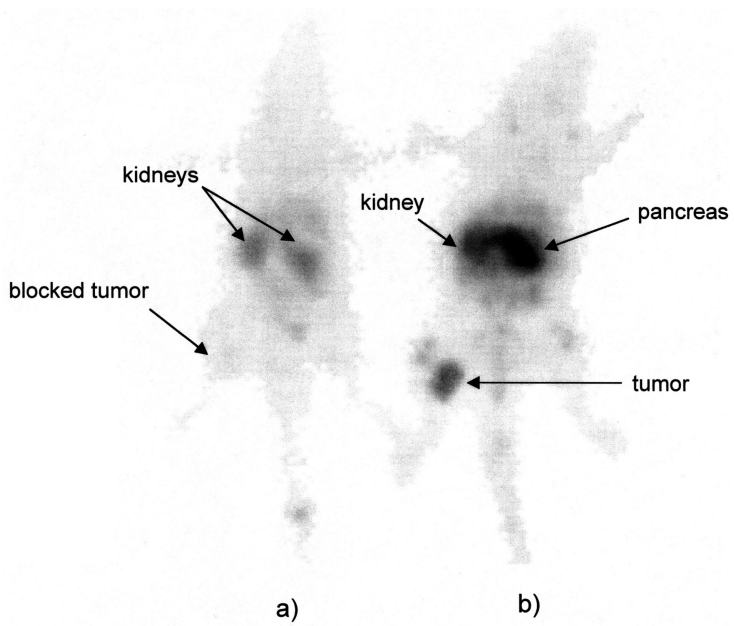

FIG. 8. Four hours postinjection scintigraphy of two Lewis rats bearing subcutaneous tumors in the left hind leg: (a) rat with a coinjection of ^{111}In-DOTA-TOC and excess of cold peptide; (b) rat injected only with ^{111}In-DOTA-TOC.

8a) about 500 times excess of non-radiolabeled peptide is co-injected with ^{111}In-DOTA-TOC, competing for the receptors; no radioactive signal is seen from the tumor and the pancreas.

The aim of biodistribution studies in animal models is the evaluation of radiolabeled peptide uptake in different organs, especially in the receptor-positive organs and in kidneys. For clinical applications of a radiopharmaceutical, the kidney toxicity is the dose limiting factor. Peptides are taken up by the tubular cells and radiometal chelates are trapped within the lysosomes, high retention of the radiolabel occurring in the kidneys, eventually causing nephrotoxicity [44].

Figure 9 shows a comparison in biodistribution in AR4-2J rat pancreatic tumor bearing Lewis rats of four compounds: ^{111}In-octreoscan (see structure in Figure 1d) and DOTA-TOC (see Figure 2a) labeled with three different radiometals: ^{111}In, ^{90}Y and ^{67}Ga, respectively [22]. The best tumor-to-kidney ratio corresponds to the gallium-labeled compound, this result being confirmed also in patients (see Section 5). As shown also in Section 3.3., the (radio)metal has a significant influence on the properties (binding affinity, internalization, biodistribution) of the radiopharmaceutical. In addition, this study shows the superiority of the new compounds over the approved ^{111}In-octreoscan and was the basis to introduce the improved versions into the clinic.

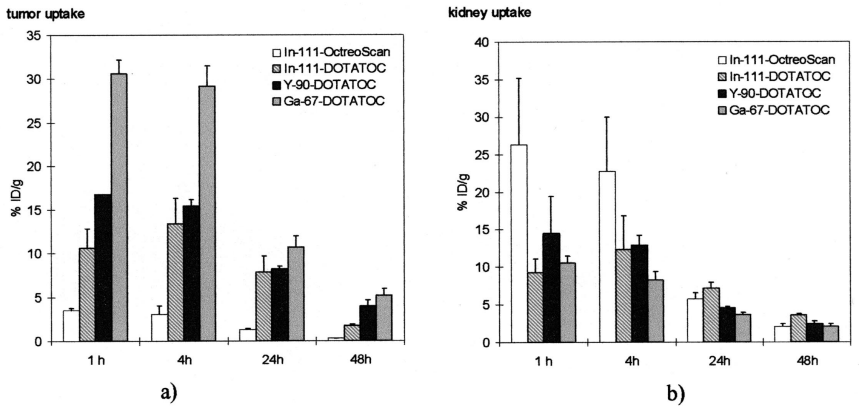

FIG. 9. (a) Tumor and (b) kidney uptake of ^{111}In-, ^{67}Ga- and ^{90}Y-DOTA-TOC in comparison with Octreoscan.

Before therapeutic clinical applications can be performed, radiotherapy studies in animals will be done. For example, Stolz et al. [47] evaluated the therapeutical effect of ^{90}Y-DOTA-TOC on rats bearing CA20948 tumors. Their result showed complete remission of tumors in five out of seven rats. De Jong et al. [45] demonstrated with different somatostatin analogs and different radiometals that the cure rate depends on tumor size, having 100% remission for small tumors. Zamora et al. [46] investigated analogues of somatostatin directly labeled with ^{188}Re in nude mice bearing xenografts of human prostate adenocarcinoma.

All these in vivo tests, along with the in vitro assays presented in Section 3 are helpful for designing and developing new and improved radiopharmaceuticals. However, compounds that look promising in animal models are not necessarily working in humans.

5. INFLUENCE OF THE (RADIO)METAL ION AND ITS COORDINATION CHEMISTRY ON THE TARGETING PROPERTIES OF RADIOMETALLOPEPTIDES

In this section we will analyze the important role of the radiometal complex geometry as well as charge, size, fluxionality, etc., on DOTA-[Tyr^3]-octreotide pharmacology.

As discussed above, the most widely used chelator for radiometals is DOTA. Except for the labeling of biomolecules with ^{99m}Tc and ^{186,188}Re, it has been used for all other radiometals of relevance in nuclear oncology. The use of one single chelator and one single chelator-peptide conjugate for a variety of radiometals has the advantage that potential clinical applications will be approved easier by ethical committees. The gold standard molecule for the *in vivo* localization of somatostatin receptor positive tumors and their targeted radionuclide therapy is [DOTA^0-Tyr^3]-octreotide. This molecule has been labeled with ^{66,67,68}Ga^{III}, ^{111}In^{III}, ^{90}Y^{III}, ^{213}Bi^{III}, and ^{57}Co^{II}. Figure 7 shows the binding characteristics of several metallo-peptides to sstr2 versus a ^{125}I-labeled SS-28 as radioligand. An important result of this experiment is that obviously the metal ion has a marked influence on the affinity of the metallo-peptide; e.g., Co^{II}-DOTATOC shows a better sstr2 binding than Ga^{III}-DOTATOC, Y^{III}-DOTATOC, and Bi^{III}-DOTATOC. As dem-

onstrated, the conjugation of the metal-DOTA complex may even result in an improved ligand compared to the natural peptide. It is not yet clear why the metal ion, which is remote from the pharmacologic part of the peptide, has such a distinct influence.

Preliminary comparative data using two-dimensional ^{1}H-NMR studies of the Ga^{III}-, In^{III}-, Y^{III}-DOTATOC are not conclusive and the peptides resist crystallization. The model peptides In^{III}-, Y^{III}-, Ga^{III}-DOTA-D-$PheNH_2$, however, could be crystallized and their X-ray crystal structure determined. The structures differ in different ways. Ga^{III}-DOTA-D-$PheNH_2$ (Figure 10a) has a pseudooctahedral structure, the macrocycle showing a cis-geometry. The equatorial plane is formed by two transannular nitrogens of the tetraaza ring and two oxygens of the respective carboxylate groups. One carboxylate group is free and the carbonyl oxygen of the peptide bond forming the linkage to D-$PheNH_2$ is not bound to the Ga^{III}. This is in contrast to $Y^{III}(In^{III})$-DOTA-D-$PheNH_2$ (Figure 10b) which are octacoordinate complexes including the amide carboxy oxygen [22]. The complex geometry is a somewhat distorted antiprism. ^{1}H-NMR studies showed that also in solution the Ga^{III}-complex is hexacoordinate whereas the Y^{III}-DOTA-D-$PheNH_2$ and In^{III}-DOTA-D-$PheNH_2$ complexes are octacoordinate, the later showing much higher fluxionality [42]

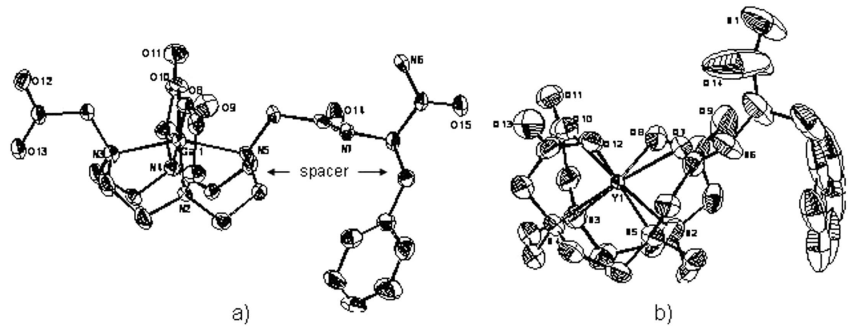

FIG. 10. (a) ORTEP plot of the crystal structure of Ga^{III}-DOTA-D-$PheNH_2$, a pseudooctahedral structure with a *cis* geometry of the macrocycle. One carboxylate group is free and the carbonyl oxygen of the peptide bond forming the linkage to D-$PheNH_2$ is not bound to Ga^{III}; (b) ORTEP representation of the crystal structure of Y^{III}-DOTA-D-$PheNH_2$, an octacoordinate complex including the amide carboxy oxygen. Reproduced by permission from ref. 22.

which may explain the differences between ^{111}In- and ^{90}Y-DOTA-TOC in the biodistribution study.

The hexacoordination of the Ga^{III}-complex may explain the improved kidney clearance of ^{68}Ga-DOTA-TOC compared to ^{90}Y-DOTA-TOC and the improved pharmacological profile may depend on the free carboxymethyl arm bound to the peptide, allowing for more flexibility due to a spacer function. This hypothesis was tested by developing a conjugate with the optimal chelator for Ga^{III} radioisotopes, NOTA (1,4,7-triaza-1,4,7-triacetic acid). NOTA was modified in order to allow a spacer between the chelator (NODAGA = 1,4,7-triaza-1-glutaric acid-4,7-diacetic acid) and the peptide, separating the signal producing chelate from the biologically active peptide (Figure 11). This combination has the additional advantage that the extremely stable Ga^{III}-NOTA complexes make any interference and false interpretation of biological and pharmacological data due to potential transchelation chemistry rather unlikely. Indeed, Ga-NODAGA-TOC conjugate shows similar pharmacologic and biodistribution parameters like Ga-DOTA-TOC [21].

Preliminary data [43] indicate that Co^{II}-DOTA-D-PheNH_2 has a very similar structure like the Ga^{III} complex and this along with the charge difference may explain the high potency of the corresponding metallo-pep-

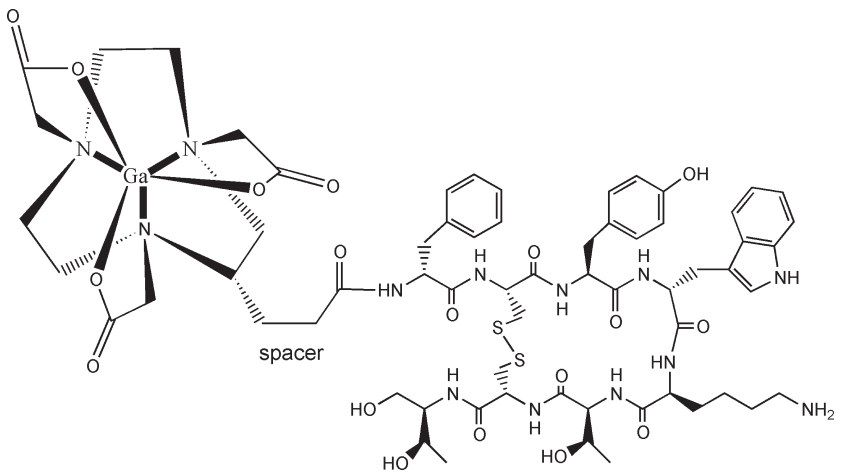

FIG. 11. Structural formula of Ga-NODAGA-TOC.

tide. The low pharmacologic potency and profile of the Bi^{III} complexed peptide is not understood at all at this moment.

6. OVERVIEW OF PATIENT STUDIES

As already mentioned, the basis of somatostatin receptor targeted radiotherapy is the overexpression of somatostatin receptor subtypes on neuroendocrine tumors (Table 1).

Herein we present a few patient studies with the gold standard DOTA-[Tyr^3]-octreotide (DOTA-TOC) (see Figure 2a for structure) radiolabeled with different radionuclides for imaging and for therapy, highlighting their superb targeting performance. Figure 12 shows the positron emission tomography scan of a patient with an abdominal carcinoid with multiple liver and bone metastases, scanned with ^{68}Ga-DOTA-TOC. This image reflects the high sensitivity and specificity of the radiogallium-modified

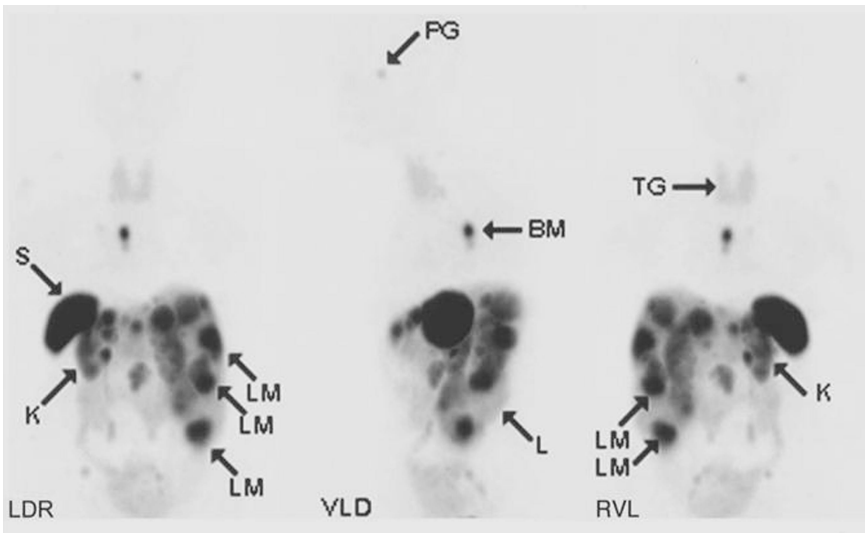

FIG. 12. Ninety minutes postinjection scans in different projections of a patient with multiple liver (LM) and bone metastases (BM) originating from a carcinoid tumor using ^{68}Ga-DOTA-[Tyr^3]-octreotide; S = spleen; K = kidney; PG = pituitary gland; TG = thyroid gland. PET slices: coronary slice: LDR = left-dorsal-right; sagital slice: VLD = ventral-left-dorsal; coronary slice: RVL = right-ventral-left.

peptide, in agreement with the preclinical results found for this radio-metallo-peptide.

Labeled with the β emitter, ^{90}Y-DOTA-TOC proved to be very efficient in targeted radiotherapy of some neuroendocrine tumors. Below three examples are shown which represent three typical subgroups of patients which have been treated at the University Hospital Basel since 1996 and which benefited from the targeted radiotherapy in different ways.

Figure 13 shows a 15 years old patient with a highly metastasized neuroendocrine tumor who had no remaining therapy option and was on morphine medication. The sequence of scans illustrates several factors which determine the potential success of targeted radiotherapy: the quick targeting, a high uptake into the target, a long residence time, specificity, fast clearance from the non-target organs. It shows images of the patient at 15 min after injection of the radiopharmaceutical (^{111}In/^{90}Y-DOTA-TOC) (Fig 13a), at 24 hours (Figure 13b), at 48 hours (Figure 13c) and after six days (Figure 13d). Already after 15 min a good targeting was seen demonstrating the fast blood clearance and localization of the radiopeptide. At 24 hours the background clearance is more advanced and the tumors are delineated more clearly. At 48 hours and also after six days the metallic radionuclide is still retained in the tumors. The reason for this long residence is the ability of the radiometal-DOTA-peptide conjugate to internalize into the tumor cells via endocytosis upon binding to the receptor. This is a crucial step not only to direct a peptide linked radiometal to the interior of the cell, potentially to the cell nucleus, but also causing a long persistence at the tumor. It is noteworthy that the patient improved remarkably during therapy and was able to change from morphine to non-steroidal drugs or even could discontinue analgesic drugs altogether. This is an example of a compassionate use of this therapy. The patient survived five years after the beginning of the therapy and is still alive with highly improved life quality.

A second example is shown in Figure 14. The scintiscan is performed with ^{111}In-DOTA-TOC, representing a patient with a primary endocrine pancreatic tumor with four small liver metastases before ^{90}Y-DOTA-TOC treatment (Figure 14a) and after therapy (Figure 14b). After radiotherapy, the metastases disappeared and the primary tumor shrunk by >50 %, becoming operable. This treatment outcome is called a partial remission.

A final example shows a patient with a Merkel cell tumor which was about the size of a fist of a child (Figure 15a). The tumor disappeared after one injection of 80 mCi ^{90}Y-DOTA-TOC (Figure 15b). This is an example of a so called complete remission.

The benefit of targeted radiotherapy with radiolabeled somatostatin analogues is documented and has been proven. Still, targeted peptide receptor-mediated radiotherapy is in its infancy and questions remain how one could enhance the efficacy of the therapy. Renal toxicity is the

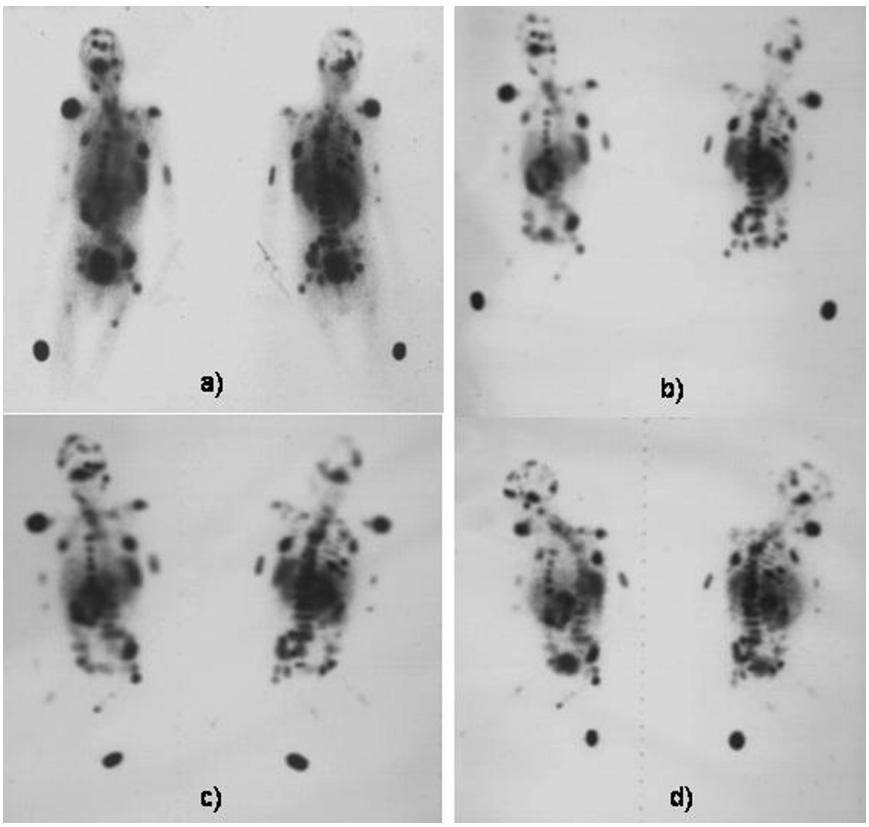

FIG. 13. Scintiscans of a patient with multiple metastases of a neuroendocrine tumor at different time points after injection: (a) at 15 min; (b) at 24 h; (c) at 48 h; (d) after six days postinjection, scanned with ^{111}In/^{90}Y-DOTA-TOC.

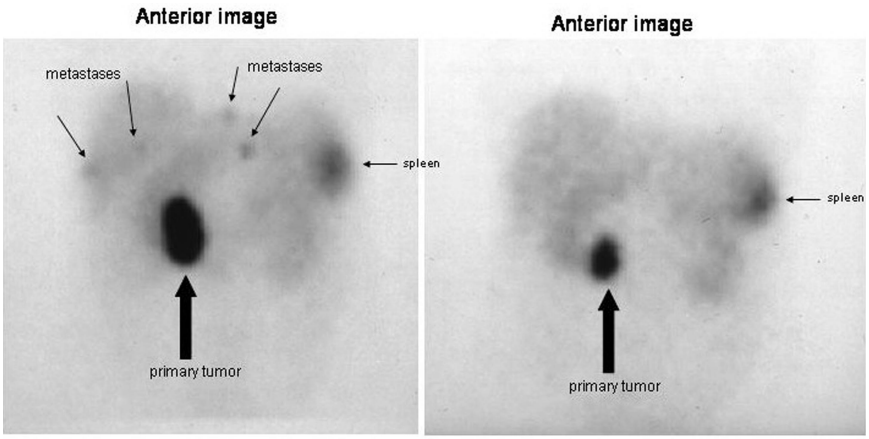

FIG. 14. Scintigraphy of a patient with a endocrine pancreatic tumor with four metastases before (a) and after radiotherapy (b): partial remission, using ^{111}In/^{90}Y-DOTA-TOC.

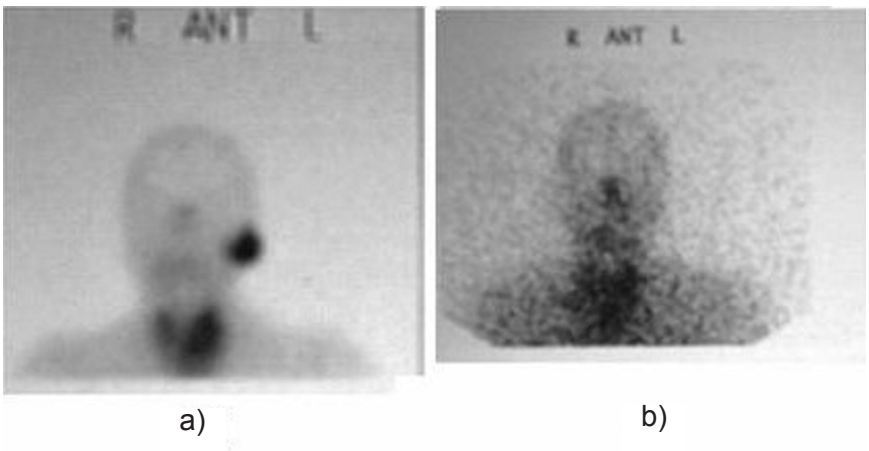

FIG. 15. Scintigraphy of a patient with a Merkel cell tumor (a) before and (b) six weeks after therapy with ^{90}Y-DOTA-TOC.

main dose limiting factor found so far. Infusion of cationic amino acids reduce the uptake of the peptides in the tubular cells of the kidneys. Eventually structural modifications of the peptides will lead to new

radiopeptides with much lower renal uptake. This improvement most likely will come from innovative developments and chelator design from medicinal inorganic chemists.

7. SUMMARY AND CONCLUSION

Radiometallo-labeled analogs of somatostatin have shown great benefit in the *in vivo* localization and targeted radiotherapy of human tumors. The progress and innovation in this clinical application came from the change in strategy, leaving the most widely used radiohalogens for a coordination chemistry approach. The use of chelators appended to the biologically active peptide which convey high thermodynamic and kinetic stability to the radiopeptides did not only improve the pharmacokinetics and pharmacodynamics of the molecules, but surprisingly the biological potency as well.

The most urgent problem to be solved in the field is to improve the kidney clearance of the radiopeptides. The kidney turned out to be the dose limiting organ in this type of targeted radiotherapy. Coordination chemical strategies have already paved the way to a successful clinical application; it is most likely that chelator modification will further help to improve the renal handling of radiometallo-peptides.

ACKNOWLEDGEMENTS

The authors would like to thank for scan pictures Dr. Hofmann and Prof. W. Knapp from the Medical University of Hannover, Germany, Prof. J. Müller, Dr. Ch. Waldherr and Dr. M. Walter from the University Hospital Basel, Switzerland, and Prof. Dr. Baum from University Hospital Frankfurt, Germany.

ABBREVIATIONS

BB	bombesin
BFC	bifunctional chelator
CCK	cholecystokinin
CPTA	4-(1,4,8,11-tetraazacyclotetradec-1-yl)methyl) benzoic acid

D-2-Nal	D-2-naphtylalanine
DFO	desferrioxamine B
DOTA	1,4,7,10-tetraazacyclododecane-1,4,7,10-tetraacetic acid
DOTAGA	1,4,7,10-tetraazacyclododecane-1,4,7,10-tetraacetic acid-1-(1-carboxy-3-carboxypropyl)
DOTASA	1,4,7,10-tetraazacyclododecane-4,7,10-triacetic acid-1-(1-carboxy-2-carboxyethyl)
DTPA	diethylenetriaminepentaacetic acid
EC	electron capture
GLP-1	glucagon-like peptide 1
GRP	gastrin releasing peptide
hsst	human somatostatin receptor
HYNIC	2-hydrazinonicotinic acid
IC_{50}	concentration of the peptide which will replace 50% of the radioligand
IT	internal transfer
LAN	lanreotide
LET	linear energy transfer
LHRH	luteinizing hormone releasing hormone
α-MSH	α-melanocyte stimulating hormone
MTC	medullary thyroid cancer
NHS	*N*-hydroxysuccinimide
NK1	neurokinin 1
NODAGA	1,4,7-triaza-1-glutaric acid-4,7-diacetic acid
NODASA	1,4,7-triazacyclononane-1-succinic acid-4,7-diacetic acid
NOTA	1,4,7-triaza-1,4,7-triacetic acid
NPY	neuropeptide Y
NTR	neurotensin receptor
OC	octreotide
PAC	pituitary adenylate cyclase
PACAP	pituitary adenylate cyclase-activating polypeptide
PET	positron emission tomography
SCLC	small cell lung cancer
SPECT	single photon emission computerized tomography

SRIF	somatotropin release inhibiting factor (somatostatin)
SS	somatostatin
sstr	somatostatin receptor
TETA	1,4,8,11-tetraazacyclotetradecane-1,4,8,11-tetraacetic acid
TOC	$[Tyr]^3$-octreotide
VIP	vasoactive intestinal peptide
VPAC	recombinant receptor for VIP and PACAP

REFERENCES

1. A. J. Fischman, J. W. Babich, and H. W. Strauss, *J. Nucl. Med*., *34*, 2253 (1993).
2. S. Liu and S. D. Edwards, *Chem. Rev*., *99*, 2235 (1999).
3. J. C. Reubi, *J. Nucl. Med*., *36*, 1825-1835 (1995).
4. J. M. Palacios, R. Cortes, M. Dietl, and A. Probst, *J. Receptor Res*., *8*, 509-520 (1988).
5. A. Heppeler, S. Froidevaux, A. N. Eberle, and H. R. Maecke, *Curr. Med. Chem*., *7*, 971-994 (2000).
6. J. C. Schär, B. Waser, G. Mengod, and J. C. Reubi, *Int. J. Cancer*, *70*, 530-537 (1997).
7. S. W. J. Lamberts, W. H. Bakker, J. C. Reubi, and E. P. Krenning, *N. Engl. J. Med*., *323*, 1246-1249 (1990).
8. C. J. Anderson and M. J. Welch, *Chem. Rev*., *99*, 2219-2234 (1999).
9. H. R. Maecke and S. Good, in Vol. 6 of *Technetium, Rhenium and Other Metals in Chemistry and Nuclear Medicine* (M. Nicolini and U. Mazzi, eds.), SGE Editoriali, Italy, 2002, pp. 35-41.
10. D. J. Kwekkeboom, W. H. Bakker, P. P. M. Kooji, M. W. Konijnenberg, A. Srinivasan, J. L. Erion, M. A. Schmidt, J. L. Budaj, M. de Jong, and E. P. Krenning, *Eur. J. Nucl. Med*., *28*, 1319-1325 (2001).
11. H. Humm, *J. Nucl. Med*., *27*, 1490-1497 (1986).
12. M. L. Thakur, H. Kolan, J. Li, R. Wiaderkiewicz, V. R. Pallela, R. Duggaraju, and A. V. Schally, *Nucl. Med. Biol*., *24*, 105-113 (1997).
13. J. M. Varnum, M. L. Thakur, A. V. Schally, S. Jansen, and K. H. Mayo, *J. Biol. Chem*., *269*, 12583-12588 (1994).

14. S. Liu and D.S. Edwards, *Bioconj. Chem*., *12*, 7-34 (2001).
15. R. Albert, C. Bruns, B. Stolz, P.M. Smith-Jones, H.R. Maecke, H. Knecht, and J. Pless, *Actualité de Chimie Thérapeutique*, *21 série*, 111-123 (1994).
16. A. Srinivasan and M. A. Schmidt, Proceedings of the Fifteenth American Peptide Symposium, 267-268 (1996).
17. H. R. Maecke, A. Riesen and W. Ritter, *J. Nucl. Med*., *30*, 1235-1239 (1989).
18. B. Stolz, , P. Smith-Jones, R. Albert, L. Tolcsvai, U. Briner, G. Ruser, H.R. Maecke, G. Weckbecker, and C. Bruns, *Digestion*, *57* (suppl. 1), 17 (1996).
19. M. de Jong, W. H. Bakker, E. P. Krenning, W. A. P. Breeman, M. E. van der Pluijm, B. F. Bernard, T. J. Visser, E. Jermann, M. Béhé, P. Powell, and H. R. Maecke, *Eur. J. Nucl. Med.*, *24*, 368 (1997).
20. J. P. André, H. R. Maecke, M. Zehnder, L. Macko, and K. G. Akyel, *Chem. Commun*., 1301-1302 (1998).
21. K. P. Eisenwiener, M. I. M. Prata, I. Buschmann, H. Zhang, A. C. Santos, S. Wenger, J. C. Reubi, and H. R. Mäcke, *Bioconj. Chem.*, *13*, 530 (2002).
22. A. Heppeler, S. Froidevaux, H. R. Mäcke, E. Jermann, M. Béhé, P. Powell, and M. Hennig, *Chem. Eur. J.*, *5*, 1974 (1999).
23. C. S. Cutler, C. J. Smith, G. J. Ehrhardt, T. T. Tyler, S. S. Jurisson, and E. Deutsch, *Cancer Biother. Radiopharm.*, *15*, 531 (2000).
24. M. R. McDevitt, D. Ma, L. T. Lai, J. P. S. Borchardt, R. K. Frank, K. Wu, V. Pellegrini, M. J. Curcio, M. Miederer, N. H. Bander, and D. A. Scheinberg, *Science*, *294*, 1537 (2001).
25. F. Hu, C. S. Cutler, T. Hoffman, G. Sieckman, W. A. Volkert, and S. S. Jurisson, *Nucl. Med. Biol.*, *29*, 423 (2002).
26. R. Albert, P. Smith-Jones, B. Stolz, C. Simeon, H. Knecht, C. Bruns, and J. Pless, *J. Bioorg. Med. Chem. Letters*, *8*, 1207-1210 (1998).
27. K. P. Eisenwiener, P. Powell, and H.R. Maecke, *Bioorg. Med. Chem. Lett*., *10*, 2133-2135 (2000).
28. P. J. Blower, J. S. Lewis, and J. Zweit, *Nucl. Med. Biol*., *23*, 957-980 (1996).
29. M. J. Abrams, M. Juweid, C. tenKate, D. A. Schwartz, M. M. Hauser, F. E. Gaul, A. J. Fuccello, R. H. Rubin, H. W. Strauss, and A. J. Fischman, *J. Nucl. Med., 31,* 2022 (1990).

30. D. S. Edwards, S. Liu, A. R. Harris, R. J. Looby, M. C. Ziegler, S. J. Heminway, J. A. Barrett, and T. R. Carroll, *Bioconj. Chem., 8,* 146 (1997).

31 T. Maina, B. Nock, A. Nikolopoulou, P. Sotiriou, G. Loudos, D. Maintas, P. Cordopatis, and E. Chiotellis, *Eur. J. Nucl. Med., 29,* 742-753 (2002).

32. A. Otte, E. Jermann, M. Behe, M. Goetze, H.C. Bucher, H.W. Roser, A. Heppeler, J. Mueller-Brand, and H.R. Maecke, *J. Nucl. Med*., *24*, 792 (1997).

33. M. J. Mattes, G.L. Griffiths, H. Diril, D. M. Goldenberg, G.L. Ong, and L. B. Shih, *Cancer*, *73* (Suppl), 787-793 (1994).

34. P. Caravan, J. J. Ellison, T. J. McMurrym, and R. B. Lauffer*, Chem. Rev*., *99*, 2293-2352 (1999).

35. D. L. Kukis, S. J. DeNardo, G. L. DeNardo, R. T. O'Donnell, and C. F. Meares, *J. Nucl. Med*., *39*, 2105-2110 (1998).

36. K. P. Pulukkody, T. J. Norman, D. Parker, L. Royle, and C. J. Broan, *J. Chem. Soc., Perkin Trans*., 605-620 (1993).

37. J. L. Cox, A. S. Craig, I. M. Helps, K. J. Jankowski, D. Parker, M. A. W. Eaton, A. T. Millican, K. Millar, N. R. A. Beeley, and B. A. Boyce, *J. Chem. Soc., Perkin Trans*., 2567-2576 (1990).

38. J. B. Stimmel and F. C. Kull, Jr., *Nucl. Med. Biol*., *25*, 117-125 (1998).

39. A. Heppeler, E. Jermann, T. Gyr, R.M. Dyson, G. Ruser, M. Hennig, M. Neuburger, M. Neuburger-Zehnder, T. Kaden, and H. R. Maecke, in *Technetium, Rhenium and Other Metals in Chemistry and Nuclear Medicine* (M. Nicolini and U. Mazzi, eds.) Vol. 5, SGE Editoriali, Padova, Italy, 1999, pp. 65-69.

40. J. Lister-James, B. R. Moyer, and T. O. Dean, *J. Nucl. Med*., *40*, 221 (1996).

41. J. C.Reubi, J. C. Schär, B. Waser, S. Wenger, A. Heppeler, J. S. Schmitt, and H. R. Maecke, *Eur. J. Nucl. Med*., *27*, 273-282 (2000).

42. H. Maecke, G. Scherer, A. Heppeler, and M. Hennig, *Eur. J. Nucl. Med., 28*, 967 (2001).

43. A. Heppeler, PhD thesis, University of Basel, Basel, Switzerland, 2000.

44. O. C. Boerman, W. J. Oyen, and F. H. Corstens, *Semin. Nucl. Med*., *25*, 201 (2000).

45. M. de Jong, W. A. P. Breeman, W. H. Bakker, B. F. Bernard, M. Schaar, A. van Gameren, J. E. Bugaj, J. Erion, M. Schmidt, A. Srinivasan, and E.P. Krenning, *Int. J. Cancer*, *92*, 628-633 (2001).

46. P. O. Zamora, H. Bender, S. Gulhke, M. J. Marek, F. F. Knapp, Jr., B. A. Rhodes, and H. J. Biersack, *Anticancer Res*., *17 (3B)*, 1803-1808 (1997).

47. B. Stolz, G. Weckbecker, P. M. Smith-Jones, R. Albert, F. Raulf, and C. Bruns, *Eur. J. Nucl. Med*., *25*, 668-674 (1998).

II

Design, synthesis and biological evaluation of new somatostatin based radiopeptides

*Mihaela Ginj,[1] Jörg S. Schmitt,[1] Jianhua Chen,[1] Beatrice Waser,[2] Jean-Claude Reubi,[2] Marion de Jong,[3] Stefan Schulz,[4] Helmut R. Maecke[1]**

[1] Division of Radiological Chemistry, Department of Radiology, University Hospital Basel, Petersgraben 4, 4031-Basel, Switzerland, [2] Institute of Pathology, University Hospital Berne, 3012-Berne, Switzerland, [3] Department of Nuclear Medicine, University Hospital Rotterdam, Rotterdam, Netherlands, [4] Otto-von-Guericke University, Magdeburg, Germany.

*Corresponding author:

Tel.: +41-61-265.46.99

Fax: +41-61-265.55.59

Email: hmaecke@uhbs.ch

Summary

The prototypes for tumor targeting with radiolabelled peptides are derivatives of somatostatin usually with high affinity mainly for sstr2 and moderate affinity to sstr5. We aimed at developing new analogs for internal radiotherapy, which recognize different receptor subtypes, to expand the present range of accessible tumors. Using parallel solid phase synthesis, we synthesized new DOTA-octapeptides based on octreotide, by replacing Phe^3 mainly with unnatural amino acids. The affinity profile was determined using transfected cell lines with sst1-5. Internalization was determined using AR4-2J and HEK-sst3 cell lines and biodistribution was studied in rat tumor models. Two of the derivatives thus obtained showed improved binding affinity profile, enhanced internalization in cells expressing sst2 and sst3, respectively, and better tumor:kidney ratios in animals. The predictions from these preclinical data are partially confirmed in initial clinical studies.

Running title: New somatostatin-based radiopeptides

Introduction

The tetradecapeptide somatostatin (SS-14) is of little therapeutic value since it has a broad spectrum of biological actions, but a short half-life in vivo. Conformational analyses and structure-function studies on somatostatin analogs indicate that the sequence required for biological activity consists of the β-turn fragment Phe-Trp-Lys-Thr corresponding to the residues 7-10 of SS-14. Many somatostatin analogs with smaller and more rigid rings have been synthesized in the search for compounds with enhanced and prolonged activity. Two lead compounds emerged from this research, the hexapeptide L-363,301 [1] and the octapeptide octreotide (Sandostatin®, SMS 201-995) [2]. One unintended consequence of such structural simplification, carried out before the discovery of multiple receptor subtypes, was the loss of broad-spectrum binding affinity. The cloning of the five somatostatin receptors (sst1-sst5) [3] has increased the understanding of somatostatin receptor structure and function. It also revealed that the short-chain synthetic analogs of somatostatin have high affinity for sst2, moderate to low affinity for sst3 and sst5, and no or very low affinity for sst1 and sst4.

In nuclear medicine oncology, the prototypical tracers used for in vivo receptor scintigraphy and targeted radionuclide therapy are derivatives of somatostatin. The molecular basis for their use is the overexpression of somatostatin receptors on a variety of human tumors, especially neuroendocrine tumors and their metastases [4], [5]. The majority of human sst-positive tumors express simultaneously multiple sst subtypes, although there is a considerable variation in sst subtype expression between the different tumor types and among tumors of the same type. Parts of these differences are also due to the method used to investigate the somatostatin receptor subtype occurrence [6]. Most of the data available up to now on somatostatin receptor expression in human tumors originates from mRNA detection, but more recently several groups provided information on sst subtype protein expression [5], [7], [8]. Undoubtedly, subtype 2 is the most frequently expressed in a majority of cancers. Nevertheless, in a significant number of tumors sst2 is absent or expressed in low density and other somatostatin receptor

subtypes are present. For instance, frequent expression of sst 1, 2, 3, and 5 was found in gastro-entero-pancreatic tumors (GEP) [8], in medullary thyroid cancers (MTC) [9] and in ovarian cancers [10]. A predominant expression of sst3 was discovered in inactive pituitary adenomas and in thymomas [11, 12]. Human lung tumors were shown to overexpress sst2, 3 and 5 [13]. The considerable heterogeneity in the expression of individual sst within and between different tumors, but also the effects associated with single sst subtypes (sst2 mediates antiproliferative effects, sst3 also mediates antiproliferative, but also proapoptotic effects, sst5 mediates GH inhibition) make evident the need for tracers that can target more than one somatostatin receptor subtype in vivo.

The predominant expression of sst2 in human tumorous tissues forms the basis for the successful clinical application of radiolabeled octapeptide somatostatin analogs in imaging of sst-positive tumors. The classical radioactive somatostatin analogs used for the *in vivo* visualization and treatment of human tumors are derivatives of octreotide, the standard for scintigraphy being [^{111}In-DTPA]-octreotide (Octreoscan®). Although remote from the pharmacophore, the addition of a metal-complex to the *N*-terminus of octreotide led to a loss in binding affinity especially for sst5, but also for sst3 and sst2 [14]. This is also applicable for the analogs used in targeted radiotherapy, having DOTA (1, 4, 7, 10-tetraazacyclododecane-1, 4, 7, 10-tetraacetic acid) as chelator and ^{90}Y or ^{177}Lu as therapeutic radionuclides (e.g., ^{90}Y-DOTA-[Tyr^3]-octreotide, a conjugate having a decade of clinical experience [15]). Chelator-derivatives of lanreotide® [16] and vapreotide® [17] have been developed as well. These octapeptides have an improved binding affinity profile, but their metal-chelator-conjugates display satisfactory affinity only to sst2 and sst5 [14].

Octreotide has been subject of extensive structural studies, including NMR [18] and X-ray diffraction [19]. Taken together these studies have demonstrated that octreotide exists in solution in two conformational families, differing mainly by the conformation of the C-terminal tail. The molecule adopts an overall antiparallel β-sheet conformation, with a type II' β-turn centered at the D-Trp^4-Lys^5

region. In one conformational family, the residues following this β-turn continue the β-sheet structure, and in the second family, the residues following the β-turn adopt a 3_{10} helical conformation. All the peptidic analogs of octreotide conserve the critical sequence D-Trp^4-Lys^5 and only subtle modifications have been done to the side amino acids of this β-turn (Phe^3 and Thr^6) [20]. Among the clinically used analogs of somatostatin (octreotide, lanreotide and vapreotide) the only modification operated in the 3rd position is the substitution of Phe^3 (in octreotide) with Tyr^3 (in lanreotide and vapreotide). Since this substitution is accompanied by other structural changes at *C*-terminus (Thr-NH_2 in lanreotide, Trp-NH_2 in vapreotide versus Thr(ol) in octreotide) and/or *N*-terminus (D-2-Nal in lanreotide instead of D-Phe in octreotide and vapreotide) and at the 6th residue (Thr in octreotide replaced by Val in lanreotide and vapreotide), it is difficult to assess the alterations in the binding affinity profile. Still, a direct comparison on the effects produced by the replacement of Phe^3 with Tyr^3 is noticeable on the metal-chelator conjugates Y^{III}-DOTA-octreotide (Y^{III}-DOTA-OC) and Y^{III}-DOTA-[Tyr^3]-octreotide (Y^{III}-DOTA-TOC) [14] (see also Table 1). The more hydrophilic conjugate having Tyr on the third position gains in the binding affinity to sst2, but significantly loses in binding potency to sst3 and sst5.

Based on these structural and empirical data we assumed that modifications at this position in metal-complexed DOTA-derivatives of octreotide could modulate the affinity profile to sst3 and sst5. Our premise was that bulky aromatic residues could improve the binding profile to sst3 and 5 without losing in potency to sst2. Radioactive conjugates with a broader affinity profile would not only lead to an extension of the present range of targeted cancers, but would also mean an increased dose of radioactivity to the tumor, given the presence of different receptor subtypes on the same tumor cell or in the same tumor entity.

In this paper we describe the synthesis and pharmacological evaluation of a small library of metal-DOTA-peptides derived from octreotide with modifications at the 3rd amino acid residue. We

have already reported a first compound resulting from this library, [^{111}In/^{90}Y-DOTA]-NOC, with improved biological properties, currently in clinical trials [21].

Results and Discussion

The DOTA-somatostatin analogs **1-24** (Figure 1) obtained by systematic modification of aa^3 in octreotide were synthesized by parallel synthesis on solid phase using the Fmoc/*t*Bu strategy and the 2-chloro-tritylchloride linker. After cleavage from the resin, cyclization in solution and total deprotection, the crude products were obtained in 25-30 % yield based on the first Fmoc-cleavage. All peptide-conjugates had a purity of > 97% confirmed by two HPLC systems. In each case the ESI-MS spectra consisted of a major $[M+2K]^{2+}$ ion peak and two minor peaks corresponding to $[M+K]^{+}$ and $[M+3K]^{3+}$ ions (Table, supplemental information). Metal-ion complexed DOTA-peptides were characterized by HPLC, MS-ESI and by the retained affinity to the somatostatin receptors. Labeling was performed in acetate buffer (pH 5, 0.4 M) by heating at 95 °C for 25 min affording > 99% labeling yields with ^{111}In at a specific activity of >37 GBq/μmol peptide.

The partition coefficients of the ^{111}In/In^{III}-labeled derivatives **1-24** between aqueous (PBS, pH 7.4) and organic (octanol) layers were determined using the shake flask method. The results are displayed in Figure 2, the most lipophilic compound being ^{111}In/In^{III}-**20** and the most hydrophilic ^{111}In/In^{III}-**22** and -**23**.

Table 1 shows the IC_{50} values of the conjugates studied in this work as their Y^{III}- or In^{III}-complexed versions for the five somatostatin receptor subtypes. The values were obtained by performing complete displacement experiments with the universal somatostatin radioligand [^{125}I][Leu^8, D-Trp^{22}, Tyr^{25}]-somatostatin-28 on membranes from cells expressing the receptor subtypes and were compared to SS-28.

Internalization studies were performed on AR42J rat pancreatic tumor cells and on HEK cells stably expressing rat sst3. The uptakes in these cell-lines after 4 h incubation with the radiopeptides are shown in Table 2. These values represent specific accumulation, being the difference between the total uptake and the non-specific accumulation in the presence of excess of non-radioactive derivative.

Phe^3 derivatives. Comprising the parent compound, DOTA-octreotide, there are six conjugates bearing a phenylalanine derivative in the 3rd position of the peptide: **1**, **8**, **9**, **10**, **11** and **12**. In the homologues series **9**, **1**, **8** there is no improvement neither in binding affinity nor internalization by varying the length of the Phe chain. Although the phenylglycine residue was previously successfully employed in this position of the β-turn in the cyclohexapeptide analog of somatostatin SOM-230 [22], its incorporation in the DOTA-octapeptide **9** causes a complete loss of affinity for sst3 and sst5, and a 2.5-fold drop for sst2. The superior Phe homolog derivative **8** maintains some affinity for sst2, 3 and 5, but at lower values compared with **1**. These results are correspondingly reflected in the internalization rates in cells expressing rsst2 (AR42J) and rsst3 (HEK). The two halogeno-Phe derivatives **11** and **12**, displaying comparable lipophilicities, the same binding affinities to sst2 and similar 4 h internalization rates in AR42J cells, differ significantly in their binding potencies against sst3 and sst5, respectively. The higher affinity of ^{111}In-**11** against sst3 is confirmed by the superior accumulation in HEK-rsst3 cells. Derivative **10**, the most lipophilic of this series, excels in the accumulation in AR42J cells with an amount (12.7 ± 1.2 %ID) superior to all the other five conjugates in this group, although it has the lowest sst2 affinity among these six derivatives.

Tyr^3 derivatives. The presence of a weak (-I, conjugate **14**) and a strong electronic deactivator (-NO_2, conjugate **15**), respectively, on the Tyr ring in the ortho position relative to the phenolic OH causes an increase in the pKa values of these residues (data not shown). This is reflected in the partition coefficients, increasing in the order **2** ≥ **14** >> **15**. Apparently, a more acidic residue in this position is not beneficial neither to the binding affinities to any of the sst nor to the internalization in sst2 or 3-

expressing cells, $^{111/115}$In-**15** showing a net inferior biological profile when compared with $^{111/115}$In-DOTA-TOC ($^{111/115}$In-**2**). Using the same reference, despite the improved sst2 affinity, $^{111/115}$In-**14** has a lower internalization rate in AR42J cells. This result does not corroborate the previous findings of Hofland et al. [23] on DOTA-[^{125}I-Tyr^3]-octreotide showing an increased uptake in sst-expressing cells and tissues.

Heterocyclic-side chain^3 derivatives. Seven residues with heterocyclic side-chain have been introduced in the 3rd position of octreotide, respectively: two pyridine derivatives (**6** and **7**), a thiophene (**17**), a benzothiophene (**5**), an indole (**16**), a benzthiazole (**18**) and a piperidine-side chain residue (**23**). Undoubtedly, the best biological profile in this series belongs to the metal complexed derivative **5**. The most lipophilic of this group, the metal-complexed-**5** conjugate confirms the starting hypothesis that a bulkier aromatic residue in this position of the octreotide would improve the sst3 and sst5 binding profile. Moreover, it also shows a significant increase in the binding affinity to sst2. The internalizations in sst2- and sst3-expressing cells mirror these results. Its *N*-analogue (**16**) has comparable lipophilicity, but significantly lower potency on sst2 and sst5 and a dramatic drop on the binding affinity and internalization rate towards sst3. Interestingly, the somewhat more hydrophilic related conjugate **18** fails in all the biological assays. The thiophenylalanine derivative **17** has a reasonable sst2 and sst3 binding profile reflected also in the internalization assays. The two pyridinylalanine derivatives **6** and **7** preserve only a reasonable affinity to sst2, but without satisfactory internalizations in AR42J cells. In the structure-activity investigations done by Hocart et al. [24] in the search for somatostatin antagonists, the substitution of 3-pyridylalanine in this position produced an antagonist with marginal affinity for sst2 (291 nM). The worst derivative of this series is the most hydrophilic one, bearing a piperidylalanine residue in the 3rd position (**23**).

Polyaromatic-side chain^3 derivatives. Two naphtylalanine derivatives (**3** and **4**), a diphenylalanine (**13**), an antranylalanine (**19**) and a pyrenylalanine (**20**) have been employed instead of Phe^3 in octreotide. The complexed version of **3** has incontestably the best biological profile of this

group [21]. The binding potency of this compound on sst2 and sst3 is reflected also in the internalization rate in the cells expressing these receptors. It has also a superior binding affinity to sst5 compared with the parent conjugate **1**. Interestingly, the 2-Nal^3 conjugate (**4)** turned out inferior in all assays, a result difficult to explain, giving the very small structural difference between the two compounds. Despite the moderate binding affinity to sst2, comparable with that of **1**, it shows insignificant accumulation in AR42J cells after 4 h incubation at 37 ^{0}C (< 0.9 %). The diphenyl-substituted derivative **13**, one of the most lipophilic conjugates of this series, loses completely the binding affinities to all sst and therefore also the capacity to activate the internalization of the receptors. The bulkiest and the most lipophilic conjugate **20** has one of the highest affinities to sst3 (18 ± 1.0 nM), confirmed also by the internalization experiments in HEK cells expressing this receptor (>12 %). The second bulkiest conjugate **19** has lower affinity to sst3, but higher for sst5, while maintaining a good binding also to sst2.

Aliphatic-side chain^3 derivatives. The three aliphatic side-chain residues Ser (**21**), Lys (**22**) and cyclohexylalanine (**24**) were employed in the 3rd position for comparison reasons, to prove the necessity of an aromatic residue in this location. All these derivatives lost their binding affinity to all sst subtypes and did not internalize neither in sst2- nor sst3-expressing cells. Previous Ala-scans studies [25] on SS-14 have also shown that the replacement of Phe^7 (corresponding to Phe^3 in octreotide) by an Ala residue led to a drop of about 90 % in the ability to inhibit the growth hormone release in vitro.

Although we started from the premise of substituting Phe^3 in octreotide with bulky aromatic residues, we studied also the influence of several phenylalanine and tyrosine derivatives in this position, along with the consequences of employing aliphatic amino acids. Summarizing, very subtle modifications in this region of the β-bend have profound effects on the pharmacological profile. Even if the binding affinity against a ligand and the capacity to internalize are two distinct features of a G

protein-coupled receptor and they do not necessarily have to correlate, most of the ligands reported herein having reasonable to good binding affinity induce also internalization to a higher or lower extent. Two intriguing exceptions from this ''rule'' are the metal complexed derivatives **4** and **10**. ^{111}In-**4** with 2-Nal as 3rd residue shows very low internalization in sst2 expressing cell-line AR42J (0.9 ± 0.3 %ID), although the 1-Nal^3 derivative ^{111}In-**3** has the best internalization in these cells (25 ± 1.5 % ID) associated with one of the best binding affinities for sst2 (3.3 ± 0.2 nM). On the contrary, ^{111}In-**10** shows a good internalization in AR42J cells (12.7 ± 1.2 %ID), similar to that of ^{111}In-DOTA-TOC (**2**), although its binding affinity to sst2 is low (85 ± 15 nM). It is difficult to explain these results, due probably to the different agonist ability (partial or total agonist) of these derivatives. Substantial evidence exists that ligand composition, receptor subtype and the cell-line used for transfection of receptor DNA are critical factors in the intracellular routing and retention of somatostatin and its analogs [26].

Generally, the bulky and lipophilic residues employed instead of Phe^3 increase the binding affinity to sst3 and they also activate the internalization of this receptor. The best conjugates for this receptor were the metal-complexed **3**, **5**, **17**, **19**, **20** conjugates. Some of them also enhance the potency of binding to sst5 (**3**, **5**, **16**, **19**).

Nevertheless, the broadest affinity profile in this series, supplemented by a good activation of internalization in sst2 and sst3 expressing cell lines, respectively, correspond to the metal-complexed conjugates **3** and **5**. We reported previously the biological evaluation of ^{111}In/In^{III}-**3** (^{111}In/In^{III}-DOTA-NOC) [21], in comparison with ^{111}In/In^{III}-labeled DOTA-TOC and DOTA-OC. This compound is actually in clinical trials, showing improved imaging properties in comparison with the other radiolabeled somatostatin analogs in clinical use, in a group of metastasized thyroid cancer patients not showing any radioiodine uptake anymore [27].

We compared ^{111}In-**5** with ^{111}In-**3** in cellular retention tests in AR42J cells and in HEK-rsst3 cells (Figure 3) and we found a similar behaviour in both cell lines. Both compounds display a higher retention of the internalized fraction in the sst3 expressing cells than in sst2 ones due probably to the difference in the receptor dynamics [26]. Nevertheless, the two conjugates behave differently in immunocytochemical internalization studies in HEK cells stably expressing hsst5 (Figure 4). Although it has been previously shown by Roth et al. [26] that in HEK cells transfected with sst5 the receptor endocytosis is promoted only by the octacosapeptide (SS-28) and not SS-14, in our assay SS-14 triggers the receptor internalization after 30 min incubation at 37 ^{0}C. Also In^{III}-**3** induces sst5 internalization to a lower extent in these cells, while In^{III}-**5** activates no internalization in these cells.

In vitro internalization studies are generally used as a predictor of in vivo tumor or sst-positive tissue accumulation. Despite the negative result obtained in sst5 internalization assay, ^{111}In-**5** has a two-fold higher accumulation in CA20948 rat pancreatic tumor (Figure 5A) than ^{111}In-**3** at 4 h after injection. This ratio between the two ligands is maintained also 24 h after injection and slightly decreases after 48 h. As this type of tumor has been shown to express several somatostatin receptor subtypes [28], we believe that this increased uptake for ^{111}In-**3** could be due to the slightly better binding profile of this compound along with the significantly higher capacity of internalization in sst3-expressing cells. In AR42J tumor the two ligands accumulate in a similar manner (Figure 5B), consequence of the sole sst2 presence in this tissue [29]. Both radioligands have favorable tumor:kidney ratios in both rat tumor bearing models as shown in Figure 5 [21]. This is an important parameter in targeted radiotherapy, as the kidney is the dose limiting organ.

Overall, in addition to DOTA-NOC (**3**), the conjugate **5** (named DOTA-BOC) originating from the same library of DOTA-octreotide derivatives with modifications at the 3rd residue has very promising preclinical data. We have recently reported the synthesis and biological evaluation of the Thr^{8}-modification of these conjugates (DOTA-NOC-ATE and DOTA-BOC-ATE) [30], also displaying promising in vitro and in vivo biological profiles. As mentioned there, this type of radioligands might

be used as imaging agents to predict the usefulness of cold octreotide (Sandostatin®) or lanreotide (Somatuline®) therapy rather than OctreoScan® which has a much less adequate binding profile for this purpose. Since there is no radioligand for SOM230, these radioligands may be also candidates to identify patients adequate for SOM230 treatment [31].

Significance

Peptide receptor mediated radionuclide imaging and targeted therapy are emerging fields in oncology. The prototypical peptides are derivatives of somatostatin. Nevertheless, the clinically used derivatives have mainly affinity for sst2. Although this receptor is overexpressed in a variety of tumors, there are several malignancies where other somatostatin receptor subtypes are present in higher density. We designed and synthesized a new series of DOTA-octreotide derivatives by exchanging the 3rd residue in octreotide principally with a variety of aromatic side-chain amino acids. We chose this position due to its involvement in the critical β-turn of this molecule and to the empirical observations on the pharmacological profile of two DOTA-derivatives used in clinic. The small library of compounds thus obtained is not only a useful structure-activity investigation tool, but also the supply of two new derivatives with improved pharmacological properties. DOTA-[1-Nal^3]-octreotide (**3**) and DOTA-[BzThi^3]-octreotide (**5**), labeled with ^{111}In, ^{90}Y, ^{177}Lu or ^{68}Ga, can efficiently target sst2, 3 and 5, having the broadest affinity profile among the radioligands used in clinic. This means not only the increase of the present range of targeted tumors, but also an enhanced cytotoxic radioactive dose to the same tumor expressing several somatostatin receptor subtypes.

Acknowledgements

M. Ginj, J. Chen and H.R. Maecke acknowledge the support from the Swiss National Science Foundation (Grant No. 3100A0-100390) and Bundesamt für Bildung und Wissenschaft (BBW, Grant

No. C00.0091). The analytical support provided by Novartis Pharma (Dieter Staab) and also the expert technical assistance of K. Hinni (Basel) and D. Meyer (Magdeburg) are also gratefully acknowledged.

Experimental procedures

Abbreviations. The nomenclature for the somatostatin receptor subtypes is in accordance with the recommendations of IUPHAR. [3] Abbreviations of the common amino acids are in accordance with the recommendations of IUPAC-IUB [32]. Additional abbreviations: 1 (or 2)-Nal = 1 (or 2)-naphthylalanine, Thi = (2-thienyl)-alanine; 3 (or 4)-Pya = 3 (or 4)-pyridylalanine; hPhe = homophenylalanine; (4-I) Phe= 4-iodophenylalanine; (4-iPr) Phe= 4-isopropyl-phenylalanine; (3-NO_2) Tyr= 3-nitro-tyrosine; (4-Pip) Ala= 4-piperidinyl-alanine; BzThi = 3-benzothienylalanine; Cha = cyclohexylalanine; Antra = antranylalanine; Pyra = 1-pyrenylalanine; PhGly = phenylglycine; DOTA = 1,4,7,10-tetraazacyclododecane-1,4,7,10-tetraacetic acid; DOTA($tBu)_3$ (prochelator) = 4, 7, 10-tricarboxymethyl-tert-butyl ester 1, 4, 7, 10-tetraazacyclododecane-1-acetate; DCM = dichloromethane; DIC = diisopropylcarbodiimide; DIPEA = diisopropylethylamine; DMF = dimethylformamide; HOBt = *N*-hydroxybenzotriazole; HATU = O-(7-azabenzotriazol-1-yl)-*N*, *N*, *N'*, *N'*-tetramethyluroniumhexafluorophosphat; TFA = trifluoroacetic acid; TFE = trifluoroethanol; TIS = triisopropylsilane.

Materials. All chemicals were obtained from commercial sources and used without further purification. H-Thr(tBu)ol-(2-chlorotritylchloride)-resin was obtained from Advanced ChemTech, Louisville, KY, and most Fmoc (9-fluorenylmethoxycarbonyl)-amino acids were purchased from NovaBiochem AG, Läufelfingen (Switzerland) and Neosystem (France). The reactive side chains of the amino acids were masked with one of the following groups: Cys, acetamidomethyl; Lys, *t*-butoxycarbonyl; Thr, *t*-butyl; Trp, *t*-butoxycarbonyl. The prochelator DOTA($tBu)_3$ was synthesized according to Heppeler et al. [33] Analytical RP-HPLC was carried out on a Hewlett Packard 1050

HPLC-system equipped with a multiwavelength-detector and a flow-through Berthold LB506C1 γ-detector. Preparative HPLC was done on a Bischof HPLC-system (Metrohm AG, Switzerland) with HPLC-pumps 2250 and a Lambda 1010 UV-detector. Quantitative γ-counting was performed on a COBRA 5003 γ-system well counter from Packard Instrument Company (Switzerland). Electrospray ionization-mass spectrometry (ESI-MS) was carried out with a Finnigan SSQ 7000 spectrometer (Bremen, Germany). $^{111}InCl_3$ was obtained from Mallinckrodt Medical (Petten, the Netherlands).

Peptide-Conjugates Synthesis. The peptide-chelator conjugates were synthesized by parallel standard Fmoc-solid phase synthesis [Atherton E., 1989 #49] on 2-chlorotritylchloride resin (substitution 0.8 mmol/g) on a Rink Engineering peptide-synthesizer Switch 24 (RinkCombichem, Bubendorf, Switzerland). A 3.0 equivalent excess of the protected amino acids based on the original substitution of the resin was used. The couplings were mediated by DIC and HOBt in DMF for 1 h and monitored by the qualitative ninhydrin [34] or TNBS test [35]. Fmoc removal was achieved with 20 % piperidine in DMF in two successive 10 min treatments. The last step on the solid phase was the coupling for 2 h of the prochelator DOTA$(tBu)_3$ to the N-terminus of the peptide, using HATU as activating agent. The fully protected conjugates were then cleaved from the resin support by using a 1 % TFA in DCM solution containing also H_2O (0.5 % v/v) and TFE (20 % v/v) as scavengers. After co-evaporation with toluene and drying in desiccator, the crude protected peptide conjugates were cyclized in aqueous MeOH by addition of iodine (10 equivalents). Thirty minutes later, acid ascorbic was added to quench the excess of iodine. For the complete deprotection the dried cyclized peptide-conjugates were dissolved in TFA with TIS (3 % v/v), thioanisole (3 % v/v) and H_2O (5 % v/v) as scavengers. After 4 h incubation at room temperature, the crude products were precipitated in cool diethyl ether.

Purification and Characterization of Peptide-Conjugates. The crude conjugates were purified by preparative RP-HPLC using an Interchrom Uptisphere 5ODB C18 column (250 × 21.2 mm) and a linear gradient from 20 % to 50 % solvent B (solvent A, 0.1 % TFA/water, solvent B,

acetonitrile) over 25 min at a flow rate of 15 mL/min. Detection was done at 254 nm. All compounds were lyophilized after purification and characterized by ESI-MS and HPLC. Pure fractions were identified by analytical multiwavelength RP-HPLC with a CC250/4 Nucleosil 120-3C18 column from Macherey-Nagel using a linear gradient from 10 % B to 60 % B over 40 min at a flow rate of 0.75 mL/min (solvent A, 0.1 % TFA/water, solvent B, acetonitrile).

Formation of Metal Complexes. The DOTA-SRIF-analogs were complexed with $InCl_3$ (anhydrous) or $Y(NO_3)_3 \bullet 5\ H_2O$ as described by Wild et al. [21] The radiopeptides were also synthesized according to Wild et al. [21] and obtained in >99% radiochemical purity at specific activities of >37 GBq/μmol peptide. For internalization, externalization and animal biodistribution experiments the DOTA-peptides were labeled to a specific activity of about 37 GBq/μmol peptide and then excess $InCl_3$ was added to afford structurally characterized homogenous ligands.

Determination of Lipophilicity. The octanol-water partition coefficients were determined using the shake flask method. Both solvents (aqueous and octanol) were presaturated with the other by leaving them in contact for at least 24 hours. To a solution of 100 nM radiolabeled peptide in 500 μL PBS (pH 7.4) 500 μL of octanol were added (n = 5). The mixtures were vigorously shaken for long enough to reach equilibrium (approx. 1 h). After equilibration for a few minutes, the mixtures were centrifugated (10 minutes at 2000 rpm) to achieve good separation. The activity concentrations in 100 μL samples of both the aqueous and the organic phase were measured in a γ-counter. The partition coefficient (log P) was calculated from the formula:

$$\log P = \log_{10} (\text{counts in octanol layer/counts in aqueous layer})$$

Receptor Binding Assays. CHO-K1 and CCL39 cells stably expressing human sst1-5 were grown as described previously [14]. All culture reagents were supplied by GIBCO/BRL and Life Technologies (Grand Island, N.Y.). Cell membrane pellets were prepared and receptor autoradiography was performed on pellet sections (mounted on microscope slides), as described in detail previously [14]. For each of the tested compounds, complete displacement experiments were performed with the

universal somatostatin radioligand [^{125}I]-[Leu^{8},D-Trp^{22},Tyr^{25}]-somatostatin-28 using increasing concentrations of the Metallo^{III}-DOTA-peptide ranging from 0.1 to 1,000 nM. Somatostatin-28 was run in parallel as control using the same increasing concentrations. IC_{50} values were calculated after quantification of the data using a computer-assisted image processing system. Tissue standards (autoradiographic [^{125}I] microscales Amersham, UK) containing known amounts of isotopes, cross-calibrated to tissue-equivalent ligand concentrations, were used for quantification [14].

Cell culture and radioligand internalization studies. The apparatus and procedures for the cell internalization experiments are based on previously described methods. [30] Briefly, the AR42J cell line was maintained by serial passage in monolayers in Dulbecco's modified Eagle's media (DMEM), supplemented with 10% fetal bovine serum, amino acids, vitamins and penicillin-streptomycin, in a humidified 5% CO_2 atmosphere at 37^{0}C. Human embryonic kidney (HEK) 293 cells stably expressing rat sst3 receptors were grown in DMEM supplemented with 10% fetal bovine serum, penicillin-streptomycin and G418 (500 μg/ml) in a humidified 5% CO_2 atmosphere at 37^{0}C. For all cell experiments, the cells were seeded at a density of 0.8 - 1.1 million cells /well in 6-well plates and incubated over night with internalization buffer (DMEM, 1% fetal bovine serum, amino acids and vitamins, pH 7.4) to obtain a good cell adherence. Medium was removed from the 6-well plates and cells were washed once with 2 mL of internalization buffer. Furthermore, 1.5 mL internalization buffer was added to each well and incubated at 37°C for about 1 h. Thereafter approximately 500,000 cpm or 0.02 MBq/well ^{111}In/In^{III}-labeled peptides (2.5 pmol/well) to a final concentration of 1.67 nM were added to the medium and the cells were incubated at 37°C for the indicated time periods in triplicates. To determine non-specific membrane binding and internalization, cells were incubated with radioligand in the presence of 1 μM [In^{III}]-**3**. Cellular uptake was stopped by removing medium from the cells and by washing twice with 1 mL of ice-cold PBS. Acid wash for 10 min with a glycine-buffer pH 2.8 on ice was also performed twice. This procedure was performed to distinguish between membrane-bound (acid-releasable) and internalized (acid-resistant) radioligand. Finally, the cells were treated with 1 N

NaOH. The culture medium, the receptor-bound and the internalized fraction were measured radiometrically in a γ-counter (Packard, Cobra II).

Cellular retention studies (AR42J and HEK cells). For cellular retention studies AR4-2J cells and respectively HEK cells stably expressing rsst3 (1 million) were incubated with 2.5 pmol/well (1.67 nM) $^{111}In/In^{III}$-labeled **2**, **3** or **5** for 120 min, respectively, then the medium was removed and the wells were washed twice with 1 mL ice-cold PBS. In each experiment an acid wash for 10 min on ice with a glycine-buffer of pH 2.8 was performed to remove the receptor-bound ligand. Cells were then incubated again at 37°C with fresh internalization buffer (DMEM containing 1% fetal bovine serum, pH 7.4). After different time points the external medium was removed for quantification of radioactivity in a γ-counter and replaced with fresh 37°C medium. The cells were solubilized in 1 N NaOH, removed and the internalized radioactivity was quantified in a γ-counter. The recycled fraction was expressed as percentage of the total internalized amount per 1 million cells and the integrity of the externalized peptides was determined using HPLC after removing the solvent by a centrifugal evaporator.

Immunocytochemistry. HEK cells stably expressing sst5 were grown on poly-L-lysine-coated coverslips overnight. After 30 min treatment with SS-14, In^{III}-**3** and In^{III}-**5**, respectively, cells were fixed with 4% paraformaldehyde and 0.2% picric acid in phosphate buffer (pH 6.9) for 40 min at room temperature and washed several times in 10 mM Tris-HCl, pH 7.4, 10 mM phosphate buffer, 137 mM NaCl and 0.05% thimerosal (TPBS). Specimens were then incubated for 3 min in 50% methanol and for 3 min in 100% methanol, washed in TPBS and preincubated with TPBS supplemented with 3% normal goat serum for 1 h at room temperature. Cells were then incubated with affinity-purified anti-sst5 antibody at a concentration of 1 μg/ml in TPBS supplemented with 1% normal goat serum overnight. After washing with TPBS, bound primary antibody was detected with cyanine 3.18-

conjugated secondary antibody (Jackson Immunoresearch, West Grove, PA). Cells were then dehydrated, cleared in xylol and permanently mounted in DPX (Fluka, Deisenhofen, Germany).

Animal biodistribution studies. Animals were kept, treated and cared for in compliance with the guidelines of the Swiss regulations (approval #789).

CA20948 rat tumor model. Male Lewis rats (Harlan, The Netherlands; 200-300 g), bearing the rat CA20948 pancreatic tumor [28] in their flank, were used in the experiments. Rats were injected under ether anesthesia with 2-3 MBq of 0.34 nmol (0.5 μg total peptide mass) [^{111}In]-DOTA-peptide in 0.5 mL saline into the dorsal vein of the penis.

AR42J rat tumor model. Five weeks old male Lewis rats were implanted subcutaneously with 10-12 millions AR4-2J cells freshly suspended in sterile PBS. Fourteen days after inoculation the rats showed solid palpable tumor masses (tumor weight 0.4-0.7 g) and were used for the experiments. Rats were injected under ether anesthesia with 2-3 MBq of 0.34 nmol (0.5 μg total peptide mass) [^{111}In]-DOTA-peptide in 0.05 mL NaCl solution 0.9% into the femoral vein.

In both animal models, at 4 h, 24 h and 48 h after injection rats were sacrificed under ether anesthesia. Organs and blood were collected and the radioactivity in these samples was determined using a γ-counter. In order to determine the non-specific uptake of the radiopeptides, rats were injected with 0.5 mg octreotide in 0.5 mL saline as a co-injection with the radioligand.

References

1. Veber, D. F., Freidinger, R.M., Schwenk-Perlow, D. et al. (1981) A potent cyclic hexapeptide analogue of somatostatin. Nature 292, 55-58.
2. Bauer, W., Briner, U., Doepfner, W. et al. (1982) SMS-201-995: a very potent and selective octapeptide analogue of somatostatin with prolonged action. Life Sci. 31, 1133-1140.
3. Hoyer, D., Bell, G.I., Berelewitz, M., et al. (1995) Classification and nomenclature of somatostatin receptors. Trends Pharmacol. Sci. 16, 86-88.
4. Reubi, J. C., Laissue, J., Krenning, E., Lamberts, S.W. (1992) Somatostatin receptors in human cancer: incidence, characteristics, functional correlates and clinical implications. J. Steroid. Biochem. Mol. Biol. 43, 27-35.
5. Reubi, J. C., Waser, B., Schaer, J.C., Laissue J.A. (2001) Somatostatin receptor sst1-sst5 expression in normal and neoplastic human tissues using receptor autoradiography with subtype-selective ligands. Eur. J. Nucl. Med. 28, 836-846.
6. Reubi, J. C. (2003) Peptide receptors as molecular targets for cancer diagnosis and therapy. Endocr. Rev. 24, 389-427.
7. Hofland, L. J., Liu, Q, Van Koetsveld, PM, et al. (1999) Immunohistochemical detection of somatostatin receptor subtypes sst1 and sst2A in human somatostatin receptor positive tumors. J. Clin. Endocrinol. Metab. 84, 775-780.
8. Kulaksiz, H., Eissele, R, Rossler, D, Schulz, S, Hollt, V, Cetin, Y, Arnold, R. (2002) Identification of somatostatin receptor subtypes 1, 2A, 3, and 5 in neuroendocrine tumours with subtype specific antibodies. Gut 50, 52-60.
9. Forssell-Aronsson, E., Nilsson, O., Benjegard, S.A., et al. (2000) ^{111}In-DTPA-D-Phe^{1}-octreotide binding and somatostatin receptor subtypes in thyroid tumors. J. Nucl. Med. 41, 636-642.

10. Halmos, G., Sun, B., Schally, A.V., Hebert, F., Nagy, A. (2000) Human ovarian cancers express somatostatin receptors. J. Clin. Oncol. Metab. 85, 3509-3512.

11. Ferone, D., Van Hagen, M.P., Kwekkeboom, D.J., et al. (2000) Somatostatin receptor subtypes in human thymoma and inhibition of cell proliferation by octreotide in vitro. J. Clin. Endocrinol. Metab. 85, 1719-1726.

12. Greenman, Y., Melmed, S. (1994) Expression of three somatostatin receptor subtypes in pituitary adenomas: evidence for preferential sst5 expresison in the mammosomatotroph lineage. J.Clin. Endocrinol. Metab. 79, 724-729.

13. Papotti, M., Croce, S., Bello, M., Bongiovanni, M., Allia, E., Schindler, M., Bussolati, G. (2001) Expresion of somatostatin receptor types 2, 3 and 5 in biopsies and surgical specimens of human lung tumours. Virchows Arch. 439, 787-797.

14. Reubi, J., Schaer, J., Waser, B., Wenger, S., Heppeler, A., Schmitt, J.S., et al. (2000) Affinity profiles for human somatostatin receptor sst1-sst5 of somatostatin radiotracers selected for scintigraphic and radiotherapeutic use. Eur. J. Nucl. Med. 27, 273-282.

15. Bodei, L., Cremonesi, M., Grana, C., Rocca, P., Bartolomei, M., Chinol, M., Paganelli, G. (2004) Receptor radionuclide therapy with ^{90}Y-[DOTA]^{0}-Tyr^{3}-octreotide (^{90}Y-DOTATOC) in neuroendocrine tumours. Eur. J. Nucl. Med. Mol. Imaging. 31, 038-046.

16. Murphy, W., Lance, V.A., Moreau, S., Moreau., J.P., Coy, D.H. (1987) Inhibition of rat prostate tumor growth by an octapeptide analog of somatostatin. Life Sci. 40, 2515-2522.

17. Cai, R., Szoke, B., Lu, R., Fu, D., Redding, T.W., Schally, A.V. (1986) Synthesis and biological activity of highly potent octapeptide analogs of somatostatin. Proc. Natl. Acad. Sci. USA 83, 1896-1900.

18. Melacini, G., Zhu, Q., Goodman, M. (1997) Multiconformational NMR analysis of Sandostatin (octreotide): equilibrium between β-sheet and partially helical structures. Biochemistry 36, 1233-1241.

19. Pohl, E., Heine, A., Sheldrick, G.M., Dauter, Z., Wilson, K.S., Kallen, J., Huber, W., Pfaffli, P.J. (1995) Structure of octreotide, a somatostatin analogue. Acta Crystallogr. D. Biol. Crystallogr. 51, 48-59.

20. Mattern, R., Moore, S.B., Tran, T.A., Rueter, J.K., Goodman, M. (2000) Synthesis, biological activities and conformational studies of somatostatin analogs. Tetrahedron 56, 9819-9831.

21. Wild, D., Schmitt, J.S., Ginj, M., Mäcke, H.R., Bernard, B.F., Krenning, E.P., De Jong, M., Wenger, S., Reubi, J.C. (2003) DOTA-NOC, a high affinity ligand of somatostatin receptor subtypes 2, 3 and 5 for labelling with various metals. Eur. J. Nucl. Med. Mol. Imaging 30, 1338-1347.

22. Lewis, I., Bauer, W., Albert, R., Chandramouli, N., Pless, J., Weckbecker, G., Bruns, C. (2003) A novel somatostatin mimic with broad somatotropin release inhibitory factor receptor binding and superior therapeutic potential. J. Med. Chem. 46, 2334-2344.

23. Hofland, L., Breeman, W.A., Krenning, E.P., de Jong, M., Waaijers, M., van Koetsveld, P.M., Macke, H.R., Lamberts, S.W. (1999) Internalization of [DOTA^{0},^{125}I-Tyr^{3}]Octreotide by somatostatin receptor-positive cells in vitro and in vivo: implications for somatostatin receptor-targeted radio-guided surgery. Proc. Assoc. Am. Physicians 111, 63-69.

24. Hocart, S. J., Jain, R., Murphy, W.A., Taylor, J.E., Morgan, B., Coy, D.H. (1998) Potent antagonists of somatostatin: synthesis and biology. J. Med. Chem. 41, 1146-1154.

25. Vale, W., Rivier, C., Brown, M., Rivier, J. Hypothalamic peptide hormones and pituitary regulation: Advances in experimental medicine and biology; Plenum Press: New York, 1977, pp 123-156.

26. Roth, A., Kreienkamp, H.J., Nehring, R.B., Roosterman, D., Meyerhof, W., Richter, D. (1997) Endocytosis of the rat somatostatin receptors: subtype discrimination, ligand specificity, and delineation of carboxy-terminal positive and negative sequence motifs. DNA Cell Biol. 16, 111-119.

27. Wild, D., Macke, H.R., Waser, B., Reubi, J.C., Ginj, M., Rasch, H., Muller-Brand, J., Hofmann, M. (2005) (68)Ga-DOTANOC: a first compound for PET imaging with high affinity for somatostatin receptor subtypes 2 and 5. Eur. J. Nucl. Med. Mol. Imaging 32, 724.

28. Stolz, B., Weckbecker, G., Smith-Jones, P.M., Albert, R., Raulf, F., Bruns, C. (1998) The somatostatin receptor-targeted radiotherapeutic [^{90}Y-DTPA-DPhe^{1},Tyr^{3}]octreotide (^{90}Y-SMT 487) eradicates experimental rat pancreatic CA 20948 tumours. Eur. J. Nucl. Med. 25, 668-674.

29. Elberg, G., Hipjin, RW, Schonbrunn, A. (2002) Homologous and heterologous regulation of somatostatin receptor 2. Mol Endocrinol 16, 2502-2514.

30. Ginj, M., Chen, J., Walter, M.A., Eltschinger, V., Reubi, J.C., and Maecke, H.R. (2005) Preclinical evaluation of new and highly potent analogs of octreotide for predictive imaging and targeted radiotherapy. Clin. Cancer Res. 11, 1136-1145.

31. Bruns, C., Lewis, I, Briner, U, Meno-Tetang, G, Weckbecker, G. (2002) SOM230: a novel somatostatin peptidomimetic with broad somatotropin release inhibiting factor (SRIF) receptor binding and a unique antisecretory profile. Eur. J. Endocrinol. 146, 707-716.

32. IUPAC-IUB Commission of Biochemical Nomenclature (CBN) (1972) Symbols for Amino-Acid Derivatives and Peptides, Recommendations 1971. Eur. J. Biochem. 27, 201-207.

33. Heppeler, A., Froidevaux, S., Maecke, H.R. et al. (1999) Radiometal-labelled macrocyclic chelator-derivatised somatostatin analogue with superb tumour targeting properties and potential for receptor-mediated internal radiotherapy. Chem. Eur. J. 5, 1974-1981.

34. Kaiser, E., Colescott, R.L., Bossinger, C.D., Cook, P.I. (1970) Color test for detection of free terminal amino groups in the solid-phase synthesis of peptides. Anal. Biochem. 34, 595-598.

35. Hancock, W. S., Battersby, J.E. (1976) A new micro-test for the detection of incomplete coupling reactions in solid-phase peptide synthesis using 2,4,6-trinitrobenzenesulphonic acid. Anal. Biochem. 71, 260-264.

Table (supplemental data). Analytical data of the compounds **1-24**.

No.	Compound name	Mass spectrum (*m/z*)		HPLC[c]
		calcd[a]	obsd[b]	(t_{R-1})[d]
1	DOTA-OC	1404.6	741.3	18.5
2	DOTA-[Tyr]^3-OC	1420.6	749.2	17.3
3	DOTA-[1-Nal]^3-OC	1454.6	767.0	19.0
4	DOTA-[2-Nal]^3-OC	1454.6	766.8	19.1
5	DOTA-[BzThi]^3-OC	1461.7	770.1	18.9
6	DOTA-[3-Pya]^3-OC	1405.6	742.0	14.7
7	DOTA-[4-Pya]^3-OC	1405.6	742.3	14.8
8	DOTA-[hPhe]^3-OC	1417.6	748.2	19.4
9	DOTA-[PhGly]^3-OC	1391.6	735.2	15.6
10	DOTA-[(4-iPr)Phe]^3-OC	1446.7	762.6	20.7
11	DOTA-[(4-F)Phe]^3-OC	1423.6	750.9	20.4
12	DOTA-[(4-I)Phe]^3-OC	1530.5	804.4	21.4
13	DOTA-[(4-Ph)Phe]^3-OC	1480.6	780.1	22.2
14	DOTA-[(3-I)Tyr]^3-OC	1546.5	762.4	19.4
15	DOTA-[(3-NO_2)Tyr]^3-OC	1465.6	772.0	18.3
16	DOTA-[Trp]^3-OC	1443.6	760.9	20.8
17	DOTA-[Thi]^3-OC	1410.6	744.4	18.2
18	DOTA-[BzTiaz]^3-OC	1462.7	770.6	17.0
19	DOTA-[Antra]^3-OC	1505.8	792.7	22.3
20	DOTA-[Pyra]^3-OC	1529.8	804.4	25.2
21	DOTA-[Ser]^3-OC	1345.5	712.3	14.2
22	DOTA-[Lys]^3-OC	1385.7	732.5	13.9
23	DOTA-[(4-Pip)Ala]^3-OC	1410.6	745.3	13.7
24	DOTA-[Cha]^3-OC	1410.7	745.9	20.5

[a] Theoretical molecular weight ($[M+H]^+$, Da). [b] Observed molecular weight ($[M+2K]^{2+}$, Da). [c]Reversed-phase HPLC (C-18, 5 μm, 4.6 × 250 mm, multiwavelength detection), retention times (min). Each compound was found to have a purity of > 98 % by HPLC. [d] HPLC-1 elution system: A, 0.1% TFA / H_2O; B, acetonitrile; 10% B to 60% B in 30 min at 0.75 mL min^{-1}.

Table 1. Affinity profiles (IC_{50}, nM)[a] for human sst receptors 1-5 (hsst 1-5).

Compound [b]	hsst1	hsst2	hsst3	hsst4	hsst5
SS-28	3.4 ± 0.3	2.7 ± 0.2	4.4 ± 0.4	3 ± 0.1	3.4 ± 0.3
M^{III}-**1**	> 10000	20 ± 2.2	27 ± 8	> 1000	58 ± 22
M^{III}-**2**	> 10000	11.4 ± 1.7	389 ± 136	> 10000	204 ± 92 (6)
M^{III}-**3**	> 1000	**3.3 ± 0.2**	**26 ± 1.9**	> 1000	**10.4 ± 1.6**
M^{III}-**4**	> 10000	25 ± 1.0	133 ± 68	> 1000	98 ± 12.5
M^{III}-**5**	> 10000	**3.1 ± 0.3**	**12 ± 1.0**	455 ± 65	**6 ± 1.8**
M^{III}-**6**	> 10000	22 ± 9	205 ± 43	> 1000	648 ± 165
M^{III}-**7**	> 10000	17 ± 6.6	617 ± 192	> 1000	647 ± 129
M^{III}-**8**	> 10000	47 ± 6.5	131 ± 69	> 1000	75 ± 45
M^{III}-**9**	> 1000	53 ± 16	649 ± 187	> 1000	> 1000
M^{III}-**10**	> 10000	85 ± 15	> 1000	> 1000	315 ± 105
M^{III}-**11**	> 1000	38 ± 2.0	52 ± 15	> 1000	283 ± 152
M^{III}-**12**	> 10000	39 ± 8.5	290 ± 160	> 1000	65 ± 7.0
M^{III}-**13**	> 10000	625 ± 25	> 1000	> 1000	495 ± 105
M^{III}-**14**	> 10000	4.0 ± 1.3	190 ± 10	> 1000	650 ± 250
M^{III}-**15**	> 10000	190 ± 50	> 1000	> 1000	775 ± 225
M^{III}-**16**	> 10000	12.3 ± 4.7	132 ± 18	960 ± 10	34 ± 3.0
M^{III}-**17**	> 10000	14 ± 1.5	22.7 ± 6.2	> 1000	137 ± 8.8
M^{III}-**18**	> 1000	161 ± 76	102 ± 53	187 ± 30	> 1000
M^{III}-**19**	> 1000	21 ± 1.0	47 ± 17	691 ± 99	20 ± 9.0
M^{III}-**20**	> 1000	93 ± 12	18 ± 1.0	> 1000	461 ± 163
M^{III}-**21**	> 1000	890 ± 74	119 ± 38	> 1000	> 1000
M^{III}-**22**	> 10000	> 1000	> 10000	> 10000	> 1000
M^{III}-**23**	> 10000	> 1000	> 1000	> 1000	> 1000
M^{III}-**24**	> 10000	285 ± 35	300 ± 130	> 1000	335 ± 5

[a] IC_{50} values are expressed as mean ± SEM; SS-28 is used as control. [b] All the compounds **1**-**24** were complexed either with Y^{III} or In^{III}.

Table 2. Internalization of ^{111}In-labeled peptides **1-24** in AR42J cells (rsst2) and in HEK-rsst3 cells after 4 h incubation at 37 ^{0}C. The results are expressed as % specific internalized from the total added radioactivity per one million cells (mean ± SEM; n = 3).

Radiopeptide	% internalized in AR42J cells	% internalized in HEK-rsst3 cells
^{111}In-**1**	6.1 ± 0.5	1.8 ± 0.7
^{111}In-**2**	11.5 ± 1.8	0.8 ± 0.2
^{111}In-**3**	25.0 ± 1.5	16.3 ± 1.9
^{111}In-**4**	0.9 ± 0.3	0.48 ± 0.2
^{111}In-**5**	17.2 ± 1.9	24.3 ± 0.9
^{111}In-**6**	1.1 ± 0.8	> 0.1
^{111}In-**7**	1.5 ± 0.3	> 0.1
^{111}In-**8**	1.9 ± 0.6	2.0 ± 0.1
^{111}In-**9**	0.7 ± 0.4	0.3 ± 0.1
^{111}In-**10**	12.7 ± 1.2	> 0.1
^{111}In-**11**	3.7 ± 0.3	5.3 ± 0.1
^{111}In-**12**	5.3 ± 0.7	1.16 ± 0.1
^{111}In-**13**	> 0.1	> 0.1
^{111}In-**14**	5.0 ± 0.4	1.2 ± 0.2
^{111}In-**15**	0.8 ± 0.2	> 0.1
^{111}In-**16**	5.3 ± 0.3	> 0.1
^{111}In-**17**	7.2 ± 0.6	12.6 ± 1.2
^{111}In-**18**	0.5 ± 0.3	> 0.1
^{111}In-**19**	2.7 ± 0.4	6.8 ± 0.3
^{111}In-**20**	2.4 ± 0.5	12.1 ± 1.0
^{111}In-**21**	> 0.1	0.8 ± 0.5
^{111}In-**22**	> 0.1	> 0.1
^{111}In-**23**	> 0.1	> 0.1
^{111}In-**24**	0.6 ± 0.3	> 0.1

Legend to the figures:

Figure 1. Structural formulae of conjugates **1**-**24**.

Figure 2. Schematic illustration of the partition coefficient values for the ^{111}In/^{115}In-labeled conjugates **1**-**24**.

Figure 3. Comparison in cellular retention after 2 h internalization of ^{111}In-**3** and ^{111}In-**5** in AR42J cells and in rsstr3-HEK cells, respectively. The values represent percentage retained in cell from the total amount internalized.

Figure 4. Immunocytochemical internalization in hsstr5-HEK cells of In^{III}-**3** and In^{III}-**5**, in comparison with SS-14.

Figure 5. Comparison in the tumor uptake kinetics and the tumor:kidney ratios between ^{111}In-**3** and ^{111}In-**5** in two animal models: CA20948 (**A**) and AR42J model (**B**).

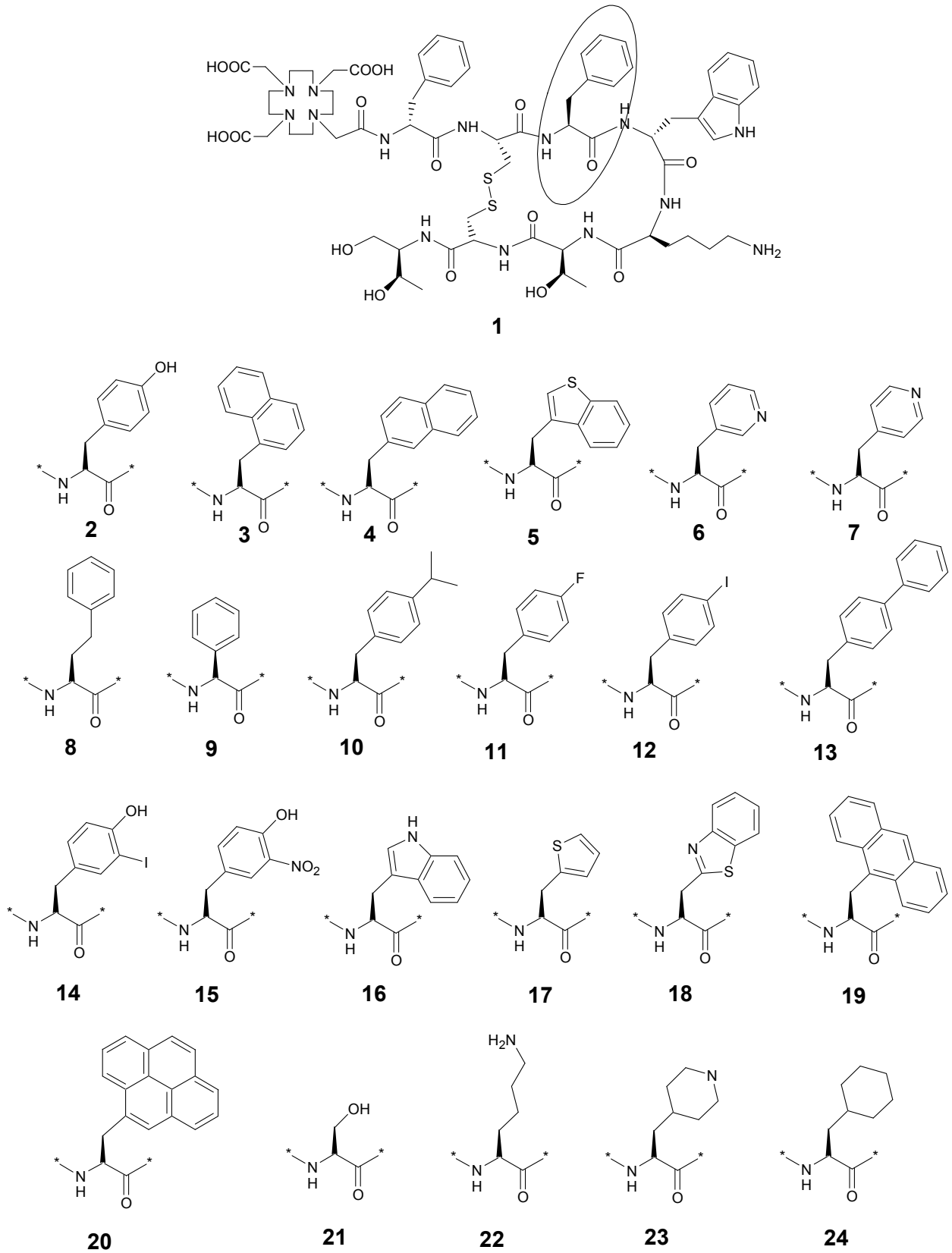

Fig.1

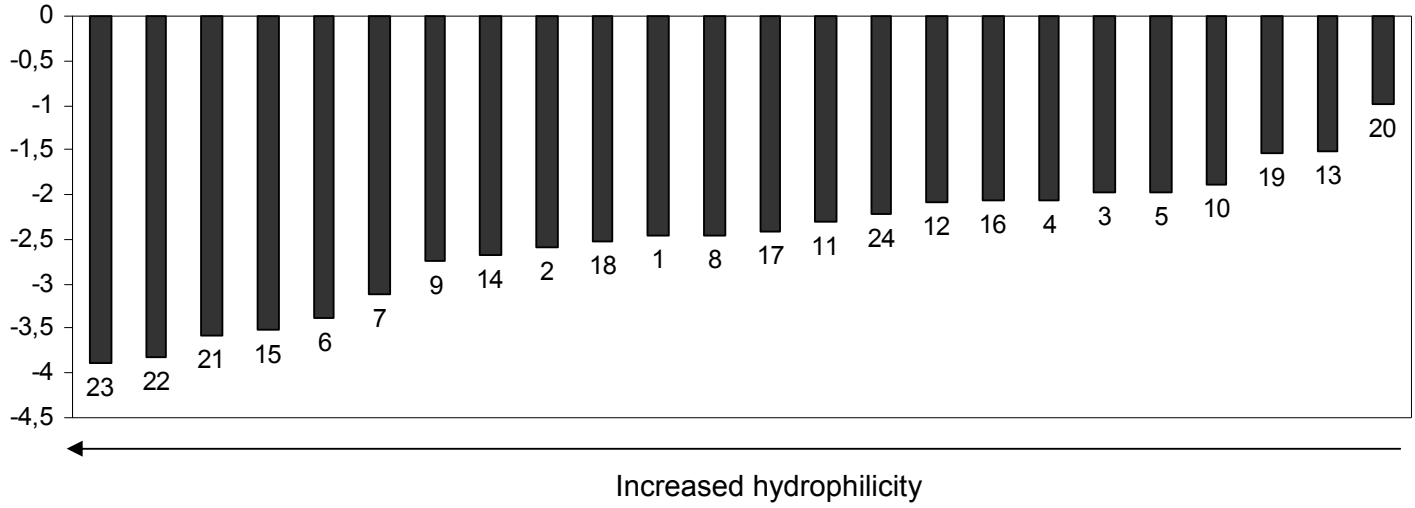
0
-0,5
-1
-1,5
-2
-2,5
-3
-3,5
-4
-4,5
23
22
21
15
6
7
9
14
2
18
1
8
17
11
24
12
16
4
3
5
10
19
13
20
Increased hydrophilicity

Fig.2

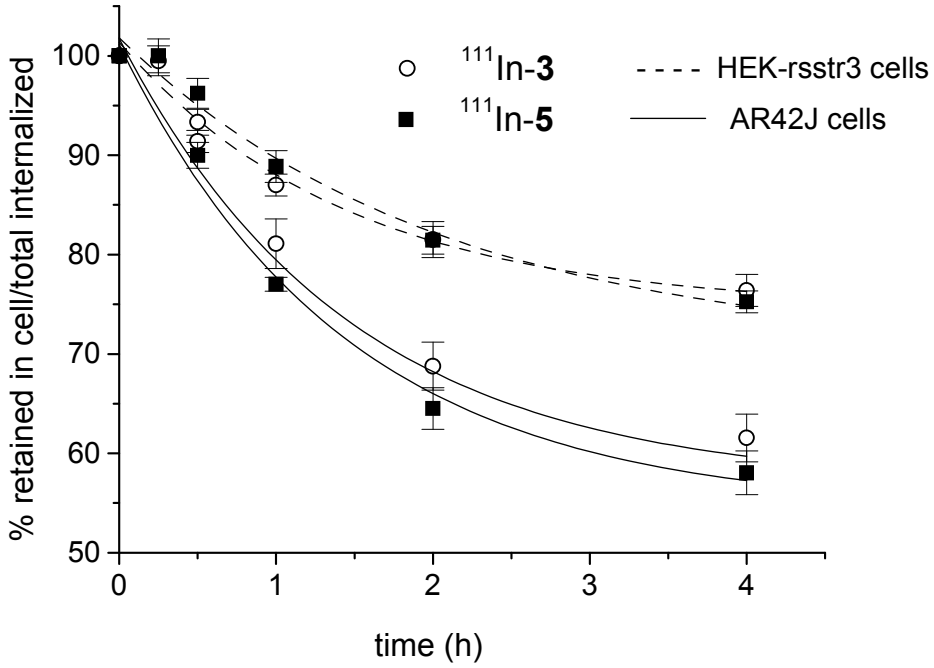
% retained in cell/total internalized
100
90
80
70
60
50
0
1
2
3
4
time (h)
111In-3
111In-5
HEK-rsstr3 cells
AR42J cells

Fig.3

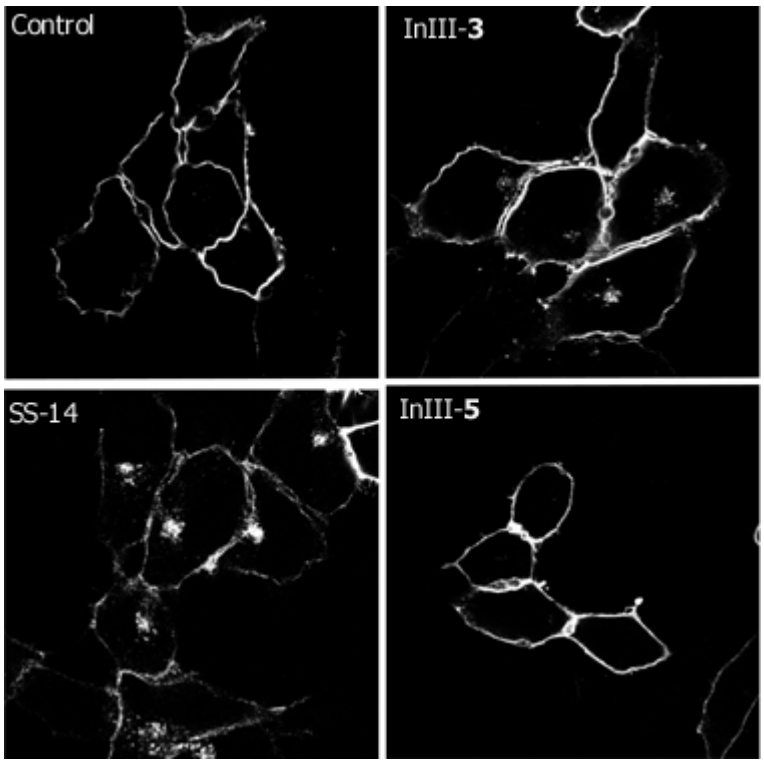

Fig.4

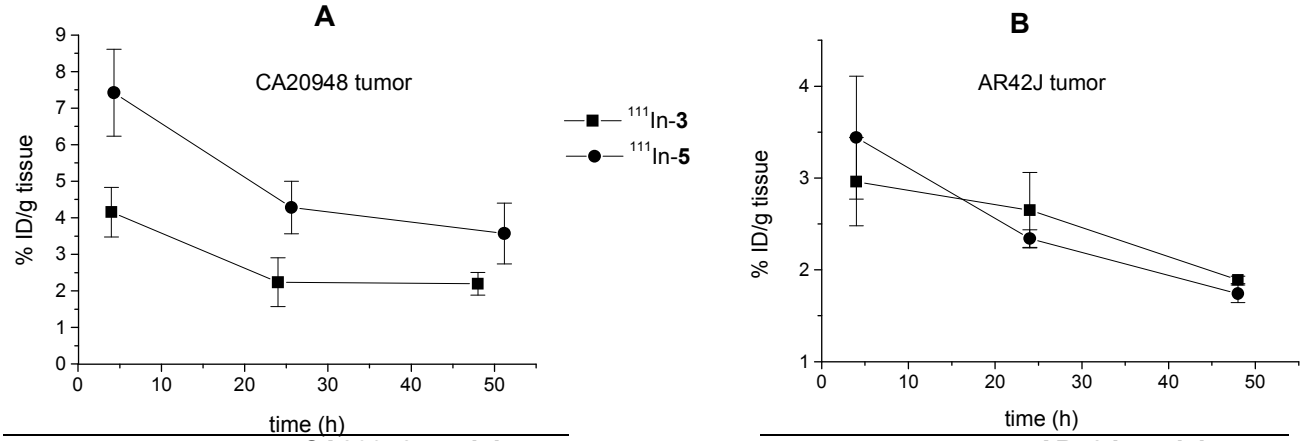

	CA20948 model	
Tumor:kidney	^{111}In-**3**	^{111}In-**5**
4h	2 ± 0.6	2.23 ± 0.3
24h	1.2 ± 0.3	1.44 ± 0.24
48h	1.12 ± 0.2	1.27 ± 0.29

	AR42J model	
Tumor:kidney	^{111}In-**3**	^{111}In-**5**
4h	2.1 ± 0.35	1.77 ± 0.3
24h	2.08 ± 0.3	1.42 ± 0.05
48h	1.5 ± 0.03	1.1 ± 0.06

Fig. 5

III

DOTA-NOC, a high-affinity ligand of somatostatin receptor subtypes 2, 3 and 5 for labelling with various radiometals

Damian Wild[1], Jörg S. Schmitt[1], Mihaela Ginj[1], Helmut R. Mäcke[1], Bert F. Bernard[2], Eric Krenning[2], Marion de Jong[2], Sandra Wenger[3], Jean-Claude Reubi[3]

[1] Division of Radiological Chemistry, Institute of Nuclear Medicine, Department of Radiology, University Hospital Basel, Basel, Switzerland
[2] Department of Nuclear Medicine, University Hospital Rotterdam, Rotterdam, The Netherlands
[3] Institute of Pathology, University of Bern, Bern, Switzerland

Received: 3 February 2003 / Accepted: 24 May 2003 / Published online: 21 August 2003

Abstract. Earlier studies have shown that modification of the octapeptide octreotide in positions 3 and 8 may result in compounds with increased somatostatin receptor affinity that, if radiolabelled, display improved uptake in somatostatin receptor-positive tumours. The aim of a recent research study in our laboratory was to employ the parallel peptide synthesis approach by further exchanging the amino acid in position 3 of octreotide and coupling the macrocyclic chelator DOTA(1,4,7,10-tetraazacyclododecane-1,4,7,10-tetraacetic acid) to these peptides for labelling with radiometals like gallium-67 or -68, indium-111, yttrium-90 and lutetium-177. The purpose was to find radiopeptides with an improved somatostatin receptor binding profile in order to extend the spectrum of targeted tumours. A first peptide, [^{111}In,^{90}Y-DOTA]-1-Nal^3-octreotide (^{111}In,^{90}Y-DOTA-NOC), was isolated which showed an improved profile. In^{III}-DOTA-NOC exhibited the following IC_{50} values (n*M*) when studied in competition with [^{125}I][Leu^8, D-Trp^{22}, Tyr^{25}]somatostatin-28 (values for Y^{III}-DOTA-NOC are shown in parentheses): sstr2, 2.9±0.1 (3.3±0.2); sstr3, 8±2 (26±1.9); sstr5, 11.2±3.5 (10.4±1.6). Affinity towards sstr1 and 4 was very low or absent. In^{III}-DOTA-NOC is superior to all somatostatin-based radiopeptides having this particular type of binding profile, including DOTA-lanreotide, and has three to four times higher binding affinity to sstr2 than In^{III},Y^{III}-DOTA-Tyr^3-octreotide (In^{III},Y^{III}-DOTA-TOC). In addition, [^{111}In]DOTA-NOC showed a specific and high rate of internalization into AR4-2J rat pancreatic tumour cells which, after 4 h, was about two times higher than that of [^{111}In]DOTA-TOC and three times higher than that of [^{111}In]DOTA-octreotide ([^{111}In]DOTA-OC). The internalized radiopeptides were externalized intact upon 2 h of internalization followed by an acid wash. After 2–3 h of externalization a plateau is reached, indicating a steady-state situation explained by reactivation of the receptors followed by re-endocytosis. Biodistribution studies in CA 20948 tumour-bearing rats showed rapid clearance from all sstr-negative tissues except the kidneys. At 4 h the uptake of [^{111}In]DOTA-NOC in the tumour and sstr-positive tissues, such as adrenals, stomach and pancreas, was three to four times higher than that of [^{111}In]DOTA-TOC. Differential blocking studies indicate that this is at least partially due to the uptake mediated by sstr3 and sstr5. These very promising preclinical data justify the use of this new radiopeptide for imaging and potentially internal radiotherapy studies in patients.

Keywords: Somatostatin receptor subtypes – Indium-111 – Yttrium-90 – Tumour targeting – Peptide receptors

Eur J Nucl Med Mol Imaging (2003) 30:1338–1347
DOI 10.1007/s00259-003-1255-5

Abbreviations of the common amino acids are in accordance with the recommendations of IUPAC-IUB [IUPAC-IUB Commission of Biochemical Nomenclature (CBN), Symbols for amino-acid derivatives and peptides, recommendations 1971. *Eur J Biochem* 1972; 27:201–207].

Helmut R. Mäcke (✉)
Division of Radiological Chemistry,
Institute of Nuclear Medicine, Department of Radiology,
University Hospital Basel, Petersgraben 4,
4031 Basel, Switzerland
e-mail: hmaecke@uhbs.ch
Tel.: +41-61-2654699, Fax: +41-61-2655559

Introduction

Radiopeptides are becoming of increasing interest in tumour targeting for either the localization or the internal radiotherapy of neoplasms [1, 2, 3, 4, 5, 6, 7, 8, 9]. Analogues of the somatotropin release inhibiting factor

(SRIF), somatostatin, radiolabelled with a variety of gamma-, positron- and beta-emitters, are the prototypes of such peptides. Somatostatin is a cyclic peptide hormone that occurs naturally in two bioactive molecular forms: somatostatin-14 and its N-terminally extended form, somatostatin-28. It exerts different biological effects in different parts of the body such as the brain, the pituitary, the pancreas, the gut and some components of the immune system. The effects include inhibition of hormone secretion and modulation of neurotransmission and cell proliferation. These actions are mediated by specific, G-protein-coupled receptors. Today five different somatostatin receptor subtypes have been characterized and cloned (sstr1–5). They are responsible for different biological responses. As some of these receptors are overexpressed in several human tumours, especially neuroendocrine tumours and their metastases, these tumours can be visualized in vivo by radiometal chelator conjugated somatostatin analogues like [^{111}In-DTPA-D-Phe^{1}]-octreotide (OctreoScan) [10]. It has also been shown that somatostatin receptor scintigraphy using this agent is the most sensitive method for localization of primary and metastatic disease in endocrine pancreatic tumours and carcinoids except insulinomas [11]. New conjugates may show higher sensitivity with regard to the localization of tumours and metastases, e.g. ^{99m}Tc-depreotide is registered in many countries and appears to show good performance in the evaluation of solitary pulmonary nodules [12], in breast tumours and even in melanoma [13]. On the other hand, a recent study comparing OctreoScan with ^{99m}Tc-depreotide in 44 patients with neuroendocrine tumours showed that the ^{111}In-labelled peptide yielded a far higher detection rate for neuroendocrine tumours, especially for liver metastases [14]. ^{111}In]DOTA-TOC and [^{90}Y]DOTA-TOC (DOTA = 1,4,7,10-tetraazacyclododecane-1,4,7,10-tetraacetic acid) have been shown to be effective targeting and therapeutic agents in animal models and patients [15, 16, 17, 18, 19, 20, 21, 22, 23]. In addition, replacement of the alcohol group at the C-terminus of the octapeptide by a carboxylic acid group led to increased sstr2 affinity [24], and [^{177}Lu-DOTA]-D-Phe^{1}-Tyr^{3}-Thr^{8}-octreotide ([^{177}Lu]DOTA-TATE) showed higher tumour uptake than [^{111}In-DTPA]-octreotide in six patients with somatostatin receptor-positive tumours [25]. These new radiopeptides show distinctly higher sstr2 affinity compared with OctreoScan. Nevertheless, they bind with high affinity only to sstr2: their affinity to sstr5 is low, and that to sstr3 almost negligible; no affinity of these new compounds was found to sstr1 and sstr4. Although the majority of tumours studied with radiolabelled somatostatin analogues express mainly sstr2 [26], recent literature data indicate that also sstr1 and sstr3–5 may be present in some human tumours. For example, in binding studies using [^{125}I]-RC-160 (D-Phe-Cys-Tyr-D-Trp-Lys-Val-Cys-Trp-NH_2; K_D=6.55 n*M*) as the radioligand, Halmos et al. [27] found somatostatin receptors to be present on 76% of human epithelial ovarian cancers. By use of in situ hybridization, Reubi et al. found m-RNAs of sstr1, 2 and 3 in a variety of human tumours, including GH-adenoma [28]. Forssell-Aronsson et al. reported the lack of sstr2 (except for medullary thyroid carcinoma) with Northern blot in most of the thyroid tumours studied in 68 patients. Nevertheless, all tumour types regularly expressed sstr1, sstr3, sstr4 and sstr5 [29]. Raderer et al. could visualize primary pancreatic adenocarcinoma in vivo with [^{111}In]DOTA-lanreotide (LAN; D-2-Nal-Cys-Tyr-D-Trp-Lys-Val-Cys-Thr-NH_2) but not with [^{111}In]DTPA-octreotide [30]. Traub et al. reported [^{111}In]DOTA-LAN to have a high sensitivity for detection of lung cancer [31]. However, their claim that this peptide targets sstr2–5 with high affinity and sstr1 with lower affinity could not be confirmed by Reubi et al. [24]. To extend the biological activity profile of radiolabelled somatostatin analogues, we started a programme to synthesize radiopeptides with affinity to all somatostatin receptor subtypes in order to potentially extend the spectrum of accessible tumours in diagnosis and internal radiotherapy. A first compound resulted from a parallel synthesis approach exchanging the amino acid in position 3 of octreotide; this led to a radiopeptide, [^{111}In/^{90}Y-DOTA]-1-Nal^{3}-octreotide ([^{111}In/^{90}Y]DOTA-NOC), which had improved affinity to sstr2 and high affinity to sstr3 and sstr5 when compared with our lead compound [^{111}In/^{90}Y]DOTA-TOC.

Here we present the preclinical evaluation of this peptide with regard to binding affinity, rate of internalization and biodistribution in a tumour-bearing rat model and compare its properties with those of [^{111}In/^{90}Y-DOTA^{0}-Tyr^{3}]-octreotide and [^{111}In/^{90}Y-DOTA^{0}]-octreotide.

Materials and methods

All chemicals were obtained from commercial sources and used without further purification. H-Thr(tBu)-ol-(2-chloro-trityl)-resin was obtained from Advanced ChemTech (Giessen, Germany) and Fmoc (9-fluorenylmethoxycarbonyl) amino acids were purchased from NovaBiochem AG (Läufelfingen, Switzerland), Bachem (Bubendorf, Switzerland) and Neosystems (France). $^{111}InCl_3$ was obtained from Mallinckrodt Medical (Petten, The Netherlands). The prochelator DOTA(tBu)$_3$ (4,7,10-tricarboxymethyl-*tert*-butyl ester 1,4,7,10-tetraazacyclododecane-1-acetate) was synthesized according to Heppeler et al. [32] or purchased from Macrocyclics (Richardson, Tex., USA). The reactive side chains of the amino acids were masked with one of the following groups: Cys, acetamidomethyl; Lys, *t*-butoxycarbonyl; Thr, *t*-butyl; Trp, *t*-butoxycarbonyl. Analytical reversed-phase high-performance liquid chromatography (RP-HPLC) was carried out on a Hewlett Packard 1050 HPLC system (Waldbronn, Germany) equipped with a multiwavelength detector and a flow-through Berthold LB506C1 gamma-detector. Preparative HPLC was done on a Bischof HPLC system (Metrohm AG, Switzerland) with HPLC-pumps 2250 and a Lambda 1010 UV detector (Metrohm AG, Switzerland). CC250/4 Nucleosil 120-3C18 columns from Macherey-Nagel were used for analytical HPLC, and a VP250/21 Nucleosil 200-5C15 column for preparative HPLC. The gradient systems consist-

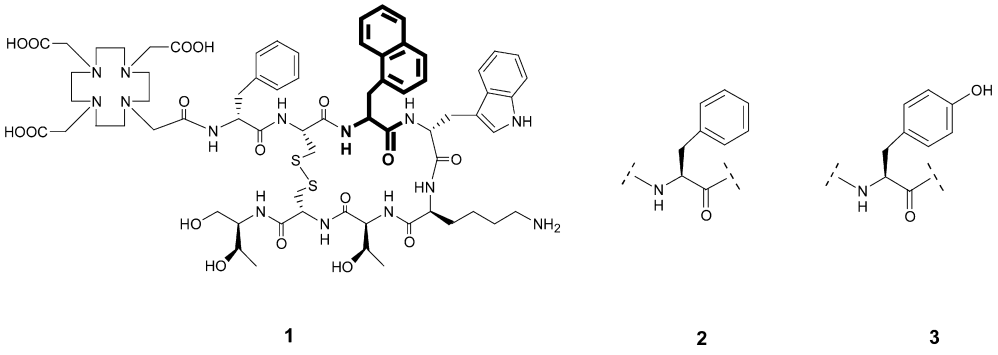

Fig. 1. Structural formulae of the DOTA-conjugated peptides. *1*, DOTA-1-Nal[3]-octreotide (DOTA-NOC); *2*, DOTA-octreotide (DOTA-OC); *3*, DOTA-Tyr[3]-octreotide (DOTA-TOC)

ed of mixtures of water with 0.1% trifluoroacetic acid (TFA) (solvent A) and acetonitrile (solvent B). Quantitative gamma-counting was performed on a COBRA 5003 gamma-system well counter from Packard Instrument Company (Switzerland). Electrospray ionization mass spectrometry (ESI-MS) was carried out with a Finnigan SSQ 7000 spectrometer (Bremen, Germany).

Synthesis. The peptide-chelator conjugates were synthesized by standard Fmoc solid phase synthesis [33] on 2-chlorotritylchloride resin (substitution 0.8 mmol/g) on a Rink peptide-synthesizer Switch 24 (RinkCombichem Technologies, Bubendorf, Switzerland), according to the general procedure described previously [32]. The last step was the coupling of the prochelator DOTA$(tBu)_3$ to the N-terminus of the peptide. Cleavage of the fully protected conjugates from the resin, oxidative cyclization using iodine, deprotection and HPLC purification led to compounds 1–3 (Table 1, Fig. 1), which could be labelled with "cold" or radioactive In^{3+} or Y^{3+} (In^{III}, Y^{III}). All compounds were lyophilized after purification and characterized by ESI-MS and RP-HPLC. In each case the MS spectra consisted of a major $[M+2Na]^{2+}$ ion peak and some other smaller peaks corresponding to $[M+Na]^{+}$ and $[M+3Na]^{3+}$ ions. All peptide-chelator conjugates had a purity >95% confirmed by RP-HPLC. The results are given in Table 1. The peptide-DOTA conjugates obtained were designated DOTA-NOC [DOTA[0]-D-Phe[1]-1-Nal[3]]-octreotide), DOTA-OC [DOTA[0]-octreotide]) and DOTA-TOC [DOTA[0]-Tyr[3]]-octreotide).

The DOTA-SRIF analogues were complexed with $InCl_3$ (anhyd.) and $Y(NO_3)_3 \cdot 5\ H_2O$, using the following procedure: ca. 20 µg of the respective DOTA-peptide was heated along with 1.5 eq. of the corresponding metal salt in 150 µl 0.2 *M* sodium acetate buffer (pH 5) for 25 min. After cooling, 20 µl 0.1 *M* DTPA (pH 5) was added to complex free metal ions. This mixture was loaded onto a SepPak C_{18} cartridge (Millipore, Switzerland), activated using 5 ml MeOH followed by 10 ml H_2O. $[M^{III}(DTPA)]^{2-}$ was washed from the cartridge using water. The M^{III}-DOTA-peptide was eluted with methanol and obtained in >97% purity after evaporation of methanol. The radiopeptides were synthesized according to Heppeler et al. [32] and obtained in >99% radiochemical purity at specific activities of >37 GBq/µmol peptide.

For internalization experiments, the DOTA-peptides were labelled to a specific activity of about 37 GBq/µmol peptide; excess $InCl_3$ was then added and the mixture was purified on a SepPak C_{18} cartridge as described above to afford [$^{111}In/In^{III}$]DOTA-peptides.

Determination of the somatostatin receptor affinity profiles. Cells stably expressing human sstr1–5 were grown as described previously [24]. All culture reagents were supplied by GIBCO/BRL and Life Technologies (Grand Island, N.Y.). Cell membrane pellets were prepared and receptor autoradiography was performed on pellet sections (mounted on microscope slides) as described in detail previously [24]. For each of the tested compounds, complete displacement experiments were performed with the universal somatostatin radioligand [^{125}I][Leu[8],D-Trp[22],Tyr[25]]somatostatin-28 using increasing concentrations of the unlabelled peptide ranging from 0.1 to 1,000 n*M*. Somatostatin-28 was run in parallel as control using the same increasing concentrations. IC_{50} values were calculated after quantification of the data using a computer-assisted image processing system. Tissue standards (autoradiographic [^{125}I]microscales Amersham, UK) containing known amounts of isotopes, cross-calibrated to tissue-equivalent ligand concentrations, were used for quantification [24]. The concentrations of the peptide solutions were measured by UV-spectroscopy ($\varepsilon_{NOC,280\ nm}$=9,855).

Cell culture and radioligand internalization studies. Sst_2 receptor expressing AR4-2J cells were obtained from Novartis Pharma (Basel, Switzerland). The AR4-2J cell line was maintained by serial passage in mono-layers in Dulbecco's Modified Eagle's Medium (DMEM), supplemented with 10% fetal bovine serum, amino acids, vitamins and penicillin-streptomycin, in a humidified 5% CO_2/air atmosphere at 37°C. Viability of the cells and cell numbers were counted under a microscope with a "Neubauer's counting chamber". For all cell experiments, the cells were seeded at a density of 0.8–1.1 million cells/well in six-well plates and incubated overnight with internalization buffer to obtain a good cell adherence. The loss of cells during the internalization experiments was below 10%. When different radiolabelled peptides were compared in cell experiments, the same cell suspension-containing plates were used. Furthermore, the internalization rate was linearly corrected to 1 million cells/well in all cell experiments.

Medium was removed from the six-well plates and cells were washed once with 2 ml of internalization buffer (DMEM, 1% fetal bovine serum, amino acids and vitamins, pH 7.4). Furthermore, 1.5 ml internalization buffer was added to each well and the plates were incubated at 37°C for about 1 h. Thereafter approximately 500,000 cpm or 0.02 MBq/well $^{111}In/^{115}In$-labelled peptides (2.5 pmol/well) to a final concentration of 1.67 n*M* were added to the medium and the cells were incubated at 37°C for the indicated time periods in triplicate. Internalization was also studied using three different concentrations of [$^{111}In/^{115}In$]DOTA-NOC (0.15 pmol/well or 0.1 n*M*, 2.5 pmol/well or 1.67 n*M*, and 10 pmol/well or 6.67 n*M*). To determine non-specific membrane binding and internalization, cells were incubated with radioligand in the presence of 1 µ*M* octreotide. Cellular uptake was stopped by removing medium from the cells and by washing twice with 1 ml of ice-cold phosphate-buffered saline (PBS). Acid wash for 10 min with a 0.1 *M* glycine buffer pH 2.8 on ice was also performed twice. This was shown previously to be suffi-

cient to remove >90% of receptor-bound radioligand. This procedure was performed to distinguish between membrane-bound (acid-releasable) and internalized (acid-resistant) radioligand. Finally, the cells were treated with 1 *N* NaOH. The culture medium, the receptor-bound and the internalized fraction were measured radiometrically in a gamma-counter (Packard, Cobra II).

Radioligand externalization studies. AR4-2J cells (1 million) were incubated with 2.5 pmol/well or 1.67 n*M* [^{111}In/^{115}In]-labelled DOTA-NOC, DOTA-TOC or DOTA-OC for 120 min, then the medium was removed and the wells were washed twice with 1 ml ice-cold PBS. In each experiment an acid wash for 10 min on ice with a glycine buffer of pH 2.8 was performed to remove the receptor-bound ligand. Cells were then incubated again at 37°C with fresh externalization buffer (DMEM containing 1% fetal bovine serum pH 7.4). After different time points the external medium was removed for quantification of radioactivity in a gamma-counter and replaced with fresh 37°C externalization medium. Internalized ligand was extracted in 1 *N* NaOH, removed and quantified in a gamma-counter. The recycled fraction was expressed as a percentage of the total internalized amount per 1 million cells, and the stability of the externalized peptides was determined using HPLC after removal of the solvent by a centrifugal evaporator.

Biodistribution. Animal experiments were performed in compliance with the regulations of our institutions and with generally accepted guidelines governing such work. Male Lewis rats (200–250 g) bearing the CA20948 pancreatic tumour (0.4–3.5 g) were used in the experiments. Rats were injected under ether anaesthesia with 2–3 MBq of 0.34 nmol (0.5 µg total peptide mass) [^{111}In]DOTA-NOC in 0.5 ml saline into the dorsal vein of the penis. At several time points, rats were sacrificed under ether anaesthesia. Organs and blood were collected and the radioactivity in these samples was determined using a gamma-counter.

In order to determine the non-specific uptake of the radiopeptides, rats were injected with 0.5 mg octreotide in 0.5 ml saline as a co-injection with the radioligand.

To study the sstr2-, 3- and 5-related specific uptake of [^{111}In]DOTA-NOC in the SRIF receptor-positive tissues, blocking studies were designed with two different somatostatin analogues: DTPA-TATE (sstr2-selective ligand) and In^{III}-DOTA-NOC (sstr2, 3, and 5 affinity). Twenty-five micrograms of these peptides was co-injected with 2–3 MBq [^{111}In]DOTA-NOC (0.34 nmol in 0.5 ml saline) into the dorsal vein of the penis of non-tumour-bearing male Lewis rats. Rats were sacrificed at 24 h and the organs of interest collected and counted for radioactivity.

Statistical methods. Student's *t* test was used to determine statistical significance. Differences at the 95% confidence level ($P<0.05$) were considered significant.

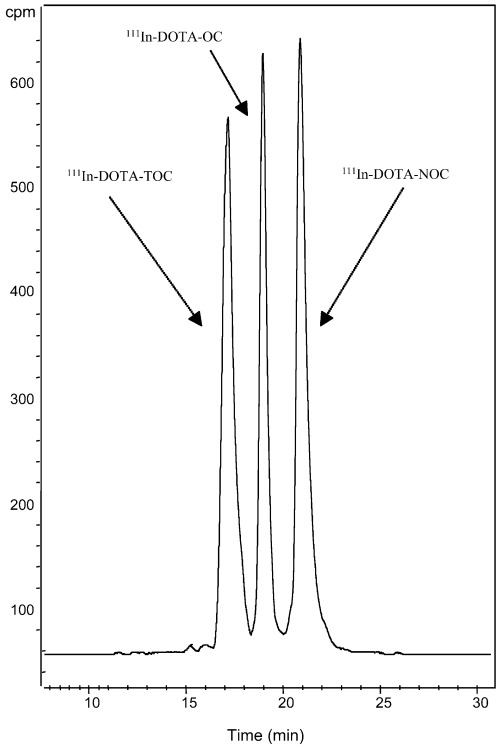

Fig. 2. Elution profile of [^{111}In]DOTA-TOC, [^{111}In]DOTA-OC and [^{111}In]DOTA-NOC on the HPLC system described in Materials and methods. The gradient applied was 0–30 min, 15% B to 40% B

Results

Synthesis and radiolabelling

The three DOTA-coupled octapeptides (Fig. 1) were obtained by parallel synthesis on a trityl chloride resin and are part of a small library. The peptides not reported here will be discussed in a more comprehensive chemistry publication. The overall yield of the DOTA peptides was about 30% based on the first Fmoc cleavage. The peptides were prepared and purified to >95% purity by HPLC analysis.

Uncomplexed and metal ion-complexed DOTA peptides were characterized by HPLC, by ESI-MS and by the retained affinity to the somatostatin receptors. Some selected analytical data are given in Table 1. Labelling

Table 1. Analytical data for each of the compounds

Compound number	Compound name	Mass spectrum		HPLC[a]	
		Calculated M (Da)	Observed M+Na$^+$ (Da)	T_R (min)	Purity (%)
1	DOTA-NOC	1,454.6	1,477.7	20.77	98.5
2	DOTA-OC	1,404.6	1,428.3	18.27	99.2
3	DOTA-TOC	1,420.6	1,444.3	16.1	99.0

[a] Elution system: flow 0.75 ml/min; A, 0.1% TFA in H_2O; B, MeCN; linear gradient: 0–30 min, 10% B to 60% B. T_R, elution time

was performed in acetate buffer (pH 5, 0.4 *M*) by heating at 95°C for 25 min, affording labelling yields with ^{111}In and ^{90}Y of >99% at a specific activity of >37 GBq/μmol peptide. The HPLC elution profile of the three ^{111}In-labelled peptides is shown in Fig. 2. The respective RF values are 17.03 min for [^{111}In]DOTA-TOC, 18.83 min for [^{111}In]DOTA-OC and 20.88 min for [^{111}In]DOTA-NOC (for a gradient see the footnote to Table 1), indicating that this is the order of increasing lipophilicity.

Receptor binding and affinity profiles

Table 2 shows the IC_{50} values of the three radiopeptides studied in this work as their Y^{III} (In^{III}) complexed versions and of Y^{III}-DOTA-LAN for the five somatostatin receptor subtypes. The values were obtained by performing complete displacement experiments with the universal somatostatin radioligand [^{125}I][Leu^8, D-Trp^{22}, Tyr^{25}]-somatostatin-28 on membranes from cells expressing the receptor subtypes and were compared with the data for somatostatin-28.

All compounds bound specifically to sstr2 with IC_{50} values between 3 and 23 n*M*. High specific binding affinities to sstr3 were also found for In^{III}-DOTA-NOC (IC_{50}=8±2 n*M*), Y^{III}-DOTA-NOC (IC_{50}=26±1.9 n*M*) and Y^{III}-DOTA-OC (IC_{50}=27±8 n*M*). Y^{III}-DOTA-TOC and Y^{III}-DOTA-LAN showed only very low affinities to sstr3 (IC_{50} ≥300 n*M*).

All metallopeptides also showed specific binding to sstr5; Y^{III}-DOTA-TOC bound with IC_{50}=204±92 n*M* and Y^{III}-DOTA-OC with IC_{50}=58±22 n*M* whereas Y^{III}-DOTA-LAN (IC_{50}=16.3±3.4 n*M*) and Y^{III}-DOTA-NOC (IC_{50}=10.4±1.6 n*M*) showed rather high affinities to sstr5.

In vitro internalization studies in AR4-2J cells

Figure 3 shows the results in respect of the time-dependent internalization of [^{111}In/^{115}In]DOTA-NOC, [^{111}In/^{115}In]DOTA-TOC and [^{111}In/^{115}In]DOTA-OC into AR4-2J rat pancreatic tumour cells during a 240-min incubation period at 37°C. About 85%–95% of totally internalized ligand was specifically internalized. At 30 min and 1.67 n*M* concentration, [^{111}In]DOTA-NOC showed 7.2%±1.0% specific cell uptake of the total activity administered which increased to 24.8%±1.6% up-

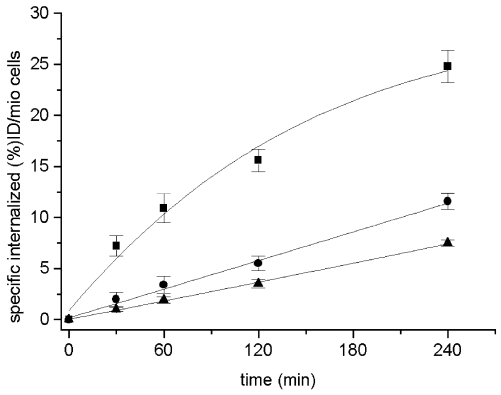

Fig. 3. Comparison of the internalization rate of [^{111}In]DOTA-NOC (■), [^{111}In]DOTA-TOC (●) and [^{111}In]DOTA-OC (▲) into AR4-2J cells. Values and standard deviations are the result of three independent experiments with triplicates in each experiment and are expressed as specific internalization (percentage of dose added to 1 million cells at 1.67 n*M* concentration, 37°C)

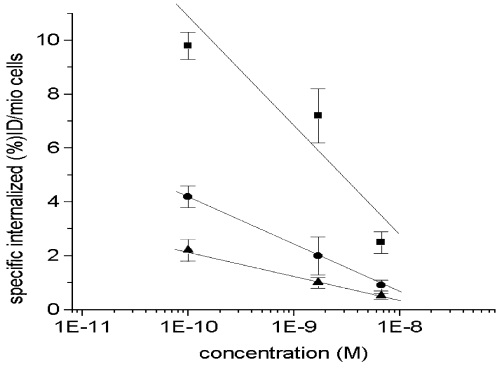

Fig. 4. Comparison of the percentage (± standard deviation) of radiopeptide internalized into AR4-2J cells (1 million cells, 37°C) after 30 min with different radiopeptide concentrations. *Symbols* are as in Fig. 3

Table 2. Affinity profiles (IC_{50}) for human sst 1–5 receptors

Compound	hsst1	hsst2	hsst3	hsst4	hsst5
SS-28	3.8±0.3 (10)	2.5±0.3 (11)	5.7±0.6 (10)	4.2±0.3 (11)	3.7±0.4 (11)
In^{III}-DOTA-NOC	>10,000 (3)	2.9±0.1 (3)	8±2 (3)	227±18 (3)	11.2±3.5 (3)
Y^{III}-DOTA-NOC	>1,000 (3)	3.3±0.2 (3)	26±1.9 (3)	>1,000 (3)	10.4±1.6 (3)
Y^{III}-DOTA-TOC	>10,000 (6)	11.4±1.7 (6)	389±136 (5)	>10,000 (6)	204±92 (6)
Y^{III}-DOTA-OC	>10,000 (5)	20±2.2 (5)	27±8 (5)	>1000 (5)	58±22 (4)
Y^{III}-DOTA-LAN	>10,000 (4)	22.8±4.9 (4)	290±105 (4)	>1000 (4)	16.3±3.4 (4)

IC_{50} values are in n*M* (mean±SEM). Number of independent studies is given in parentheses. SS-28 was used as control

Using an assay based on rat brain cortex membranes and [^{125}I]-Tyr^3-octreotide as radioligand, In^{III}-DOTA-D-Phe^1-octreotide and In^{III}-DOTA-Tyr^3-octreotide were shown to be equipotent to the corresponding Y^{III}-DOTA-peptides (data not shown or Heppeler et al. [32])

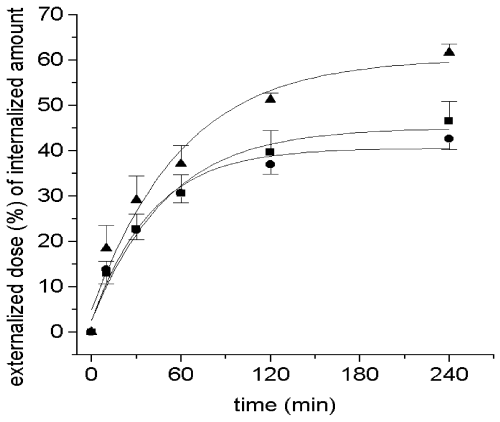

Fig. 5. Comparison of the externalization rate (± standard deviation) after 120-min internalization of the three radiopeptides. *Symbols* are as in Fig. 3

take at 4 h. A tendency to reach a plateau was found at 24 h for all three peptides (data not shown). The uptake of [^{111}In]DOTA-OC at 30 min was only 1.0%±0.2% and increased to 7.5%±0.3% at 4 h, whereas [^{111}In]DOTA-TOC showed 2.0%±0.7% internalization at 30 min, rising to 11.6%±0.8% at 4 h. The percentage of internalized peptide measured at 30 min as a function of concentration is shown in Fig. 4.

The rate of externalization is shown in Fig. 5. In these experiments, ^{111}In labelled peptides were allowed to internalize for 120 min; cells were then washed twice with PBS before removing the receptor-bound ligand with the glycine buffer. Medium was then added and removed after 10 min, 30 min, 60 min, 120 min and 240 min and measured for radioactivity. Up to 60 min, the three peptides showed insignificant differences in the externalization rate. Thereafter the extent of externalized ligand was highest for [^{111}In]DOTA-OC, with about 60% at 4 h compared with 47%±4% for [^{111}In]DOTA-NOC and

Table 3. Biodistribution and tissue radioactivity ratios in organs, blood and CA 20948 tumour of rats 4 h, 24 h and 48 h after injection of [^{111}In]DOTA-NOC and [^{111}In]DOTA-TOC

Time	Organ	[^{111}In]DOTA-TOC unblocked, *n*=3 rats	*P*	[^{111}In]DOTA-NOC unblocked, *n*=5 rats	[^{111}In]-DOTA-NOC blocked[c], *n*=3 rats
4 h	Blood[a]			0.014±0.001	
24 h	Blood[a]	0.002±0.000	0.009	0.003±0.0005	0.003±0.0001
4 h	Kidneys[a]			1.91±0.07	
24 h	Kidneys[a]	2.32±0.13	<0.0001	1.73±0.14	1.88±0.02
48 h	Kidneys[a]				1.81±0.14
4 h	Liver[a]			0.18±0.018	
24 h	Liver[a]	0.05±0.000	0.0004	0.11±0.020	0.10±0.008
24 h	Spleen[a]	0.04±0.000	0.0001	0.05±0.009	0.05±0.007
4 h	Femur[b]			0.127±0.010	
24 h	Femur[b]	0.05±0.010	0.0004	0.098±0.016	0.022±0.005
48 h	Femur[b]			0.084±0.014	
4 h	Pancreas[b]	2.57±0.08	<0.0001	7.75±1.39	
24 h	Pancreas[b]	1.70±0.13	0.01	2.93±0.69	0.33±0.05
4 h	Adrenals[b]	3.62±0.14	<0.0001	7.43±0.42	
24 h	Adrenals[b]	3.19±0.27	<0.0001	7.21±1.02	1.32±0.28
48 h	Adrenals[b]	1.80±0.13	<0.0001	5.85±0.60	
4 h	Stomach[b]			0.91±0.12	
24 h	Stomach[b]	0.25±0.04	0.0014	0.56±0.13	0.08±0.01
4 h	Pituitary[b]	1.48±0.07	019 ns	1.66±0.20	
24 h	Pituitary[b]	1.22±0.03	0.064 ns	1.89±0.55	0.21±0.06
4 h	Tumour[b]	1.15±0.16	0.0004	3.86±0.63	
24 h	Tumour[b]	1.12±0.11	0.021	2.08±0.62	0.36±0.10
48 h	Tumour[b]	0.51±0.04	<0.0001	2.04±0.29	
Tumour to tissue ratios					
24 h	Tumour/blood	520		693	
24 h	Tumour/liver	22.4		18.9	
4 h	Tumour/kidneys			2.02	
24 h	Tumour/kidneys	0.48		1.20	
48 h	Tumour/kidneys			1.12	

Values are the mean of % ID/g±SE
[a] Somatostatin receptor-negative organs
[b] Somatostatin receptor-positive organs
[c] Blocked with 0.5 mg octreotide as a co-injection with the radiopeptide

43%±2% for [^{111}In]DOTA-TOC. At 4 h the externalization curve of all peptides showed a plateau. Study of the chemical structure of the externalized [^{111}In]DOTA-NOC and [^{111}In]DOTA-TOC by HPLC gave no indication of metabolites. The peptides externalized were intact.

Biodistribution studies in rats

The 4-h, 24-h and 48-h uptake values of [^{111}In]DOTA-NOC and [^{111}In]DOTA-TOC in sst receptor-positive organs, including pancreas, adrenals, pituitary, stomach and CA 20948 rat pancreatic tumour, as well as the kidneys, liver, spleen, femur and blood are shown in Table 3. Both radiopeptides displayed rapid blood clearance with less than 0.02% ID/g remaining in the blood at 4 h. There was also fast clearance from all sstr-negative tissues except the kidneys. The excretion of both peptides was mainly by the kidneys. [^{111}In]DOTA-NOC had a significantly higher uptake than [^{111}In]DOTA-TOC in all sstr-positive tissues at all time points, e.g. at 4 h (tumour, 3.9%±0.6% ID/g vs 1.15%±0.16% ID/g; pancreas, 7.75%±1.4% ID/g vs 2.57%±0.08% ID/g; adrenals, 7.43%±0.42% ID/g vs 3.62%±0.14% ID/g; pituitary, 1.66%±0.20% ID/g vs 1.48%±0.07% ID/g).

To estimate the uptake in sstr-positive organs which may be due to receptor subtype expression other than sstr2, in vivo blocking studies were performed in normal rats using different blocking agents like [DTPA^0-Tyr^3-Thr^8]-octreotide (DTPA-TATE), an sstr2-specific ligand (IC_{50}=3.9±1 n*M*), and In^{III}-DOTA-NOC (IC_{50}: sstr2=2.9±0.1 n*M*, sstr3=8±2 n*M*, sstr5=11.2±3.5 n*M*). In the adrenals, blocking with only 25 µg of In^{III}-DOTA-NOC showed a very efficient reduction of about 95% whereas 25 µg of the sstr2-selective ligand DTPA-TATE resulted in only about 75% blocking.

A significantly higher blocking effect was also found with In^{III}-DOTA-NOC in the pancreas, pituitary and stomach (data not shown).

Discussion

Receptor scintigraphy with ^{111}In-DTPA-octreotide has become the "gold standard" for the localization, staging and management of neuroendocrine tumours [34]. The high sensitivity of somatostatin receptor scintigraphy and its ability to change the management of patients with neuroendocrine tumours has been demonstrated in several studies [35, 36, 37, 38, 39]. The same agent has been used for receptor-mediated radionuclide therapy with some success if injected in high doses (6 GBq every 4 weeks) for total doses of up to about 100 GBq [40, 41, 42]. This agent only binds with reasonably high affinity to sstr2 and with low affinity to sstr5 [24]; in addition, ^{111}In is not an ideal therapeutic radionuclide. Therefore several groups have developed agents based on somatostatin for improved targeting with positron emitters like ^{68}Ga, ^{64}Cu and the gamma emitter ^{111}In, and most importantly for labelling with therapeutic radionuclides like ^{90}Y and ^{177}Lu. The most successful peptides have been [Tyr^3]-octreotide (TOC) and [Tyr^3, Thr^8]-octreotide (octreotate = TATE) coupled to the macrocyclic chelator DOTA (DOTA-TOC, DOTA-TATE) [32, 43, 44, 45]. These agents bind with high affinity only to sstr2. Although sstr2 is probably the most abundantly expressed SRIF receptor in human cancer [26], subtypes sstr1, sstr3, sstr4 and sstr5 may also be of interest. So, our approach is focussed on the identification of analogues with a pan-somatostatin binding profile carrying functional groups for radiolabelling [46] and we have started a programme to use parallel synthesis methods to produce DOTA-coupled octapeptides with the aim of improving the affinity to subtypes other than 2 while maintaining the sstr2 affinity. In a series of compounds we found that [DOTA^0-1-naphthyl^3]-octreotide shows promising properties owing to its high affinity to sstr2, with an IC_{50} value of 3.3±0.2 n*M* if complexed to Y^{III} and 2.9±0.1 n*M* if complexed to In^{III}, which is three- to four-fold higher than the corresponding value for Y^{III}-DOTA-TOC (IC_{50}=11.4±1.7 n*M*). The new metallopeptides are equipotent to somatostatin-28 on sstr2 and a factor of 7 more potent than Y^{III}-DOTA-LAN. Moreover, they show good affinity to sstr3 and are significantly more potent at sstr5 than Y^{III}-DOTA-LAN. These data do not confirm the pan-somatostatin-like binding affinities of DOTA-LAN published earlier by Smith-Jones et al. [47]. In addition, In^{III}- and Y^{III}-DOTA-NOC show the highest affinities on sstr3. A metal ion dependence is found at sstr3 and sstr4, In^{III}-DOTA-NOC being about three to four times more potent than Y^{III}-DOTA-NOC. A potential explanation for this phenomenon is the difference in the coordination geometry of the two DOTA-metal^{III} complexes, which was documented using ^{1}H-NMR spectroscopy and X-ray crystallography [48]. Y^{III}-DOTA-OC and Y^{III}-DOTA-NOC are equipotent on sstr3 and about a factor of 6 less potent than the endogenous ligand. There is no metal ion dependence in affinity to sstr5.

Cell uptake and release

In order to obtain a defined and homogeneous metallopeptide, [^{111}In]DOTA-NOC was complexed with "cold" In^{III} to yield [^{111}In, ^{115}In]DOTA-NOC. At 4 h of internalization, [^{111}In/^{115}In]DOTA-NOC showed a factor of 2 higher specific cell uptake than [^{111}In/^{115}In]DOTA-TOC and a factor of about 3 higher than [^{111}In/^{115}In]DOTA-OC at 1.67 n*M* peptide concentration per 1 million cells. The difference was even more pronounced at 0.1 n*M* concentration (Fig. 4). This order follows the receptor affinity of the three radiopeptides, indicating that receptor affinity is the major factor determining the rate of internalization.

As the addition of excess cold octreotide inhibits 90% of the uptake, it can be considered as specific and recep-

tor mediated. In the time interval of the study, no steady state was reached, but the distinct leveling off of [^{111}In/^{115}In]DOTA-NOC uptake indicates that steady state was closely approached; we explain this by the onset of efflux of radiopeptides that were shown to be structurally intact.

If, upon internalization of the radioligand for 2 h, the cells were exposed to the culture medium, a time-dependent efflux of the radiopeptides could again be observed, indicating rapid recycling to the extracellular medium. A steady state was reached already after 2–3 h of release (Fig. 5). This is in agreement with data that we have published previously on [^{67}Ga]NODAGA-TOC [49]. We interpret this as beginning reactivation of the receptors by the intact externalized peptides and concomitant reendocytosis. The finding that the weakest binder [^{111}In]DOTA-OC apparently shows the most efficient externalization fits with this explanation. The fact that the externalized peptides are still intact upon release is another indication that this is the correct interpretation. It is also in keeping with the conclusion drawn from data obtained by Koenig et al. [50].

Biodistribution studies

The biodistribution studies in CA20948-bearing tumour rats demonstrated superior uptake of [^{111}In]DOTA-NOC compared with [^{111}In]DOTA-TOC at 4 h, 24 h and 48 h in receptor-positive normal tissues (except the pituitary) and the tumour. An estimated area under the curve showed an improvement of approximately 2.5-fold in the tumour. This improvement is likely due to the improved sst2, sst3 and sst5 receptor affinity and the significantly faster rate of internalization, as exemplified in the AR4-2J cell line. The octreotide co-injection experiment demonstrated that the uptake is specific and receptor mediated.

Radiometal labelled radiopeptides show high and persistent kidney uptake, limiting their therapeutic potential. One of the goals in the design of new somatostatin-based radioligands is to reduce their uptake in the kidney. Indeed, the tumour-to-kidney ratio of [^{111}In]DOTA-NOC is improved 2.5-fold compared with [^{111}In]DOTA-TOC.

Despite the distinctly higher lipophilicity of [^{111}In]DOTA-NOC over [^{111}In]DOTA-TOC, the uptake in the liver and the intestines is surprisingly low. In addition, the long residence time of the new radiopeptide in the tumour indicates that it is not only suitable for imaging but also efficacious in targeted radiotherapy when labelled with ^{90}Y and/or ^{177}Lu provided that there is no significant difference among these M^{III} radiometals.

To understand the contribution of the high uptake values in SRIF receptor-positive organs due to the different subtype affinities of [^{111}In]DOTA-NOC, the uptake in these tissues was studied using different blocking agents, namely DTPA-TATE, an sstr2-specific ligand with IC_{50}=3.9±1 n*M*, and In^{III}-DOTA-NOC, which has a high affinity to sstr2, sstr3 and sstr5. The higher blocking efficiency of In^{III}-DOTA-NOC in the adrenals, pancreas, stomach and pituitary may indicate that part of the radioligand uptake is due to the improved receptor subtype profile. These organs have previously been shown to express different receptor subtypes, at least at the mRNA level: sstr2: adrenals, pituitary and pancreas; sstr3: pituitary, pancreas and stomach; sstr5: adrenals, pituitary, pancreas and stomach [51].

In conclusion, we have developed a new radiopeptide based on somatostatin which promises to target a broader range of somatostatin receptors and concomitantly a larger spectrum of tumours. These preclinical data indicate that [^{111}In]DOTA-NOC is superior to existing and well-studied radiolabelled somatostatin analogues. Indeed, the predictions from these preclinical studies have been confirmed in initial clinical studies in which excellent images of thyroid cancer patients have been obtained. We assume that [^{90}Y]/[^{177}Lu]DOTA-NOC will have similar favourable properties.

Acknowledgements. M. Ginj, D. Wild, J. Schmitt and H. Maecke acknowledge support from the Swiss National Science Foundation project No. 31-52969.97, BBW No. C00.0091 and BBT project 4668.1 EUS. The support provided by Novartis Pharma in respect of MS and NMR is gratefully acknowledged.

This work was performed within the COST B12 action.

References

1. Behr TM, Béhé M, Becker W. Diagnostic applications of radiolabeled peptides in nuclear endocrinology. *Q J Nucl Med* 1999; 43:268–280.
2. Breeman WAP, de Jong M, Kwekkeboom DJ, et al. Somatostatin receptor-mediated imaging and therapy: basic science, current knowledge, limitations and future perspectives. *Eur J Nucl Med* 2001; 28:1421–1429.
3. Fischman A, Babich J, Strauss H. A ticket to ride: peptide radiopharmaceuticals. *J Nucl Med* 1993; 34:2253–2263.
4. Heppeler A, Froidevaux S, Eberle A, Maecke H. Receptor targeting for tumor localization and therapy with radiopeptides. *Curr Med Chem* 2000; 7:971–994.
5. Lamberts SW, Van der Lely AJ, De Herder WW, Hofland LJ. Octreotide. *N Engl J Med* 1996; 25:246–254.
6. Lister-James J, Moyer B, Dean T. Small peptides radiolabeled with ^{99m}Tc. *Q J Nucl Med* 1996; 40:221–233.
7. Liu S, Edwards D. ^{99m}Tc-labeled small peptides as diagnostic radiopharmaceuticals. *Chem Rev* 1999; 99:2235–2268.
8. Reubi JC. Neuropeptide receptors in health and disease: the molecular basis for in vivo imaging. *J Nucl Med* 1995; 36: 1825–1835.
9. Thakur M. Radiolabelled peptides: now and the future. *Nucl Med Comm* 1995; 16:724–732.
10. Krenning EP, Kwekkeboom DJ, Bakker WH, et al. Somatostatin receptor scintigraphy with [^{111}In-DTPA-D-Phe^1]- and [^{123}I-Tyr^3]-octreotide: the Rotterdam experience with more than 1000 patients. *Eur J Nucl Med* 1993; 20:716–731.
11. Gibril F, Reynolds JC, Doppman JL, et al. Somatostatin receptor scintigraphy: its sensitivity compared with that of other im-

aging methods in detecting primary and metastatic gastrinomas—a prospective study. *Ann Intern Med* 1996; 125:24–26.
12. Blum JE, Handmaker H, Rinne NA. The utility of a somatostatin-type receptor binding peptide radiopharmaceutical (P829) in the evaluation of solitary pulmonary nodules. *CHEST* 1999; 115:224–232.
13. Virgolini I, Leimer M, Handmaker H, et al. Somatostatin receptor subtype specificity and in vivo binding of a novel tumor tracer, ^{99m}Tc-P829. *Cancer Res* 1998; 58:1850–1859.
14. Lebtahi R, Le Cloirec J, Houzard C, et al. Detection of neuroendocrine tumors: ^{99m}Tc-P829 scintigraphy compared with ^{111}In-pentetreotide scintigraphy. *J Nucl Med* 2002; 43:889–895.
15. de Jong M, Bakker WH, Krenning EP, et al. Yttrium-90 and indium-111 labelling, receptor binding and biodistribution of [DOTA^0,D-Phe^1,Tyr^3]octreotide, a promising somatostatin analogue for radionuclide therapy. *Eur J Nucl Med* 1997; 24: 368–371.
16. Stolz B, Weckbecker G, Smith-Jones PM, Albert R, Raulf F, Bruns C. The somatostatin receptor-targeted radiotherapeutic [^{90}Y-DPTA-DPhe^1,Tyr^3]octreotide (^{90}Y-SMT 487) eradicates experimental rat pancreatic CA 20948 tumours. *Eur J Nucl Med* 1998; 25:668–674.
17. Otte A, Herrmann R, Heppeler A, et al. Yttrium-90-DOTATOC: first clinical results. *Eur J Nucl Med* 1999; 26:1439–1447.
18. Otte A, Mueller-Brand J, Dellas S, Nitzsche E, Herrmann R, Maecke H. Yttrium-90-labelled somatostatin-analogue for cancer treatment. *Lancet* 1998; 351:417–418.
19. Cremonesi M, Ferrari M, Zoboli S, et al. Biokinetics and dosimetry in patients administered with ^{111}In-DOTA-Tyr^3-octreotide: implications for internal radiotherapy with ^{90}Y-DOTATOC. *Eur J Nucl Med* 1999; 26:877–886.
20. Waldherr C, Pless M, Maecke H, et al. Tumor response and clinical benefit in neuroendocrine tumors after 7.4 GBq ^{90}Y-DOTATOC. *J Nucl Med* 2002; 43:610–616.
21. Paganelli G, Zoboli S, Cremonesi M, et al. Receptor-mediated radiotherapy with ^{90}Y-DOTA-Phe^1-Tyr^3-octreotide. *Eur J Nucl Med* 2001; 28:426–434.
22. Waldherr C, Pless M, Maecke H, Haldemann A, Mueller-Brand J. The clinical value of [^{90}Y-DOTA]-D-Phe^1-Tyr^3-octreotide (^{90}Y-DOTATOC) in the treatment of neuroendocrine tumours: a clinical phase II study. *Ann Oncol* 2001; 12: 942–945.
23. de Jong M, Breeman WA, Bernard BF, et al. Tumor response after [^{90}Y-DOTA^0,Tyr^3]octreotide radionuclide therapy in a transplantable rat tumor model is dependent on tumor size. *J Nucl Med* 2001; 42:1841–1846.
24. Reubi J, Schaer J, Waser B, et al. Affinity profiles for human somatostatin receptor sst1–sst5 of somatostatin radiotracers selected for scintigraphic and radiotherapeutic use. *Eur J Nucl Med* 2000; 27:273–282.
25. Kwekkeboom DJ, Bakker WH, Kooij PP, et al. [^{177}Lu-DOTA^0,Tyr^3]octreotate: comparison with [^{111}DTPA^0]octreotide in patients. *Eur J Nucl Med* 2001; 28:1319–1325.
26. Reubi JC, Waser B, Schaer J, Laissue JA. Somatostatin receptor sst1–sst5 expression in normal and neoplastic human tissues using receptor autoradiography with subtype-selective ligands. *Eur J Nucl Med* 2001; 28:836–846.
27. Halmos G, Sun B, Schally AV, Hebert F, Nagy A. Human ovarian cancers express somatostatin receptors. *J Clin Endocrinol Metab* 2000; 85:3509–3512.
28. Reubi JC, Schaer J, Waser B, Mengod G. Expression and localization of somatostatin receptor sstr1, sstr2, and sstr3 messenger RNAs in primary human tumors using in situ hybridization. *Cancer Res* 1994; 54:3455–3459.
29. Forssell-Aronsson E, Nilsson O, Benjegard SA, et al. ^{111}In-DTPA-D-Phe^1-octreotide binding and somatostatin receptor subtypes in thyroid tumors. *J Nucl Med* 2000; 41:636–642.
30. Raderer M, Pangerl T, Leimer M, et al. Expression of human somatostatin receptor subtype 3 in pancreatic cancer in vitro and in vivo. *J Nat Cancer Inst* 1998; 90:1666–1668.
31. Traub T, Petkov V, Ofluoglu S, et al. ^{111}In-DOTA-lanreotide scintigraphy in patients with tumors of the lung. *J Nucl Med* 2001; 42:1309–1315.
32. Heppeler A, Froidevaux S, Maecke HR, et al. Radiometal-labelled macrocyclic chelator-derivatised somatostatin analogue with superb tumour targeting properties and potential for receptor-mediated internal radiotherapy. *Chem Eur J* 1999; 5:1974–1981.
33. Atherton E, Sheppard R. Fluorenylmethoxycarbonyl-polyamide solid phase peptide synthesis. General principles and development. Oxford: Oxford Information Press, 1989.
34. Oberg K. Established clinical use of octreotide and lanreotide in oncology. *Chemotherapy* 2001; 47:40–53.
35. Chiti A, Fanti S, Savelli G, et al. Comparison of somatostatin receptor imaging, computed tomography and ultrasound in the clinical management of neuroendocrine gastro-entero-pancreatic tumours. *Eur J Nucl Med* 1998; 25:1396–1403.
36. Lebtahi R, Cadiot G, Sarda L, et al. Clinical impact of somatostatin receptor scintigraphy in the management of patients with neuroendocrine gastroenteropancreatic tumors. *J Nucl Med* 1997; 38:853–858.
37. Cadiot G, Bonnaud G, Lebtahi R, et al. Usefulness of somatostatin receptor scintigraphy in the management of patients with Zollinger-Ellison syndrome. *Gut* 1997; 41:107–114.
38. Termanini B, Gibril F, Reynolds JC, et al. Value of somatostatin receptor scintigraphy: a prospective study in gastrinoma of its effect on clinical management. *Gastroenterology* 1997; 112:335–347.
39. Gibril F, Doppman JL, Reynolds JC, et al. Bone metastases in patients with gastrinomas: a prospective study of bone scanning, somatostatin receptor scanning, and MRI in their detection, their frequency, location and effect of their detection on management. *J Clin Oncol* 1998; 16:1040–1053.
40. Krenning EP, de Jong M, Kooij PP, et al. Radiolabelled somatostatin analogue(s) for peptide receptor scintigraphy and radionuclide therapy. *Ann Oncol* 1999; 10 (Suppl 2):S23–S29.
41. Janson E, Eriksson B, Oberg K. Treatment with high dose [^{111}In-DTPA-D-Phe^1]-octreotide in patients with neuroendocrine tumors. *Acta Oncol* 1999; 38:373–377.
42. Valkema R, de Jong M, Bakker WH, et al. Phase 1 study of peptide receptor radionuclide therapy with [^{111}In-DTPA^0]-octreotide: the Rotterdam experience. *Semin Nucl Med* 2002; 32:110–123.
43. de Jong M, Breeman WA, Bernard BF, et al. [^{177}Lu-DOTA^0,Tyr^3]Octreotate for somatostatin receptor-targeted radionuclide therapy. *Int J Cancer* 2001; 92:628–633.
44. Lewis J, Lewis M, Srinivasan A, Schmidt MA, Wang J, Anderson CJ. Comparison of four ^{64}Cu-labeled somatostatin analogues in vitro and in tumor-bearing rat model: evaluation of new derivatives for positron emission tomography imaging and targeted radiotherapy. *J Med Chem* 1998; 42:1341–1347.
45. Froidevaux S, Heppeler A, Eberle A, et al. Preclinical comparison in AR4-2J tumor bearing-mice of four radiolabeled 1,4,7,10-tetraazacyclododecane-1,4,7,10-tetraacetic acid-somatostatin analogs for tumor diagnosis and internal radiotherapy. *Endocrinology* 2000; 141:3304–3312.

46. Reubi JC, Eisenwiener KP, Rink H, Waser B, Maecke H. A new peptide somatostatin agonist with high affinity to all five somatostatin receptors. *Eur J Pharmacol* 2002; 456: 45–49.
47. Smith-Jones PM, Bischof C, Leimer M, et al. DOTA-lanreotide: a novel somatostatin analog for tumor diagnosis and therapy. *Endocrinology* 1999; 140:5136–5148.
48. Maecke H, Scherer G, Heppeler A, Hennig M. Is In-111 an ideal surrogate for Y-90? If not why? *Eur J Nucl Med* 2001; 28:967.
49. Eisenwiener KP, Prata MIM, Buschmann I, et al. NODAGATOC, a new chelator-coupled somatostatin analogue labeled with [$^{67/68}$Ga] and [^{111}In] for SPECT, PET, and targeted therapeutic applications of somatostatin receptor (hsst2) expressing tumors. *Bioconj Chem* 2002; 13:530–541.
50. Koenig JA, Kaur R, Dodgeon I, Edwardson JM, Humphrey PPA. Fates of endocytosed somatostatin sst2 receptor and associated agonists. *Biochem J* 1998; 336:291–298.
51. Raulf F, Pérez J, Joyer D, Bruns C. Differential expression of five somatostatin receptor subtypes, sstr1-5, in the CNS and peripheral tissue. *Digestion* 1994; 55 (Suppl 3):46–53.

IIIa

^{68}Ga-DOTANOC: a first compound for PET imaging with high affinity for somatostatin receptor subtypes 2 and 5

Damian Wild[1], Helmut R. Mäcke[1], Beatrice Waser[2], Jean Claude Reubi[2], Mihaela Ginj[1], Helmut Rasch[1], Jan Müller-Brand[1], Michael Hofmann[3]

[1] Clinic and Institute of Nuclear Medicine, University Hospital Basel, Petersgraben, 4, 4031, Basel, Switzerland
[2] Institute of Pathology, University of Bern, 3010, Bern, Switzerland
[3] Department of Nuclear Medicine, Hannover University Medical School, Hannover, Germany

Published online: 18 November 2004

Eur J Nucl Med Mol Imaging (2005) :724
DOI 10.1007/s00259-004-1697-4

Existing somatostatin-based radiotracers (e.g. ^{111}In-DOTATOC) have sole affinity for somatostatin receptor subtype 2 (sst_2). This represents a drawback, given that sst_{1-5} have been shown to be over-expressed in different tumours, alone or concomitantly [1]. Our goal, therefore, was to develop radiopeptides with broader receptor subtype profiles.

^{68}Ga-DOTANOC is a first compound for PET imaging with high affinity for sst_2 and sst_5 [2]. Its affinity profile (IC_{50} nM) for human sst_{1-5} is, respectively, >10,000, 1.9±0.4, 40±5.8, 260±74 and 7.2±1.6. For comparison, the values for the standard compound, ^{111}In-DOTATOC, are >10,000, 4.6±0.2, 120±26, 230±82 and 130±17.

Here we present the 60 min p.i. ^{68}Ga-DOTANOC PET images and the 21 h p.i. ^{111}In-DOTATOC planar images of a 52-year-old patient with an advanced neuroendocrine tumour. The two examinations were performed within 4 weeks. During this time interval the patient received bisphosphonates.

Preparation and application of ^{68}Ga-DOTANOC PET and ^{68}Ga-DOTATOC PET are comparable [3].

In the reported case study, the ^{68}Ga-DOTANOC PET scan shows high radioligand uptake in the liver and bone metastases. Although many bone metastases appeared visually similar in the two scans, the right sixth rib and left occipital bone metastases (arrows) are much more visible on the ^{68}Ga-DOTANOC PET scan. This selective difference cannot be explained simply by the advantages of the PET technique. The possible predominance of sst_5 in these two bone metastases and the high sst_5 affinity of ^{68}Ga-DOTANOC are in fact the probable reasons for the high

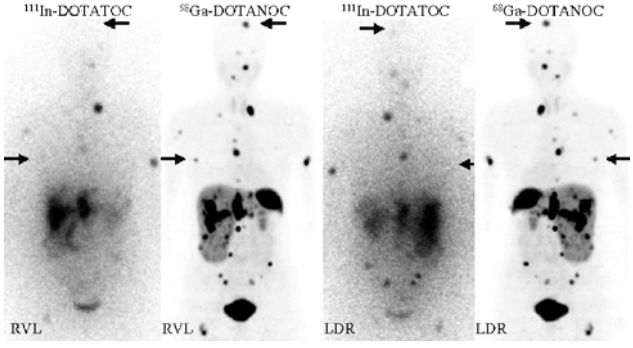

^{68}Ga-DOTANOC and low ^{111}In-DOTATOC uptake. The enlarged liver and somatostatin receptor-positive organs such as the spleen (high uptake) and pituitary gland and thyroid (moderate uptake) are also visible. These normal organs, known to express more sst than just sst_2, are better visualised with ^{68}Ga-DOTANOC (see in particular the spleen).

We conclude that ^{68}Ga-DOTANOC is an excellent candidate for primary diagnostic and follow-up investigations in patients with suspected or proven somatostatin receptor-positive tumours. Furthermore, in this case, predictive imaging indicates that ^{90}Y- or ^{177}Lu-DOTANOC has greater potential for treatment of this patient than ^{90}Y- or ^{177}Lu-DOTATOC.

References

1. Reubi JC, Waser B. Concomitant expression of several peptide receptors in neuroendocrine tumours: molecular basis for in vivo multireceptor tumour targeting. Eur J Nucl Med Mol Imaging (Review) 2003;30:781–93.
2. Wild D, Schmitt JS, Ginj M, Macke HR, Bernard BF, Krenning E, et al. DOTA-NOC, a high-affinity ligand of somatostatin receptor subtypes 2, 3 and 5 for labelling with various radiometals. Eur J Nucl Med Mol Imaging 2003;30:1338–47.
3. Hofmann M, Maecke HR, Börner AR, Weckesser E, Schöffski P, Oei ML, et al. Biokinetics and imaging with the somatostatin receptor PET radioligand ^{68}Ga-DOTATOC: preliminary data. Eur J Nucl Med 2001;28:1751–7.

Damian Wild (✉)
Clinic and Institute of Nuclear Medicine, University Hospital Basel, Petersgraben 4, 4031, Basel, Switzerland
e-mail: dwild@uhbs.ch
Tel.: +41-61-265-4796, Fax: +41-61-265-4925

IV

Preclinical Evaluation of New and Highly Potent Analogues of Octreotide for Predictive Imaging and Targeted Radiotherapy

Mihaela Ginj,[1] Jianhua Chen,[1] Martin A. Walter,[1] Veronique Eltschinger,[2] Jean Claude Reubi,[2] and Helmut R. Maecke[1]

[1]Division of Radiological Chemistry, Department of Radiology, University Hospital Basel, Basel, Switzerland and [2]Institute of Pathology, University of Berne, Berne, Switzerland

ABSTRACT

Purpose: **Molecular imaging and targeted radiotherapy are emerging fields in nuclear oncology. Five human somatostatin receptors (hsstr1-hsstr5) are known to be overexpressed to some degree on various tumors, sstr2 being the most important one. Clinically used somatostatin based radiopeptides target exclusively sstr2. The aim of this study was to develop novel analogues with a broader sstr profile for diagnostic (positron emission tomography and single-photon emission computed tomography) and radiotherapeutic applications.**

Experimental Design: **The following promising structures emerged from a parallel synthetic approach: [1,4,7,10-tetraazacyclododecane-1,4,7,10-tetraacetic acid ($DOTA^0$),1-Nal^3,Thr^8]-octreotide (1, DOTA-NOC-ATE) and [$DOTA^0$,$BzThi^3$,Thr^8]-octreotide (2, DOTA-BOC-ATE). The conjugates were labeled with cold and radioactive ^{111}In. Pharmacologic properties were compared with [^{111}In-DOTA,Tyr^3]-octreotide ([^{111}In-DOTA]-TOC).**

Results: **The receptor affinity profile showed high affinity of both peptides to hsstr2, hsstr3, and hsstr5 and some intermediate affinity to hsstr4, whereas [^{111}In-DOTA]-TOC shows affinity only to sstr2. The internalization is fast in sstr2 expressing AR4-2J and in transfected sstr3 expressing human embryonic kidney 293 cells. Both radiopeptides internalize much more efficiently than [^{111}In-DOTA]-TOC. Animal biodistribution studies showed very high and specific uptake of [^{111}In]-1 and [^{111}In]-2 in s.c. implanted AR4-2J tumors (Lewis rats) and in somatostatin receptor expressing normal tissues. The uptake was at least 2-fold higher in these tissues and in the tumor compared with [^{111}In-DOTA]-TOC. In addition, the kidney uptake was significantly lower for both radiopeptides.**

Conclusions: **These data suggest that the novel radiopeptides are superior to [^{111}In/^{90}Y-DOTA]-TOC and show great promise for the clinical application in the imaging of somatostatin receptor–positive tumors and their targeted radiotherapy.**

INTRODUCTION

Targeted radiotherapy using different vector molecules like monoclonal antibodies, peptides, and others has made remarkable progress in recent years. The breakthrough has centered around the first Food and Drug Administration–approved therapeutic radiolabeled monoclonal antibody, Zevalin, an anti-CD20 antibody labeled with ^{90}Y (1). Nevertheless, peptides have several advantages over the antibodies (faster clearance, rapid tissue penetration, no antigenicity, readily synthesized and GMP produced, etc.) and the most commonly used receptor-targeting agents are a variety of somatostatin analogs. The molecular basis for the use of radiolabeled somatostatin analogues in peptide receptor–mediated radionuclide therapy is provided by the overexpression of the five somatostatin receptors (sstr1-sstr5) on a variety of human tumors, especially neuroendocrine tumors and their metastases (2, 3). It is now more than a decade since the first radiolabeled analogue of somatostatin, [^{111}In-diethylentriaminepentaacetic acid (DTPA)]-octreotide (OctreoScan), was approved for scintigraphy of patients with neuroendocrine tumors (4) and it is still one of the best imaging agents (5). Because a β^- particle emitter, such as ^{90}Y, in most cases seems more suitable for tumor therapy (peptide receptor–mediated radionuclide therapy) than the Auger electron emitter ^{111}In, derivatives like 1,4,7,10-tetraazacyclododecane-1,4,7,10-tetraacetic acid (DOTA)-[Tyr^3]-octreotide (DOTA-TOC) have been developed, enabling stable labeling with ^{90}Y, ^{111}In, or ^{177}Lu (6, 7). Numerous preclinical and clinical studies with [^{111}In]- and [^{90}Y]-labeled DOTA-TOC have shown the effective targeting and therapy using these conjugates (7–13). In addition, replacement of the alcohol group at the COOH terminus of the octapeptide by a carboxylic acid group led to increased sstr2 affinity (14, 15) if peptides are labeled with Y^{III}- and Cu^{II}-based radiometals and [^{177}Lu]-[$DOTA^0$,Tyr^3,Thr^8]-octreotide ([^{177}Lu-DOTA]-TATE) showed higher tumor uptake than [^{111}In-DTPA]-octreotide in six patients with somatostatin receptor–positive tumors (16). These new radiopeptides show distinctly higher sstr2 affinity compared with OctreoScan and [In^{III}/Y^{III}-DOTA]-TOC. Nevertheless, they bind with high affinity only to sstr2.

Expression of different somatostatin receptor subtypes in human tumors has been extensively investigated using different methods: mRNA detection [Northern blots (17), *in situ* hybridization (18), RNase protection assays, and reverse transcription-PCR (19)], immunohistochemical studies (20) and receptor autoradiography with subtype-selective ligands (3).

Received 9/7/04; revised 10/26/04; accepted 11/4/04.
Grant support: Swiss National Science Foundation grant 3100A0-100390 (M. Ginj, M. Walter, and H. Maecke) and Bundesamt für Bildung und Wissenschaft grant C00.0091 (M. Ginj and H. Maecke).
The costs of publication of this article were defrayed in part by the payment of page charges. This article must therefore be hereby marked *advertisement* in accordance with 18 U.S.C. Section 1734 solely to indicate this fact.
Note: This work was done within the COST B12 action.
Requests for reprints: Helmut R. Maecke, Division of Radiological Chemistry, Department of Radiology, University Hospital Basel, Petersgraben 4, CH-4031 Basel, Switzerland. Phone: 41-61-265-46-99; Fax: 41-61-265-55-59; E-mail: hmaecke@uhbs.ch.

Although each of these methods has its own disadvantage and the results from all these studies cannot always be compared with each other, they all lead to some common important conclusions. That is, there is a considerable heterogeneity in the expression of individual sstr within and between different tumors, sstr2 being predominantly expressed in a variety of tumors. However, in a significant number of tumors this was being absent or expressed in lower density. For example, correlating immunohistochemical and mRNA detection data with OctreoScan scintigraphy, Papotti et al. (21) found sstr2, sstr3, and sstr5 in human lung tumors. Growth hormone producing adenomas frequently have sstr2 and sstr5; a predominant sstr3 expression has been reported in inactive pituitary adenomas (3, 22) and in thymomas (23); recently, a high incidence of sstr1, sstr2, and sstr3 has been revealed in human cervical and endometrial cancers (24). The expression of sstr1, 2, 3 and 5 is frequently found in gastro-entero-pancreatic tumors (25), medullary thyroid cancers (17) and in epithelial ovarian cancers (26). Therefore, it is obvious that new radiolabeled somatostatin analogues with improved binding affinity profiles are needed.

To extend not only the present range of targeted cancers but also to increase the tumor uptake, given the presence of different receptor subtypes on the same tumor cell or in the same tumor entity, we started a program to design and synthesize radiopeptides with affinity to all sstr. Our strategy was based on two methods: (a) progressive extension of the peptide cycle from octreotide to somatostatin-14 (27) and (b) modification of octreotide. The second approach was realized through parallel solid phase synthesis, mainly by exchanging the amino acids in the positions 3 and 8 of octreotide. We have already reported a first compound resulting from this small library, [^{111}In/^{90}Y-DOTA]-NOC, with improved biological properties, currently in clinical trials (28).

In the present study, we investigated the biological activity profile of two new [^{111}In/In^{III}]-labeled DOTA-peptide conjugates, [DOTA^0,1-Nal^3,Thr^8]-octreotide (**1**, DOTA-NOC-ATE) and [DOTA^0,BzThi^3,Thr^8]-octreotide (**2**, DOTA-BOC-ATE) by means of receptor binding affinity, rate of internalization, cellular retention, and biodistribution in a tumor-bearing rat model. These two compounds are also part of the library acquired through octreotide modification, and their evaluation has been done in comparison with [^{111}In/In^{III}-DOTA]-TOC which in our laboratory is the gold standard of somatostatin receptor imaging and, labeled to ^{90}Y, of targeted radiotherapy.

MATERIALS AND METHODS

All chemicals including 9-fluorenylmethoxycarbonyl–protected amino acids were obtained from commercial sources and used without further purification. Tritylchloride resin was obtained from PepChem (Tübingen, Germany) and $^{111}InCl_3$ from Mallinckrodt Medical (Petten, the Netherlands). The prochelator DOTA(tBu)$_3$ was synthesized according to Heppeler et al. (6). The reactive side chains of the amino acids were masked with one of the following groups: Cys, acetamidomethyl; Lys, *t*-butoxycarbonyl; Thr, *t*-butyl; Trp, *t*-butoxycarbonyl. Analytic reverse phase-high performance liquid chromatography (HPLC) was carried out on a Hewlett-Packard 1050 HPLC system equipped with a multiwavelength detector and a flow-through Berthold LB506C1 γ-detector. Preparative HPLC was done on a Bischof HPLC system (Metrohm AG, Herisau, Switzerland) with HPLC pumps 2250 and a Lambda 1010 UV detector. CC250/4 Nucleosil 120-3C18 columns from Macherey-Nagel (Düren, Germany) were used for analytic HPLC and a VP250/21 Nucleosil 200-5C15 column for preparative HPLC. The gradient systems consisted of mixtures of acetonitrile and water with 0.1% trifluoroacetic acid. Quantitative γ-counting was done on a COBRA 5003 γ-system well counter from Packard Instrument Co. (Hombrechtikon, Switzerland). Electrospray ionization-mass spectrometry was carried out with a Finnigan SSQ 7000 spectrometer (Bremen, Germany).

Synthesis. The peptide-chelator conjugates were synthesized by standard 9-fluorenylmethoxycarbonyl-solid phase synthesis (29) on tritylchloride resin (substitution, 0.8 mmol/g) on a Rink Engineering peptide-synthesizer Switch 24 (RinkCombichem Technologies, Bubendorf, Switzerland) according to the general procedure described previously (28) affording compounds **1** and **2** (Fig. 1), which could be labeled with natural or radioactive indium or yttrium. The compounds were characterized by electrospray ionization-mass spectrometry and reverse phase-HPLC.

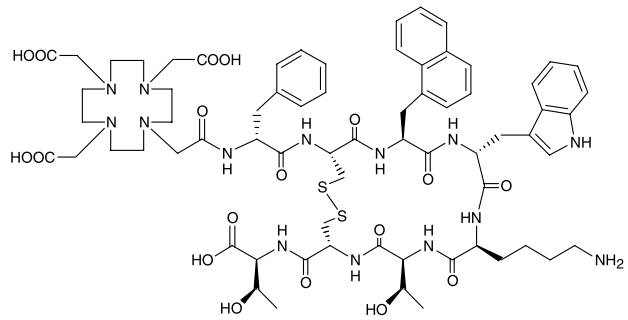

DOTA-NOC-ATE **1**

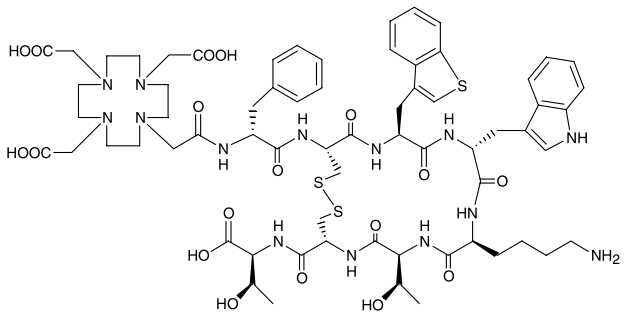

DOTA-BOC-ATE **2**

Fig. 1 Structural formulae of DOTA-[1-Nal^3, Thr^8]-octreotide (DOTA-NOC-ATE, **1**) and DOTA-[BzThi^3, Thr^8]-octreotide (DOTA-BOC-ATE, **2**).

Formation of Metal Complexes. The DOTA-somatotropin release-inhibitingfactor analogues were complexed with $InCl_3$ (anhydrous) and $Y(NO_3)_3{\cdot}5H_2O$ as described by Wild et al. (28). The radiopeptides were also synthesized according to Wild et al. (28) and obtained in >99% radiochemical purity at specific activities of >37 GBq/μmol peptide. For internalization experiments, the DOTA peptides were labeled to a specific activity of about 37 GBq/μmol peptide and then excess $InCl_3$ was added to afford structurally characterized homogenous ligands.

Determination of Somatostatin Receptor Affinity Profiles. CHO-K1 and CCL39 cells stably expressing human sstr1-5 were grown as described previously (14). All culture reagents were supplied by Life Technologies (Grand Island, NY). Cell membrane pellets were prepared and receptor autoradiography was done on pellet sections (mounted on microscope slides), as described in detail previously (14). For each of the tested compounds, complete displacement experiments were done with the universal somatostatin radioligand [^{125}I]-[Leu^{8},D-Trp^{22},Tyr^{25}]-somatostatin-28 using increasing concentrations of the Metallo^{III}-DOTA-peptide ranging from 0.1 to 1,000 nmol/L. Somatostatin-28 was run in parallel as control using the same increasing concentrations. IC_{50} values were calculated after quantification of the data using a computer-assisted image processing system. Tissue standards (autoradiographic [^{125}I] microscales, Amersham, Buckinghamshire, United Kingdom) containing known amounts of isotopes, cross-calibrated to tissue-equivalent ligand concentrations, were used for quantification (14). The concentrations of the peptide solutions were measured by UV spectroscopy ($\varepsilon_{NOC\text{-}ATE,\ 280\ nm}$ = 9,855 and $\varepsilon_{BOC\text{-}ATE,\ 280\ nm}$ = 7,570).

Cell Culture, Radioligand Internalization, and Cellular Retention Studies. The AR4-2J cell line was maintained by serial passage in monolayers in DMEM, supplemented with 10% fetal bovine serum, amino acids, vitamins, and penicillin-streptomycin, in a humidified 5% CO_2 atmosphere at 37°C. Human embryonic kidney 293 cells stably expressing rat $sstr_3$ receptors were a gift from Dr. S. Schulz (Magdeburg, Germany; ref. 30) and were grown in DMEM supplemented with 10% fetal bovine serum, penicillin-streptomycin, and G418 (500 μg/mL) in a humidified 5% CO_2 atmosphere at 37°C. Cell numbers were counted under the microscope with a ''Neubauer's counting chamber''. For all cell experiments, the cells were seeded at a density of 0.8 to 1.1 million cells per well in 6-well plates and incubated over night with internalization buffer to obtain a good cell adherence. The loss of cells during the internalization experiments was <10%. When different radiolabeled peptides were compared in cell experiments, the same cell suspension containing plates were used. Furthermore, the internalization rate was linearly corrected to 1 million cells per well in all AR4-2J cell experiments.

Medium was removed from the 6-well plates and cells were washed once with 2 mL of internalization buffer [DMEM, 1% fetal bovine serum, amino acids, and vitamins (pH 7.4)]. Furthermore, 1.5 mL internalization buffer were added to each well and incubated at 37°C for about 1 hour. Thereafter ~500,000 cpm or 0.02 MBq per well ^{111}In/In^{III}-labeled peptides (2.5 pmol per well) to a final concentration of 1.67 nmol/L were added to the medium and the cells were incubated at 37°C for the indicated time periods in triplicates. To determine nonspecific membrane binding and internalization, cells were incubated with radioligand in the presence of 1 μmol/L [In^{III}]-**1**. Cellular uptake was stopped by removing medium from the cells and by washing twice with 1 mL of ice-cold PBS. Acid wash for 10 minutes with a glycine-buffer (pH 2.8) on ice was also done twice. This procedure was done to distinguish between membrane-bound (acid releasable) and internalized (acid resistant) radioligand. Finally, the cells were treated with 1 N NaOH. The culture medium, the receptor bound and the internalized fraction were measured radiometrically in a γ-counter (Packard, Cobra II). Internalization into AR4-2J cells was also studied using three different concentrations of [^{111}In]-**1** and [^{111}In]-2 (6.67 nmol/L or 10 pmol per well, 1.67 nmol/L or 2.5 pmol per well, and 0.167 nmol/L or 0.25 pmol per well).

For cellular retention studies AR4-2J cells (1 million) were incubated with 2.5 pmol per well (1.67 nmol/L) [^{111}In/In^{III}]-labeled DOTA-NOC-ATE, DOTA-BOC-ATE, or DOTA-TOC for 120 and 240 minutes, respectively, then the medium was removed and the wells were washed twice with 1 mL ice-cold PBS. In each experiment, an acid wash for 10 minutes on ice with a glycine-buffer of pH 2.8 was done to remove the receptor-bound ligand. Cells were then incubated again at 37°C with fresh internalization buffer [DMEM containing 1% fetal bovine serum (pH 7.4)]. After different time points, the external medium was removed for quantification of radioactivity in a γ-counter and replaced with fresh 37°C medium. The cells were solubilized in 1 N NaOH, removed and the internalized radioactivity was quantified in a γ-counter. The recycled fraction was expressed as percentage of the total internalized amount per 1 million cells and the integrity of the externalized peptides was determined using HPLC after removing the solvent by a centrifugal evaporator.

Biodistribution and Imaging Studies in Rats. Animals were kept, treated, and cared for in compliance with the guidelines of the Swiss regulations (approval 789). Five-week-old male Lewis rats were implanted s.c. with 10 to 12 millions AR4-2J cells freshly suspended in sterile PBS. Fourteen days after inoculation, the rats showed solid palpable tumor masses (tumor weight, 0.4-0.7 g) and were used for the experiments. Rats were injected under ether anesthesia with 2 to 3 MBq of 0.34 nmol (0.5 μg total peptide mass) [^{111}In]-**1**, [^{111}In]-**2** and [^{111}In-[^{111}In-DOTA]-TOC, respectively, in 0.05 mL NaCl solution 0.9% into the femoral vein. At 4, 24, and 48 hours after injection rats were sacrificed under ether anesthesia. Organs and blood were collected and the radioactivity in these samples was determined using a γ-counter.

To determine the nonspecific uptake of the radiopeptides, rats were injected with 25 μg [In^{III}]-**2** in 0.05 mL NaCl solution 0.9% as a coinjection with the radioligand. To study a potential sstr2, sstr3, and sstr5 related specific uptake of [^{111}In]-**1** in the somatostatin receptor–positive tissues, blocking studies were designed with different somatostatin analogs: DTPA-TATE [sstr2-selective ligand, IC_{50}(sstr2) = 3.9 ± 1 nmol/L], [In^{III}-DTPA]-TATE [sstr2-selective ligand, IC_{50}(sstr2) = 1.3 ± 0.2 nmol/L], and [In^{III}]-2 (sstr2, sstr3, and sstr5 affinity). In a first series, 25 μg of these peptides were coinjected with 2 to 3 MBq

[^{111}In]-1 (0.34 nmol in 0.05 mL NaCl solution 0.9%) into the femoral vein of AR4-2J tumor-bearing male Lewis rats. In a second series, increased amounts of DTPA-TATE (50 μg) and 25 μg of In^{III}-DTPA-TATE were coinjected. Rats were sacrificed at 4 hours and the organs of interest collected and counted for radioactivity. The radioactivity uptake in the tumor and normal tissues of interest was expressed as a percentage of the injected radioactivity dose per gram tissue (% ID/g).

Two rats were used for imaging studies. One rat was injected with 3 MBq of 0.34 nmol [^{111}In]-**1** and the other one was coinjected with the same amount and type of radioligand and 25 μg [In^{III}]-**2** into the femoral vein. Four hours after injection, rats were anaesthetized and images were acquired in the prone position using a γ-camera equipped with a medium energy parallel hole collimator (Basicam, Siemens, Erlangen, Germany).

Statistical Methods. To compare differences between the radiopeptides the Student's *t* test was used.

RESULTS

Synthesis and Labeling. The DOTA-coupled octapeptides **1** and **2** (Fig. 1) were obtained by solid phase synthesis on a tritylchloride resin. The overall yield of the DOTA peptides was about 30%. Uncomplexed and metal-complexed DOTA peptides were characterized by analytic HPLC and electrospray ionization-mass spectrometry. Table 1 lists the calculated and measured molecular weights and also the HPLC retention time of the conjugates and their labeled versions.

Receptor Binding and Affinity Profiles. Table 2 shows the IC_{50} values of the radiopeptides studied in this work as their In^{III} complexed versions in comparison with [In^{III}-DOTA]-TOC for the five somatostatin receptor subtypes. Additionally, the binding profile of the compounds used for the blocking studies in rats are also listed along with the unmodified octapeptides in Table 2. The values were obtained by performing complete displacement experiments with the universal somatostatin radioligand [^{125}I][Leu^{8}, D-Trp^{22}, Tyr^{25}]-somatostatin-28 on membranes from cells expressing the receptor subtypes and were compared with somatostatin-28. All compounds bind specifically to sstr2, with IC_{50} values ranging from 0.8 to 4.6 nmol/L. High binding affinities for sstr3 were found for [In^{III}]-2 (IC_{50} = 5.5 ± 0.8 nmol/L) and [In^{III}]-1 (IC_{50} = 13 ± 4.0 nmol/L), whereas [In^{III}-DOTA]-TOC showed very low sstr3 affinity (IC_{50} = 120 ± 26 nmol/L). [In^{III}]-1 and [In^{III}]-2 displayed moderate affinity for sstr4 (IC_{50} = 160 ± 3.8 and 135 ± 32 nmol/L,respectively).

Table 1 Analytic data of compounds **1**, **2**, [In^{III}]-**1**, and [In^{III}]-**2**

Compound	Calculated MW	Measured MW	RP-HPLC* retention time (min)
DOTA-NOC-ATE, **1**	1,469.68	1,508.2 (M + K^{+})	22.73
DOTA-BOC-ATE, **2**	1,475.71	1,515.4 (M + K^{+})	22.45
[In^{III}-DOTA]-NOC-ATE, [In^{III}]-**1**	1,580.6	1,582.5 (M + H^{+})	23.15
[In^{III}-DOTA]-BOC-ATE, [In^{III}]-**2**	1,587.7	1,589.2 (M + H^{+})	22.9
[In^{III}-DOTA]-TOC	1,533.64	1,534.8 (M + H^{+})	18.23

*Elution system: flow, 0.75 mL/min; solvent A, 0.1% trifluoroacetic acid in H_2O; solvent B, acetonitrile; linear gradient: 0 to 30 minutes, 90% A to 40% A.

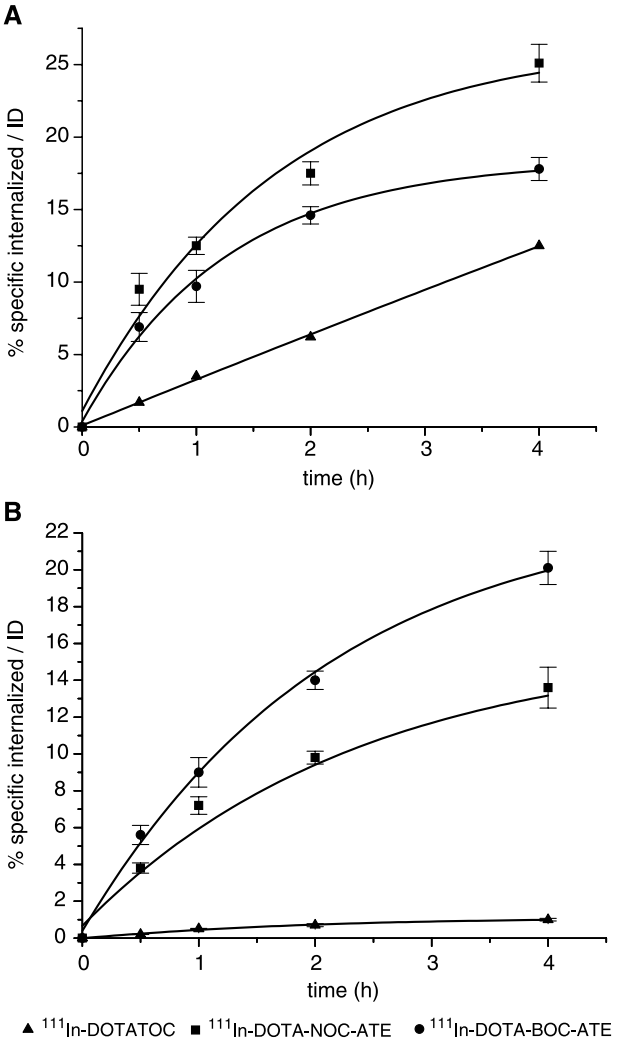

Fig. 2 Comparison of the internalization rate of [^{111}In]-**1**, [^{111}In]-**2**, and [^{111}In-DOTA]-TOC into AR4-2J cells (*A*) and in rsstr$_3$-HEK cells (*B*), respectively. Specific internalization (% dose added to 1 million cells at 1.67 nmol/L concentration) and result of three independent experiments with triplicates in each experiment.

Specific sstr5 affinity was found for [In^{III}]-1 and [In^{III}]-2 (IC_{50} = 4.3 ± 0.5 and 3.9 ± 0.2 nmol/L, respectively).

***In vitro* Internalization Studies in AR4-2J and rsstr3-Human Embryonic Kidney Cells.** Figure 2*A* shows the results of the specific internalization of [^{111}In]-**1** and [^{111}In]-**2** in comparison with [^{111}In-DOTA]-TOC into AR4-2J rat pancreatic tumor cells. The highest rate of internalization corresponds to [^{111}In]-**1** with 25.1 ± 1.3% specific cellular uptake at 4 hours, followed by [^{111}In]-**2** with 17.8 ± 0.8% and [^{111}In-DOTA]-TOC with 12.5 ± 0.7%. The percentage of internalized peptide at 30 minutes as a function of concentration showed a linear dependence (data not shown). Figure 2*B* shows the internalization of [^{111}In]-**1** and [^{111}In]-**2** in sstr3 transfected human embryonic kidney cell lines compared with [^{111}In-DOTA]-TOC. During 4 hours, [^{111}In]-2 internalized 20.1% of the added radiopeptide and [^{111}In]-**1** 13.5%, whereas [^{111}In-DOTA]-TOC showed <0.8% specific internalization.

Table 2 Affinity profiles (IC_{50}) of a series of somatostatin analogues for human somatostatin receptors sstr1 to sstr5

Compound	hsstr1	hsstr2	hsstr3	hsstr4	hsstr5
SS-28	3.6 ± 0.7	2.3 ± 0.6	3.3 ± 0.5	2.7 ± 0.5	2.3 ± 0.3
[In^{III}-DOTA]-NOC-ATE	>10,000	2 ± 0.35	13 ± 4	160 ± 3.8	4.3 ± 0.5
[In^{III}-DOTA]-BOC-ATE	>1,000	1.4 ± 0.37	5.5 ± 0.8	135 ± 32	3.9 ± 0.2
NOC-ATE	>1,000	3.6 ± 1.6	302 ± 137	260 ± 95	16.7 ± 9.9
BOC-ATE	>1,000	0.8 ± 0.4	33 ± 5.5	80 ± 20	3.6 ± 1.5
Octreotide*	>10,000	2.0 ± 0.7	187 ± 55	>10,000	22 ± 6
[In^{III}-DOTA]-TOC*	>10,000	4.6 ± 0.2	120 ± 26	230 ± 82	130 ± 17
DTPA-TATE*	>10,000	3.9 ± 1	>10,000	>1,000	>1,000
[In^{III}-DTPA]-TATE*	>10,000	1.3 ± 0.2	>10,000	433 ± 16	>1,000

NOTE. IC_{50} values are in nmol/L (mean ± SE) and are the mean of at least three experiments. Somatostatin-28 is used as reference.
*Data from Reubi et al. (14).

Cellular Retention. Cellular retention of [^{111}In]-**1,** [^{111}In]-**2** and [^{111}In-DOTA]-TOC was analyzed and compared in AR4-2J cells. In these experiments, the radiopeptides were allowed to internalize for 120 and 240 minutes, respectively; cells were then washed twice with PBS before removing the receptor-bound ligand with glycine buffer (pH 2.8). Warm medium (37°C) was then added and removed after 15, 30, 60, 120, and 240 minutes and measured for radioactivity. Figure 3 illustrates the cellular radioactivity retention of these three compounds in AR4-2J cells over time after two different internalization times. There is no significant difference between the cellular retention after 2 and 4 hours of internalization for the studied conjugates, respectively, except for [^{111}In]-**1** which maintained after 4 hours 30 ± 4.0% ($P < 0.05$) of the 2 hours of internalized fraction and 41.6 ± 6.0% of the 4 hours of internalized fraction, respectively. As shown in Fig. 3, after 4 hours, the percentage of cellular retention for all three conjugates reaches a plateau. HPLC study of the externalized [^{111}In]-**1** and [^{111}In]-**2** gave no indication of metabolites (data not shown).

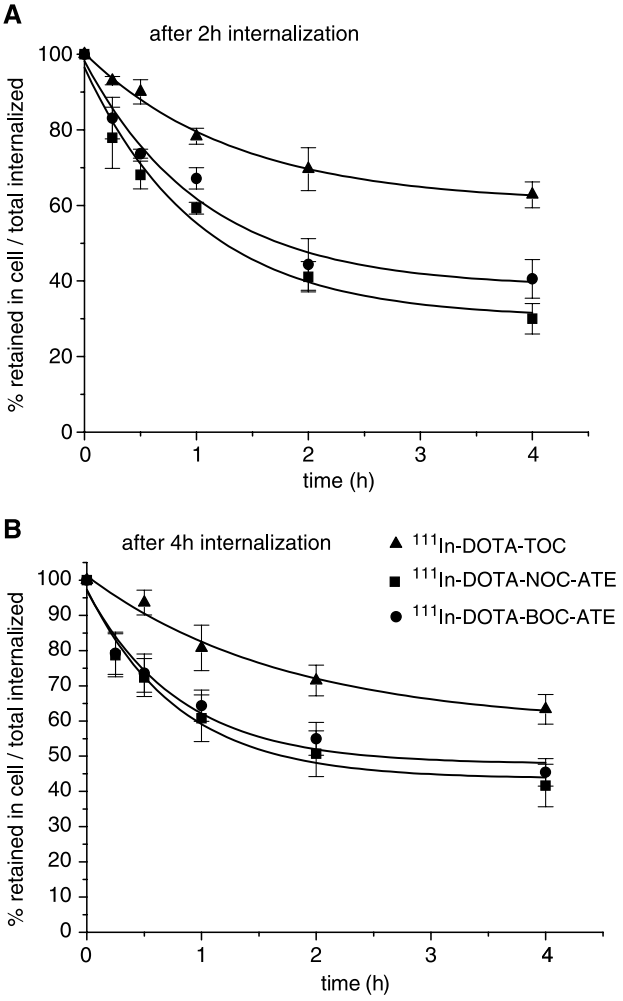

Fig. 3 Comparison of cellular retention over time between[^{111}In]-**1**, [^{111}In]-**2** and [^{111}In-DOTA]-TOC in AR4-2J cells at 37C, after 2 hours of internalization (*A*) and 4 hours of internalization (*B*). % Radioactivity retained in the cell from the total internalized conjugate.

Biodistribution and Imaging Studies in Rats. Pharmacokinetics. The 4, 24, and 48 hours uptake values of [^{111}In]-**1** and [^{111}In]-**2** in somatostatin receptor–positive organs including, pancreas, adrenals, stomach, and AR4-2J rat pancreatic tumor as well as in other tissues are summarized in Table 3. Both radiopeptides displayed rapid blood clearance with <0.04% ID/g remaining in the blood at 4 hours. There is also fast clearance from all sstr-negative tissues except the kidneys which is the main organ of excretion. The two radioligands have a similar biodistribution profile in this rat tumor model except for the adrenals where [^{111}In]-**1** shows a higher uptake than [^{111}In]-**2** (calculated area under the curve: 299.4 versus 164.54% ID/g h). The area under the curve for tumors is 97.2% ID/g h for [^{111}In]-**2** and 95.5% ID/g h for [^{111}In]-**1**, respectively.

Comparison. Figure 4 shows a comparison of the biodistribution properties between [^{111}In]-**1**, [^{111}In]-**2** and [^{111}In-DOTA]-TOC at 4 hours after injection. The tumor uptake for [^{111}In-DOTA]-TOC is 1.95 ± 0.23% ID/g, whereas for [^{111}In]-**1** and [^{111}In]-**2** the values are 4.01 ± 0.49 and 4.12 ± 0.62% ID/g, respectively. Also the uptake in sstr-positive organs (pancreas, adrenals, stomach) is superior for [^{111}In]-**1** and [^{111}In]-**2** (see Table 3) in comparison with [^{111}In-DOTA]-TOC (pancreas, 2.47 ± 0.17% ID/g; adrenals, 1.59 ± 0.16% ID/g; stomach, 0.34 ± 0.02% ID/g). The situation is reversed for the kidney uptake: 2.6 ± 0.12% ID/g for [^{111}In-DOTA]-TOC versus 1.51 ± 0.08% ID/g for [^{111}In]-**1** and 1.79 ± 0.15% ID/g for [^{111}In]-**2**. An evaluation of the tumor-to-different tissues ratios for the three conjugates is presented also in Table 3.

Table 3 Biodistribution in AR4-2J tumor-bearing rats at 4, 24, and 48 hours (n = 4-5 rats per time point) after injection of [^{111}In-DOTA]-NOC-ATE and [^{111}In-DOTA]-BOC-ATE and tissue radioactivity ratios in comparison with [^{111}In-DOTA]-TOC at 4 hours after injection

		[^{111}In-DOTA]-NOC-ATE (%ID/g tissue ± SD)		[^{111}In-DOTA]-BOC-ATE (%ID/g tissue ± SD)	
Organ	Time (h)	Nonblocked	Blocked*	Nonblocked	Blocked*
Blood	4	0.04 ± 0.001	0.014 ± 0.005	0.02 ± 0.003	0.015 ± 0.007
	24	0.004 ± 0.0002		0.005 ± 0.0008	
	48	0.003 ± 0.0001		0.004 ± 0.0002	
Tumor	4	4.01 ± 0.5	0.30 ± 0.03†	4.12 ± 0.62	0.38 ± 0.04†
	24	1.82 ± 0.26		2.04 ± 0.75	
	48	1.11 ± 0.04		1.1 ± 0.17	
Kidneys	4	1.51 ± 0.08	1.56 ± 0.60	1.8 ± 0.15	1.9 ± 0.5
	24	0.74 ± 0.12		1.82 ± 0.16	
	48	0.73 ± 0.07		0.93 ± 0.30	
Adrenals	4	10.75 ± 0.55	0.34 ± 0.03†	5.71 ± 0.53	0.3 ± 0.08†
	24	5.87 ± 1.40		3.34 ± 0.72	
	48	5.22 ± 0.30		2.83 ± 0.63	
Pancreas	4	12.30 ± 0.88	0.32 ± 0.04†	10.33 ± 0.34	0.77 ± 0.03†
	24	2.44 ± 0.30		3.30 ± 0.20	
	48	2.15 ± 0.24		2.52 ± 0.56	
Spleen	4	0.10 ± 0.009	0.04 ± 0.01	0.052 ± 0.005	0.04 ± 0.02
	24	0.03 ± 0.0009		0.048 ± 0.002	
	48	0.03 ± 0.004		0.045 ± 0.01	
Stomach	4	1.83 ± 0.62	0.056 ± 0.001†	0.811 ± 0.22	0.07 ± 0.02†
	24	0.92 ± 0.11		0.65 ± 0.35	
	48	0.41 ± 0.20		0.47 ± 0.06	
Bowel	4	0.25 ± 0.06	0.03 ± 0.01†	0.151 ± 0.023	0.04 ± 0.01†
	24	0.16 ± 0.002		0.13 ± 0.006	
	48	0.14 ± 0.007		0.127 ± 0.001	
Liver	4	0.087 ± 0.05	0.081 ± 0.03	0.095 ± 0.011	0.09 ± 0.02
	24	0.04 ± 0.006		0.067 ± 0.01	
	48	0.038 ± 0.001		0.065 ± 0.01	
Lung	4	0.085 ± 0.008	0.033 ± 0.01†	0.061 ± 0.002	0.04 ± 0.02†
	24	0.02 ± 0.003		0.0445 ± 0.004	
	48	0.018 ± 0.003		0.03 ± 0.0	
Heart	4	0.02 ± 0.001	0.01 ± 0.001	0.013 ± 0.001	0.01 ± 0.005
	24	0.006 ± 0.001		0.008 ± 0.0007	
	48	0.005 ± 0.001		0.008 ± 0.0004	
Bone	4	0.01 ± 0.002	0.01 ± 0.0002	0.012 ± 0.006	0.01 ± 0.005
	24	0.005 ± 0.0009		0.006 ± 0.001	
	48	0.003 ± 0.0007		0.005 ± 0.0004	

Tumor-to-tissue ratios (4 h p.i./24 h p.i.)	[^{111}In-DOTA]-NOC-ATE	[^{111}In-DOTA]-BOC-ATE	[^{111}In-DOTA]-TOC
Tumor/blood	100.3/455	171.6/408	65.5/47.17
Tumor/liver	50.1/45.5	45.7/31	25.8/20.2
Tumor/kidneys	2.7/2.5	2.3/1.12	0.64/0.32

*Blocked with 25 μg [In^{III}-DOTA]-BOC-ATE.
†$P < 0.001$.

Selective Blocking. To estimate the uptake in sstr-positive organs which may be due to receptor subtype expression other than sstr2, *in vivo* blocking studies were done in AR4-2J tumor-bearing rats using different blocking agents like [DTPA^0-Tyr^3-Thr^8]-octreotide (DTPA-TATE) and [In^{III}-DTPA]-TATE, two sstr2-specific ligands and [In^{III}]-**2**, sstr2, sstr3, and sstr5 ligand (see Table 2 for IC_{50} values). Two series of experiments were done, using different amounts of these blocking compounds (Table 4*A* and *B*). As already mentioned in Table 3, 25 μg [In^{III}]-**2** per rat are enough for 95% blocking of the uptake in tumor and sstr-positive organs ($P < 0.001$). Table 4*A* displays the selective blocking of tumor, adrenals, pancreas, and stomach when using only 25 μg DTPA-TATE. As the AR4-2J rat pancreatic tumor expresses only sstr2, the blocking with DTPA-TATE should be as effective as that with [In^{III}]-**2**. In our assay, however, only 70% of the tumor uptake were blocked by the sstr2-selective ligand. In the second selective blocking experiment (Table 4*B*), increased amounts of DTPA-TATE (50 μg per rat) were employed as well as the sstr2-selective ligand [In^{III}-DTPA]-TATE (25 μg per rat) with its improved affinity to this receptor (see Table 2). The two sstr2 ligands were found to be equipotent in decreasing the tumor uptake (85%) but slightly different in their effect on the pancreas and adrenal uptake. The kidney uptake is not influenced by any of these added ligands.

Rat Images. Figure 5 shows the γ-scintigraphy of two Lewis rats s.c. bearing AR4-2J tumors on the thorax 4 hours after injection of [^{111}In]-**1** with (Fig. 5*A*) and without (Fig. 5*B*) coinjection of excess of [In^{III}]-**2**. Coinjection led to a visible

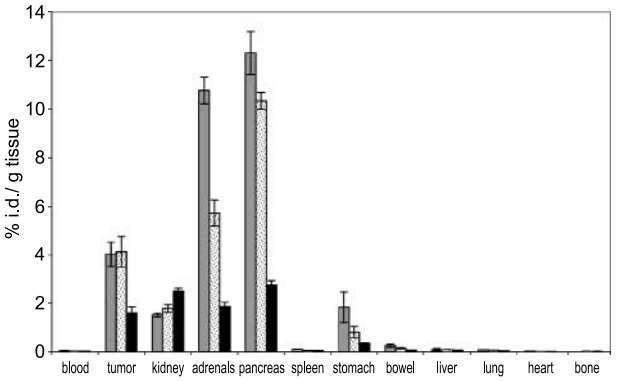

Fig. 4 Biodistribution comparison between [^{111}In-DOTA]-NOC-ATE (▩), [^{111}In-DOTA]-BOC-ATE (▨), and [^{111}In-DOTA]-TOC (■) in AR4-2J tumor-bearing rats at 4 hours after injection.

decrease of the tumor and pancreas uptake, proving the effective blocking of somatostatin receptors. Furthermore, the images show the fast clearance of the radiopeptide from sstr-negative organs and the good target-to-nontarget ratios.

DISCUSSION

This study describes the design, synthesis, and preclinical evaluation of two new somatostatin-based DOTA-coupled peptides for the labeling with a variety of hard acid radiometals like ^{111}In, ^{67,68}Ga, ^{90}Y, and the lanthanides.

The pharmacologic profiles as well as the biological properties of the ^{111}In-labeled peptides are compared with [^{111}In, ^{90}Y-DOTA-Tyr^3]-octreotide (6, 9). The two peptide structures emerged from a parallel synthesis approach with modifications at position 3 of the octapeptide octreotide and the COOH-terminal replacement of Thr(ol) for Thr (14, 15).

The rationale to develop these new peptides came from the desire to develop radiopeptides with a broader spectrum of targeted tumors and a potentially higher uptake in tumors expressing different receptor subtypes concomitantly.

A first radiopeptide emerging from this library of compounds was [^{111}In, ^{90}Y-DOTA]-[1-Nal^3]-octreotide which showed improved affinities towards sstr2, sstr3, and sstr5 if compared with [^{111}In-DOTA]-[Tyr^3]-octreotide (28). The new compounds have several advantages over existing radiopeptides. First, the affinity for sstr2 is as high as the best radiopeptides studied thus far (14). In addition, high affinity to sstr3 and sstr5 was found as well and some emerging sstr4 affinity, thus representing the broadest sstr profile of any somatostatin-based radioligands whereas maintaining a very high sstr2 affinity. The structural features determining the broader affinity profile are not fully understood yet. We observed earlier that the modification of Phe^3 by Tyr^3 in DOTA-coupled octapeptides led to a 3-fold improved sstr2 affinity but the sstr3 affinity dropped by a factor of >10 (14, 28). The higher lipophilicity of benzothienyl-Ala (BzThi) and 1-Nal probably improves sstr3 and sstr5 affinity. The sstr2 affinity increase is most likely a combination of the Thr(ol) versus Thr replacement and the increased lipophilicity at aa^3 position.

A comparison of the affinity profiles of the metallo-chelated peptides with the unmodified peptides BOC-ATE and NOC-ATE showed that BOC-ATE could represent an improved alternative for octreotide (Sandostatin) in the treatment of acromegaly and/or the carcinoid syndrome as it has a higher potency on the receptor subtypes 2-5. Also, the coupling of a DOTA-based metal complex to the N_3-terminus may improve the affinity to some receptor subtypes. [In^{III}-DOTA]-NOC-ATE and [In^{III}-DOTA]-BOC-ATE are at least equipotent to the nonchelated peptide on sstr2 but distinctly more potent on sstr3. On sstr5 [In^{III}-DOTA]-BOC-ATE is equipotent to BOC-ATE but [In^{III}-DOTA]-NOC-ATE is more potent than NOC-ATE.

Somatostatin receptors belong to the family of G-protein coupled receptors (31). There are several important consequences of the coupling of agonists to this type of receptors like desensitization, Ca^{2+} mobilization, cyclic AMP production, and internalization. The latter is of special relevance to the targeting aspects of using G-protein coupled receptor targeting radioligands as it allows long retention times on the tumor which is of special importance in therapeutic applications but may also contribute to the diagnostic sensitivity due to an increased tumor-to-background ratio with time. Both radiopeptides internalize distinctly faster than [^{111}In-DOTA]-TOC in AR4-2J tumor cells. The efflux rate of both radiopeptides from AR4-2J cells is similar, the total amount of cell released radiopeptide is lower if more time is allowed for internalization, indicating that pathways inside the cell slow down the efflux of radiopeptides (32). [^{111}In]-**1** and [^{111}In]-**2** internalize very efficiently into sstr3 cells, [^{111}In]-**2** being clearly superior to [^{111}In]-**1** which may be explained with the higher affinity of [^{111}In]-**2** on sstr3 (see Table 2). [^{111}In-DOTA]-TOC having a

Table 4 Radioactivity uptake in AR4-2J tumor-bearing rats, 4 hours after coinjection of [^{111}In-DOTA]-NOC-ATE and different blocking agents (n = 4 rats per blocking experiment)

Blocking compound	Amount injected per rat (μg)	Radioactivity uptake in organs and tumor (%ID/g tissue ± SD)				
		AR4-2J tumor	Adrenals	Pancreas	Stomach	Kidneys
None		4.01 ± 0.49	10.75 ± 0.55	12.3 ± 0.88	1.83 ± 0.62	1.51 ± 0.08
[InIII-DOTA]-BOC-ATE	25	0.30 ± 0.03*	0.34 ± 0.03*	0.32 ± 0.04*	0.056 ± 0.001*	1.56 ± 0.06*
(A) DTPA-TATE	25	1.26 ± 0.16†	2.13 ± 0.07*	1.85 ± 0.09*	0.24 ± 0.01*	1.57 ± 0.1
(B) DTPA-TATE	50	0.6 ± 0.08*	1.36 ± 0.46*	0.85 ± 0.02*	0.09 ± 0.01*	1.47 ± 0.18
[InIII-DTPA]-TATE	25	0.56 ± 0.07*	0.78 ± 0.11*	0.70 ± 0.09*	0.10 ± 0.02*	1.4 ± 0.29

*$P < 0.001$.

†$0.05 > P > 0.001$ compared with nonblocked data series.

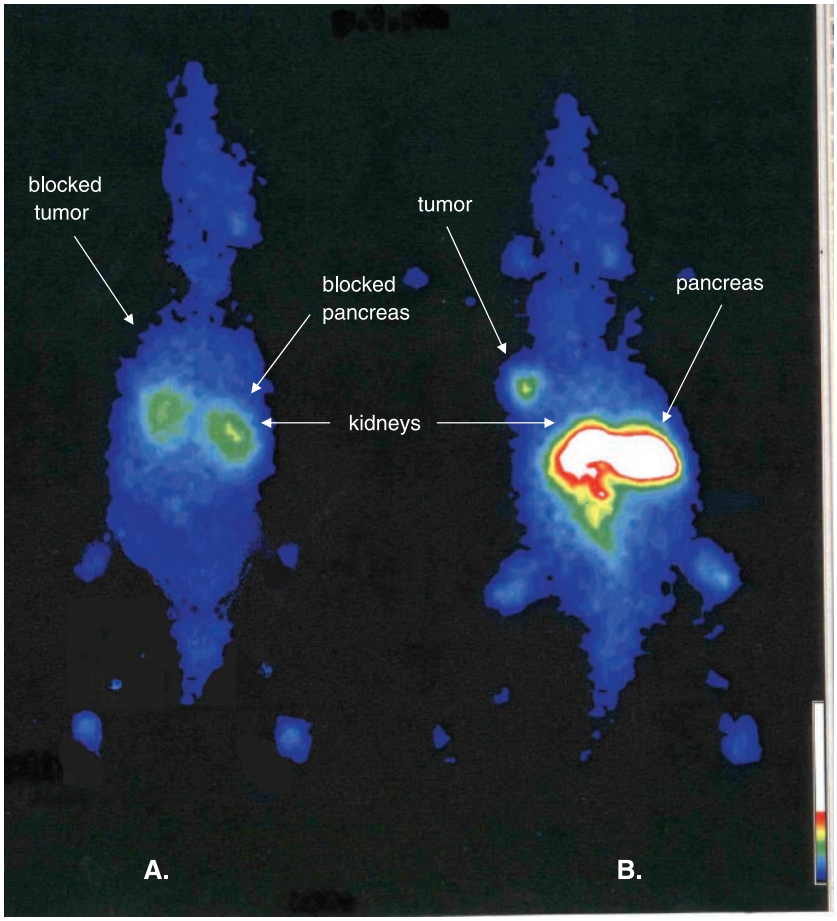

Fig. 5 Four hours post injection scintigraphy of two Lewis rats bearing AR4-2J s.c. tumors: rat with a coinjection of [^{111}In-DOTA]-NOC-ATE and excess [In^{III}-DOTA]-BOC-ATE (*A*) and rat injected only with [^{111}In-DOTA]-NOC-ATE (*B*).

low affinity to sstr3 shows negligible internalization. These data clearly show that [^{111}In]-**1** and [^{111}In]-**2** have a much higher potential to target tumors with sstr3 expression, either alone or concomitantly with other subtypes. The high sstr5 affinity indicates that this also holds for sstr5 expressing tumors.

The efflux rate of the new radiopeptides is faster than the one of [^{111}In-DOTA]-TOC, an effect that we cannot explain at the moment. As the externalized radiopeptides are intact, a faster metabolic degradation cannot be the justification for this. Nevertheless, the amount retained in the cell remains higher for [^{111}In]-**1** and [^{111}In]-**2** than for [^{111}In-DOTA]-TOC, due to the higher internalization rate of the first two. In internalization, we found a close approximation to a steady state after 4 hours of internalization of both new radiopeptides and also the efflux kinetics showed a distinct leveling off after 4 hours. We have explained similar results recently assuming rapid recycling of the radiopeptides to the extracellular medium and reactivation of the receptors by the intact externalized peptides followed by reendocytosis (28). This explanation is also in accordance with the work of Koenig et al. (33).

The *in vivo* pharmacokinetics in the AR4-2J rat model of [^{111}In]-**1** and [^{111}In]-**2** shows a rapid and specific targeting of the somatostatin receptor 2 expressing tumor and somatostatin receptor–positive tissue like the pancreas (Fig. 5*B* for [^{111}In]-**1**). The specificity of this uptake is shown by the blocking experiment which shows lack of uptake in the tumor and the pancreas, even if only 25 μg [In^{III}]-**2** are coinjected with 0.5 μg [^{111}In]-**1** (Fig. 5*A*).

A quantitative analysis of the biodistribution at 4, 24, and 48 hours showed a high uptake in the tumor which was similar for [^{111}In]-**1** and [^{111}In]-**2** but 2-fold higher than for [^{111}In-DOTA]-TOC at 4 hours. The uptake in other somatotropin release-inhibiting factor receptor–positive tissues like the pancreas, adrenals, stomach, and bowel was also very high, specific, and receptor mediated as shown by the blocking experiment. Already a coinjection of 25 μg [In^{III}]-**2** blocks the tumor uptake by >90%, the adrenals by 97%, the pancreas by 95%, the stomach by 97%, and the bowel by 88%, illustrating the potential advantage of the broader affinity profile of this ligand. The almost 7- and 4-fold higher uptake in the adrenals and 5- and 4-fold higher uptake in the pancreas may be explained by the expression of sstr3 and sstr5 in these organs (34). The more efficient blocking capability of [In^{III}]-**2** compared with the sstr2-selective ligands DTPA-octreotate and [In^{III}-DTPA]-octreotate also indicates that this radioligand is superior to other somatostatin-based radiopeptides. The residence time of [^{111}In]-**1** and [^{111}In]-**2** in the tumor is somewhat shorter than that of other somatostatin-based radiopeptides and parallels the efflux rate from AR4-2J cells compared with

[^{111}In-DOTA]-TOC. The area under the curve determining the dose given to the tumor is still very high and justifies diagnostic and therapeutic studies in patients in the near future.

Despite an increased lipophilicity of the new radiopeptides the liver uptake is low and resembles the low uptakes of more hydrophilic radiopeptides like [^{111}In-DTPA-Tyr^3, Thr^8]-octreotide (35) but is much lower than for other hydrophilic radiopeptides like [^{64}Cu-TETA-Tyr^3, Thr^8]-octreotide (15).

Radiometal-labeled peptides show persistent kidney uptake due to proximal tubular cell reabsorption after glomerular filtration, which still makes kidneys the critical organ for therapeutic applications. Both compounds, [^{111}In]-**1** and [^{111}In]-**2** show an improved tumor-to-kidney ratio at all time points which makes these two radiopeptides very promising candidates for somatostatin receptor targeted radiotherapy.

New cold somatostatin-based peptides with superior therapeutic potential and a more universal binding profile than octreotide or lanreotide are currently being developed. Most advanced is SOM230, a cyclohexapeptide that has high binding affinity to sstr1, sstr2, sstr3, sstr5 and is currently under evaluation in phase 1 clinical trials (36). Because there is no radioligand for SOM230, [^{111}In]-**1** and [^{111}In]-**2** may be candidates to identify patients adequate for SOM230 treatment. In addition, [^{111}In]-**1** and [^{111}In]-**2** may be much better alternatives to predict the usefulness of cold octreotide (Sandostatin) or lanreotide (Somatuline) therapy than OctreoScan, which has a much less adequate binding profile for this purpose.

CONCLUSION

We have designed and characterized chemically and pharmacologically two new DOTA-based peptides for diagnostic and therapeutic applications, [^{111}In-DOTA-Nal^3, Thr^8]-octreotide and [^{111}In-DOTA-BzThi^3, Thr^8]-octreotide. The peptides were compared with our clinical gold standard [^{111}In/^{90}Y-DOTA-Tyr^3]-octreotide. They show superior pharmacologic properties when compared with the latter. Both peptides are currently prepared for clinical studies.

The combined preclinical data indicate that [^{111}In, ^{90}Y-DOTA]-NOC-ATE and [^{111}In, ^{90}Y-DOTA]-BOC-ATE are very promising new somatostatin-based radioligands for the diagnosis and targeted radiotherapy of a broader range of tumors expressing somatostatin receptors. They represent the first somatostatin-based radiopeptides, which show high affinity to sstr2, sstr3, and sstr5 and intermediate affinity to sstr4. For the first time, efficient internalization into a sstr3 expressing cell line using radiometallolabeled somatostatin analogues was shown.

We also propose [^{111}In-DOTA]-NOC-ATE and [^{111}In-DOTA]-BOC-ATE as imaging agents to predict the successful use of cold octreotide or lanreotide therapy, as Octreoscan has very low affinity to sstr3 and sstr5.

ACKNOWLEDGMENTS

We thank Dr. S. Schulz for the sstr3-transfected human embryonic kidney 293 cells and Novartis Pharma for the support regarding MS and NMR.

REFERENCES

1. Witzig TE, Gordon LI, Cabanillas F, et al. Randomized controlled trial of yttrium-90-labeled ibritumomab tiuxetan radioimmunotherapy versus rituximab immunotherapy for patients with relapsed or refractory low-grad, follicular, or transformed B-cell non-Hodgkin's Lymphoma. J Clin Oncol 2002;20:2453–63.

2. Reubi JC, Laissue J, Krenning E, Lamberts SW. Somatostatin receptors in human cancer: incidence, characteristics, functional correlates and clinical implications. J Steroid Biochem Mol Biol 1992; 43:27–35.

3. Reubi JC, Waser B, Schaer JC, Laissue JA. Somatostatin receptor sst1-sst5 expression in normal and neoplastic human tissues using receptor autoradiography with subtype-selective ligands. Eur J Nucl Med 2001;28:836–46.

4. Krenning EP, Kwekkeboom DJ, Bakker WH, et al. Somatostatin receptor scintigraphy with [^{111}In-DTPA-D-Phe^1]- and [^{123}I-Tyr^3]-octreotide: the Rotterdam experience with more than 1000 patients. Eur J Nucl Med 1993;20:716–31.

5. Lebtahi R, Le Cloirec J, Houzard C, et al. Detection of neuroendocrine tumors: ^{99m}Tc-P829 scintigraphy compared with ^{111}In-pentetreotide scintigraphy. J Nucl Med 2002;43:889–95.

6. Heppeler A, Froidevaux S, Mäcke HR, et al. Radiometal-labelled macrocyclic chelator-derivatised somatostatin analogue with superb tumour-targeting properties and potential for receptor-mediated internal radiotherapy. Chemistry A European Journal 1999;5:1016–23.

7. de Jong M, Bakker WH, Krenning EP, et al. Yttrium-90 and indium-111 labelling, receptor binding and biodistribution of [DOTA^0, D-Phe^1,Tyr^3]octreotide, a promising somatostatin analogue for radionuclide therapy. Eur J Nucl Med 1997;24:368–71.

8. Otte A, Mueller-Brand J, Dellas S, Nitzsche E, Herrmann R, Maecke H. Yttrium-90-labelled somatostatin-analogue for cancer treatment. Lancet 1998;351:417–8.

9. Waldherr C, Pless M, Maecke H, Haldemann A, Mueller-Brand J. The clinical value of [^{90}Y-DOTA]-D-Phe^1-Tyr^3-octreotide (^{90}Y-DOTATOC) in the treatment of neuroendocrine tumours: a clinical phase II study. Ann Oncol 2001;12:941–5.

10. Cremonesi M, Ferrari M, Zoboli S, et al. Biokinetics and dosimetry in patients administered with ^{111}In-DOTA-Tyr^3-octreotide: implications for internal radiotherapy with ^{90}Y-DOTATOC. Eur J Nucl Med 1999; 26:877–86.

11. Stolz B, Weckbecker G, Smith-Jones PM, Albert R, Raulf F, Bruns C. The somatostatin receptor-targeted radiotherapeutic [^{90}Y-DPTA-DPhe^1,Tyr^3]octreotide (^{90}Y-SMT 487) eradicates experimental rat pancreatic CA 20948 tumours. Eur J Nucl Med 1998;25:668–74.

12. Bushnell D, O'Dorisio T, Menda Y, et al. Evaluating the clinical effectiveness of ^{90}Y-SMT 487 in patients with neuroendocrine tumors. J Nucl Med 2003;44:1556–60.

13. Warner RR, O'Dorisio TM. Radiolabeled peptides in diagnosis and tumor imaging: clinical overview. Semin Nucl Med 2002;32:79–83.

14. Reubi JC, Schar JC, Waser B, et al. Affinity profiles for human somatostatin receptor subtypes SST1-SST5 of somatostatin radiotracers selected for scintigraphic and radiotherapeutic use. Eur J Nucl Med 2000;27:273–82.

15. Lewis JS, Lewis MR, Srinivasan A, Schmidt MA, Wang J, Anderson CJ. Comparison of four ^{64}Cu-labeled somatostatin analogues *in vitro* and in a tumor-bearing rat model: evaluation of new derivatives for positron emission tomography imaging and targeted radiotherapy. J Med Chem 1999;42:1341–7.

16. Kwekkeboom DJ, Bakker WH, Kooij PP, et al. [^{177}Lu-DOTA^{0}-Tyr^3]octreotate: comparison with [^{111}In-DTPA^0]octreotide in patients. Eur J Nucl Med 2001;28:1319–25.

17. Forssell-Aronsson EB, Nilsson O, Bejegard SA, et al. ^{111}In-DTPA-D-Phe^1-octreotide binding and somatostatin receptor subtypes in thyroid tumors. J Nucl Med 2000;41:636–42.

18. Reubi JC, Schaer JC, Waser B, Mengod G. Expression and localization of somatostatin receptor SSTR1, SSTR2, and SSTR3

messenger RNAs in primary human tumors using *in situ* hybridization. Cancer Res 1994;54:3455–9.

19. Buscail L, Saint-Laurent N, Chastre E, et al. Loss of sst2 somatostatin receptor gene expression in human pancreatic and colorectal cancer. Cancer Res 1996;56:1823–7.

20. Reubi JC, Kappeler A, Waser B, Laissue J, Hipkin RW, Schonbrunn A. Immunohistochemical localization of somatostatin receptors sst2A in human tumors. Am J Pathol 1998;153:233–45.

21. Papotti M, Croce S, Bello M, et al. Expression of somatostatin receptor types 2, 3 and 5 in biopsies and surgical specimens of human lung tumours. Correlation with preoperative octreotide scintigraphy. Virchows Arch 2001;439:787–97.

22. Greenman Y, Melmed S. Expression of three somatostatin receptor subtypes in pituitary adenomas: evidence for preferential SSTR5 expression in the mammosomatotroph lineage. J Clin Endocrinol Metab 1994;79:724–9.

23. Ferone D, van Hagen MP, Kwekkeboom DJ, et al. Somatostatin receptor subtypes in human thymoma and inhibition of cell proliferation by octreotide *in vitro*. J Clin Endocrinol Metab 2000;85:1719–26.

24. Schulz S, Schmitt J, Weise W. Frequent expression of immunoreactive somatostatin receptors in cervical and endometrial cancer. Gynecol Oncol 2003;89:385–90.

25. Reubi JC, Waser B. Concomitant expression of several peptide receptors in neuroendocrine tumours: molecular basis for *in vivo* multireceptor tumour targeting. Eur J Nucl Med Mol Imaging 2003;30:781–93.

26. Halmos G, Sun B, Schally AV, Hebert F, Nagy A. Human ovarian cancers express somatostatin receptors. J Clin Endocrinology & Metabolism 2000;85:3509–12.

27. Reubi JC, Eisenwiener KP, Rink H, Waser B, Maecke HR. A new peptidic somatostatin agonist with high affinity to all five somatostatin receptors. Eur J Pharmacol 2002;456:45–9.

28. Wild D, Schmitt JS, Ginj M, et al. DOTA-NOC, a high-affinity ligand of somatostatin receptor subtypes 2, 3 and 5 for labelling with various radiometals. Eur J Nucl Med Mol Imaging 2003;30:1338–47.

29. Atherton E, Sheppard R. Fluorenylmethoxycarbonyl-polyamide solid phase peptide synthesis. General principles and development. In: Solid phase peptide synthesis. A practical approach. Oxford: Oxford Information Press; 1989. p. 25–38.

30. Tulipano G, Stumm R, Pfeiffer M, Kreienkamp HJ, Hollt V, Schulz S. Differential β-arrestin trafficking and endosomal sorting of somatostatin receptor subtypes. J Biol Chem 2004;27:21374–82.

31. Pierce K, Premont R, Lefkowitz R. Seven-transmembrane receptors. Nature Reviews Mol Cell Biol 2002;3:639–50.

32. Wang M, Caruano AL, Lewis MR, Meyer LA, VanderWaal RP, Anderson CJ. Subcellular localization of radiolabeled somatostatin analogues: implications for targeted radiotherapy of cancer. Cancer Res 2003;63:6864–9.

33. Koenig JA, Kaur R, Dodgeon I, Edwardson JM, Humphrey PP. Fates of endocytosed somatostatin sst2 receptors and associated agonists. Biochem J 1998;336:291–8.

34. Raulf F, Perez J, Hoyer D, Bruns C. Differential expression of five somatostatin receptor subtypes, SSTR1-5, in the CNS and peripheral tissue. Digestion 1994;55 Suppl 3:46–53.

35. de Jong M, Breeman WA, Bakker WH, et al. Comparison of ^{111}In-labeled somatostatin analogues for tumor scintigraphy and radionuclide therapy. Cancer Res 1998;58:437–41.

36. Bruns C, Lewis I, Briner U, Meno-Tetang G, Weckbecker G. SOM230: a novel somatostatin peptidomimetic with broad somatotropin release inhibiting factor (SRIF) receptor binding and a unique antisecretory profile. Eur J Endocrinol 2002;146:707–16.

V

Available online at www.sciencedirect.com
SCIENCE DIRECT®
Tetrahedron Letters
Tetrahedron Letters 46 (2005) 2821–2824

Synthesis of trifunctional somatostatin based derivatives for improved cellular and subcellular uptake

Mihaela Ginj and Helmut R. Maecke*

Division of Radiological Chemistry, Department of Radiology, University Hospital Basel, 4031 Basel, Switzerland

Received 25 January 2005; revised 18 February 2005; accepted 22 February 2005

Abstract—It is now well established that the biological effects of Auger-emitting radionuclides are critically dependent on their subcellular location. Therefore, for their use in molecular imaging and targeted radionuclide therapy, attempts should be made to increase the nuclear specificity of the carriers. In the present paper the synthesis of novel trifunctional somatostatin derivatives containing a nuclear localization motif is described. These derivatives of [DOTA^0, Tyr^3]-octreotide (DOTATOC, DOTA = 1,4,7,10-tetraazacyclododecane-1,4,7,10-tetraacetic acid) were obtained in high yields using Fmoc peptide synthesis in solid and in solution phase.

The molecular basis for the use of radiolabeled somatostatin (SS) analogs in peptide receptor mediated radionuclide therapy (PRRT) is provided by the overexpression of the five somatostatin receptors (sstr1–5) on a variety of human tumors, especially neuroendocrine tumors and their metastases.[1] The 'gold standard' is represented by DOTATOC (DOTA = 1,4,7,10-tetraazacyclododecane-1,4,7,10-tetraacetic acid, TOC = Tyr^3-octreotide), a radiopeptide which, labeled with ^{90}Y,[2] has almost a decade of clinical experience mainly in the targeted radiotherapy of neuroendocrine tumors.[3] ^{90}Y is a high energy β-emitter radionuclide, therefore more suitable for large tumors, its cytotoxicity being primarily due to the crossfire effect.[4] This is clinically significant, because it means that metastatic small cell clusters cannot be efficiently killed using β-emitters.

Auger-electron emitting radionuclides like ^{111}In, ^{67}Ga, ^{125}I, or ^{195m}Pt have potential for the therapy of small size cancers due to their high level of cytotoxicity, low energy and short-range biological effectiveness. Biological effects are critically dependent on the subcellular (and even subnuclear) localization of these nuclides.[5] [^{111}In-DTPA]-octreotide (DTPA = diethylenetriaminepentaacetic acid) has already been used for radionuclide therapy in patients with somatostatin receptor-positive tumors and its usefulness has been shown to be clearly dependent on the high accumulation of the radioligand in the tumor.[6] Therefore derivatives with a longer retention time in the cell and aiming at the nucleus would increase the potential of Auger-electron emitters in radiotherapy, but also improve other targeted therapy strategies.

Bearing this in mind we assumed that a new functional unit for nucleus targeting and prolonged cell retention could be added to the DOTATOC conjugate. For this we have chosen the nuclear targeting signal (NLS) of the SV40 large T antigen, the heptapeptide H-Pro-Lys-Lys-Lys-Arg-Lys-Val-OH.[7] This sequence serves as a tag to proteins, indicating their destination to the cell nucleus and assisting in the transport through the nuclear membrane. To function properly, the NLS conjugates must be located in the cytoplasm, but they are not readily incorporated into cells.[8] We report herein the design and synthesis of new trifunctional conjugates of a truncated analog of somatostatin bearing a function for receptor binding and internalization (TOC), one for the nucleus transfer (NLS) and one for the cytotoxic or reporter effect (^{111}In-DOTA).

The pharmacological profile of DOTATOC-like conjugates is greatly influenced by any structural alterations and care should be taken when designing new modifications. In order to test the best architecture for such a trifunctional derivative of somatostatin we incorporated

Keywords: NLS; DOTA-peptide; Radiotherapy; Auger electron emitter; Peptide synthesis.
* Corresponding author. Tel.: +41 61 265 4699; fax: +41 61 265 5559; e-mail: hmaecke@uhbs.ch

0040-4039/$ - see front matter © 2005 Elsevier Ltd. All rights reserved.
doi:10.1016/j.tetlet.2005.02.117

the NLS in three different positions relative to the somatostatin analog sequence. The C-terminus modification (compound **I**) and the two N-terminus derivatives (compounds **II** and **III**) thus synthesized are shown in Figure 1. Compound **III** has a branched structure in which the NLS sequence is inverted (H-Val-Lys-Arg-Lys-Lys-Lys-Pro-OH).

Compounds **I** and **II** were fully synthesized on the solid phase using stepwise Fmoc peptide chemistry. Conjugate **I** was assembled on trityl-chloride resin (TCP). Coupling of Fmoc-Val-OH to the solid support was performed in dry dichloromethane in the presence of an excess of DIPEA (*N*-ethyldiisopropylamine). Conjugate **II** was anchored to 2-chlorotrityl chloride resin (CTCP) pre-loaded with Fmoc-Thr(*t*Bu)-ol. Additions of subsequent Fmoc-protected amino acids were carried out using DIC (*N*,*N*′-diisopropylcarbodiimide), HOBt (*N*-hydroxybenzotriazole), and DIPEA in DMF and 20% piperidine in DMF was used for Fmoc removal. 6-Aminohexanoic acid (Ahx) spacers were chosen between the NLS part and TOC for all three derivatives, and an additional β-Ala spacer between the chelator DOTA and the NLS sequence in compound **II** in order to circumvent the potential steric hindrance. The syntheses were straightforward despite the relatively long sequences; nevertheless capping with acetic acid anhydride was carried out after each coupling, starting from the fifth residue from the resin, as a safety measure. The DOTA-tris(*tert*-butyl) ester[9] was coupled on solid phase at the N-terminus of the peptides, using 2-(1-*H*-9-azabenzotriazole-1-yl)-1,1,3,3-tetramethyluronium hexafluorophosphate (HATU) and DIPEA in NMP (*N*-methylpyrrolidone) for 2–4 h. The formation of the disulfide bridge in both conjugates was achieved in solution at room temperature, after cleavage of the fully protected linear conjugate from the resin, with I_2 in aqueous methanol. Total deprotection using TFA–water–triisopropylsilane (TIS)–thioanisole (95:2.5:1.25:1.25) for 4 h afforded the desired conjugates **I** and **II**, respectively, in good purities (75±5%), as assessed by multiwavelength detection HPLC.

Compound **III** was synthesized by either one of two strategies: solid phase peptide synthesis alone or by a convergent approach, involving the synthesis of protected fragments in solid phase and combination of these units in solution as illustrated in Scheme 1. The orthogonally-protected lysine derivative Fmoc-Lys-(ivDde)-OH[10] was chosen for the branching of this conjugate on the resin. The ivDde group is considerably more stable to piperidine than Dde, and is less prone to migrate from protected to unprotected lysine side chains.[11] After Fmoc cleavage the prochelator was coupled, thus allowing subsequently the ε-NH-ivDde removal with 3% hydrazine in DMF. Following cleavage from the resin, cyclization in solution and total deprotection, the crude product **III** obtained using method **A** (Scheme 1) had a purity of approximatively 85% as indicated by analytical HPLC. The overall yield of this synthesis was 21%.

We supposed that the synthesis of **III** would be more efficient and rapid via a convergent approach, involving synthesis and coupling of the component fragments (**1**), [Tyr^3, Lys^5(ivDde)]-octreotide, and (**2**) (Scheme 1, **B**). We opted for a minimal protection in this case to facilitate the succeeding conditions for coupling in solution. For the construction of the second fragment we utilized again the versatile Fmoc-Lys(ivDde)-OH derivative in a similar manner as in method **A**. As solid support we chose the TCP resin for its acid sensitivity, allowing cleavage with preservation of protecting groups Boc and *t*Bu. Following removal from the resin with 20% AcOH in DCM, fragment (**2**) was obtained with a purity of 80 ± 5% as revealed by HPLC and used without

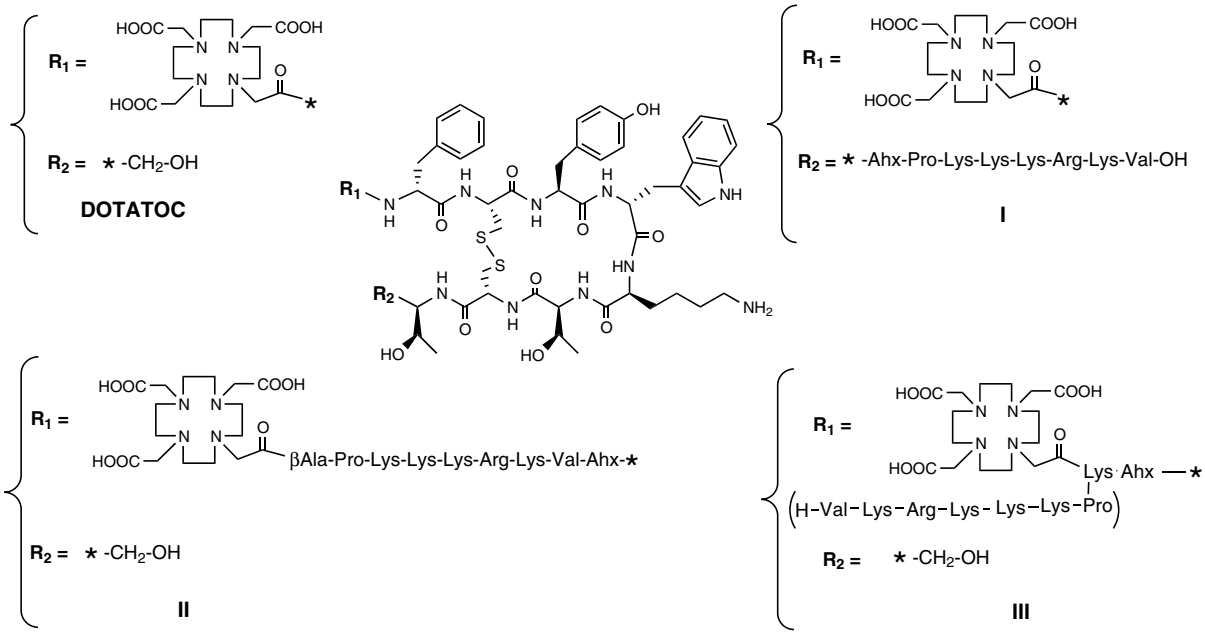

Figure 1. Chemical structures of the synthesized conjugates **I**–**III** and DOTATOC.

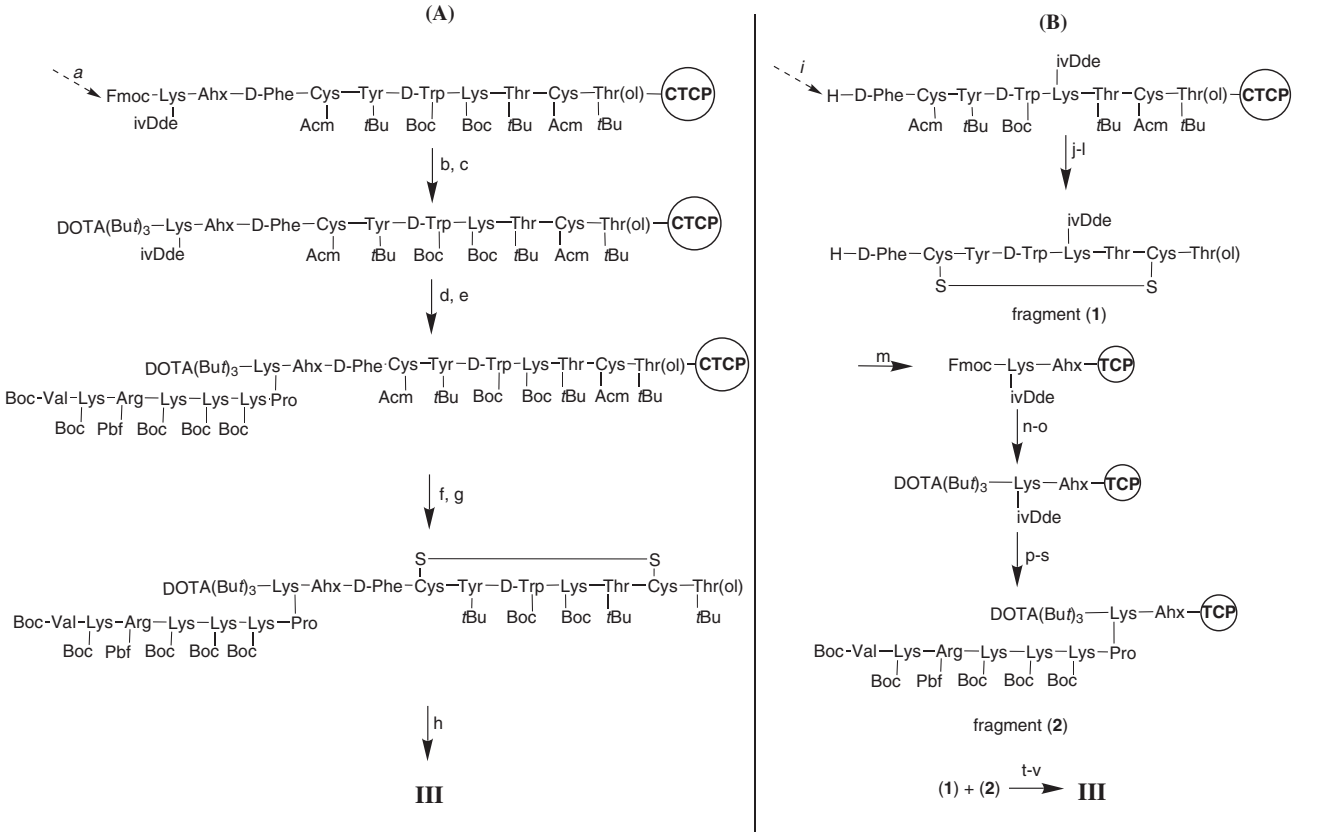

Scheme 1. Preparation of compound **III** using two methods: **A**—solid phase synthesis approach, **B**—mixed solid and solution phase synthesis. Reagents and conditions: (a) stepwise elongation of protected Fmoc-Lys(ivDde)-Ahx-Tyr^3-octreotide on CTCP resin; (b), (n) 20% piperidine/DMF; (c), (o) DOTA(tBu)$_3$, HATU/DIPEA; (d), (p), (u) 3% hydrazine/DMF; (e), (r) stepwise coupling of the NLS protected residues with DIC/HOBt/DIPEA; (f), (k) 1% TFA/CH_2Cl_2; (g) I_2/MeOH aq; (h), (l), (v) 95% TFA, 2.5% H_2O, 1.25% TIS, 1.25% thioanisole; (i) assembling of [Tyr^3, Lys^5(ivDde)]-octreotide on CTCP resin; (j) Tl(TFA)$_3$; (m) assembling of Fmoc-Lys(ivDde)-Ahx on TCP resin; (s) 20% AcOH/CH_2Cl_2; (t) HATU/DIPEA/DMF.

further purification. After investigating the efficacy of several coupling agents (DIC; dicyclohexylcarbodiimide, DCC; benzotriazole-1-yl-oxy-tris-(dimethylamino)-phosphonium-hexafluorophosphate, BOP; 2-(1-*H*-benzotriazole-1-yl)-1,1,3,3-tetramethyluronium hexafluorophosphate, HBTU) for the activation of fragment (**1**) for the solution coupling with fragment (**2**) in various solvents (DMF, NMP, THF), we selected HATU (3 equiv) in DMF, with DIPEA (3 equiv). This choice was based on the observed coupling efficacy. After 4 h of stirring at room temperature, the solvent was evaporated in vacuo and the residue was dissolved in ethyl acetate and washed with 1 N $NaHCO_3$ and brine, then dried with anhydrous Na_2SO_4, and evaporated. Afterwards the product was re-suspended in DMF with 3% hydrazine and incubated for 30 min at room temperature for ivDde deprotection. The mixture was then acidified with TFA and evaporated. After drying in a desiccator, the residue was dissolved in a TFA–water–TIS–thioanisol (95:2.5:1.25:1.25) solution for total deprotection, followed by precipitation in diethyl ether and washed with dry ether. The crude peptide thus obtained was purified by HPLC,[12] affording compound **III** in a 23% overall yield.

Homogeneity and identity of the conjugates were assessed by analytical HPLC and MALDI mass spectrometry.[13] These compounds were readily labeled with ^{111}In as previously described[14] and a comparison of the retention times on HPLC of the ^{111}In-labeled derivatives of **I**, **II**, **III** and DOTATOC is given in Figure 2.

In conclusion, we designed and synthesized new trifunctional derivatives of somatostatin **I**–**III** intended for enhanced cellular and nuclear uptake in sstr-positive tissues and prolonged retention time in tumors. The mixed solid phase solution approach employed for compound **III** did not confirm a significant improvement compared with the solid phase scheme alone. Both methods can be used for preparing such compounds in relatively good yields. Still, we consider the solid phase approach more convenient for this type of synthesis. To support our hypothesis regarding the use of these conjugates, internalization, cellular retention, and nuclear uptake experiments are in progress. Nevertheless, one of the most important properties of these derivatives should be the preservation, if not improvement of binding affinity to sstr2, as for DOTATOC. We have already completed a series of binding affinity measurements of **I**–**III** on HEK 293 cells transfected with rat and human receptor sstr2, respectively (data not shown) and the results confirm one of our hypotheses: C-terminus modification of DOTATOC causes a significant loss in binding affinity for either rat or human sstr2, but the N-terminal

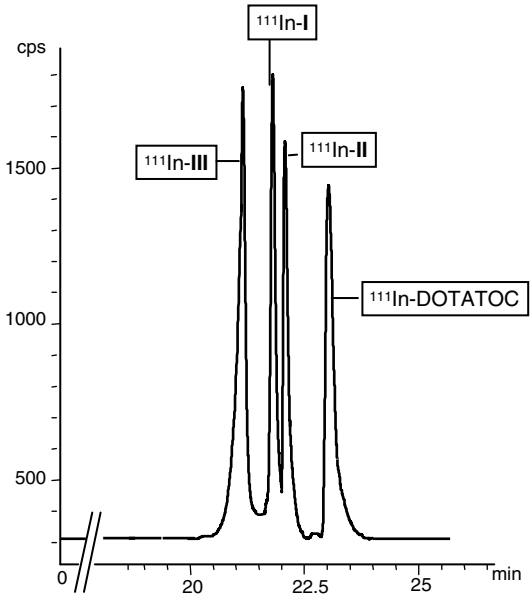

Figure 2. Comparison of retention times for the ^{111}In-labeled compounds **I**–**III** and DOTATOC on a HPLC system, using the gradient described in Ref. 12.

functionalization fully preserves the pharmacological integrity.

Acknowledgements

The authors acknowledge the support from the Swiss National Science Foundation. The precious assistance of Dieter Staab from Novartis Pharma Basel regarding the MALDI-MS is gratefully acknowledged.

References and notes

1. Reubi, J. C.; Waser, B.; Schaer, J. C.; Laissue, J. A. *Eur. J. Nucl. Med.* **2001**, *28*, 836–846.
2. Otte, A.; Mueller-Brand, J.; Dellas, S.; Nitzsche, E.; Herrmann, R.; Maecke, H. *Lancet* **1998**, 417–418.
3. Bodei, L.; Cremonesi, M.; Grana, C.; Rocca, P.; Bartolomei, M.; Chinol, M.; Paganelli, G. *Eur. J. Nucl. Med. Mol. Imaging* **2004**, *31*, 38–46.
4. Ginj, M.; Maecke, H. R. In *Radiometallo-Labeled Peptides in Tumor Diagnosis and Therapy*; Sigel, A., Sigel, H., Eds.; Metal ions in biological systems; Marcel Dekker: New York, 2004; Vol. 42, pp 109–142.
5. O'Donoghue, J. A.; Wheldon, T. E. *Phys. Med. Biol.* **1996**, *41*, 1973–1992.
6. Krenning, E. P.; Valkema, R.; Kooij, P. P.; Breeman, W. A.; Bakker, W. H.; deHerder, W. W.; vanEijck, C. H.; Kwekkeboom, D. J.; deJong, M.; Pauwels, S. *Ital. J. Gastroenterol. Hepatol.* **1999**, *31*, S219–S223.
7. Conti, E.; Uy, M.; Leighton, L.; Blobel, G.; Kuriyan, J. *Cell* **1998**, *94*, 193–204.
8. Yoneda, Y.; Hieda, M.; Nagoshi, E.; Miyamoto, Y. *Cell Struct. Funct.* **1999**, *24*, 425–433.
9. Synthesized according to: Heppeler, A.; Froidevaux, S.; Mäcke, H. R.; Jermann, E.; Béhé, M.; Powell, P.; Hennig, M. *Chem. Eur. J.* **1999**, *5*, 1974–1981.
10. All the protected amino acids were purchased from NovaBiochem AG, Läufelfingen, Switzerland.
11. Chhabra, S. R.; Hothi, B.; Evans, D. J.; White, P. D.; Bycroft, B. W.; Chan, W. C. *Tetrahedron Lett.* **1998**, *39*, 1603–1606.
12. Analytical HPLC was carried out on a Hewlett Packard 1050 HPLC system equipped with a multiwavelength detector and a flow-through Berthold LB506C1 γ-detector. Preparative HPLC was done on a Bischof HPLC system (Metrohm AG, Switzerland) with HPLC-pumps 2250 and a Lambda 1010 UV-detector. CC250/4 Nucleosil 120-3C18 columns from Macherey-Nagel were used for analytical HPLC, and a VP250/21 Nucleosil 200-5C15 column for preparative HPLC. The gradient systems consisted of mixtures of acetonitrile and water with 0.1% TFA. The gradient used for Figure 2 is linear from 85% to 60% 0.1% TFA/H_2O in 30 min.
13. Matrix-assisted laser desorption ionization-mass spectrometry (MALDI-MS) measurements were performed on a Voyager sSTR equipment with a Nd:YAG laser (Applied Biosystems, Framingham, NY).
14. Ginj, M.; Chen, J.; Walter, M. A.; Eltschinger, V.; Reubi, J. C.; Maecke, H. R. *Clin. Cancer Res.* **2005**, *11*, 1136–1145.

VI

Trifunctional Somatostatin-Based Derivatives Designed for Targeted Radiotherapy Using Auger Electron Emitters

Mihaela Ginj, PhD[1]; Karin Hinni[1]; Sibylle Tschumi[1]; Stefan Schulz, PhD[2]; and Helmut R. Maecke, PhD[1]

[1]*Division of Radiological Chemistry, Department of Radiology, University Hospital Basel, Basel, Switzerland; and*
[2]*Department of Pharmacology and Toxicology, Otto-von-Guericke University, Magdeburg, Germany*

Auger electron–emitting radionuclides have potential for the therapy of small-size cancers because of their high level of cytotoxicity, low-energy, high linear energy transfer, and short-range biologic effectiveness. Biologic effects are critically dependent on the subcellular (and even subnuclear) localization of these radionuclides. Our goals were the design, synthesis, and in vitro preclinical assessment of new trifunctional conjugates of somatostatin that should aim at the nucleus and, therefore, ensure a longer retention time in the cell, a close approximation to the DNA, and the success of Auger electron emitters in targeted radionuclide therapy as well as also improve other targeted therapy strategies. **Methods:** Three trifunctional derivatives of [(1,4,7,10-tetraazacyclododecane-1,4,7,10-tetraacetic acid)^0,Tyr^3]octreotide (DOTA-TOC) bearing the nuclear localization signal (NLS) (of simian virus 40 large-T antigen) PKKKRKV in 3 different positions relative to the somatostatin analog sequence were synthesized using solid and solution phase peptide synthesis. These compounds together with DOTA-TOC and DOTA-NLS derivatives were labeled with ^{111}In and tested for binding affinity, internalization, externalization, and nuclei localization on AR4-2J cells and on human embryonic cells stably transfected with sst2A. **Results:** The two N-terminal derivatives preserved the sstr2A binding affinity. Their rate of internalization in all tested sstr-expressing cell lines was always superior for the trifunctional derivatives in comparison with the parent compound. A 6-fold increase in cellular retention from the total internalized activity and a 45-fold higher accumulation in the cell nuclei were found for one of the N-terminally modified compounds compared with [^{111}In]-DOTA-TOC. The C-terminal conjugate was inferior in all tests compared with the parent compound. **Conclusion:** These encouraging results support our hypothesis that an additional NLS sequence to the DOTA-TOC could not only provide a better carrier for Auger electron–emitting radionuclides but also ensure a longer radioactivity retention time in the tumor cell.

Key Words: nuclear localization signal; Auger electron emitter; nuclear uptake; ^{111}In

J Nucl Med 2005; 46:2097–2103

Given the overexpression of somatostatin receptors in a variety of neuroendocrine tumors and their metastases (*1*), peptide receptor–mediated radiotargeted therapy (PRRT) using radiolabeled somatostatin derivatives is the method of choice for their treatment. The gold standard in our clinic is represented by DOTA-TOC (DOTA = 1,4,7,10-tetraazacyclododecane-1,4,7,10-tetraacetic acid; TOC = Tyr^3-octreotide), a radiopeptide that, labeled with ^{90}Y (*2*), has now almost a decade of clinical experience in therapy (*3*). ^{90}Y is a β-particle emitter with a maximum electron energy of 2.3 MeV and an optimal range in tissue of up to 42 mm, its cytotoxicity being primarily due to the crossfire effect (*4*). However, ^{90}Y seems less suitable for the therapy of small metastases or disseminated single tumor cells, because very small tumors will not be able to absorb all electron energy emitted by ^{90}Y in the tumor cells (*5*). In very small lesions, PRRT with Auger electron–emitting radiopharmaceuticals may be a better choice. Auger electron emitters decaying in the neighborhood of the DNA produce similar amounts of reactive chemical radical species as do α-emitters, which are regarded as the classical form of high linear energy transfer (LET) radiation (*6*).

Several encouraging accounts on radiotherapy using internalizing antibodies conjugated to radionuclides emitting low-energy electrons have been recently published (*7–9*). Accompanied by studies on comparison of the usefulness of Auger electron emitters versus β-particle emitters in radioimmunotherapy (*6,10,11*), these reports demonstrate the superior cell killing efficacy of Auger electron emitters in small tumors. Also, [^{111}In-DTPA]octreotide (DTPA = diethylenetriaminepentaacetic acid) has already been used for radionuclide therapy in patients with somatostatin receptor–positive tumors (*12*). An additional advantage of using low-energy emitters such as ^{111}In is the lack of renal toxicity. It was shown that the kidney is the major critical organ for PRRT with ^{90}Y-DOTA-TOC (*13*), whereas the use of [^{111}In-DTPA]octreotide did not show any renal toxicity even though calculated kidney doses were higher than 40 Gy (*12*). Along with the in vitro therapy investigations performed by Capello et al. (*14*), these studies show that the

Received Jun. 16, 2005; revision accepted Aug. 11, 2005.
For correspondence or reprints contact: Helmut R. Maecke, PhD, Division of Radiological Chemistry, Department of Radiology, University Hospital Basel, Petersgraben 4, CH-4031 Basel, Switzerland.
E-mail: hmaecke@uhbs.ch

usefulness of this type of PRRT using low-energy emitters is clearly dependent on the high accumulation of the radioligand in the tumor cell. Moreover, Tiensuu Janson et al. (*15*) have shown that the clinical effectiveness of [^{111}In-DTPA]octreotide could be explained by the translocation of ^{111}In to the perinuclear and nuclear area of the cell. Consequently, enhancing the tumor uptake and retention of radiolabeled somatostatin analogs could provide more effective in situ radiotherapy, optimizing the energy transfer from Auger electron emitters to tumor DNA (*16*).

In this respect we reasoned that a new functional unit for nucleus targeting and prolonged cell retention could be added to the DOTA-TOC conjugate. For this we have chosen the classical nuclear localization signal (NLS) of the simian virus 40 large-T antigen, the heptapeptide H-Pro-Lys-Lys-Lys-Arg-Lys-Val-OH (*17*). This sequence serves as a tag to proteins, indicating their destination to the cell nucleus and assisting in the transport through the nuclear membrane. To function properly, the NLS conjugates must be located in the cytoplasm, but they are not readily incorporated into cells (*18*). We synthesized previously 3 such derivatives bearing the NLS unit in 3 different positions relative to the somatostatin analog sequence (*19*). In this study we investigated the biologic in vitro outcome of these NLS-DOTA-TOC derivatives (**1**), (**2**), and (**3**) (Fig. 1) labeled with ^{111}In, by means of receptor-binding affinity, rate of internalization, cellular retention, and cellular nuclear uptake. This evaluation was done in comparison with the parent compound, ^{111}In-DOTA-TOC, but also with the ^{111}In-DOTA-Ahx-Pro-Lys-Lys-Lys-Arg-Lys-Val-OH (**4**) derivative, which served as a control (Ahx = aminohexanoic acid).

MATERIALS AND METHODS

Radiolabeled Peptide Derivatives

DOTA-TOC and the conjugates (**1**), (**2**), and (**3**) were synthesized as previously described (*19*). Also, DOTA-Ahx-Pro-Lys-Lys-Lys-Arg-Lys-Val-OH (**4**) was synthesized as recently reported (*19*). DOTA was coupled as a tris(*t*-butyl ester) using the monoamide approach. $^{111}InCl_3$ was obtained from Mallinckrodt Medical. All of the conjugates were labeled with $^{111}InCl_3$ as described (*20*).

Cell Culture

The AR4-2J cell line was maintained by serial passage in mono-layers in Dulbecco's modified Eagle medium (DMEM; Cambrex Bio Science), supplemented with 10% fetal bovine serum, amino acids, vitamins, and penicillin–streptomycin, in a humidified 5% CO_2 atmosphere at 37°C. Human embryonic kidney (HEK) 293 cells stably expressing sstr2A receptors were transfected as described (*21*) and were grown in DMEM supplemented with 10% fetal bovine serum, penicillin–streptomycin, and G418 (500 μg/mL) in a humidified 5% CO_2 atmosphere at 37°C.

Saturation Binding Assays

HEK cells stably expressing sstr2A were grown as described previously (*21*). All culture reagents were supplied by BioConcept. For each of the tested compounds, saturation binding experiments on intact cells were performed, using increasing concentrations of the $^{111/nat}$In-DOTA-peptide ranging from 0.1 to 1,000 nmol/L. $^{111/nat}$In-DOTA-TOC was run in parallel as a control using the same increasing concentrations. ^{nat}In-DOTA-TOC at 1 μmol/L was used to quantify the nonspecific binding. Cells were seeded near confluence into 6-well plates using the growth medium and incubated overnight. The medium was removed on the next day, binding buffer (DMEM with 1% fetal bovine serum, pH 7.4) was added to the wells, and the cells were incubated for 1 h at 37°C. For each radioligand, triplicates were prepared for every concentration, for both total binding and nonspecific binding. Before adding the radioligands to the wells, the plates were placed on ice for 30 min. After adding the radioligands and ^{nat}In-DOTA-TOC for nonspecific binding, the plates were incubated for 2 h at 4°C. After this interval, the binding buffer was aspirated and the cells were washed twice with ice-cold phosphate-buffered saline (PBS, pH 7.4); this represented the free fraction. Finally, the cells were collected with 1N NaOH; this corresponded to the bound fraction. A control for each radioligand was prepared to check the amount of conjugate that internalizes at 4°C. The radioactivity in the free and bound fractions was measured using a γ-counter (Cobra II; Packard Instrument Co.). Specific binding was calculated as the

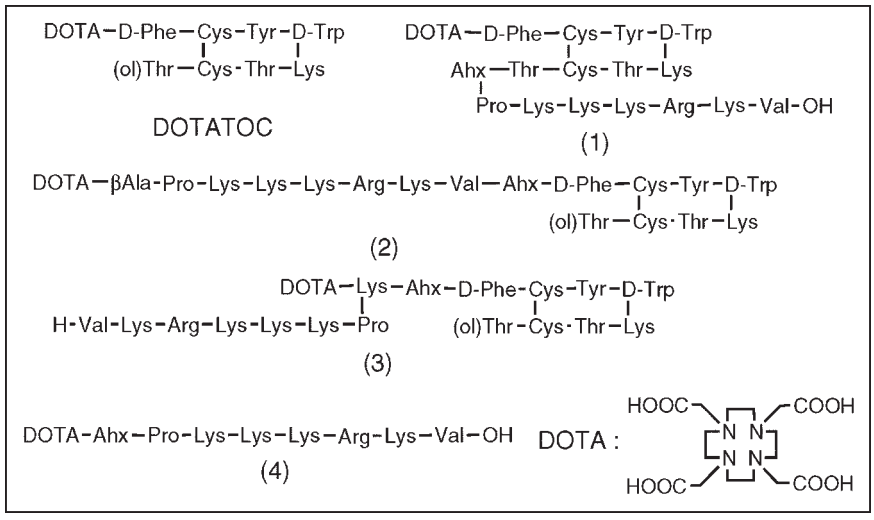

FIGURE 1. Structures of DOTA-TOC and of NLS-conjugates (**1**), (**2**), (**3**), and (**4**).

difference between the radioactive levels without versus with 1 μmol/L ^{nat}In-DOTA-TOC. Dissociation constant (K_d) values were calculated from Scatchard plots of the obtained data using Origin 5.0. software (Microcal Software, Inc.).

Radioligand Internalization Studies

The apparatus and procedures for the cell internalization experiments are based on previously described methods (*20*). Briefly, for all cell experiments, the cells were seeded at a density of 0.8–1.1 million cells per well in 6-well plates and incubated overnight with internalization buffer to obtain good cell adherence. When different radiolabeled peptides were compared in cell experiments, the same cell suspension–containing plates were used. Furthermore, the internalization rate was linearly corrected to 1 million cells per well in all cell experiments. Medium was removed from the 6-well plates and cells were washed once with 2 mL of internalization buffer (DMEM, 1% fetal bovine serum, amino acids, and vitamins, pH 7.4). Next, 1.5 mL of internalization buffer were added to each well and incubated at 37°C for about 1 h. Thereafter, approximately 500,000 cpm or 0.02 MBq of $^{111/nat}$In-labeled peptides per well (2.5 pmol/well) to a final concentration of 1.67 nmol/L were added to the medium and the cells were incubated at 37°C for the indicated time periods in triplicates. To determine nonspecific membrane binding and internalization, cells were incubated with radioligand in the presence of 1 μmol/L ^{nat}In-DOTA-TOC. Cellular uptake was stopped by removing medium from the cells and by washing twice with 1 mL of ice-cold PBS. Acid wash for 10 min with a pH 2.8 glycine buffer on ice was also performed twice. This procedure was performed to distinguish between membrane-bound (acid releasable) and internalized (acid resistant) radioligand. Finally, the cells were treated with 1N NaOH. The culture medium, the receptor-bound fraction, and the internalized fraction were measured radiometrically in a γ-counter (Cobra II).

Cellular Retention Studies

For cellular retention studies, HEK cells sstr2 stably transfected (1 million) were incubated with 2.5 pmol per well (1.67 nmol/L) of $^{111/nat}$In-labeled DOTA-peptide for 120 min; then the medium was removed and the wells were washed twice with 1 mL of ice-cold PBS. In each experiment, an acid wash for 5 min on ice with a pH 2.8 glycine buffer was performed twice to remove the receptor-bound ligand and a PBS wash was performed quickly afterward to restore the physiologic pH. Cells were then incubated again at 37°C with fresh internalization buffer (DMEM containing 1% fetal bovine serum, pH 7.4). After different time points, the external medium was removed for quantification of radioactivity in a γ-counter and replaced with fresh 37°C medium. The cells were solubilized in 1N NaOH and removed, and the internalized radioactivity was quantified in a γ-counter. The recycled fraction was expressed as the percentage of the total internalized amount per 1 million cells.

Nuclei Isolation Assay

A nuclei isolation kit (Nuclei EZ Prep Kit; Sigma-Aldrich Chemie Gmbh) was used to separate and quantify the amount of radioactivity stored in the nuclei. The preparation was done according to the manufacturer's instructions. HEK cells stably expressing sstr2 were seeded in Petri dishes at a density of 18–20 million per dish with growth medium and incubated overnight at 37°C. On the next day the medium was removed, the cells were washed twice with PBS, and internalization medium was added to the dishes (DMEM, 1% fetal bovine serum, amino acids, and vitamins, pH 7.4). The cells were incubated at 37°C for 1 h. The conjugates (**3**) and DOTA-TOC were radiolabeled with ^{111}In at a specific activity of 37 GBq/μmol. Fifty picomoles from each radioconjugate were added to the cells, followed by incubation at 37°C for 4 h (triplicates were used for each compound). After this interval, the dishes were placed on ice, the media were aspirated, and the plates were washed 4 times with ice-cold PBS. Subsequently, the cells were harvested and lysed according to the Nuclei EZ Prep Kit manufacturer's instructions. The purity of the final nuclei was determined by careful visual microscopic inspection of the nuclei diluted in trypan blue counting solution (Fluka Chemie Gmbh), using a hemacytometer. The radioactivity in the nuclei and the cytoplasmatic fractions collected for each of the 2 compounds was quantified in the γ-counter.

Statistical Methods

The Student *t* test was used to determine statistical significance. Differences at the 95% confidence level ($P < 0.05$) were considered significant.

RESULTS

Radiolabeled Peptide Derivatives

The structures of the investigated derivatives are shown in Figure 1. Following the same procedure as for (**1**), (**2**), (**3**), and DOTA-TOC (*19*), compound (**4**) was synthesized to be used as a negative control for the in vitro studies described herein. The efficient radiolabeling of these derivatives with ^{111}In was confirmed by high-performance liquid chromatography equipped with a γ-detector (data not shown).

Binding Affinity Profiles

Table 1 shows the K_d values of the radiopeptides studied in this work as their $^{111/nat}$In-complexed versions in comparison with $^{111/nat}$In-DOTA-TOC for the somatostatin receptor subtype 2. The values were obtained by performing saturation binding experiments on intact cells expressing sstr2A. Except for $^{111/nat}$In-(**4**), all synthesized derivatives show specific binding affinity to this receptor. Whereas the two N-terminally modified DOTA-TOC derivatives, $^{111/nat}$In-(**2**) and $^{111/nat}$In-(**3**), maintain a good affinity to this receptor subtype with values comparable to those of $^{111/nat}$In-DOTA-TOC, the C-terminally modified DOTA-TOC derivative (**1**) labeled with $^{111/nat}$In displays a 100-fold drop in the binding affinity.

TABLE 1
Binding Affinities ($K_d \pm$ SD, nmol/L; $n = 3$) of NLS-Derivatives and DOTA-TOC Labeled with ^{111}In for sstr2A

Compound	K_d (sstr2A)
^{111}In-DOTA-TOC	2.48 ± 0.51
^{111}In-(**1**)	280 ± 140
^{111}In-(**2**)	15.6 ± 1.2
^{111}In-(**3**)	7.4 ± 1.3
^{111}In-(**4**)	>10,000

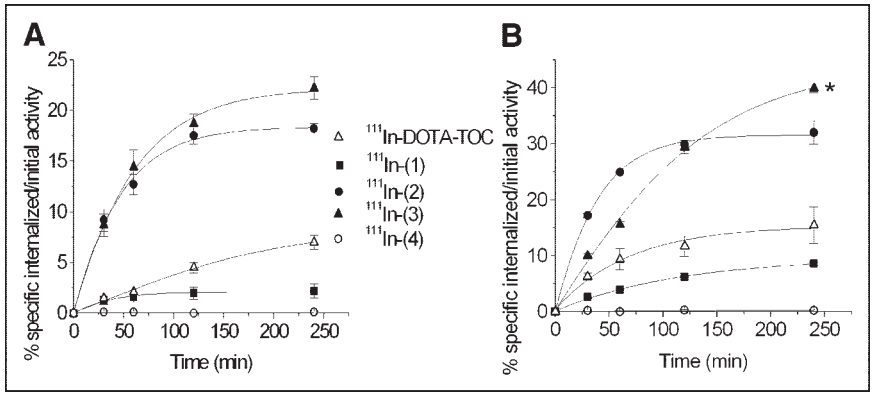

FIGURE 2. Comparison of internalization rates of ^{111}In-labeled conjugates (**1**), (**2**), (**3**), and (**4**) and DOTA-TOC in AR4-2J cells (A) and in sstr2A-HEK cells (B). Values represent specific internalization (% initial activity to 1 million cells at 1.67 nmol/L concentration) and are results of 3 independent experiments with triplicates in each experiment. *$P < 0.001$.

In Vitro Internalization Studies

Figure 2 displays the rates of internalization of all 5 ^{111}In-labeled compounds in 2 cell lines: AR4-2J rat pancreatic tumor cell line (Fig. 2A) and HEK cells stably expressing sstr2A (Fig. 2B). In both cases, the highest rate of internalization at 4 h corresponds to ^{111}In-(**3**) (22.2% in AR4-2J and 39.9% in HEK-sstr2). The control performed with ^{111}In-(**4**) shows no uptake in any of the cell lines used. At 4 h, ^{111}In-(**2**) and ^{111}In-(**3**) have a 3-fold and a 3.6-fold, respectively, higher uptake in AR4-2J compared with ^{111}In-DOTA-TOC. Correlating with the affinity profile, ^{111}In-(**1**) reveals a significant decrease in the internalization rate in AR4-2J, compared with the parent compound (2.2% vs. 6.0%). The same order of uptake at 4 h is maintained in HEK cells expressing sstr2, but with higher absolute values for all of the somatostatin-based derivatives investigated. In this cell line, the 30-min and 1-h uptake of ^{111}In-(**3**) is lower than that for ^{111}In-(**2**), but after a 2-h incubation both compounds have similar cellular uptakes. At 4 h, ^{111}In-(**3**) has a significantly higher accumulation than that for ^{111}In-(**2**) ($P < 0.001$). Blocking studies were performed at all time points in both cell lines with 1 μmol/L ^{nat}In-DOTA-TOC, demonstrating that internalization was receptor mediated.

In the same internalization experiment we collected the membrane surface-bound radioligand performing twice acid washes with pH 2.8 glycine buffer before the treatment with 1N NaOH for each compound. The results are shown in Figure 3. No surface-bound radioligand was found for ^{111}In-(**4**) in both cell lines. Very low amounts of cell-surface–associated activity were also recovered for ^{111}In-DOTA-TOC. In contrast, all 3 NLS-derivatives of DOTA-TOC exhibit relatively high amounts of surface-bound radioactivity in both cell lines, in the order ^{111}In-(**3**) > ^{111}In-(**2**) > ^{111}In-(**1**). The pattern of the percentage of surface-bound radioligand of the total amount (2.5 pmol/well) is the same for all compounds, including ^{111}In-DOTA-TOC: a rapid increase within 30 min and a descent from 1 to 4 h.

Cellular Retention of ^{111}In-(3) and ^{111}In-DOTA-TOC in HEK Cells Expressing sstr2A

Cellular retentions of ^{111}In-(**3**) and ^{111}In-DOTA-TOC were analyzed and compared in HEK cells expressing sstr2A. In these experiments, the radiopeptides were allowed to internalize for 120 min; cells were then washed twice with PBS before removing the receptor-bound ligand with glycine buffer, pH 2.8. Warm medium (37°C) was then added and removed after 15, 30, 60, 120, and 240 min and measured for radioactivity. Figure 4A illustrates the cellular radioactivity retention of these compounds over time, expressed as the percentage left in the cell from the total amount internalized. As ^{111}In-(**3**) seems to reach a plateau after 4 h, ^{111}In-DOTA-TOC continues to externalize. Almost 80% from the 2-h internalized ^{111}In-(**3**) is still in the cells after 4 h, whereas only 50% of the ^{111}In-DOTA-TOC

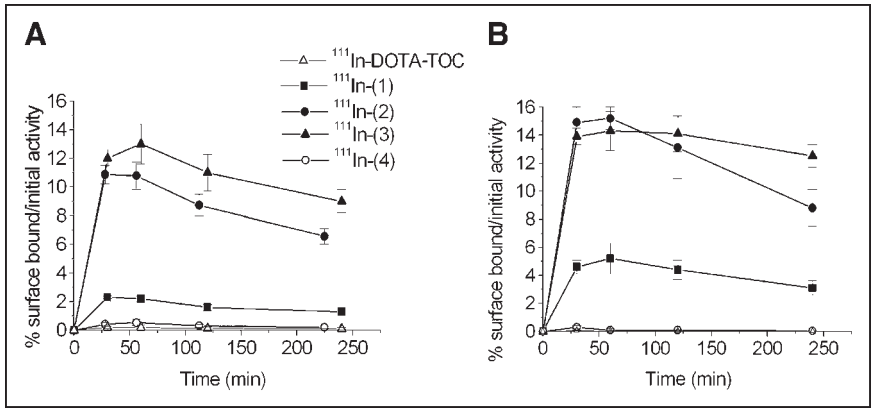

FIGURE 3. Comparison of surface-bound amounts of ^{111}In-labeled conjugates (**1**), (**2**), (**3**), and (**4**) and DOTA-TOC in AR4-2J cells (A) and in sstr2A-HEK cells (B). Values represent specific binding (% initial activity to 1 million cells at 1.67 nmol/L concentration) and are results of 3 independent experiments with triplicates in each experiment.

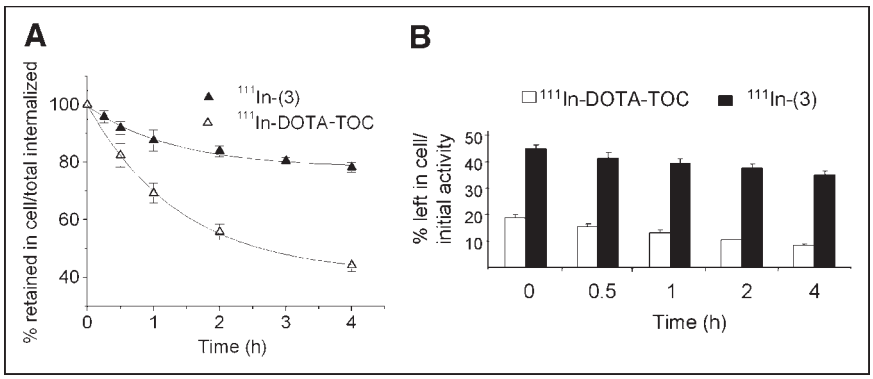

FIGURE 4. Comparison of cellular retention over time between ^{111}In-(**3**) and ^{111}In-DOTA-TOC in sstr2A-HEK cells at 37°C after 2 h of internalization. Values are expressed as percentage retained in cell from total amount internalized (A) and from total amount of added radioligand (B).

2-h uptake is still maintained at this interval. This difference becomes more prominent if the retention in the cell is expressed as the percentage from the total amount of radiopeptide added to the wells (2.5 pmol/well/million cells), as shown in Figure 4B. Thus, after 2 h of internalization, followed by 4 h of externalization, 35% of the NLS-derivative is still retained in the cells (equivalent with 0.88 pmol/well/million cells), whereas only 8.2% of the ^{111}In-DOTA-TOC added remained intracellular (equivalent with 0.2 pmol/well/million cells).

Uptake of ^{111}In-(3) and ^{111}In-DOTA-TOC in Nuclei of HEK Cells Expressing sstr2A

The isolation of HEK-sstr2 nuclei using the Nuclei EZ Prep Kit yielded high- purity nuclei, as revealed by the trypan blue staining test. This experiment was done to determine and compare the amount of radioactivity stored in nuclei after 1-, 4-, and 24-h continuous incubation of ^{111}In-(**3**) and ^{111}In-DOTA-TOC at 37°C with HEK cells expressing sstr2A. The results are shown in Figure 5 and Table 2. Thus, independently of the unit of measure used to express this outcome, there is a massive difference between the nuclear uptakes of the 2 radioligands especially at 1 and 4 h. If the total internalized radioactivity is taken as reference, then ^{111}In-(**3**) has a 15-times higher nuclear accumulation at 1 h compared with that of the parent compound and the difference becomes even larger at 4 h with an 82-fold increase in the percentage in the nuclei in favor of ^{111}In-(**3**) (Fig. 5). Reported as the percentage of the added radioligand or the amount of radiopeptide added (Table 2), the gap between the nuclear uptake of the 2 conjugates goes from 20-fold at 1 h to 45-fold at 4 h and a 16-fold difference at 24 h, always in favor of ^{111}In-(**3**).

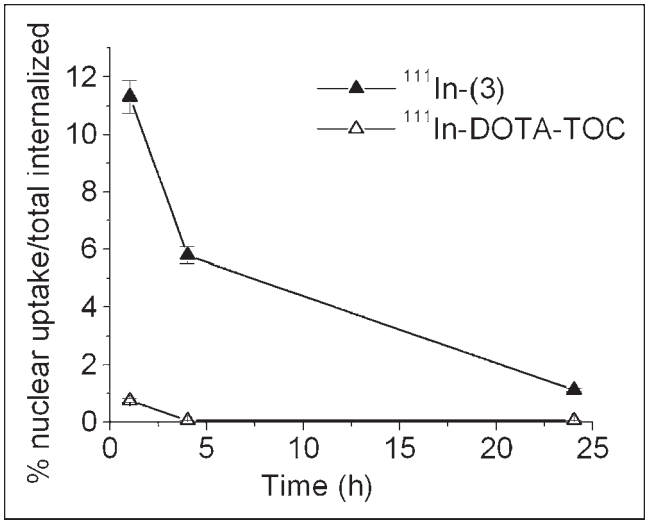

FIGURE 5. Percentage of nuclear uptake of radioactivity in sstr2A-HEK cells incubated with ^{111}In-(**3**) and ^{111}In-DOTA-TOC for 1, 4, and 24 h. Values represent percentage from total amount internalized.

DISCUSSION

The design of effective Auger electron– or low-energy electron–emitting targeting agents for in vivo targeting and treatment of cancers becomes of increasing interest. Neglected initially for therapeutic purposes because of their low-energy and consequent short range, Auger electron cascades are now being seriously considered. The majority of low-energy Auger electrons emitted during radioactive decay deposit their energy over subcellular dimensions, producing highly localized energy density in the immediate vicinity of the decay site (*22*). In vivo and in vitro studies demonstrate that the toxicity of Auger electron emitters approximates that for low-LET radiation when the emitter is localized on the membrane or in the cytoplasm and that for high-LET α-particles when localized in the nucleus or in its proximity (*23*). Recently, the hypothesis that the radiotoxicity of Auger electrons is caused only by direct ionization of the DNA has been proven inaccurate. Apparently 90% of Auger electrons' toxicity is due primarily to indirect mechanisms (*24,25*). Lacking the crossfire effect, for a long time it was assumed that the toxicity and therapeutic potential of low-energy electron emitters requires the radiotargeting of each and every tumor cell. This concept has been recently established as inexact, as the decay of such isotopes leads to a so-called "bystander effect," proven by the in vivo use of ^{125}I-deoxyuridine (*26*). This is translated into an in vivo inhibition or retardation of tumor growth in nonradiotargeted cells by signals produced in Auger electron–labeled cells. Nevertheless, a long enough time of retention in the

TABLE 2
Comparison of Cell Nuclear Uptake Between ^{111}In-(**3**) and ^{111}In-DOTA-TOC in HEK Cells Stably Expressing sstr2A

Expression of nuclear uptake	^{111}In-(**3**)			^{111}In-DOTA-TOC		
	1 h	4 h	24 h	1 h	4 h	24 h
% added radiopeptide	3.6 ± 0.2	2.8 ± 0.1	0.9 ± 0.1	0.18 ± 0.05	0.06 ± 0.01	0.02 ± 0.01
pmol	1.8 ± 0.3	1.36 ± 0.1	0.4 ± 0.1	0.09 ± 0.04	0.03 ± 0.01	0.025 ± 0.005

targeted cells and intranuclear location of the radioligand would increase the potential success of this type of therapy (*27*).

On the basis of previous work reporting targeted radiotherapy using ^{111}In-labeled somatostatin derivatives (*12,28*) and persuaded by the interesting findings on the therapeutic effects of internalizing antibodies labeled with Auger electron–emitting radionuclides (*6*), we envisaged the design of new trifunctional conjugates of a truncated analog of somatostatin bearing a function for receptor binding and internalization (TOC): one for the nucleus transfer (NLS; PKKKRKV) and one for the cytotoxic or reporter effect (^{111}In-DOTA) (*19*). Combining these two targeting strategies, we aimed to achieve a higher accumulation of radioactivity in the cell nuclei and a prolonged retention time of the radioligand in the tumor cells, both conditions being necessary for effective Auger electron DNA cytotoxicity transfer. As the pharmacologic profile of DOTA-TOC–like conjugates is greatly influenced by any structural alterations, we incorporated the NLS in 3 different positions relative to the somatostatin analog sequence, respectively. The first experiment done to test the best assembly of the trifunctional derivatives (**1**), (**2**), and (**3**) was the binding affinity profile to somatostatin sst2 receptors. Because ^{nat}In-DOTA-TOC has suitable affinity only for the sstr2 subtype (*20*), we used HEK cells transfected with sstr2A. Confirming one of our hypotheses, the C-terminal modification of DOTA-TOC (compound **3**) showed a significant loss in binding affinity for this receptor, whereas the N-terminal functionalizations (compounds **2** and **3**) preserved the pharmacologic integrity. This result was also confirmed in the internalization studies, with ^{111}In-(**1**) displaying significantly lower internalization rates in both AR4-2J and HEK-sstr2A cell lines in comparison with ^{111}In-DOTA-TOC. On the other hand, the ^{111}In-labeled derivatives (**2**) and (**3**) revealed increased specific accumulation in both cell lines. Nevertheless, ^{111}In-(**3**) proved to be the best design, not only because of the binding affinity but also because it shows the highest internalization rates (at 4 h, 2-fold internalization rate when compared with the parent compound in both cell lines studied). Confirming the premise that the NLS has to be located in the cytoplasm to drive the cargo to the nucleus (*18*), ^{111}In-(**4**) has no uptake and no binding in both the rat (AR4-2J) and the human (HEK-sstr2A) cell lines.

In addition to the high specific cellular uptake, ^{111}In-(**3**) reveals also a low externalization rate in HEK-sstr2A cells. Although this derivative seems to reach a plateau after 4 h of externalization, with >70% of the 2-h internalized radiopeptide retained intracellularly, the ^{111}In-DOTA-TOC retained in the cell is only 40% and continues to decrease gradually. The gap between the 2 externalization rates becomes even clearer when the cellular retention is expressed as a percentage of the added radioligand.

The most explicit confirmation of the hypothesis on which the design of these NLS-somatostatin derivatives was based comes from the nuclei isolation experiment. The fast nuclear targeting is supported by the 11.2% uptake of ^{111}In-(**3**) in the nuclei in comparison with only 0.7% for ^{111}In-DOTA-TOC at just 1 h after incubation at 37°C. Both compounds show a gradual decrease in the cellular nuclear accumulation from 1 to 24 h, with the ratio of this uptake between the 2 conjugates reaching a maximum at 4 h (82 times higher nuclear uptake for ^{111}In-(**3**)).

The higher internalization rate, the prolonged cellular retention and the significantly higher nuclear uptake of ^{111}In-(**3**) in comparison with the parent compound are proofs that the principle of 2-step targeting may work in practice. It was previously shown that some radiolabeled somatostatin analogs translocate to the nucleus after internalization (*29,30*), usually after longer incubation times. Our results support this theory, but they also show that the addition of a NLS moiety dramatically increases the rate of nuclear targeting, enhancing the efficacy of a potential Auger electron-emitter cytotoxic effect. Although both the complete mechanisms of endocytosis of somatostatin analogs (*31*) and of translocation through the nuclear pores of NLS-cargo conjugates (*32*) still remain to be clarified, at this point we can only assume that a part of the internalized radioligand escapes the lysosomal degradation (*33*). The use of strongly fluorescing lanthanides such as Eu^{3+} or Tb^{3+} used as surrogates of In^{3+} may represent the best proof of nuclear localization of such conjugates (*34*). Nevertheless, it is not crucial that the radiolabeled conjugate remains intact after endocytosis, being sufficient if only the ^{111}In-DOTA-NLS portion of ^{111}In-(**3**) arrives in nuclear proximity. A longer retention in the nuclear compartment may necessitate an additional functional group intercalating into the DNA.

CONCLUSION

The research dealing with the molecular design of new targeting agents is rapidly expanding in the field of nuclear medicine. We have designed and characterized in vitro new NLS-conjugated DOTA-somatostatin–based derivatives.

The peptides were compared with our clinical gold standard [^{111}In-DOTA-Tyr^3]octreotide. These first series of in vitro data demonstrate that the concept of 2-step targeting can work in practice if the conjugates have a suitable design. Future experiments will show the extent to which this approach may improve the cytotoxic effect of such conjugates. This type of strategy could be of real interest particularly for the treatment of disseminated tumor cells, using Auger electron–emitting radionuclides. Or it can be used as a neoadjuvant therapy in combination with β-emitting targeted radiotherapy in neoplasia having both large tumors and small malignancies.

Moreover, this model can be extended also to other ligands of G-protein–coupled receptors or to other cytotoxic moieties, thus further improving the targeting strategies.

ACKNOWLEDGMENTS

We acknowledge the financial support from the Swiss National Science Foundation (project 3100A0-100390), European Molecular Imaging Laboratories, and COST (European Cooperation in the Field of Scientific and Technical Research) B12 (Action B12: "Radiotracers for the in vivo assessment of biologic functions").

REFERENCES

1. Reubi JC, Waser B, Schae JC, Laissue JA. Somatostatin receptor sst1-sst5 expression in normal and neoplastic human tissues using receptor autoradiography with subtype-selective ligands. *Eur J Nucl Med.* 2001;28:836–846.
2. Otte A, Mueller-Brand J, Dellas S, Nitzsche E, Herrmann R, Maecke HR. Yttrium-90-labelled somatostatin-analogue for cancer treatment. *Lancet.* 1998; 351:417–418.
3. Bodei L, Cremonesi M, Grana C, et al. Receptor radionuclide therapy with ^{90}Y-[DOTA]^0-Tyr^3-octreotide (^{90}Y-DOTATOC) in neuroendocrine tumours. *Eur J Nucl Med Mol Imaging.* 2004;31:38–46.
4. O'Donoghue JA, Bardies M, Wheldon TE. Relationship between tumor size and curability for uniformly targeted therapy with beta-emitting radionuclides. *J Nucl Med.* 1995;36:1902–1909.
5. de Jong M, Breeman WA, Bernard BF, et al. Tumor response after [^{90}Y-DOTA^0,Tyr^3]octreotide radionuclide therapy in a transplantable rat tumor model is dependent on tumor size. *J Nucl Med.* 2001;42:1841–1846.
6. Behr T, Behe M, Lohr M, et al. Therapeutic advantages of Auger electron- over beta-emitting radiometals or radioiodine when conjugated to internalizing antibodies. *Eur J Nucl Med.* 2000;27:753–765.
7. Behr T, Sgouros G, Vougiokas V, et al. Therapeutic efficacy and dose-limiting toxicity of Auger-electron vs. beta emitters in radioimmunotherapy with internalizing antibodies: evaluation of ^{125}I- vs. ^{131}I-labeled CO17-1A in a human colorectal cancer model. *Int J Cancer.* 1998;76:738–748.
8. Michel R, Castillo ME, Andrews PM, Mattes MJ. In vitro toxicity of A-431 carcinoma cells with antibodies to epidermal growth factor receptor and epithelial glycoprotein-1 conjugated to radionuclides emitting low-energy electrons. *Clin Cancer Res.* 2004;10:5957–5966.
9. Michel R, Rosario AV, Andrews PM, Goldenberg DM, Mattes MJ. Therapy of small subcutaneous B-lymphoma xenografts with antibodies conjugated to radionuclides emitting low-energy electrons. *Clin Cancer Res.* 2005;11:777–786.
10. Michel R, Brechbiel MW, Mattes MJ. A comparison of 4 radionuclides conjugated to antibodies for single-cell kill. *J Nucl Med.* 2003;44:632–640.
11. Govindan S, Goldenberg DM, Elsamra SE, et al. Radionuclides linked to a CD74 antibody as therapeutic agents for B-cell lymphoma: comparison of Auger electron emitters with beta-particle emitters. *J Nucl Med.* 2000;41:2089–2097.
12. Valkema R, De Jong M, Bakker WH, et al. Phase I study of peptide receptor radionuclide therapy with [In-DTPA]octreotide: the Rotterdam experience. *Semin Nucl Med.* 2002;32:110–122.
13. Moll S, Nickeleit V, Mueller-Brand J, et al. A new cause of renal thrombotic microangiopathy: yttrium 90-DOTATOC internal radiotherapy. *Am J Kidney Dis.* 2001;37:847–851.
14. Capello A, Krenning EP, Breeman WAP, Bernard BF, De Jong M. Peptide receptor radionuclide therapy in vitro using [^{111}In-DTPA^0]octreotide. *J Nucl Med.* 2003;44:98–104.
15. Tiensuu Janson E, Westlin JE, Ohrvall U, Oberg K, Lukinius A. Nuclear localization of ^{111}In after intravenous injection of [^{111}In-DTPA-D-Phe^1]-octreotide in patients with neuroendocrine tumors. *J Nucl Med.* 1999;41:1514–1518.
16. Mariani G, Bodei L, Adelstein SJ, Kassis AI. Emerging roles for radiometabolic therapy of tumors based on Auger electron emission. *J Nucl Med.* 1999;41:1519–1521.
17. Kalderon D, Roberts BL, Richardson WD, Smith AE. A short amino acid sequence able to specify nuclear location. *Cell.* 1984;39:499–509.
18. Yoneda Y, Hieda M, Nagoshi E, Miyamoto Y. Nucleocytoplasmic protein transport and recycling of Ran. *Cell Struct Funct.* 1999;24:425–433.
19. Ginj M, Maecke HR. Synthesis of trifunctional somatostatin based derivatives for improved cellular and subcellular uptake. *Tetrahedron Lett.* 2005;46:2821–2824.
20. Ginj M, Chen J, Walter MA, Eltschinger V, Reubi JC, Maecke HR. Preclinical evaluation of new and highly potent analogs of octreotide for predictive imaging and targeted radiotherapy. *Clin Cancer Res.* 2005;11:1136–1145.
21. Tulipano G, Stumm R, Pfeiffer M, Kreienkamp HJ, Hollt V, Schulz S. Differential beta-arrestin trafficking and endosomal sorting of somatostatin receptor subtypes. *J Biol Chem.* 2004;279:21374–21382.
22. Adelstein S, Kassis AI. Radiobiologic implications of the microscopic distribution of energy from radionuclides. *Int J Rad Appl Instrum B.* 1987;14:165–169.
23. Kassis A, Sastry KS, Adelstein SJ. Kinetics of uptake, retention, and radiotoxicity of ^{125}IUdR in mammalian cells: implications of localized energy deposition by Auger processes. *Radiat Res.* 1987;109:78–89.
24. Walicka M, Adelstein SJ, Kassis AI. Indirect mechanisms contribute to biological effects produced by decay of DNA-incorporated iodine-125 in mammalian cells in vitro: clonogenic survival. *Radiat Res.* 1998;149:142–146.
25. Walicka M, Ding Y, Adelstein SJ, Kassis AI. Toxicity of DNA-incorporated iodine-125: quantifying the direct and indirect effects. *Radiat Res.* 2000;154: 326–330.
26. Xue L, Butler NJ, Makrigiorgios GM, Adelstein SJ, Kassis AI. Bystander effect produced by radiolabeled tumor cells *in vivo. Proc Natl Acad Sci USA.* 2002;99: 13765–13770.
27. Kassis AI. Cancer therapy with Auger electrons: are we almost there? *J Nucl Med.* 2003;44:1479–1481.
28. Buscombe JR, Caplin ME, Hilson AJW. Long-term efficacy of high-activity ^{111}In-pentetreotide therapy in patients with disseminated neuroendocrine tumors. *J Nucl Med.* 2003;44:1–6.
29. Hornick CA, Anthony CT, Hughey S, Gebhard BM, Espenan GD, Woltering EA. Progressive nuclear translocation of somatostatin analogs. *J Nucl Med.* 2000;41: 1256–1263.
30. Wang M, Caruano AL, Lewis MR, Meyer LA, VanderWaal RP, Anderson CJ. Subcellular localization of radiolabeled somatostatin analogues: implications for targeted radiotherapy of cancer. *Cancer Res.* 2003;63:6864–6869.
31. Koenig JA, Edwardson JM. Endocytosis and recycling of G-protein coupled receptors. *Trends Pharmacol Sci.* 1997;18:276–287.
32. Kaffman A, O'Shea EK. Regulation of nuclear localization: a key to a door. *Annu Rev Cell Dev Biol.* 1999;15:291–339.
33. Duncan JR, Stephenson MT, Wu HP, Anderson CJ. Indium-111-diethylentriaminepentaacetic acid-octreotide is delivered in vivo to pancreatic, tumor cell, renal, and hepatocyte lysosomes. *Cancer Res.* 1997;57:659–671.
34. Parker D, Dickins RS, Puschmann H, Crossland C, Howard JAK. Being excited by lanthanide coordination complexes: aqua species, chirality, excited-state chemistry, and exchange dynamics. *Chem Rev.* 2002;102:1977–2010.